Memory T cell responses in influenza A infection and vaccination in humans

Thesis Submitted for the Degree of Doctor of Philosophy



Cecilia Chui

St Cross College

Supervisors:
Professor Sir Andrew J. McMichael, FRS
Dr. Xiaoning Xu

MRC Human Immunology Unit
Weatherall Institute of Molecular Medicine
Nuffield Department of Clinical Medicine
University of Oxford

Trinity Term 2012

To my parents, grandparents and sister, who supported me each step of the way.

Contents

1 Introduction **4**

1.1 Influenza virus . . . 4

1.1.1 Molecular biology of influenza virus . . . 5

1.1.2 Transmission, viral entry, replication and host range . . . 7

1.1.3 Clinical manifestations . . . 10

1.1.4 Animal models . . . 11

1.1.5 Epidemiology . . . 12

1.1.6 Treatments: antivirals, current vaccine strategies and universal vaccine . 12

1.1.6.1 Antivirals . . . 12

1.1.6.2 Influenza vaccine . . . 13

1.1.6.3 Universal vaccine . . . 16

1.2 Immune responses to influenza A infection . . . 16

1.2.1 Innate immune response . . . 16

1.2.2 Adaptive immune response . . . 18

1.2.2.1 Humoral immune response . . . 18

1.2.2.2 Cellular immune response . . . 22

1.2.2.3 Assessment of T cell-mediated immunity to influenza in animal models . . . 26

1.2.2.4 Assessment of T cell mediated immunity to influenza in humans . . . 28

1.2.3 T cell-mediated immunity in influenza A infection . . . 28

1.2.3.1 Antigen presentation and activation of T cells . . . 29

1.2.3.2 T- cell recognition, cross-reactivity and immunodominance . 30

1.2.3.3 Heterosubtypic immunity to influenza virus . . . 32

1.2.4 Memory $CD4^+$ and $CD8^+$ T cells in long-lived protective cellular immunity . . . 34

1.3 Aims . . . 36

2 Materials and Methods **40**

2.1 Materials . . . 40

2.1.1 Plasticware and other laboratory supplies . . . 40

2.1.2 Buffers . . . 40

2.1.3 Plasmids and viruses . . . 41

2.1.4 Restriction Enzymes . . . 41

2.1.5 Kits and beads . . . 41

2.1.6 Media . . . 41

2.1.7 Cytokines . . . 42
2.1.8 Cell lines . . . 42
2.1.9 Tissue culture reagents . . . 42
2.1.10 Chemical and biological reagents . . . 42
2.1.11 Flow cytometry antibodies . . . 43
2.1.12 Other antibodies . . . 45
2.2 Methods . . . 46
2.2.1 Subjects and study cohorts . . . 46
2.2.1.1 Experimental influenza infection . . . 46
2.2.1.2 Viruses . . . 47
2.2.1.3 Experimental H1N1 infection (2010) . . . 48
2.2.1.4 Pandemic H1N1 vaccine trials . . . 48
2.2.1.5 Pandemic H1N1 convalescence study (Siren study RHM Med 0914) . . . 51
2.2.1.6 Healthy adult donors . . . 52
2.2.2 Cellular immunology . . . 52
2.2.2.1 Isolation of peripheral blood mononuclear cells (PBMCs) . . . 52
2.2.2.2 Synthetic peptides . . . 53
2.2.2.3 ELISpot assay for human IFN-γ . . . 54
2.2.2.4 Validation of ELIspot assays . . . 55
2.2.2.5 $CD8^+$ T cells depletion . . . 55
2.2.2.6 Generation of antigen-specific $CD4^+$ and $CD8^+$ T cell lines . . . 56
2.2.2.7 Generation of B cell lines (BCLs) . . . 56
2.2.2.8 Maintenance of short-term T cell lines . . . 56
2.2.2.9 Cytotoxicity assay . . . 56
2.2.2.10 Isolation of genomic DNA and HLA typing . . . 57
2.2.2.11 Cultured ELISpot . . . 58
2.2.2.12 Intracellular cytokine staining (ICS) and flow cytometry . . . 58
2.2.2.13 Immunophenotyping of activated cells . . . 61
2.2.2.14 Epithelial Cell MHC Class II Expression . . . 61
2.2.2.15 Virology and Serology Assays . . . 62
2.2.3 Molecular Biology . . . 63
2.2.3.1 Construction of recombinant vaccinia viruses (rVACVs) . . . 63
2.2.4 Assays for circulating follicular T helper cells . . . 70
2.2.4.1 T cell proliferation assay . . . 70
2.2.4.2 Phenotyping of blood and tonsillar follicular helper cells . . . 70
2.2.4.3 Isolation of B cells . . . 70
2.2.4.4 Isolation of $CD4^+$ T cells . . . 71
2.2.4.5 Co-culture of $CD4^+$ T cells and B cells . . . 71
2.2.4.6 ELISA for IgA, IgM and IgG . . . 72
2.2.4.7 ELISA for IL-21 . . . 72
2.2.4.8 Cell stimulation . . . 73
2.2.4.9 Intracellular staining for IL-21 . . . 73
2.2.4.10 $CD154^+$ assay for antigen-specific cells . . . 73
2.2.4.11 Co-culture of $CD154^+$ cells and autologous B cells . . . 74

2.2.5 Statistical Analysis . . . 74

3 Experimental human acute influenza challenge 75
3.1 Introduction . . . 75
3.2 Results . . . 77
3.2.1 Validation of experimental approach . . . 77
3.2.2 Experimental influenza infection and symptom pattern of the study groups . . . 77
3.2.3 T cell responses of infected volunteers . . . 81
3.2.4 Phenotypes of the pre-existing T cell responses . . . 82
3.2.5 Role of T cell in viral control and symptom development . . . 85
3.2.6 Kinetics of T cells during influenza infection . . . 85
3.2.7 HLA-DR was expressed in the respiratory epithelium . . . 87
3.3 Discussion . . . 88
3.3.1 Experimental infection of influenza A viruses . . . 88
3.3.2 Roles of $CD4^+$ T cells in protection . . . 89

4 Functional studies of influenza-specific $CD4^+$ T cells 103
4.1 Introduction . . . 103
4.2 Results . . . 106
4.2.1 Pre-existing T cell immunity in healthy individuals against seasonal H3N2 and H1N1 . . . 106
4.2.2 Functional avidity of seasonal H1N1-specific T cells that cross-react with pandemic H1N1 epitopes . . . 106
4.2.3 Cytotoxic ability of flu-specific T cells . . . 107
4.2.4 Recognition of target cells infected with rVACVs expressing seasonal or pandemic H1N1 M protein . . . 108
4.2.5 Polyfunctionality of T cells in an acute influenza infection . . . 108
4.2.5.1 Cytokine profile of flu-specific T cells . . . 108
4.2.5.2 Flu-specific T cells expressed other cytokines in addition to IFN-γ . . . 110
4.2.5.3 IFN-γ -producing flu-specific T cells differentially expressed other functions . . . 111
4.2.6 Memory phenotype of responding $CD4^+$ and $CD8^+$ cells . . . 112
4.2.7 Polyfunctional analysis of influenza-specific $CD4^+$ and $CD8^+$ T cell responses . . . 112
4.2.8 Relationship between polyfunctional T cell responses and clinical parameter . . . 113
4.3 Discussion . . . 114

5 T cell responses to an inactivated influenza vaccine 134
5.1 Introduction . . . 134
5.2 Results . . . 136
5.2.1 Study subjects . . . 136
5.2.2 Safety of the vaccines evaluated . . . 137
5.2.3 Immunogenicity of the vaccines evaluated . . . 137

5.2.4 Antigen-specific T cell responses in 2009 pandemic H1N1 and seasonal vaccine trials . . . 139
5.2.5 CD4 dependent responses of vaccine-induced flu-specific T cells 140
5.2.6 Inverse correlation between baseline cell-mediated immune response and fold increase in influenza-specific response post vaccination 145
5.2.7 Phenotype of memory T cells in vaccination . . . 145
5.2.8 Antigen-specific T cell responses in pandemic H1N1 convalescent patients . . . 146
5.3 Discussion . . . 149

6 Circulating T follicular helper cells and their capacity to provide B cell help 164
6.1 Introduction . . . 164
6.2 Results . . . 167
6.2.1 Phenotype of $CD4^+$ $CXCR5^+$ cells in human blood . . . 167
6.2.2 Human blood $CD4^+$ $CXCR5^+$ cells induce differentiation of the naïve B cells towards plasmablasts that produce class-switched antibodies . . . 167
6.2.3 The human blood $CD4^+$ $CXCR5^+$ subset can contain influenza virus-specific cells . . . 168
6.2.4 IL-21 production by influenza virus-specific $CD4^+$ T cells . . . 169
6.2.5 Analysis of the expression of Tfh markers on peripheral blood $CD4^+$ T cells during acute influenza infection . . . 170
6.2.6 Relationship between circulating memory $CXCR5^+$ $CD4^+$ T cells and antibody responses after immunization with inactivated influenza vaccine 171
6.2.7 Influenza-specific cells from peripheral blood are able to help memory but not naive B cells . . . 172
6.3 Discussion . . . 175

7 General discussion 194
7.1 T cells in acute infection . . . 194
7.2 $CD4^+$ T cells in influenza infection . . . 196
7.3 Future studies and prospect for future vaccine development . . . 198
7.4 Concluding remarks . . . 200

List of Figures

1.1 Structure and subtypes of the influenza virus 6
1.2 Schematic diagram of influenza A virus fusion and entry processes 9
1.3 Influenza hemagglutinin 21
1.4 $CD4^+$ T cell effector subsets 24
1.5 T follicular helper (Tfh) cells 26
1.6 Sequence comparisons between H3N2, seasonal and pandemic H1N1 33
1.7 Functionality of T cells during viral infections 37
1.8 Approaches used in mapping epitopes of influenza virus 39

2.1 Enrolment and outcomes of H3N2 (October 2008) and H1N1 (August 2009) challenge studies 48
2.2 Enrolment and outcomes of pandemic H1N1 vaccine studies 51
2.3 Enrolment and outcomes of the China CDC vaccination cohort 52

3.1 *Ex vivo* IFN-γ ELISpot with cell depletion 92
3.2 Viral shedding in nasal wash, seroconversion and symptom development in seronegative healthy volunteers experimentally challenged with influenza A viruses 93
3.3 Symptom scores in each volunteer infected with influenza virus 94
3.4 IFN-γ- ELISpot layout of experimental infection in humans 95
3.5 T cell responses in seronegative healthy volunteers experimentally infected with influenza A viruses 96
3.6 T cell responses to *ex vivo* stimulation in the H1N1 group 97
3.7 Antigen-specific responses to viral peptides in infected subjects 98
3.8 Relationship between influenza-specific T cell responses and illness severity . . 99
3.9 Relationship between viral shedding, total symptom score and illness duration against total T cells on day 7 100
3.10 Kinetics of T cells in influenza infection 101
3.11 Expression of MHC Class II on the respiratory epithelium 102

4.1 Flu-specific T cell responses of healthy individuals 117
4.2 Cross- reactivity study of CD4 memory cells from H1N1 infected subjects to matrix peptides from pandemic H1N1. 118
4.3 Cross- reactivity study of CD4 memory cells from H1N1 infected subjects to nucleoprotein peptides from pandemic H1N1 119
4.4 Killing activities displayed by T cell lines generated from H3N2 infected volunteers upon recognition of target cells by chromium release assay 120
4.5 Killing activities displayed by T cell lines generated from subjects with a memory responses to H1N1 121

4.6 Gating Strategy of determining influenza-specific polyfunctional analysis of $CD8^+$ and $CD4^+$ T cells producing IL-2, IFN-γ, TNF-α , perforin and CD107a . 122
4.7 Influenza-specific T cells express multiple effector functions 123
4.8 Frequency of IFN-γ producing $CD4^+$ and $CD8^+$ T cells as measured by intracellular cytokine staining 124
4.9 Cytokine responses of flu-specific $CD4^+$ and $CD8^+$ T cells 125
4.10 IFN-γ and CD107a production of Flu-, M- or NP- specific $CD4^+$ and $CD8^+$ T cells on baseline and day 7 126
4.11 Percentage of IFN-γ^+ $CD4^+$ and $CD8^+$ T cells performing different functions were analysed on day 0, 7 and 28 127
4.12 Memory phenotype of flu-specific $CD4^+$ and $CD8^+$ cells 128
4.13 Functional profile of SEB- stimulated T cells of infected volunteers 129
4.14 Functional repertoire of $CD4^+$ T cells in response to flu peptides stimulation . . 130
4.15 Functional repertoire of $CD4^+$ T cells of in response to M or NP peptide pools . 131
4.16 Functional repertoire of $CD8^+$ T cells in response to flu peptides stimulation . . 132
4.17 Functional repertoire of $CD8^+$ T cells in response to M or NP peptide pools . . 133

5.1 IFN-γ ELISpot layout of pandemic H1N1 vaccine trials 153
5.2 T cell responses in volunteers vaccinated with inactivated influenza vaccines . . 154
5.3 Antigen-specific responses to viral peptides in vaccinated subjects 155
5.4 Correlation between humoral and cellular immune responses in vaccinated subjects 156
5.5 Relationship between influenza-specific T cell responses at baseline and the fold-increase in spot-forming cells in IFN-γ ELISpot on day 7 post-vaccination 157
5.6 T cell responses in a group of volunteers from China CDC vaccinated with seasonal and pandemic H1N1 vaccine 158
5.7 Memory phenotype of activated proliferating T cells 159
5.8 Activated and proliferative ($CD38^+$ Ki-67^+) $CD4^+$ and $CD8^+$ T cells in vaccination. 160
5.9 Frequency of naïve and non-naïve $CD4^+$ and $CD8^+$ T cells in the course of vaccination in Group A. 161
5.10 Frequency of naïve and non-naïve $CD4^+$ and $CD8^+$ T cells in the course of vaccination in Group B. 162
5.11 Flu-specific T cell responses of pandemic H1N1 convalescent subjects and healthy PBMCs collected before 2009 163

6.1 Expression of CXCR5 by circulating $CD4^+$ T cells from blood. 179
6.2 Expression of various Tfh markers by circulating $CXCR5^+$ $CD4^+$ T cells 180
6.3 Expression of various Tfh markers by $CXCR5^+$ cells from tonsil 181
6.4 Strategy used for isolation of $CXCR5^+$ and $CXCR5^-$ memory $CD4^+$ T cells and autologous naïve B cells for use in Tfh assays 182
6.5 Blood $CXCR5^+CD4^+$ T cells induce naïve B cells to differentiate into antibody-producing plasma cells 183
6.6 Blood $CXCR5^+CD4^+$ T cells induce naïve B cells to differentiate into antibody-producing plasma cells 184
6.7 Blood $CXCR5^+CD4^+$ T cells induce naïve B cells to differentiate into plasmabasts 185
6.8 Cytokine response of $CXCR5^+$ and $CXCR5^-$ memory $CD4^+$ T cell populations to activating stimuli 186

6.9 Response of CXCR5$^+$ and CXCR5$^-$ memory CD4$^+$ T cell populations to activating stimuli 187
6.10 Proliferation of CXCR5$^+$ and CXCR5$^-$ memory CD4$^+$ T cell populations in response to monocytes pulsed with inactivated flu vaccine 188
6.11 Use of intracellular staining to assess IL-21 production by CD4$^+$ T cells 189
6.12 Expression of various Tfh markers on CD4$^+$ T cells in the peripheral blood at different timepoints after a live influenza challenge 190
6.13 Frequency of memory CXCR5$^+$ CD4$^+$ T cells after influenza vaccination 191
6.14 Development of a method for assessing the ability of flu-specific CD4$^+$ T cells to provide help for B cells 192
6.15 Development of a method for assessing the ability of flu-specific CD4$^+$ T cells to provide help for B cells 193

List of Tables

3.1 Demography, virus shedding and antibody titre of the study groups 78
3.2 Summary of infected subjects in the challenge studies 80
3.3 T cell peptides in H3N2 challenge study 84
3.4 T cell peptides in H1N1 challenge study 86

4.1 Summary of stimulations used for each subject 110

5.1 Demography and antibody titre of the study groups 138
5.2 Seasonal H1N1 HA-specific T cell responses elicited by the three groups 141
5.3 Pandemic H1N1 HA-specific T cell responses elicited by the three groups . . . 142
5.4 T cell peptides in pandemic H1N1 vaccine study 144
5.5 List of H1N1 T cell peptides identified 148

Abbreviations

aa	amino acid
Ab	Antibody
Ag	Antigen
ALP	Alkaline phosphatase
APC	Allophycocyanin
APC	Antigen presenting cell
ASC	Antibody-secreting cells
BCL	B lymphoblastoid cell line
BFA	Brefeldin A
bp	base pair
BSA	Bovine serum albumin
BUdR	5-bromodeoxyuridine
CD	Cluster of differentiation
CDC	Center for Disease Control and Prevention
CFSE	Carboxyfluorescein diacetate succinimidyl ester
CMA	Concanamycin A
cpm	Counts per minute
Cr	Chromium
CTL	Cytotoxic T Lymphocytes
CXCR5	Chemokine (CXC-motif) receptor 5
D10	DMEM with 10% heat inactivated FCS
DAB	Diaminobenzidine
DMSO	Dimethyl sulphoxide
DNA	deoxyribonucleic acid
EBV	Epstein-Barr virus
EDTA	Ethylenediamine tetraacetic acid

ELISA	Enzyme-linked Immunosorbent Assays
ELISpot	Enzyme-linked immunospot assay
ER	Endoplasmic reticulum
EtBr	Ethidium bromide
FACS	Fluorescent activated cell sorting
FCS	Foetal Calf Serum
FITC	Fluorescine isothiocyanate
GC	Germinal Centre
GMT	Geometric Mean Titer
H10	RPMI with 10% heat inactivated Human AB serum
H5	RPMI with 5% heat inactivated Human AB serum
HA	Hemagglutinin
HAI titer	Haemagglutinin-specific antibody titer
HI	Haemagglutination-inhibition
HLA	Human Leukocyte Antigen
HPAI	Highly pathogenic avian influenza
IAV	Inactivated influenza vaccine
ICS	Intracellular cytokine staining
IFN	Interferon
Ig	Immunoglobulin
IL	Interleukin
ION	Ionomycin HCl
LAIV	Live attenuated influenza vaccine
LB	Luria-Bertani
M	Matrix Protein
M1	Matrix protein 1
M2	Matrix protein 2
mAb	Monoclonal Antibody
MBC	Memory B cells
MFI	Mean fluorescent intensity
MHC I	Major Histocompatibility Complex class I

MHC II	Major Histocompatibility Complex class II
MN	Microneutralization
NA	Neuraminidase
nAb	Neutralizing Antibody
NDA	No Detectable Activity
NK	Natural killer cell
NP	Nucleoprotein
PB	Pacific Blue
PBMC	Peripheral blood mononuclear cell
PBS	Phosphate Buffered Saline
PE	Phycoerythrin
PerCP	Peridin chlorophyll protein
Pfn	Perforin
Pfu	Plaque forming unit
pH1N1	Pandemic H1N1 (A/CA/07/2009)
PHA	Phytohemagglutinin
PMA	Phorbol myristate acetate
R10	RPMI with 10% heat inactivated FCS
R2	RPMI with 2% heat inactivated FCS
RNA	ribonucleic acid
RT	Room Temperature
rVACV	Recombinant vaccinia virus
SD	Standard division
SEB	Staphylococcal enterotoxin B
SEM	Standard error of the mean
SFU	Spot Forming Unit
Tcm	Central memory T cells
TCR	T-cell receptor
Tem	Effector memory T cells
Tfh	T follicular helper cells
TGF	Transforming growth factor

TNF	Tumor necrosis factor
VDM	Virus dilution medium
w/v	Weight per volume
WHO	World Health Organisation

Amino acid abbreviations

A	Alanine
C	Cysteine
D	Aspartic acid
E	Glutamic acid
F	Phenylalanine
G	Glycine
H	Histidine
I	Isoleucine
K	Lysine
L	Leucine
M	Methionine
N	Asparagine
P	Proline
Q	Glutamine
R	Arginine
S	Serine
T	Threonine
V	Valine
W	Tryptophan
Y	Tyrosine

Acknowledgements

First of all, I would like to express my most sincere gratitude for my supervisor, Prof. Sir Andrew McMichael, who always offered me intellectual guidance and invaluable advice. Special thanks must go to him for kindly arranging financial support for me during my thesis writing. I would also like to thank my supervisor Dr. Xiaoning Xu for his guidance and giving me the opportunity to do my DPhil in Oxford. My doctoral would not be complete without the mentorship and help of Dr. Chris Li, who has guided me and taught me many necessary skills since the first day. I would like to thank Prof. Alain Townsend for his advice and support in the production of recombinant vaccinia virus. Thanks also to Dr. Tao Dong who has given me advice and help from time to time. Lastly, I am very grateful for the kind help of Dr. Persephone Borrow, who has always been so kind and knowledgeable in giving me a lot of helpful ideas, and without her guidance one of my result chapters would not be complete.

I would like to take this opportunity to thank my collaborators, Dr. Tom Wilkinson from Southampton Medical School for providing me with clinical samples, scientists from China CDC for their help and friendship during our stay, and Dr. Molly Perkins from N.I.H. for her help in the development of flow panels. I would also like to thank Medical Research Council, for providing me with financial support throughout my studies. For the cohorts described in this thesis, the challenge studies were funded by Medical Research Council, Retroscreen and Duke University, while the vaccine studies were funded by Medical Research Council together with the Chinese government. I would like to thank Prof. Nick Willcox for providing me with tonsillar cells. I would also like to express my gratitude to all study participants and colleagues who have kindly donated blood for me in the past few years. Nonetheless, thanks to all the WIMM staff especially Kevin and Craig, who have sorted cells for my assays many, many times.

This journey won't be the same without the help of a lot of wonderful and kind people here in Oxford. My most heartfelt gratitude to Nicky, who proofread every chapter of my thesis and my transfer report. Many thanks to Arthur and Liye, who have helped me take countless blood samples in the past four years. Thanks to my past and present colleagues Ushani, Christy, Qiongyu and Lili, who have helped me in one way or another, from weighing and pooling peptides in the middle of the night to cooking dinner for me. I am fortunate enough to have met many lovely friends here in HIU - Lucas, Dongdong, Jason, Xiaoxiao, Peng, Oliver, Elizabeth... I will always miss the times with you all dearly. Thanks also to all my very supportive friends Marcella, Betty, Alva, Tracy, Ant, Cynthia, Rebecca and Sook Teng etc..Thanks Leo for your encouragement and kind words. Special thanks to Wilfred for hours of technical help and formatting my thesis for me. You all have made my life in the U.K. special.

I would like to dedicate this thesis to my family, particularly to my late grandparents, por por and gong gong, who both passed away in 2010. Thank you for your faith in me and I miss you both so much. Thank you to my mother and sister who have been so supportive and understanding all these years – I love you all very much.

Lastly, I would like to thank my boyfriend Derek who might be one of the best things that Oxford has ever brought to me. I am so lucky to have you and Sushi by my side - thanks for being so supportive in both the hard and good times - and that is when I realise that we are growing up together. Those bittersweet moments of us working through our DPhil together in the lab are somewhat comforting and will always be part of me in many more years to come.

Memory T cell responses in influenza A infection and vaccination in humans

Cecilia Chui, *D. Phil. Candidate*
MRC Human Immunology Unit, Weatherall Institute of Molecular Medicine
Nuffield Department of Clinical Medicine
St Cross College, University of Oxford
Trinity Term 2012

Abstract

Protective immunity against influenza virus infection is believed to be mediated by neutralising antibodies. Despite substantial evidence in animal models which suggests critical roles for T cells in viral clearance, the precise role of cellular immunity in human influenza immunity remains uncertain. The first aim of this project was to determine cellular immune responses in sero-negative human volunteers following nasal challenge with live seasonal H3N2 or H1N1 viruses. T cell responses before and during infection were mapped. A large increase in both breadth and magnitude in influenza-specific $CD4^+$ T cell responses was seen in the blood by day 7, when virus was completely cleared from nasal samples and serum antibodies were still undetectable. These acutely expanded T cells were shown to be highly activated ($CD38^+$) and proliferating ($Ki\text{-}67^+$). Pre-existing $CD4^+$ T cells, but not $CD8^+$, specific to internal proteins nucleoprotein and matrix proteins, were associated with lower virus shedding and less severe illness. These influenza-specific T cells also responded to A/California/07/2009 (H1N1) peptides, were able to kill antigen-loaded autologous B cell lines *in vitro* and were polyfunctional in cytokine production. The second aim was to assess the cellular immune responses to unadjuvanted, inactivated seasonal and pandemic A/California/07/2009 (H1N1) influenza vaccines. 151 healthy adult volunteers were vaccinated: modest influenza-specific T cell responses were induced, and specific responses to HA and NA peptide pools were found to be mediated by $CD4^+$ T cells. Activated and proliferating cells induced during vaccination were found to be of a central memory phenotype. Lastly, I explored the link between antibody production and $CD4^+$ T cells. The ability of $CXCR5^+$ $CD4^+$ T cells from peripheral blood to support antibody production was examined and antigen-specific $CD4^+$ T cells with helper functions could be found in the peripheral blood of healthy volunteers with memory influenza-specific T cells. This thesis suggests that influenza-specific $CD4^+$ T cells have an important role in limiting the severity of influenza infection in the absence of specific antibody responses through a number of mechanisms. This work provides information on how cellular immunity can be targeted in conferring broad protection against different subtypes of influenza A viruses in the development of universal flu vaccine.

Publication arising from the thesis

1. Wilkinson, T.M.*, C.K. Li*, **C.S. Chui**, A.K. Huang, M. Perkins, J.C. Liebner, R. Lambkin-Williams, A. Gilbert, J. Oxford, B. Nicholas, K.J. Staples, T. Dong, D.C. Douek, A.J. McMichael, and X.N. Xu. 2012. Preexisting influenza-specific CD4+ T cells correlate with disease protection against influenza challenge in humans. *Nat Med* 18:274-280

2. Wu, J., X. Zhong, C.K. Li, J.F. Zhou, M. Lu, K.Y. Huang, M. Dong, Y. Liu, F.J. Luo, N. Du, **C. Chui**, L.Q. Liu, N.M. Smith, B. Li, N.M. Shi, L.F. Song, Y. Gao, D.Y. Wang, X. Wang, W.F. Zhu, Y. Yan, Z. Li, J.T. Chen, A.J. McMichael, W.D. Yin, X.N. Xu, and Y. Shu. 2010. Optimal vaccination strategies for 2009 pandemic H1N1 and seasonal influenza vaccines in humans. *Vaccine* 29:1009-1016.

Chapter 1

Introduction

1.1 Influenza virus

Influenza is an acute respiratory illness that is highly contagious leading to profound morbidity and mortality. Potential danger of influenza was first recognized in 1918-1919, when the virus infected one third of the world's population and killed 20-50 million people worldwide (Barry, 2004). Seasonal epidemics cause 250,000-500,000 deaths around the globe annually and huge economic losses (Graham-Rowe, 2011). In recent years, outbreaks of highly pathogenic influenza viruses such as the H5N1 virus which has a fatality rate of 60% (Van Kerkhove et al., 2011), and pandemic H1N1 virus that caused significant morbidity and mortality in children and young adults, have posed a serious threat to the protective capacity of immune memory responses against influenza viruses in humans. The heterogeneity and diversity of influenza virus in its natural reservoir of wild waterfowl suggests that future human infection with virus of pandemic potential may occur. Therefore it is essential to understand the immune responses to influenza that may confer protection. Moreover, several features of influenza A virus, including the fact that the virus is effectively cleared a few days following infection (without the use of antiviral drugs) and most individuals are not naïve to the virus, provides an excellent model for us to extensively analyse human immune responses to acute viral infections. Immune responses to influenza virus infection have been a research topic for more than 70 years. Understanding immune responses induced by seasonal influenza A virus can help identify immune correlates of protection which is a prerequisite in developing a successful universal vaccine.

1.1.1 Molecular biology of influenza virus

Influenza A virus was first isolated from infected pigs in 1931 (Shope, 1931), and from humans later in 1933 (Smith W, 1933). It is a pathogen of avian origin but regularly infects mammals. Influenza A viruses, together with influenza B and C viruses, cause respiratory illness. Resulting in morbidity and mortality worldwide in seasonal epidemics, the virus can potentially become pandemic. Influenza belongs to the orthomyxovirus family, with an eight single stranded negative-sense RNA segmented genome encoding ten viral proteins. The viral envelope is a lipid bilayer, containing three types of transmembrane proteins: hemagglutinin (HA), neuraminidase (NA) and matrix protein 2 (M2); and an interior matrix protein 1 (M1). The viral core consists of the viral RNA (vRNA), nucleoprotein (NP) and three polymerase proteins (PB1, PB2 and PA), making up the viral ribonucleoprotein complex (vRNP) (**Fig. 1.1a**). HA is required for virus attachment to the host cells (Skehel and Wiley, 2000), while NA is responsible for the release of viral particles from the host cells. PB1-F2, which is encoded from a shifted reading frame of the PB1 gene, is not expressed by all virus strains, but is thought to be involved in viral pathogenicity by inducing macrophage cell death (Chen et al., 2001; Zamarin et al., 2006). M1 and M2 form a matrix on the interior of the virion lipid envelope (Nayak et al., 2004). Lastly, NS1 protein is responsible for inhibiting the host's interferon immune responses, and NS2 mediates the export of vRNPs.

Influenza A virus is subtyped according to the antigenic and genetic nature of their surface proteins HA and NA. To date, 16 subtypes of HA and 9 subtypes of NA have been identified. While the natural reservoir for viruses bearing these subtypes is waterfowl in the wild, only a few subtypes have established themselves in mammals such as humans (HA [H1, H2 and H3] and NA [N1 and N2]), pigs (HA [H1 and H3] and NA [N1 and N2]) and horses (H3N8 and H7N7) (Wright PF, 2001). The HA subtypes are classified into two groups (or lineages) based on their structural features and antigenic properties. Members of group 1 include the H1a, H1b and H9 clades, which include the H1 subtypes from both the seasonal H1N1 strains and the pandemic 1918 and 2009 H1N1 strains, plus the H5 HA subtypes which include the highly pathogenic avian influenza (HPAI) H5N1 strains. Members of group 2 include the H3 and H7 clades, which consist of the human seasonal H3N2 strains and the HPAI H7N7 strains respectively (Van Kerkhove et al., 2011) (**Fig. 1.1b**).

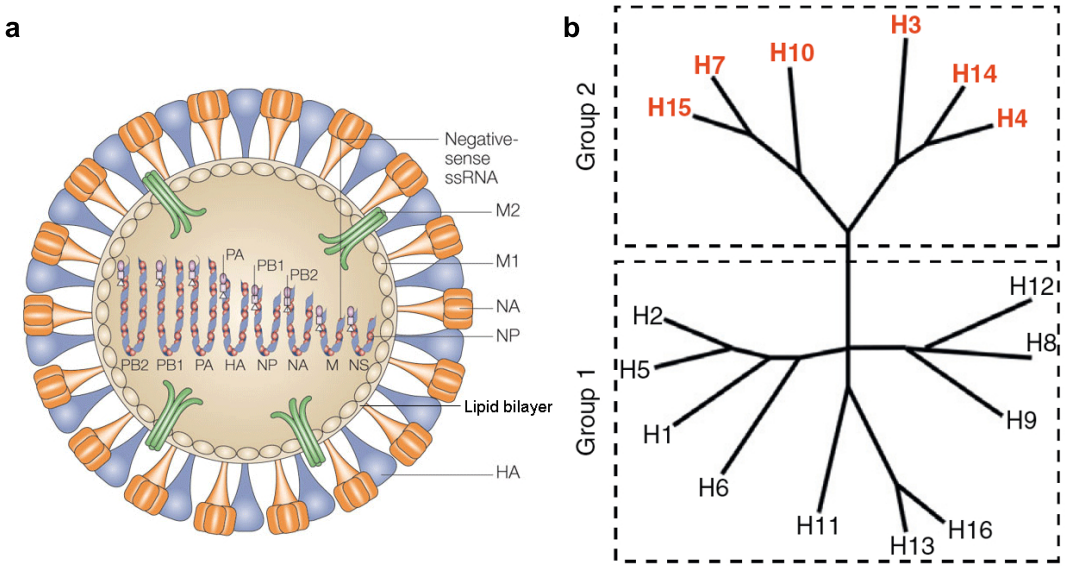

Figure 1.1 Structure and subtypes of the influenza virus. (a) Three viral proteins are exposed on the outside of virus particles: Haemagglutinin (HA, which forms trimers), neuraminidase (NA) (which forms tetramers) and M2 (which forms tetramers that make up ion-channels) are expressed on the outside of the virus. HA0 is processed to HA1 and HA2 upon enzymatic cleavage. The influenza virus matrix protein M1 associates with the inner side of the envelope. The viral genome consists of eight negative-strand RNA segments and is packaged as a helical ribonucleoprotein in complex with nucleocapsid protein (NP) and the viral polymerases PA, PB1 and PB2. **(b)** The 16 hemagglutinin subtypes of influenza A viruses fall into two major phylogenetic groups (Group 1 and 2) [Adapted from (Horimoto and Kawaoka, 2005) and (Ekiert and Wilson, 2012)].

Influenza A H1N1, H3N2 virus and influenza B virus constitute the major circulating strains among human population. In influenza A, antigenic variation that takes place in HA and NA in turn renders an individual susceptible to variant strains despite previous vaccination or exposure to the virus. Influenza virus RNA polymerase lacks proofreading mechanisms giving rise to non-silent point mutations (antigen drift) within the genome; these genetic changes encode amino acid changes in the surface proteins that allow the virus to escape from neutralizing antibodies elicited from previous infections or vaccinations (Both et al., 1983; Holmes, 2003). Furthermore, because of its segmented genome, the gene segments are able to reassort with those of other influenza viruses in the event of a coinfection in the same cell (antigenic shift) [reviewed in (Doherty et al., 2006)]. Antigenic shift can occur when an animal influenza virus crosses the species barrier and is transmitted from an animal reservoir to humans or when a new HA is introduced to the human population via genetic reassortment between animal and human influenza A viruses (Glezen, 1996; Schweiger et al., 2006; Taubenberger and Morens, 2008). Thus novel and highly pathogenic zoonotic strains (such as avian H5N1) capable of infecting humans, or viruses that give rise to pandemics [1918 (H1N1), 1955 (H2N2) and 1968 (H3N2)] have emerged.

In April 2009, an outbreak of pandemic H1N1 swine-origin influenza A virus emerged in Mexico. Distinct from the circulating H1N1, the virus posed a new threat to global population which had little pre-existing immunity; and the World Health Organization (WHO) declared a pandemic in June 2009. This H1N1 pandemic virus resulted from the reassortment of recent North American H3N2 and H1N2 swine virus (itself a triple reassortant virus from a reassortment between human H3N2, North American avian, and classical swine viruses) with Eurasian avian-like viruses. Thus this virus contains PB2 and PA genes of North American avian virus origin, PB1 gene of human H3N2 origin, HA, NP and NS gene of classical swine origin, and NA and M genes of Eurasian avian-like swine virus origin (Dawood et al., 2009; Garten et al., 2009; Smith et al., 2009). The pandemic H1N1 viruses appeared to be causing high rates of illness and severe diseases particularly among children and young adults. Patients with chronic diseases or obesity, as well as pregnant women, have are also been shown to have an increased risk of severe outcome (Peiris et al., 2009b; Singanayagam et al., 2011).

Influenza B only infects humans and undergoes antigenic drift to a lesser extent than influenza A; however, it can cause severe disease in children and the elderly. Influenza B viruses have diverged into two antigenically distinct lineages: the Yamagata and Victoria lineages (Kanegae et al., 1990; Rota et al., 1990).

1.1.2 Transmission, viral entry, replication and host range

Influenza is transmitted from person to person via aerosols and droplets. The virus enters the host via the respiratory tract. The main target cells of the virus are the columnar epithelial cells lining the airway where the viral receptors are present and functional. HA glycoproteins play a pivotal role in infection as they bind the virus to the host cell and bring about fusion. Human seasonal influenza virus binds sialic acid linked to galactose via an α-2, 6 linkage predominantly found on the epithelial cells of the human respiratory tract. On the other hand, avian virus preferentially recognizes the α-2, 3 linkage form, which predominantly found in the lower respiratory tract in human. In birds, avian influenza receptors are highly expressed in intestinal tract where virus replicates and is transmitted via faecal materials. The epithelial cells of the pig trachea contain both types of sialic acid thus pigs are highly susceptible to both human and avian viruses (Imai and Kawaoka, 2012). Due to the nature of HA, transmission of influenza virus highly depends on the tissue tropism of the virus. Avian viruses however can infect humans and have resulted

in lethal infection despite these differences in receptor specificity (Ito et al., 1998; Rogers and Paulson, 1983). Influenza A viruses require exogenous serine proteases for activation. The highly pathogenic viruses, H5 and H7, possess polybasic amino acids at the HA cleavage site and can be recognized by ubiquitous proteinases that allow the viruses to replicate in the lower respiratory tract of humans and lead to systemic infections (The Writing Committee of the World Health Organization (WHO) Consultation on Human Influenza A/H5, 2005). The HA protein (**Fig. 1.3**) is synthesized as a precursor protein HA0 that is cleaved extracellularly at conserved arginine residues into 2 subunits (HA1 and HA2) by a host cell trypsin-like protease in the respiratory tract. For seasonal influenza such as H1 and H3 viruses, tryptase Clara produced by cells of the bronchiolar epithelium is likely to be the enzyme recognizing the conserved Q/E-X-R motif found at the HA cleavage site (Chen et al., 1998). HA0 monomers associate non-covalently to form homotrimers. When the HA0 binds to the sialic acid residues on the host cell surface, this initiates endocytosis and formation of the endosome. At low pH, HA-mediated fusion of viral and endosomal membrane is activated. A conformational change in HA is then triggered and the N termini of the HA2 fusion peptides are exposed (Wiley and Skehel, 1987). The HA2 subunit thus twists to form a three-stranded coiled-coil with the hydrophobic fusion peptides inserting into the lipid bilayer of the endocytic membrane, while the C-terminal ends remained attached to the virus. The N and C region of the C-terminal end associates and brings the whole complex into a hairpin structure, allowing the lipid cell and viral membranes to fuse. The M2 ion channel pumps H^+ ions into the virion interior, dissociating the viral RNA from M1. The viral RNA is then free to be imported into the cell nucleus via an ATP-dependent manner allowing viral replication to take place (Flint SJ, 2004) (**Fig. 1.2**).

Influenza viruses transcribe and replicate their genomes in the nucleus of infected cells, thus relying on the host's nuclear functions to perform these functions. Parental RNPs are first transcribed (primary transcription) to make the new viral proteins which are necessary for RNA replication. The primary transcription is initiated by cap snatching, which involves the cleavage of 5' methylguanosine cap as well as ten to thirteen nucleotides from host pre-mRNAs by the viral endonuclease (PB2). These are then used as the primer to copy the template, and the mRNAs are polyadenylated. Virus RNA replication occurs in two steps: eight complementary positive sense RNA (cRNAs) strands are synthesized from the eight negative sense RNA segments first to generate a large amount of progeny virus vRNPs. These can then act as templates for late

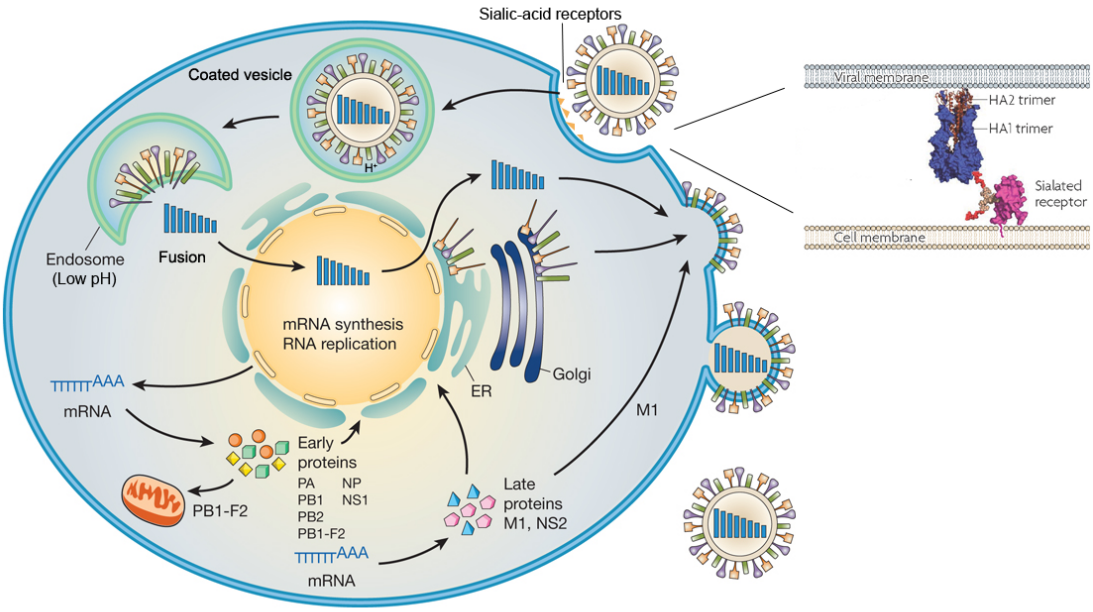

Figure 1.2 Schematic diagram of influenza A virus fusion and entry processes. Trimeric HA1 proteins bind to sialated glycoproteins. Following receptor interaction and internalization, the trimeric HA2 proteins mediate fusion of the viral membrane and the endosomal membrane in the low pH endosomal compartments, allowing viral entry. It is then followed by the release of viral RNA, replication within the nucleus, synthesis of structural and envelope proteins, budding and release of virions capable of infecting neighboring epithelial cells [Modified from (Hedestam et al., 2008; Neumann et al., 2009a)].

transcription and eventually exit the nucleus and enter the cytoplasm of the host cell, and be incorporated into virions at the plasma membrane (Cros and Palese, 2003; Nayak et al., 2004).

Influenza A has been shown to infect a variety of animals including humans, wild and domestic birds, swine, horses, seals, whales, canines, minks and others (Wright PF, 2007). Cases of transmission from animals to human are uncommon; however, interspecies transmission is possible when the human virus and avian virus infect and reassort in an intermediate host such as a pig. Although HPAI such as H5N1 can replicate in infected humans and has resulted in death, the virus has not yet adapted towards human-human transmission. Human viruses replicate well at 33°C at the upper respiratory tract of humans, while avian viruses replicate in the intestinal tract of birds with a body temperature of 41°C but replication is not as efficiently at the colder temperature (Massin et al., 2001). The ability of influenza virus to replicate efficiently in a specific host is a multigenic trait often related to receptor-binding specificity, virulence and host range adaptation. In 2003 H5N1 viruses were isolated from a father and a son in Hong Kong that had replacement at residue 227 of the receptor binding site allowing the virus to bind both α-2, 3 and α-2, 6 sialic receptors (Shinya et al., 2005; Yassine et al., 2010). Recently, the ability of

H5N1 to acquire transmission capacity has been explored. Two reports described the generation of mutant isolates of H5N1 virus that permit viral transmission between ferrets via the respiratory routes (Herfst et al., 2012; Imai et al., 2012) and emphasizing the need for influenza surveillance and pandemic preparedness.

1.1.3 Clinical manifestations

Influenza A is generally self-limiting and resolves after 3-6 days in patients. Viral clearance in the respiratory tract occurs after 3-5 days in most people. Duration of infectivity is considered to be from the day before the onset of symptoms until about 5 days after the onset. However, for some patients intensive care is required because of exacerbation of underlying diseases and complications from severe respiratory illnesses (Giannella et al., 2010). Prolonged viral shedding (detection of viral RNA at or beyond 7 days) has been reported in immunocompetent children and immunocompromised patients, and in hospitalized patients who are older and/or have chronic illnesses (Leekha et al., 2007).

Influenza A viruses cause a sudden onset (24-48 h) of febrile respiratory illness (> 38°C), as the virus infects the respiratory epithelium from the nasal passages to bronchioles. Local and systematic reactions such as high fever, chills, headache, myalgia, dry cough and diarrhea are common. Infection of the respiratory tracts may lead to primary pneumonitis, which can result in secondary streptococcal, staphylococcal and *Haemophilus influenzae* infections with severe pulmonary complications (Cox and Subbarao, 1999). Patients can be more susceptible to secondary bacterial pneumonia after influenza infection. Indeed, bacterial superinfections caused by *Streptococcus pneumoniae* and *Staphylococcus aureus* are one of the main causes of death during influenza epidemics and pandemics (McCullers, 2006; Morens et al., 2008). It has been suggested that influenza infection leads to a weakened NK cell response in the lung, which might predispose the host to subsequent bacterial superinfection (Small et al., 2010). Pathology, on the other hand, differs according to the level of virulence. Low-virulence viruses (e.g. seasonal H3N2 and H1N1) tend to cause inflammation, congestion and epithelial necrosis of the larger airways (trachea, bronchi and bronchioles); whereas high virulence viruses (e.g. 1918 H1N1, H5N1 and 2009 H1N1) not only cause inflammation in these areas but also in the alveoli, as they infect pneumocytes and intra-alveolar macrophages (Guarner and Falcon-Escobedo, 2009). The induction of a cytokine storm has been proposed to explain the pathology of fatal H5N1 infections

(de Jong et al., 2006). There is evidence that influenza A/H5N1 viruses can disseminate to other organs. Gastrointestinal symptoms such as diarrhoea, vomiting, and abdominal pain are common in H5N1 patients. Involvement of the central nervous system has also been reported in one case (Gambotto et al., 2008).

1.1.4 Animal models

Different animal models have been used for influenza research since ferrets were first used during the initial isolation of influenza viruses in 1933. Ferret models (*Mustela putorius furo*) are used as a mammalian model for influenza studies because of their relatively small size and their susceptibility to both human and avian viruses. They share similar lung physiology to humans and also share similar patterns of sialic acids, throughout the respiratory tract (van Riel et al., 2007). Both human and avian viruses replicate efficiently in ferrets without adaptation. Importantly, ferrets also emulate the clinical features associated with human disease when they are infected with influenza, making these animals an excellent model in which to address research questions concerning influenza pathogenesis and transmission following infection (Belser et al., 2011). Recently, two different groups have used ferrets to study mutated H5N1 avian virus that is transmissible between mammals. Both groups (Herfst et al., 2012; Imai et al., 2012) suggested that a few mutations are likely to be required for H5N1 to adapt to humans, but the mutated virus did not kill any of the animals, transmitted less efficiently than the pandemic H1N1 strains, and was sensitive to current antivirals and vaccines. Their research, however, has set off debates in the public domain as to whether it is appropriate to publish the details of their results and how these generated viruses should be handled.

Although mice have also been frequently used as a model to study disease pathogenesis and the associated innate and adaptive immune responses, due to the good availability of immunological reagents, the model itself does not support the replication of human influenza viruses without prior virus adaptation. Many clinical signs of infection in humans, such as fever and the sneeze reflex, are also not present in mice, limiting the suitability of mice as models to study virus transmission (Belser et al., 2011).

1.1.5 Epidemiology

Understanding the epidemiology of influenza infection is important in the selection of the seasonal vaccine strain. Influenza is highly seasonal, outbreaks in the northern hemisphere begin in late November and last about 12 weeks, first dominated by circulating influenza A then followed by influenza B (Lipsitch and Viboud, 2009). These annual outbreaks are termed epidemics. However, when a new subtype of influenza virus to which the population has no pre-existing immunity has emerged, a pandemic can result. A pandemic can be viewed as a worldwide epidemic, which spreads quickly and affects a large number of people in the world.

Five pandemics caused by the influenza A viruses have been recognized. Among those, the pandemic of 1918-19 caused by H1N1 was the most deadly, killing over 20 million people. The 1918 virus was identified based on serological studies and the complete sequencing of hemagglutinin and neuraminidase from formalin-fixed, paraffin-embedded, lung tissue samples from patients who died of influenza during the pandemic, as well as from a frozen sample obtained by *in situ* biopsy of the lung of a victim buried in permafrost in Alaska since 1918 (Cox and Subbarao, 2000). H1N1 was then replaced by H2N2, and the new serotype emerged to cause the Asian flu pandemic of 1957. In 1968, H3N2 emerged to cause the Hong Kong flu pandemic (Harper et al., 2005; Stephenson and Zambon, 2002). A H1N1 virus that closely resembled viruses that had circulated in the early 1950s re-emerged in the former Soviet Union, Hong Kong and northeastern China in 1977, causing the "Russian" influenza, and since then have co-circulated with H3N2 viruses in the human population (Nakajima et al., 1978). In early 2009, a novel swine-origin influenza A (H1N1) virus emerged from North America. Currently, both H3N2 and H1N1 circulate together in the population.

1.1.6 Treatments: antivirals, current vaccine strategies and universal vaccine

1.1.6.1 Antivirals

The two currently licensed class of drugs for treating influenza virus infection are the M2 blocker adamantanes (amantadine and rimantadine), and NA inhibitors (zanamivir and oseltamivir). Adamantanes are effective against influenza A but not influenza B viruses. However, human

influenza develops resistance to adamantanes rapidly. For instance, circulating 2009 H1N1 virus strains are resistant to adamantanes. Isolates of H5N1 virus from Cambodia, Thailand, and Vietnam have also been found to carry mutations in the M2 protein which makes amantadine ineffective (Cheung et al., 2006; Guan and Chen, 2005; Hurt et al., 2007).

On the other hand, NA inhibitors are active against both Influenza A and B. Oseltamivir is sold under the trade name Tamiflu and is currently the frontline drug recommended by the World Health Organization for treating pandemic influenza (World Health Organization, 2007). Oseltamivir-resistant viruses, although infrequent, have been reported in seasonal H1N1, avian H5N1 viruses and pandemic H1N1 2009 strains, and all of these viruses have a neuraminidase mutation (H275Y). In these patients, zanamivir remains a treatment option (de Jong et al., 2005; Dharan et al., 2009; World Health Organization, 2009).

1.1.6.2 Influenza vaccine

Currently, two distinct influenza vaccines are licensed for use in humans. Both vaccines include antigenic components from three type-specific virus strains updated annually to closely match the dominated circulating strain. The trivalent inactivated influenza vaccine (IAV) is delivered intramuscularly and is standardized according to the hemagglutinin (HA) content. On the other hand, the live attenuated influenza vaccine (LAIV) is a mucosal vaccine delivered intranasally. Both vaccines provide varying degree of protection depends on the age of the recipients and how closely the vaccine is matched to the circulating epidemic strains.

Inactivated influenza vaccine (IAV)

IAV induces neutralizing antibodies against surface proteins HA and NA, thus is strain specific and needs to be updated annually. Most inactivated vaccines are prepared by infecting embryonated chicken eggs with influenza virus vaccine strains. Allantoic fluids of infected eggs are then harvested, followed by purification of the egg-derived virus. IAV contains either the entire whole inactivated virus (whole virus vaccines), virus disrupted by detergents or solvents (split vaccines), or purified HA and NA (subunit vaccines). Anti-HA antibodies inhibit the infectivity of the virus while anti-NA cannot cause sterilizing immunity but reduce disease severity. Serum antibody responses are measured by HI (hemagglutinin inhibition) tests and are used to assess the immunogenicity of the IAV vaccine. At least one of following three requirements must be

met in order for the vaccine to get licensed for use: (i) seroprotection, i.e. achievement of a HI titer of $\geq$ 1:40 in >70% of subjects; (ii) seroconversion, i.e. a $\geq$ 4-fold increase in HI antibody titer, reaching a titer of $\geq$ 1:40 in > 40% of subjects; and (iii) a > 2.5-fold increase in geometric mean titers (GMTs), according to the criteria of the European Union Committee for Human Medicinal Products and the European Centre for Disease Prevention and Control with regard to interpandemic and prepandemic influenza vaccines (Committee for Proprietary Medicinal Products - European Agency for the Evaluation of Medicinal Products, 1997).

IAV is licensed for almost everyone except for infants younger than 6 months old, or those allergic to eggs or a previous vaccination. The effectiveness of this vaccine approach depends on the age of the recipients, with the elderly and children responding poorer than adults. The inactivated vaccine could be less immunogenic in a population naive to the virus. The standard dose of a seasonal vaccine is one dose of 15 µg HA; however, in the clinical development of a vaccine against avian H5N1 virus, to which the population was naïve, two 30 µg doses of vaccine were still unable to generate an antibody response in adults, highlighting the important role of initial priming of the immune response in generating immunogenicity (Bresson et al., 2006).

The immunogencity of a vaccine can be improved by the use of an adjuvant. Adjuvants function by enhancing the time the antigen is seen by the immune system, facilitating the delivery of antigen to antigen-presenting cells, or by providing immunostimulatory signals to improve efficacy. Aluminum hydroxide ("Alum") adjuvant has been employed in influenza vaccines but its effectiveness has been doubtful (Bresson et al., 2006). The adjuvant Fluad (Novartis), which was licensed in 1997, contains the component MF59 (O'Hagan et al., 2007). It is an oil-in-water sub-micron emulsion prepared with cholesterol metabolite squalene and has a good overall safety profile. Studies suggest that MF59 exerts its effect through a TLR-independent pathway: by attracting effector cells into the muscles at the injection sites through induction of chemokines. It also allows muscle fibers and mononuclear cells to produce a local environment that induces the differentiation of monocytes into DCs, and promotes antigen uptake by dendritic cells by upregulating the expression of a variety of relevant genes (Mosca et al., 2008; Seubert et al., 2008). The main feature of MF59 is its ability to induce and enhance the breadth of long-lasting T- and B- cell responses against the virus. Studies have shown that MF59 increases the cross-reactivity of the antibody response and the antibody titers, and sparing the amount of antigen needed to elicit a protective response (Baras et al., 2008; Stephenson et al., 2008).

The H5N1 vaccine adjuvanted with MF59 increased antibody levels and was able to generate a virus-specific $CD4^+$ T cell response (Galli et al., 2009). Other variants of squalene-based adjuvants for use in influenza vaccine are AS03 included in Pandemrix (GlaxoSmithKline) (Roman et al., 2010) and AF03 included in Humenza (Sanofi-Pasteur) (Levie et al., 2008).

Live attenuated influenza vaccine (LAIV)

LAIV is a trivalent vaccine produced by genetic reassortment between a wild-type virus and attenuated master donor viruses. The master donor viruses (A/Ann Arbor/6/60 and B/Ann Arbor/1/66) acquired the phenotype of cold-adapted (*ca*) (replicate efficiently at 25°C), temperature-sensitive (*ts*) (restricted in replication at 37°C or 39°C), and attenuated (*att*) (do not produce influenza-like illnesses) by having multiple mutations in the internal protein gene segments, after serial passage at sequentially lower temperatures in specific pathogen-free primary chicken kidney cells (Murphy and Coelingh, 2002). Each LAIV vaccine virus harbours two gene segments encoding the hemagglutinin and neuraminidase from the wild-type virus, and the remaining six-gene segments encode proteins responsible for temperature sensitivity and attenuation, thus a 6:2 reassortment. This live virus is not able to replicate in the lower respiratory tract and the lung, but is able to replicate efficiently in the ciliated epithelial cells of the nasopharyngeal mucosa to induce immune responses, which mimics those generated in a natural infection.

FluMist, a LAIV, was first licensed for human use in 2003 (Plotkin, 2008). Currently, it is licensed for healthy, non-pregnant individuals aged 2 to 49 years old. It is not licensed to children under 2 because of concerns over excess hospitalization and wheezing (Belshe et al., 2008; Bergen et al., 2004), or to those over 50 because of the failure to demonstrate efficacy (Ambrose et al., 2008; Belshe et al., 2008; Block et al., 2008). Comparing the IAV and LAIV in a meta-analysis in all age groups revealed no significant difference in overall reactogenicity or efficacy and the ability to protect against drifted strains between the two (Beyer et al., 2002). However, the efficacy of LAIV and the durability of protection induced by LAIV appeared to be greater in children in a meta-analysis of various studies (Rhorer et al., 2009). Moreover LAIV appeared to be more efficacious among subjects who have limited exposure to influenza vaccination, compared to those who were immunized annually (Eick et al., 2009; Wang et al., 2009). It is important to note that, unlike IAV, no immune correlate of protection has been

established for LAIV, and they protect without eliciting any serum HI titers (Ambrose et al., 2008).

1.1.6.3 Universal vaccine

The current vaccination strategies of IAV aimed at inducing neutralizing antibodies are strain-specific and can not offer long lasting protection against antigenic drifting strains and emerging pandemic viruses. A promising direction of vaccine research would be to develop an influenza vaccine that targets an "universal" or conserved antigen that is essential for virus function. Such vaccine could provide heterosubtypic immunity and could prevent another pandemic. Also, a vaccine that provides long-acting protection is of great need as the current seasonal influenza vaccines appear to be less effective in elderly population as the capacity of their immune system wanes (Osterholm et al., 2012). Promising candidate T- cell antigens for an universal vaccine include conserved antigens: NP and M1; while antibody targets include the stalk and the nonglobular portions of HA and M2 moieties (Hamad, 2011; Kang et al., 2011). Heterosubtypic immunity offered by T cells, although incapable of neutralizing the virus, could control the course of infection by facilitating clearance of the virus and eliciting cellular immune responses that are cross-protective across subtypes.

1.2 Immune responses to influenza A infection

1.2.1 Innate immune response

The first line of defence against influenza A viruses is led by the innate immune system, which unlike adaptive immune responses, lacks specificity and memory. Innate immune cells, such as natural killer (NK) cells, alveolar macrophages and dendritic cells are involved in the control of viral replication and regulation of adaptive immune responses following an infection (McGill et al., 2009). Immune responses are initiated upon the recognition of pathogen-associated molecular patterns (PAMPs), such as viral nucleic acids, by pattern recognition receptors (PRRs) (Schmolke and Garcia-Sastre, 2010). These receptors include: 1) the Toll-like receptors (TLR)-3, -7/8 and 9 which recognize double stranded RNA, single stranded RNA and CpG motifs respectively; 2) the retinoic acid inducible helicase RIG-I, which recognize cytoplasmic 5'-triphosphates

on single-stranded RNA and 3) the NOD (Nucleotide Oligomerization Domain receptors)-like receptors [reviewed in (Ehrhardt et al., 2010; Wolff and Ludwig, 2009)].

When influenza virus infects respiratory epithelial cells or the alveolar macrophages, the single-stranded RNA genome of the virus is recognized by TLR-7 and RIG-I. NK cells fight influenza primarily through NKp46-mediated recognition (Mandelboim et al., 2001). The downstream signalling pathways activate the immune cells to release proinflammatory cytokines and chemokines are also released in order to attract and activate more immune cells from the peripheral blood to the site of infection via the vascular endothelium. Among the cytokines released, type I interferons (IFN) IFN-α and IFN-β are the most potent. IFN stimulation induces transcription of several IFN-responsive genes, many of which can protect uninfected cells from an infection (Ehrhardt et al., 2010).

The NS1 protein of the virus, however, evades the host immune responses by antagonizing IFN response by inhibiting transcription factors such as ATF-2/c-Jun, NF-$\varkappa$B, and IRF-3/5/7. NS1 works by binding to the double-stranded RNA, thereby inhibiting the action of dsRNA-activated of $2'$-$5'$ oligo(A) synthetase and the subsequent activation of RNase L, which is involved in the innate immune response (Neumann et al., 2009b). NS1 inhibits the functions of the tripartite motif (TRIM)25 in the ubiquitination of RIG-1, which is essential in the type I IFN response. NS1 also binds to the protein kinase R (PKR), an antiviral protein. The NS1 gene of H5N1 viruses, on the other hand, contains several amino acid mutations which confer resistance to the antiviral effects of IFN, and at the same time allows the continued production of high levels of pro-inflammatory cytokines and subsequent lung pathology (Peiris et al., 2004). A recent study showed that NS1 protein of H3N2 carried a histone-like sequence which allowed the virus to bind to human transcriptional elongation complex PAF1C (hPAF1C), a key mediator of antiviral and pro-inflammatory gene expression. Thus NS1 interferes with the host transcriptional machinery and suppresses the antiviral responses (Marazzi et al., 2012).

On the other hand, a regulatory mechanism also exists in the lungs. CD200 is a glycoprotein expressed on the cell surface of the respiratory epithelial cells, and CD200 receptor (CD200R) is expressed by myeloid cells including macrophages and dendritic cells. CD200R expression on alveolar macrophages is maintained by IL-10 and TGF-β when the lungs are uninfected. However, in lungs infected by influenza, CD200 is upregulated on alveolar macrophages by TNF-α and IL-6. Studies using a CD200 knockout mouse found that CD200 activated CD200R activation

resulted in an inhibition of recruitment of immune cells, hence the production of inflammatory cytokines. This negative feedback loop maintains the homeostasis of the respiratory immune system (Snelgrove et al., 2008)

However, innate immunity is like a two-edged sword in the pathogenesis of influenza infection. The unregulated and excessive response of proinflammatory cytokines and chemokines can lead to severe and detrimental lung inflammation. Highly pathogenic viruses such as avian H5N1 are thought to induce a cytokine storm, characterized by an inflammatory infiltrate and dysregulation of inflammatory cytokines, which in turn, mediates lung pathology following an infection (Peiris et al., 2009a). For instance, high serum levels of IL-6, TNF-α, IFN-γ and sIL-2R and elevated serum levels of chemokines IP-10, MCP-1 and monokine induced by IFN-γ (MIG) were found in patients infected with H5N1 in the outbreaks in Vietnam and Hong Kong (La Gruta et al., 2007).

1.2.2 Adaptive immune response

1.2.2.1 Humoral immune response

Adaptive immunity, which includes antigen-specific antibodies and T cells, provides essential protection from influenza infection and prevents re-infections. RAG -/- mice that are immunodeficient of B cells or T cells are highly susceptible to influenza infection (Jayasekera et al., 2007). The adaptive immune response to influenza A viruses contains both humoral and cellular components. The role of humoral immunity in influenza infection was highlighted in the 2009 H1N1 pandemic, when the virus disproportionately affected children and young adults, sparing the older population. It suggests a partial immunity to the virus in the elderly population; indeed, 34% of subjects who were over the age of 60 were shown to have pre-existing cross-reactive antibodies to A (H1N1) 2009, compared to only 4% in subjects who were born after 1980 (Hancock et al., 2009).

Antiviral responses to influenza by B cells are mainly via the production of antibodies. Distinct B cell subsets with different immunoglobulin repertoires produce a multifaceted humoral response that generates protective antibodies both locally and systemically. Within human peripheral blood mononuclear cells (PBMCs) there are ~5-20% B cells, among which approximately 30-50% are $CD27^{+}$, denoted as memory B cells (MBCs), while the others are naïve B cells. Naïve B

cells interact with antigen in the secondary lymphoid organs and develop into antigen-specific memory cells. Primed B cells interact with T follicular helper cells, a T cell subset specialized in providing B cell help, and differentiate along two different pathways in the secondary lymphoid organs. B cells can differentiate into extrafollicular short-lived plasmablasts that are important for rapid antibody production (MacLennan et al., 2003). Alternatively, they can enter the germinal centre and differentiate into antibody-secreting plasma cells (ASCs) to secret antibodies and undergo affinity maturation, or to become MBC, which confer long-term protection against the pathogen (MacLennan, 1994). ASCs are the main source of serum antigen-specific antibodies (Ab). Primary and secondary immune responses generate these long-lived ASCs in the spleen, which then migrate to the bone marrow and persist throughout life. MBCs circulate between the peripheral blood and secondary lymphoid organs, and are capable of rapid proliferation and differentiation into ASC when they re-encounter the same pathogen in a secondary response. The marrow plasma cell pools are replenished from the pool of MBCs when depleted, maintaining long-lived antibody production (LeBien and Tedder, 2008). B cells can also be activated independent of T cell help, by bacterial capsular polysaccharides and microorganism-derived TLR ligands. For example, B-1 cells, a subset of specialized B cells, constitutively produce natural virus-binding immunoglobulin M (IgM) in the absence of antigens (Choi and Baumgarth, 2008).

In influenza infection or vaccination, B cells residing within the respiratory tract are activated when their B cell receptors engage with influenza virus antigens, becoming primed and differentiate into ASC. Recent studies in humans found that plasmablasts highly enriched for influenza-specific antibody secreting cells, appear in blood within 7 days postinfection or vaccination with influenza [(He et al., 2010; Sasaki et al., 2007; Wrammert et al., 2008) and personal communication with Dr. A. Huang]. The major sites of B cell responses are the local draining lymph nodes. IgG and IgA memory B cells to influenza are strongly induced locally in the respiratory tract, whereas effectors spread systemically and thus memory B cells appear to distribute more widely and are maintained for many months in about every tissue. ASCs are maintained by the bone marrow and the lung microenvironment, thus they both contribute to the long-term maintenance of specific IgG and IgA Ab production after influenza virus infection of mice and humans (Joo et al., 2008). For instance, cross-protective Abs to the pandemic H1N1 2009 virus were found in up to 96% of people born between 1909 and 1919 (Ikonen et al., 2010).

Neutralizing antibodies, produced by plasma cells, are directed primarily against the viral surface glycoproteins HA and to a lesser extent NA. For protection against influenza viruses, antibody of isotypes IgG, IgM and IgA are important. Secretory IgA prevents infections at the mucosal epithelial of the upper airway at the time of virus exposure thus providing sterilizing immunity (Swain et al., 2006); however, due to technical difficulties in quantifying IgA at mucosal surfaces the protective role of IgA in influenza infection is unclear. Serum IgG against HA, on the other hand, correlates well with protection (Plotkin, 2010) and is used as a surrogate marker for influenza vaccine licensing.

Protection from influenza infection is mediated by anti-HA antibodies which effectively neutralize virus infectivity *in vitro* and *in vivo* (Gerhard et al., 1997). The structure of HA consists of a globular head that mediates virus attachment to target cells, and a stem domain that is relatively stable and conserved (**Fig. 1.3**). Current vaccine strategies induce neutralizing antibodies to bind to exposed loops surrounding the receptor binding sites of the HA globular head receptor-binding domain and restrict viral entry into the host cells, preventing infection. These loops undergo periodic structural changes thus antibodies against them are strain-specific. The receptor binding sites are also relatively small which limits the conserved footprint that can be specifically recognized by an antibody to acquire cross-reactivity against different strains (Burton et al., 2012). Some neutralizing anti-HA antibodies have also been shown to block viral- cell membrane fusion at a concentration where receptor binding is not blocked *in vitro* (Knossow and Skehel, 2006; Skehel, 2009). In contrast to anti-HA, anti-NA antibodies work by reducing the efficient release of virus from the infected cells. Anti-NA antibodies are more difficult to quantify though recently assays have been developed which allow NA inhibition titers to be measured (Hassantoufighi et al., 2010).

Antibodies appear one to two weeks following vaccination, peak at 4 weeks after infection, then decline thereafter (Waffarn and Baumgarth, 2011). The current inactivated subunit influenza vaccines, which WHO formulates annually based on serological and epidemiological studies, elicit sufficient antibody responses to prevent the disease (Castellino et al., 2009). Serum HA-inhibiting titers of 1:40 or greater are supposed to confer protection against an infection. Although effective in protecting an individual upon exposure to a homologous virus, such protection will be ineffective against variants or a new subtype in which HA and NA are antigenically distinct.

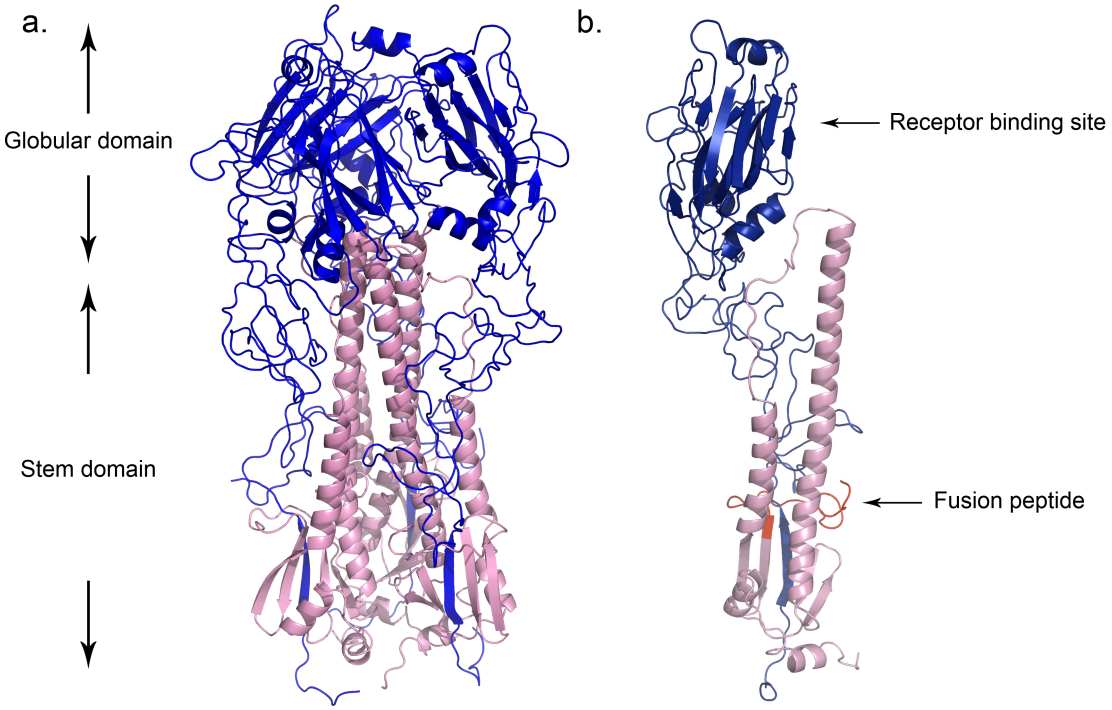

Figure 1.3 Influenza hemagglutinin. (a) Structure of hemagglutinin, which is a trimeric glycoprotein. The three HA1 chains making up the globular domain are coloured blue, and three HA2 chains making up the stem domains are coloured pink. **(b)** Structure of a hemagglutinin monomer. Each monomer is made up of HA1 (blue), which is the receptor binding domain and contains the sialic acid binding site, and the relatively conserved HA2 (pink) constitutes the stem domain including the fusion peptide (red). The receptor binding site and fusion peptide are as indicated. Broadly neutralizing antibodies can block receptor engagement, virus attachment or membrane fusion. Figure was generated and rendered using MacPyMol (DeLano Scientific) using PDB file 2HMG.

Antibodies that recognize multiple influenza subtypes have also been discovered. A panel of monoclonal antibodies against the ectodomain of M2 protein, M2e, were isolated and shown to be protective. M2e is more highly conserved than either HA and NA, thus making it a plausible target for induction of broadly protective mAbs (Grandea et al., 2010). Antibodies targeting the stem region of HA can also potentially induce cross-reactive immunity. Recently, novel broadly neutralizing antibodies that protect animals against influenza have been described. Ekiert *et al.* (Ekiert et al., 2011) describe an antibody CR8020 that is able to neutralize influenza A group 2 (but not group 1) subtypes and protects mice against virus challenge. Corti *et al.* (Corti et al., 2012) isolated another human antibody, FI6, using high-throughput screening of immortalized antibody-secreting cells. This antibody is able to recognize all 16 HA subtypes using both heavy and light chains. Both antibodies bind to highly conserved epitopes at the HA stem, and work by inhibiting conformational changes in HA and thereby blocking membrane fusion and viral entry. Broadly neutralizing antibodies that target the head region of HA around the receptor binding site have also been described (Krause et al., 2011a; Krause et al., 2011b; Whittle et al., 2011). A

recent study shows that such antibodies can bind the virus in a highly focused way with a single loop, which allow antibodies to avoid the hypervariable regions but target the small, conserved functional sites (Ekiert et al., 2012).

1.2.2.2 Cellular immune response

The milder nature of the 2009 pandemic compared to other pandemics could be due to the cross-reactive cellular immunity to the virus in the population. There is considerable sharing of T cell epitopes between the H1N1 2009 virus and the seasonal H1N1 influenza virus strains. Based on the information in the Immune Epitope Database, epitopes recognized by $CD8^+$ T cells were most frequently conserved, followed by $CD4^+$ T cells epitopes, then B-cell epitopes (Greenbaum et al., 2009b). This highlights the importance of targeting T-cell immunity in the design of a vaccine against influenza. It will be essential to better understand the generation and maintenance of effective memory T cell responses during influenza infection in order to devise an optimal vaccine strategy. T cells are derived from precursors in the hematopoietic tissues, undergo differentiation in the thymus and then migrate to the peripheral lymphoid tissue and the circulating pool of lymphocytes. T cells express CD3 and antigen-binding receptors called T-cell receptors (TCR). The majority of T cells express receptors made up of α and β chains, and others express receptors bearing the γ/δ chains. The γ/δ T cells consist of about 10% of PBMC in humans (Re et al., 2005). In humans, α/β T cells and γ/δ T cells differ in their contribution in immune responses. Among the α/β T cells are two important lineages of T cells involved in the adaptive immune responses, those that express CD4 co-receptor ($CD4^+$ T cells), and CD8 co-receptor ($CD8^+$ T cells). These cells differ in their ways of recognizing antigens and mediating effector functions. During influenza infection, both $CD4^+$ and $CD8^+$ T cells mediate control (Woodland, 2003).

Influenza-specific T cells are thought to promote viral clearance and enhance recovery via the production of pro-inflammatory cytokines and the direct lysis of virally infected cells. T cell responses are initiated when lung resident dendritic cells acquire antigens from invading virus and migrate to the draining lymph nodes (cervical and mediastinal). In the lymph nodes, antigens are presented by the mature dendritic cells to naïve T cells. Antigen-specific T cells are primed, activated and proliferate, then acquire effector functions and migrate to the site of infection (respiratory epithelium) where they mediate their antiviral effects. Once the virus is cleared, the

effector T cell population contracts, leaving a pool of long-lived and antigen-specific memory T cells capable of inducing a rapid secondary response.

$CD4^+$ T cells

The primary roles of $CD4^+$ T cells are to provide help to $CD8^+$ T cells and to early clonal expansion of B cells. Their helper function depends on the expression of the activation marker CD154 and an array of cytokines they secrete upon activation. $CD4^+$ T helper cells promote the generation of virus-specific $CD8^+$ cytotoxic T cells. They also promote the initiation and maintenance of germinal centre reactions, somatic hypermutation and the generation of antigen-specific long-lived plasma cells and MBCs (Allen et al., 2007; Lanzavecchia, 1985). Cytotoxic $CD4^+$ T cells capable of killing virally infected cells directly have also been described in chronic viral infection (Appay et al., 2002b; Landais et al., 2004; Norris et al., 2004; van Leeuwen et al., 2004). Antigen-specific $CD4^+$ T cells capable of producing multiple cytokines are also found to be superior to single cytokine producers, and their capacity to produce cytokines is associated with their other functional characteristics (Kannanganat et al., 2007).

Effector $CD4^+$ T cells are very diverse and are often characterized by plasticity and heterogeneity in terms of their cytokine profile (**Fig. 1.4**). They can be further subdivided into at least Th1, Th2, Th17 or Tfh (Sallusto and Lanzavecchia, 2009; Zhu and Paul, 2008; Zhu and Paul, 2009; Zhu and Paul, 2010; Zhu et al., 2010). Differentiation of $CD4^+$ T cells is controlled by expression of unique lineage-specific master regulator transcription factors: T-bet for Th1, GATA3 for Th2, retinoic-acid-receptor-related orphan receptor-γt (ROR-γt) for Th17, Foxp3 for Treg and Bcl-6 for Tfh subsets (Sallusto and Lanzavecchia, 2009; Zhu and Paul, 2008; Zhu and Paul, 2009; Zhu and Paul, 2010; Zhu et al., 2010).

Upon antigenic stimulation, naïve $CD4^+$ T cells can differentiate to these different effectors to mediate protection against different pathogens. Type I effector Th1 cells predominately produce IFN-γ that promotes clearance of viruses and intracellular bacteria, as well as IL-2 and TNF-α. Th2 cells produce IL-4, IL-5 and IL-13 that promote clearance of helminths and extracellular parasites. Th17 responses control fungal infections and represent a link between innate and adaptive immunity. They recruit effector cells to inflamed mucosal sites by inducing the production of chemokines. Recently, studies on different respiratory pathogens including influenza viruses suggested that IL-17 secreting Th17 cells are important in lung mucosal defense

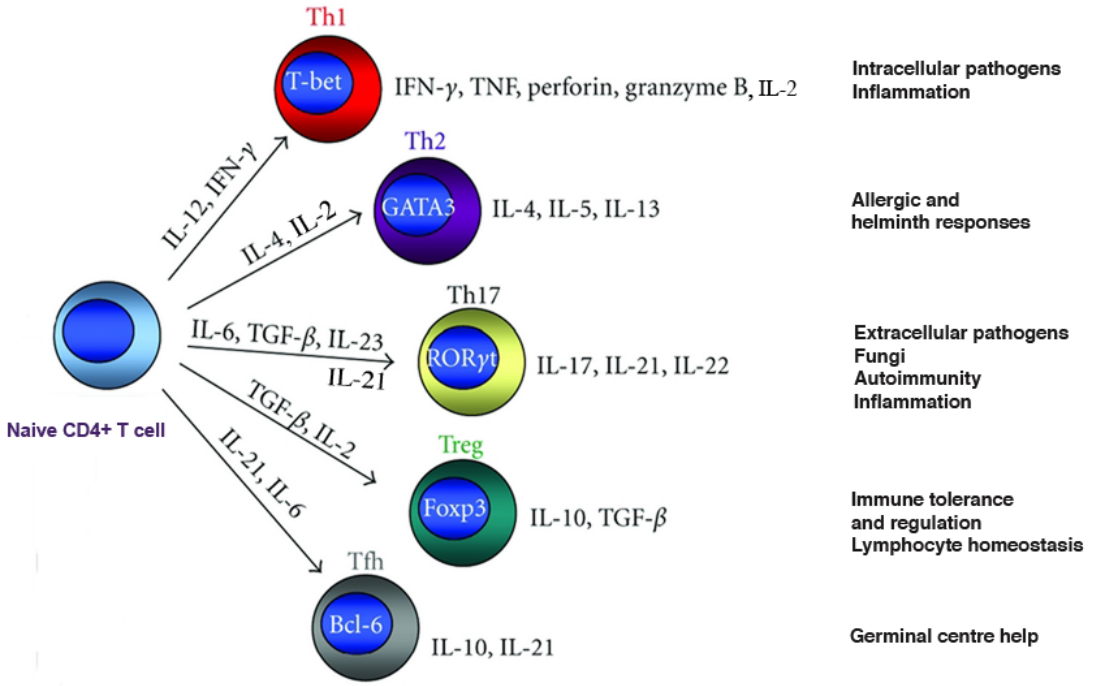

Figure 1.4 CD4⁺ T cell effector subsets. Naïve CD4⁺ T cells can differentiate into distinct effector T helper subsets upon encountering antigens, determined in part by the polarizing cytokine factors that are present. Effector subsets (Th1, Th2, Th17, Treg and Tfh) are classified by cytokine profiles, expression of transcription factors and chemokine receptors, and functional attributes. Bcl-6, B-cell lymphoma 6; CXCR, CXC receptor; Foxp3, Forkhead box p3; IFN, interferon; GATA3, Trans-acting T-cell-specific transcription factor; ROR, retinoic acid-related orphan receptor; T-bet, T-box-expressed-in-T-cells; Tfh, T follicular helper; TGF, transforming growth factor; Th, T helper; Treg, regulatory T [modified from (Marshall and Swain, 2011)].

against respiratory pathogens, e.g. by promoting secretion of IgA in the airway lumen (Jaffar et al., 2009). Influenza-specific Th17 cells during IL-10 deficiency can protect naïve mice after lethal influenza challenge (McKinstry et al., 2009). Cellular immune responses can be induced by an influenza vaccine adjuvanted by cationic adjuvant formulation (CAF01) which induced Th17 cells in mice (Rosenkrands et al., 2011).

T follicular helper cells (Tfh) (**Fig. 1.5**) represent a subset of CD4⁺ T cells involved in helping B-cell response in germinal centres (GCs) within secondary lymphoid organs (Crotty, 2011; King, 2011). GCs are discrete structures that develop within B cell follicles of secondary lymphoid organs following antigenic stimulation, in which the processes of B cell affinity maturation, class switch recombination, plasma cell differentiation and memory B cell differentiation occurs (Vinuesa et al., 2005). Tfh cells express markers such as chemokine (CXC-motif) receptor 5 (CXCR5), which allow them to respond to the specific ligand CXCL13, a chemokine that is secreted by follicular stromal cells, and home to follicles (Cyster et al., 2000; Schaerli et al., 2000). Tfh also expresses other surface markers that are essential for helper function, such as

CD40-ligand (CD40L), inducible co-stimulator (ICOS) and Programmed Death-1 (PD-1) (King et al., 2008). They secrete IL-4, IL-10 and IL-21 that are important for development of B cells and to promote antibody production (Ettinger et al., 2005; Good et al., 2006; Pene et al., 2004). Tfh generation is controlled by the balance of two transcriptional repressors, the expression of B cell lymphoma 6 (Bcl-6), which is necessary for the development of Tfh (Chtanova et al., 2004; Rasheed et al., 2006; Yu et al., 2009), and the expression of B lymphocyte-induced maturation protein 1 (Blimp-1), which regulates the function of Bcl-6 and inhibits the generation of Tfh cells (Johnston et al., 2009). Recent identification of cells with Tfh lineage markers and functional activity in the peripheral blood of humans suggests that it may be possible to use this subset of $CD4^+$ cells as a biomarker for assessing vaccine responses (Chevalier et al., 2011; Morita et al., 2011). Understanding Tfh function is essential to rational vaccine design, as nearly all licensed human vaccines protect on the basis of protective T cell-dependent antibody responses.

$CD8^+$ T cells

Effector functions of $CD8^+$ T cells include granule-mediated cytotoxicity, which involves perforin and granzymes, expression of Fas ligand (CD95L) to induce apoptosis in a Fas-Fas ligand dependent manner, and the production of pro-inflammatory cytokines including IFN-γ and TNF-α (Topham et al., 1997; Fujimoto et al., 1998; Trapani and Smyth, 2002). $CD8^+$ T cells recognize infected target cells through MHC Class I molecules bearing viral peptides, and lyse target cells directly before the release of progeny virus. The viral load is hence reduced for the subsequent neutralization by the developing antibody response. Granzyme B production has been shown to correlate with clinical symptoms in human influenza infections (McElhaney et al., 1998). Similar to that of $CD4^+$ T cells, specific cytokines direct the fates that effector $CD8^+$ T cells can adopt: T-bet expressing Tc1 required IL-12 while GATA-3 expressing Tc2 require IL-4 (Sad et al., 1995). IL-17- producing CD8 T cells (Tc17) have also been described (Huber et al., 2009) and are found in lungs in response to primary challenge with influenza (Hamada et al., 2009). The pattern of $CD8^+$ effector function may relate to the differences in antigen presentation of different pathogens. For instance HIV-specific T cells deficient in cytotoxicity produce antiviral cytokines efficiently (Appay et al., 2000). In other studies, EBV-specific T cells exhibit inverse relationships between cytotoxicity and secretion of Tc2 cytokines IL-4 and IL-10 (Nazaruk et al., 1998). $CD8^+$ T cells are associated with protective antiviral immunity in different viral infections (Duvall et al., 2008; Nemes et al., 2010; Seder et al., 2008). Immunization with

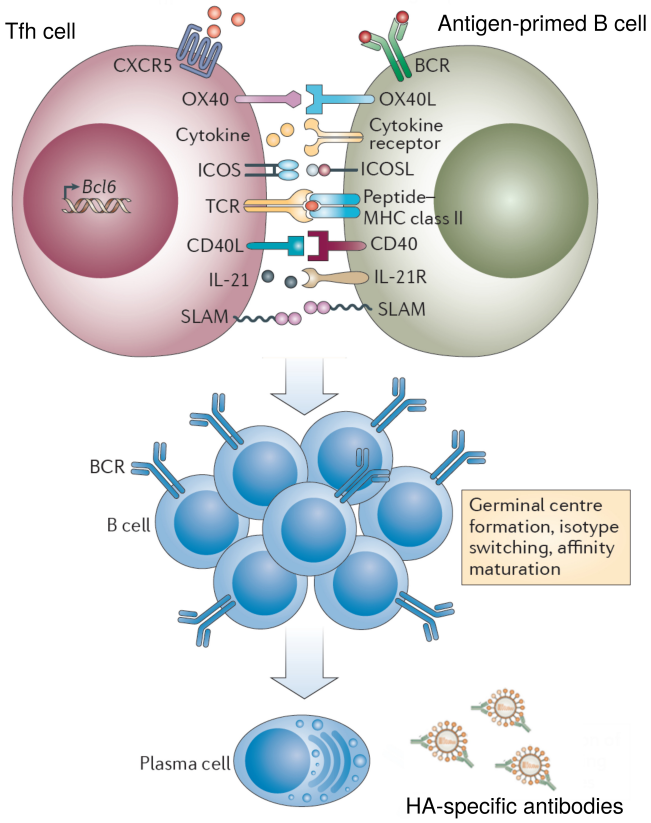

Figure 1.5 T follicular helper (Tfh) cells. T follicular helper (Tfh) cells are a specialized subset of $CD4^+$ T cells that provide help for B cells in germinal centre formation, isotype switching and affinity maturation of antibody responses. Signalling of activated $CD4^+$ T cells through TCR, ICOS and IL-21 receptor (IL-21R) leads to the expression of cell surface molecules that are important for migration and T cell–B cell interactions, such as CXC-chemokine receptor 5 (CXCR5), ICOS, CD40 ligand (CD40L), OX40 and signalling lymphocytic activation molecule (SLAM) family members. T cell help to B cells support the selection of activated antibody-secreting plasma cells in germinal centres and the generation of neutralizing antibodies, which is crucial in protecting against many viral pathogens including influenza. BCL-6, B cell lymphoma 6; BCR, B cell receptor; CXCR5, CXC-chemokine receptor 5; ICOS, inducible T cell co-stimulator; ICOSL, ICOS ligand; IL-21R, IL-21 receptor; L, ligand; SLAM, signalling lymphocytic activation molecule; TCR, T cell receptor [modified from (McHeyzer-Williams et al., 2012; Swain et al., 2012)].

the smallpox vaccine vaccinia, which elicits an immune response similar to that of an acute infection, also induced polyfunctional $CD8^+$ T cells, suggesting that they may be an important correlate of protection (Precopio et al., 2007). In long-term nonprogressors of HIV infection, HIV-specific polyfunctional $CD8^+$ lymphocytes are present at a higher frequency than patients with progressive disease (Betts et al., 2006; Harari et al., 2007).

1.2.2.3 Assessment of T cell-mediated immunity to influenza in animal models

Although mice are not as good as ferrets as a model for influenza infection, the abundance of reagents for murine studies (inbred, transgenic, knockouts) allow scientists to study the properties of the T cell response in viral immunity using influenza model. During primary

influenza infection, the cellular immune response peaks at day 10 after infection, while it peaks at day 8 following a secondary challenge (Thomas et al., 2006a). On the other hand, the recall responses in lungs are comprised of several phases. The first phase is mediated by memory T cells that are resident in the lung airways. These T cells produce cytokines to limit viral replication and spread in the epithelium. The second phase is mediated by T cells that are rapidly recruited to the airway in the first few days of the response. In the final stage, memory T cells in the secondary lymphoid organs undergo an antigen-driven expansion, and are then recruited to the lung airways after 5 days of infection (Woodland and Randall, 2004). In mice, influenza infection induces strong Th1 responses, which is thought to provide protective immunity, although Th2 cytokines (IL-4, IL-5, IL-6 and IL-10) have also been found in lungs of infected animals. Influenza-specific $CD4^+$ cells provide cognate help for antibody production, and to $CD8^+$ T cells through direct cell-cell interactions, via antigen-presenting cells, or via production of cytokines. Both primary and the recall $CD8^+$ T cells responses are diminished in Ig(-/-) μMT mice lacking $CD4^+$ cells (Riberdy et al., 2000). Size of the memory pool and the magnitude of the recall responses were also significantly reduced in the absence of $CD4^+$ T cell help (Belz et al., 2002). Transfer of virus-specific memory $CD4^+$ T cells to naïve animals before influenza infection enhanced innate inflammatory responses that contributed to viral clearance, by upregulating pulmonary and systemic levels of several pro-inflammatory mediators including IFN-γ, IL-12, IL-1 and IL-6 etc. (Strutt et al., 2010).

A large amount of data supports the roles of $CD8^+$ T cells in reducing the severity of the disease and promoting recovery upon an infection. $CD8^+$ T cells are able to mediate direct cell lysis via perforin or Fas-L dependent pathway (Topham et al., 1997). Reduction in viral load and protection in mice correlated with $CD8^+$ responses (Yap et al., 1978). Antigen-specific $CD8^+$ T cells expressed multiple cytokines in a hierarchical manner as they differentiate, as CTLs first produce IFN-γ, followed sequentially by TNF-α, then IL-2 (La Gruta et al., 2004). T cells also play a role in maintaining the homeostasis of the respiratory immune system. IL-10 producing effector $CD8^+$ T cells, which are enriched in the respiratory tract, controls lung inflammation by producing IL-10, a major regulatory cytokine, during acute lung infection in influenza (Sun et al., 2009).

1.2.2.4 Assessment of T cell mediated immunity to influenza in humans

In contrast to mice, human studies of T cell-mediated protection in influenza are more difficult as the readout of responses is taken at the periphery, and it is not easy to obtain blood samples at the onset of a human acute infection. Thus knowledge comes from epidemiological evidence where those surveillance studies require large numbers of people to obtain statistical power. Human challenge studies, however, can provide a lot of useful information with a smaller number of samples. Asymptomatic infections are common after excluding those with pre-existing hemagglutination inhibiting antibodies to the challenge strain from a meta-analysis of a number of human challenge studies (Carrat et al., 2008). In the absence of antibody protection, T cells can confer partial protection against the virus by promoting viral clearance and reducing disease severity (McMichael et al., 1983b; Yap et al., 1978). Pre-existing influenza-specific T cell cytolytic activity has been found to correlate with enhanced virus clearance upon subsequent intranasal challenge with live virus, even in the absence of antibodies to HA and NA (McMichael et al., 1983). In one study, some individuals still had detectable CTL responses at the end of 5-year study in a period of low influenza prevalence (McMichael et al., 1983a), showing that harnessing longevity of T-cell memory maybe useful for control of influenza. A study in the elderly population showed cellular immune responses correlate with protection in the absence of strong serum Ab responses (McElhaney et al., 2006).

Most adults have circulating memory T cells and the persistence of these populations could protect against subsequent infections. The emergence of the 2009 H1N1 pandemic virus (pH1N1) especially highlighted the protection mediated by T cells. PBMCs isolated from 2007, before pH1N1 emerged, showed cross-reactivity with pH1N1 sequences in ELISpot assay (Greenbaum et al., 2009a). Cross-reactivity with pH1N1 antigens is observed even in peptides which differ from their seasonal homologues (Ge et al., 2010). Taken together, T cell immunity may be important in protection against disease especially in promoting early viral clearance and providing cross-protection.

1.2.3 T cell-mediated immunity in influenza A infection

In order to further understand the immune responses to influenza, it is necessary to gain insight into what controls the specificity and diversity of T- cell epitopes upon infection and vaccination

with this virus. Antiviral responses elicited by T cells have several important features that can determine the outcome of an infection.

1.2.3.1 Antigen presentation and activation of T cells

T cells recognize processed peptide antigens that are presented on antigen-presenting cells. $CD8^+$ and $CD4^+$ T cells are primed and activated when they recognize fragments of antigens (peptides) associated with major histocompatibility complex (MHC) class I and II molecules respectively. The process of antigen degradation and peptide loading onto MHC molecules occurs intracellularly in antigen presenting cells (APC), such as dendritic cells (DC). These APCs migrate to the lymph nodes and present foreign antigens to T cells that bear a wide array of T cell receptors. In fact, the observation that influenza A virus-specific CTLs are cross-reactive, and specifically recognize target cells expressing peptides derived from relatively conserved nucleoprotein led to the discovery of the molecular basis of T cell recognition in the 1980s (Bastin et al., 1987; Townsend et al., 1985).

$CD8^+$ T cells recognize virally infected cells that display on their surface MHC Class I presenting peptides 8-10 amino acids long derived from viral proteins. MHC Class I molecules consist of a polymorphic heavy chain (alpha chain), encoded by three genes (*HLA-A, HLA-B* and *HLA-C*) in humans, in conjunction with an invariant light chain known as β2-microglobulin. They are expressed by all nucleated cells to present endogenous peptides. Most peptides to be loaded on MHC class I molecules are generated by proteosome degradation of newly synthesized ubiquitinated proteins. The resulting peptide fragments are transported to the endoplasmic reticulum (ER) by the transporter associated with antigen presentation (TAP) complex, and are loaded on nascent MHC class I molecules under the control of a peptide-loading complex composed of several ER resident chaperons (including tapasin, calnexin, calreticulin, ERp57). The MHC class I molecules loaded with peptides are then rapidly transferred via Golgi apparatus to the plasma membrane to present to the T cells. This is known as the classical Class I pathway (Neefjes et al., 2011; Vyas et al., 2008). However, in some circumstances, antigens from the extracellular environment can be presented to the $CD8^+$ T cells in a process called cross-presentation (Bevan, 1976). In this process, professional APCs acquire proteins from other tissues via endocytic mechanisms, e.g. phagocytosis and macropinocytosis. The internalized antigens are then processed and presented on the MHC class I molecules.

On the other hand, $CD4^+$ T cells respond to peptides of 12-18 amino acids long that are derived from the endocytic pathway (internalized or membrane proteins) and are bound to MHC-class II molecules. MHC class II molecules are primarily expressed by professional APCs such as DCs, macrophages and B cells. However, expression of MHC class II molecules can also be induced in non-APCs which include fibroblasts, endothelial cells and epithelial cells (Bland, 1988; Geppert and Lipsky, 1985), by IFN-γ and other stimuli, under the control of the MHC class II transactivator (CIITA) (Neefjes et al., 2011). MHC class II molecules are encoded by three polymorphic genes (*HLA-DR, HLA-DQ* and *HLA-DP*) in humans. In the ER, MHC class II α- and β- chains associate with the invariant (Ii) chain soon after synthesis. The Ii-MHC class II heterotrimer exits the ER and passes through the Golgi apparatus before being transported to a late endosomal compartment called MHC class II compartment. Once within the compartment, the Ii chain is digested by resident proteases, leaving the residual class II associated Ii peptide (CLIP) in the peptide-binding groove of the MHC class II dimers. The groove is free to bind antigenic peptide when CLIP has been removed, catalysed by two nonpolymorphic MHC class II molecules HLA-DM and HLA-DO in humans (Denzin et al., 2005). Once the peptide is loaded on the MHC class II, the Ii-chain free MHC class II peptide complexes are transported to the plasma membrane to present to the $CD4^+$ T cells (Cresswell, 2005; Heemels and Ploegh, 1995; Rudolph et al., 2006).

In the process of immune surveillance, the encounter of a peptide-MHC complex that is recognized by a T cell receptor will only lead to T cell activation when costimulatory signal by APCs is provided. This signal includes the interaction between CD28 on T cells, and costimulatory molecules, CD80 and CD86, expressed on APCs (Greenwald et al., 2005). T- cell activation results in the expression of activation markers, cytokine production, proliferation of T cells and their differentiation into effector and memory cells.

1.2.3.2 T- cell recognition, cross-reactivity and immunodominance

Recognition of peptides bound to the MHC is not the only means by which immune responses are initiated, but also is the key in the generation and maintenance of the body's T cell repertoire. During T cell development in the thymus, immature T cells express a TCR that is capable of binding self-peptide and MHC. Receiving a survival signal, these T cells are positively selected to form a self-MHC restricted T- cell repertoire. However, potentially autoimmune T cells with

a high affinity for self-peptide-self-MHC complexes are eliminated through negative selection. Therefore, cross-reactivity should be a property of T-cell recognition for all mature T cells that reached the periphery after thymic development (Ignatowicz et al., 1996). The total number of T cells that have different antigen specificities in the body is relatively limited compared to the vast diversity of peptide antigens. Therefore to allow the adaptive immune system to respond to all pathogens, each T cell receptor must be able to recognize multiple peptides presented by the same MHC molecules (Mason, 1998). Indeed, the TCR repertoire is diverse and degenerate, and potentially allowing the T cell mediated immune responses to prevent immune escape through viral mutations. This leads to the idea that T cell recognition is highly cross-reactive and that a single T cell clone might be stimulated by a number of cross-reactive peptides (Evavold et al., 1995; Sospedra and Martin, 2006). Indeed, it has been shown from crystallographic studies that cross-reactive T cell responses could be elicited when peptides retain stretches of sequences or anchor positions that are required for MHC or TCR binding (Wucherpfennig, 2004).

The nature of T cell recognition implies that, in any viral infection, the range of viral peptides selected to display to the T cell repertoire will be determined by the antigen availability and the avidity of the peptides to the MHC alleles. Yet, the T cell responses during the course of an infection are driven by a relatively small number of viral antigens, and not by the rest of the vast diversity of the viral sequence that also have MHC-binding motifs (Welsh and Fujinami, 2007). With regards to their capacity to induce a response, epitopes can be arranged in an immunodominance hierarchy. Immunodominance is influenced by the intracellular processing of the antigens, the affinity of peptide binding to MHC molecule, and the repertoire of the TCRs that are able to recognize the peptide-MHC combination. Most abundant cognate T cell populations will recognize the immunodominant epitopes, followed by the subdominant ones, resulting in a highly focused response to pathogens (Welsh and Selin, 2002). However, refocusing immune responses to subdominant but protective determinants in vaccination is possible. In mice, experimental immunogens that focus on conserved regions of HIV-1 proteome, which are mainly subdominant during natural infection, have been demonstrated to confer protection against the whole virus when the usual patterns of immunodominance are overcome (Im et al., 2011; Letourneau et al., 2007).

HLA is the most polymorphic region in the human genome with over 8,000 HLA alleles, according to the HLA database (http://www.ebi.ac.uk/imgt/hla/stats.html). HLA can be grouped

into families (HLA supertypes) that shared similar binding motifs. Supermotifs are those that can bind to a number of HLA molecules, and peptides present with supermotifs should be able to be recognized by a broader range of individuals within a population. Thus universal vaccine targeting conserved immunodominant epitopes presented by HLA superfamilies should elicit effective immune responses.

1.2.3.3 Heterosubtypic immunity to influenza virus

The phenomenon of T cell cross-reactivity and immunodominance thus shape the pre-existing T-cell memory pool laid down in an individual by previous infections, and would influence the pathogenesis of subsequent infection. For influenza A virus, the internal viral proteins NP or M1 are the most conserved between variant strains and are more resistant to antigenic drift/shift, as shown in **Fig. 1.6** (Lamb et al., 1982). Recognition of conserved T-cell epitopes presented by MHC molecules is vital for heterosubtypic immunity. The majority of the virus-specific $CD8^+$ T cell response is indeed directed against peptides derived from either NP and M1 protein (Townsend et al., 1985). Due to similarity in sequences between different subtypes, T cell responses elicited against these immunodominant viral proteins should be cross-reactive.

Protection against virus of a different subtype is termed heterosubtypic immunity. It is defined as immunity induced by a given influenza subtype, or its antigens, that is protective against subsequent challenge or infection with influenza virus of other subtypes. Heterosubtypic immunity was first described more than 40 years ago (Schulman and Kilbourne, 1965). Heterosubtypic T cell–mediated immunity has been well reported (Jameson et al., 1998; Boon et al., 2004; Lee et al., 2008; Roti et al., 2008; Greenbaum et al., 2009a; Hillaire et al., 2011). Analysis of the 1957 pandemic data has shown that people who experienced an H1N1 infection before 1957 less likely developed flu during the H2N2 pandemic (Epstein, 2006). In animal experimental systems where mice were primed and challenged with serologically distinct H1N1 and H3N2 influenza A viruses (Doherty et al., 1977), which to some extent mimics what happens in the natural epidemiology of influenza, suggested that T cell immunity is important in protection against disease as an enhanced effector function was provided by cross-reactive cytotoxic T lymphocytes (CTLs). Using human PBMCs and CTL clones, pre-existing T cell responses from healthy individuals have been shown to recognize serologically distinct strains of influenza virus, such as H5N1. Although such protection does not prevent an infection (i.e. non-sterilizing),

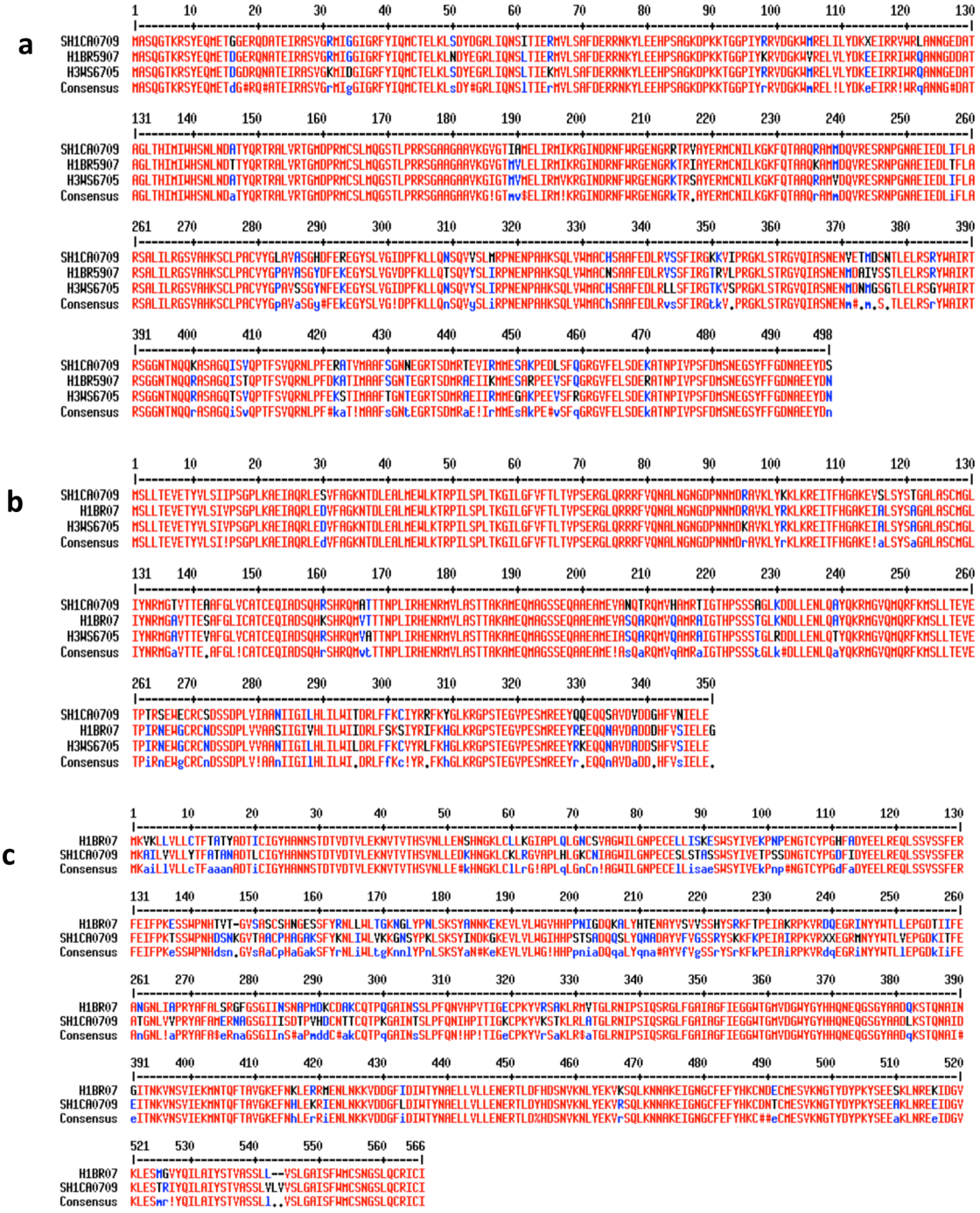

Figure 1.6 Sequence comparisons between H3N2, seasonal and pandemic H1N1. (a) Amino acid sequence alignment between full-length nucleoprotein (NP) of H3N2 (WS/67/05) virus, H1N1 (BR/59/07) and pandemic H1N1 (CA/07/09) viruses. **(b)** Amino acid sequence alignment between full-length matrix protein (M) of H3N2 (WS/67/05) virus, H1N1 (BR/59/07) and pandemic H1N1 (CA/7/09) viruses. Both proteins showed a sequence homology of higher than 97%. **(c)** Amino acid sequence alignment between full-length hemagglutinin protein (HA) of H1N1 (BR/59/07) and pandemic H1N1 (CA/7/09) viruses. Sequence homology is about 73%.

cross-reactive T cells enhanced recovery by reducing pathogenesis and mortality. It has been reported that healthy individuals that have never been exposed to avian influenza H5N1 virus

possess memory T-cells that are capable of recognizing H5N1 epitopes, where internal proteins are the major targets (Lee et al., 2008). T cell cultures generated from healthy individuals against A/PR/8/34 (H1N1) are able to lyse target cells infected with various strains of swine and avian influenza A *in vitro* (Jameson et al., 1999; Kreijtz et al., 2008). Once again, most of the T cell lines characterized in this study recognized internal viral proteins such as M1 and NP. Heterosubtypic immunity against influenza A viruses from other species has also been demonstrated (Richards et al., 2009). Experiments with murine models demonstrated that cross-protection mediated by T cells were able to provide improved virus clearance and survival during subsequent homologous or heterosubtypic virus challenges (Thomas et al., 2006b; Ulmer et al., 1993). Collectively, these reports suggest that the immune repertoire of most healthy subjects consists of T cells directed against the internal proteins from other heterosubtypic variants including those subtypes to which the population is naive. By targeting viral components that are immunogenic and conserved among heterologous strains, T cell memory can be boosted in order to activate cross-protective and heterosubtypic immunity (Thomas et al., 2006b). Taken together, a broadly protective and more effective vaccination strategy should include a component to stimulate cross-reactive T cells, in addition to the current antibody-based strategy (Tan et al., 2010).

1.2.4 Memory $CD4^+$ and $CD8^+$ T cells in long-lived protective cellular immunity

In addition to examining the extent of cross-reactivity of T cells to heterosubtypic strains and identifying the viral immune epitopes that trigger effective T cell responses, dissecting the presence and characteristics of immune memory against influenza virus is also a focus of this study. The establishment of an immunological memory ensures an individual can better control re-infection with the same pathogen, and maintenance of memory $CD8^+$ and $CD4^+$ cells against viral infection has been studied extensively (Sprent and Surh, 2001).

A goal of any T cell- based vaccine is to induce antigen-specific T cells that are able to persist after the pathogen is cleared and to confer protection against a re-infection. T cell differentiation driven by infection or vaccination can lead to a population of cells with functional and phenotypical heterogeneity. Expression of adhesion molecules and chemokine receptors distinguish immunological memory based on homing properties and tissue localization. Naïve T cells express CD45RA, and lymph node homing receptors CD62 ligand (CD62L) and CCR7

(Sallusto et al., 2004a). During acute infection, activation of antigen specific T cells results in the acquisition of primary effector functions, such as production of IFN-γ and cytotoxicity in response to antigen. Surface expression of lymph node homing molecules CCR7 and CD62L are then lost to enable movement from secondary lymphoid organs and allow extravasation from the vascular endothelium to the location of primary infection (Keating et al., 2005). These cells undergo an antigen-driven expansion, followed by a contraction phase, where most (90-95%) undergo apoptosis. The remaining fraction establishes a pool of memory T cell precursors. In the immunization with yellow fever vaccine YFV-17D or smallpox vaccine Dryvax, a systematic acute infection is caused leading to a substantial clonal expansion of effector $CD8^+$ T cells, allowing responses to the vaccines to be quantified (Ahmed and Akondy, 2011).

Once primed, these T cells have greater trafficking and proliferative capacities that allow quicker and more robust responses to secondary infection than the primary response. Memory T cells consists of two populations: central memory T cells (Tcm) which have a greater proliferative potential and reside in secondary lymphoid organs; and effector memory T cells (Tem), which lack CD62L and CCR7 and localize in peripheral tissues and spleen, and display a greater capacity for effector functions such as cytotoxicity (Owen et al., 2010; Sallusto et al., 2004a). Therefore circulating or tissue-resident Tem cells provide immediate protection for incoming pathogen upon antigen recognition, while recall responses are mediated by Tcm which proliferate rapidly in response to antigens presented by dendritic cells (Sallusto et al., 2004b). Surface markers other than homing markers can be used to segregate different memory subsets, for instance costimulatory molecules CD28 and CD27 are expressed on Tcm but are lost on most differentiated Tem cells. Apart from using homing receptor expression, memory T cells can also be distinguished according to their expression of determining transcription factors and the arrays of cytokines produced (Angelosanto and Wherry, 2010).

In developing a T cell-based vaccine, it is crucial to understand the migratory, proliferative and protective capacity of these long-lived and functional memory T cells in order to come up with a rational vaccination strategy. For influenza infection, to identify the cellular correlates of protection, several questions need to be answered: which cell types are most relevant and which function(s) can mediate control? Despite the vast number of markers that are used to define the diversity in memory T cell populations, it is not known how T cell memory is generated during an influenza infection, or the relationship between memory T cells that express different

functional/phenotypic markers, and how they confer protection. Particular T-cell memory phenotypes are shown to relate to control in certain viral infections, including CMV, EBV, HCV and HBV [reviewed in (Makedonas and Betts, 2011)]. By assessing the antigen-specific T cell function, it may be possible to establish whether a certain balance between Tcm and Tem cells is required for effective protection. For example, individuals that are capable of controlling chronic infectious diseases such as HIV-1 and HCV have an increased frequency of antigen-specific cells producing high level of IL-2 within their Tcm population [reviewed in (Zielinski et al., 2011)]. In HIV, low level of T cell activation together with a strong, broad and polyfunctional cytokine response is likely to play a role in the control of infection (Owen et al., 2010). It has not been examined in the context of influenza infection how such functional capacities are related to control over viral replication (**Fig. 1.7**).

1.3 Aims

Understanding T- cell mediated immunity following acute viral infection represents an area of research with broad implications for fundamental immunology. It offers new insights for the generation of more effective vaccines that elicit T- cell memory with the combination of different functional attributes required for inducing protective anti-viral immunity. In particular, immune correlates of protection other than neutralizing antibodies are needed for immunity mediated by T cells in influenza infection. The main objective of this DPhil project was to elucidate what constitutes a successful T cell response against acute influenza infection in humans. Despite our understanding on cross-reactive T cell responses to influenza A virus, the underlying mechanism of protective cell-mediated immunity in the absence of established humoral immunity remains poorly understood. The extent of cross-reactivity to heterologous strains, together with the overall influenza-specific memory T cells responses, are required to give a complete account of how such immunity could modulate the severity of illness caused by a novel strain of viruses. The breadth, magnitude and immunodominance hierarchy of such responses can be used to dissect the immunological basis of heterosubtypic immunity induced by both natural infection and immunization.

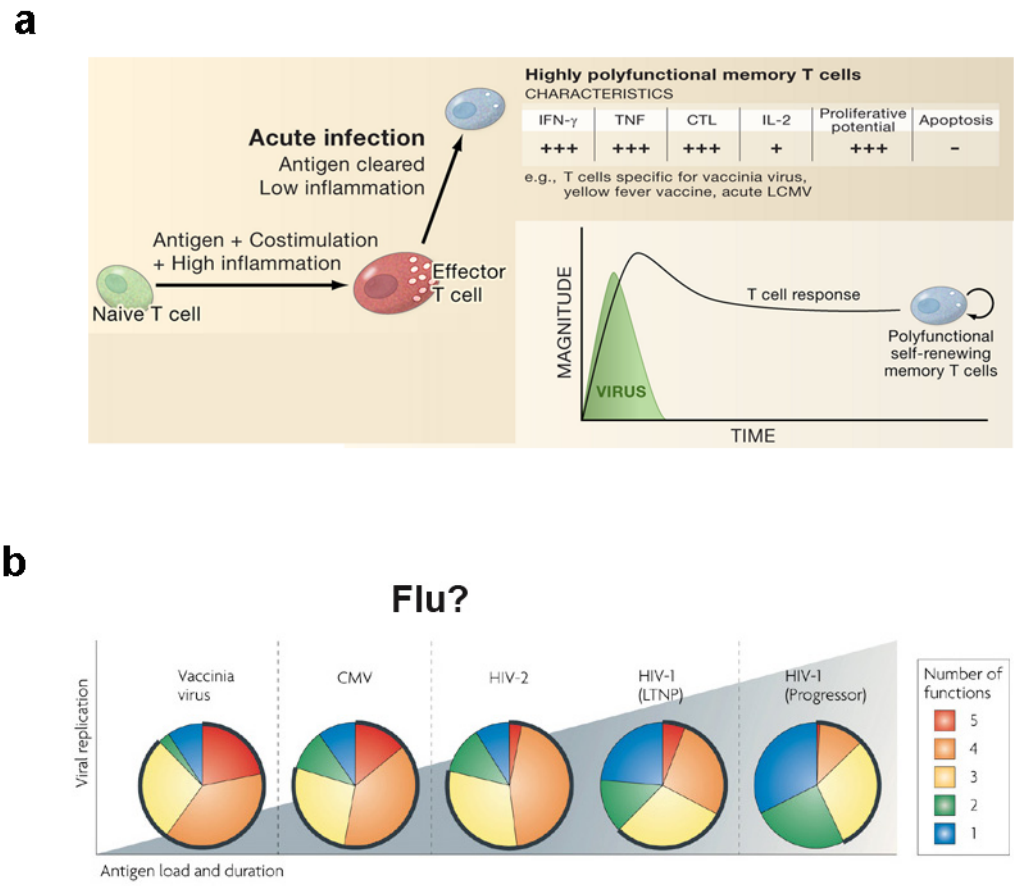

Figure 1.7 Functionality of T cells during viral infections. **(a)** During acute viral infection, naïve T cells are primed and differentiated into effector T cells. After the clearance of infection, T cells further differentiate into a pool of stable, highly polyfunctional memory T cells that are capable of producing multiple cytokines. These cells are maintained for a long time via self-renewal in the absence of antigens. In humans, T cells specific for vaccinia virus or the live attenuated yellow fever virus vaccine have these properties. **(b)** Schematic diagram of correlation of antigen-specific $CD8^+$ T cell quality and viral load.T cell functional quality in humans infected with different viruses was determined by measuring expression of IL-2, IFN-γ, TNF-α and CCL4 following stimulation with antigens. The black arcs highlight the fraction of the multifunctional (3-5 expressing) $CD8^+$ T cells within each response. Level of antigen load is indicated by background shading. CMV, cytomegalovirus; LTNP, long-term non-progressor [Adapted from (Seder et al., 2008; Virgin et al., 2009)].

In the present study, the role of pre-existing memory T cells established from previous infection/vaccination in response to acute infection is examined. The specific aims are as follows:

1) To define the role(s) of T cells in the control of acute influenza A infection in the absence of an antibody response.

2) To describe the kinetics, breadth, size, quality and functions of the influenza -specific T cell response following an acute infection.

3) To examine the patterns of T cell recognition across variant subtypes of influenza A viruses.

4) To determine the memory T cell responses to non- replicating antigens (inactivated pandemic H1N1 vaccine).

5) To analyse the possible relationship between the circulating follicular T helper cells and the antibody responses.

To achieve the above aims, two influenza challenge studies were conducted by infecting healthy adult volunteers who had no detectable antibodies to the challenge strains with live seasonal H3N2 or H1N1 viruses. In addition, another cohort of 151 adult volunteers, who were vaccinated with pandemic H1N1 vaccine, was also set up to answer the timely call of the H1N1 pandemic.

In this thesis, I first describe the kinetics and quantities of influenza-specific memory T cell populations circulating in the peripheral blood during infection or vaccination. Using IFN-γ enzyme-linked immunosorbent spot (ELISpot) assays, PBMCs are stimulated with overlapping peptides spanning the whole virus proteome set out in a 2-dimensional (2-D) matrix system so as to identify influenza virus-specific T cell epitopes (**Fig. 1.8**) (Anthony and Lehmann, 2003; Hoffmeister et al., 2003; Precopio et al., 2008). Subsequently, I examined whether these immune epitopes are likely to be targets of heterosubtypic immunity. The functions of these circulating memory T cells were explored by looking at their phenotypes through multiparameter flow cytometry, their killing capacity by chromium release assays, and the extent of cross-reactivity by using peptides from variant subtypes. Finally, this project looked at whether memory $CD4^+$ T cells that express CXCR5 have an intrinsic ability to provide help to responding naïve B cells by various *in vitro* assays.

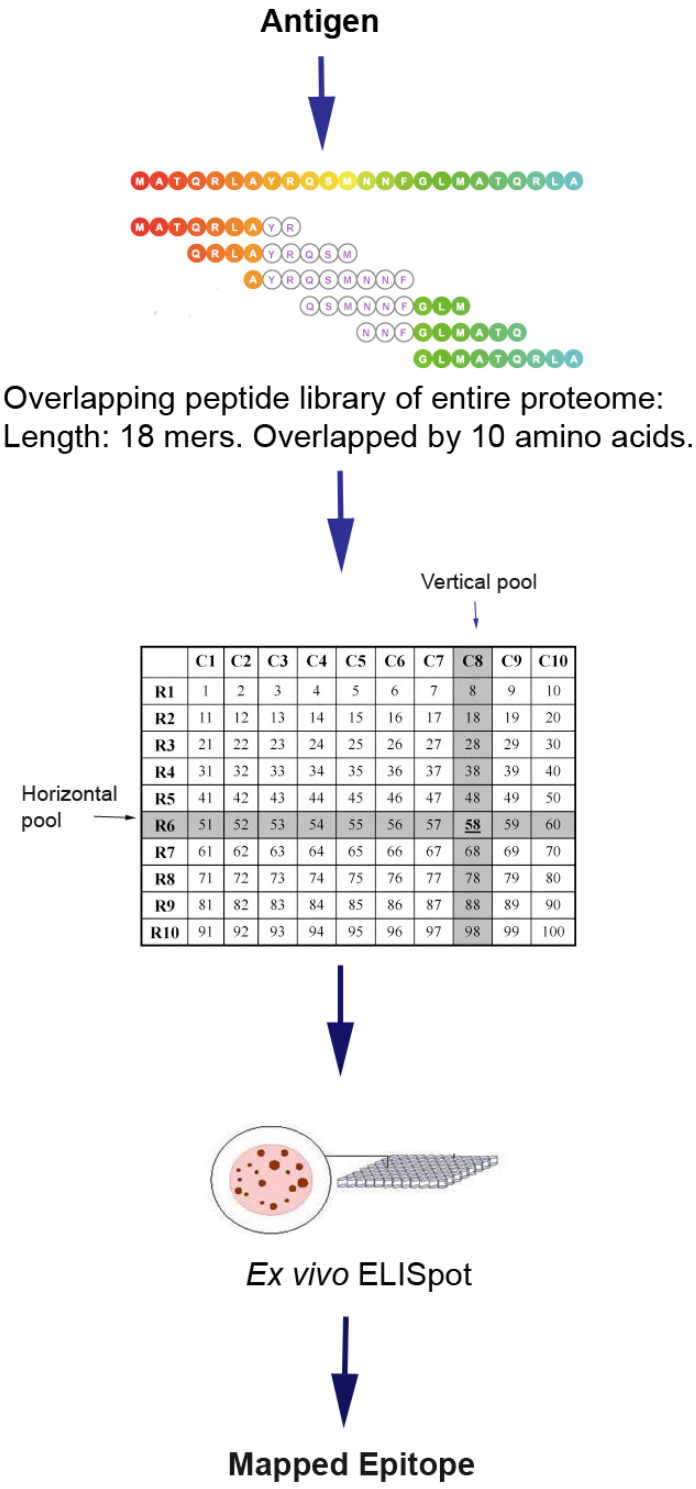

	C1	C2	C3	C4	C5	C6	C7	C8	C9	C10
R1	1	2	3	4	5	6	7	8	9	10
R2	11	12	13	14	15	16	17	18	19	20
R3	21	22	23	24	25	26	27	28	29	30
R4	31	32	33	34	35	36	37	38	39	40
R5	41	42	43	44	45	46	47	48	49	50
R6	51	52	53	54	55	56	57	**58**	59	60
R7	61	62	63	64	65	66	67	68	69	70
R8	71	72	73	74	75	76	77	78	79	80
R9	81	82	83	84	85	86	87	88	89	90
R10	91	92	93	94	95	96	97	98	99	100

Figure 1.8 Approaches used in mapping epitopes of influenza virus. Amino acid sequence of the proteome of the virus is used to design the overlapping peptides library. A 2-dimensional matrix is then laid out where each peptide was contained in two pools, one down the row and one across the column. For each peptide that made a response, there must be a vertical pool and a horizontal pool that appeared positive in an IFN-γ ELIspot. The putative peptide could then be identified by finding the intersection of the two positive pools in the arrays.

Chapter 2

Materials and Methods

2.1 Materials

2.1.1 Plasticware and other laboratory supplies

Product	Cat. No.	Supplier
6-well plates	353224	BD Biosciences, UK
12-well plates	353225	BD Biosciences, UK
24-well plates	353047	BD Biosciences, UK
15 ml Falcon tubes	352096	BD Biosciences, UK
50 ml Falcon tubes	352070	BD Biosciences, UK
96-well Multiscreen Filter plate, PVDF membrane	MAIPS4510	Millipore, UK
BD Vacutainer Heparin Blood Tubes	368480	BD Vacutainer Systems, UK
CellTrics® disposable filters	04-0042-2316	Partec, UK
ELISA plates (F96 Maxisorp NUNC Immuno plate)	442404	Nunc, USA
Leucosep tubes	227289	Greiner Bio-One, UK
PureCol collagen coated flasks	5029	Inamed Biomaterials, USA

2.1.2 Buffers

Product	Composition/Catalogue No.	Supplier
Cytofix/Cytoperm	554722	BD Biosciences, UK
Dynabeads buffer	0.1% BSA and 2 mM EDTA in PBS, pH7	N/A
ELISA incubation buffer	0.1% BSA in PBS-Tween	N/A
FACS Buffer	1% FCS, 0.1% NaN3 in PBS	N/A
FACS Fix	1% Paraformaldehyde in PBS	N/A
MACS buffer	0.5% BSA and 2 mM EDTA[1] in PBS, pH7	N/A
PBS-Tween	0.05% Tween-20 in PBS	N/A
Tris Buffer	50mM Tris and 150mM NaCl	N/A

[1] Ethylenediaminetetraacetic acid

2.1.3 Plasmids and viruses

Materials	Provided by
pSC11 plasmid	Prof. Alain Townsend, WIMM, Oxford
Inactivated A/Brisbane/59/2007 (H1N1) virus	Prof. John McCauley, NIMR, London
Inactivated A/Brisbane/10/2007 (H3N2) virus	Prof. John McCauley, NIMR, London
Influenza A virus strain X31	3VBiosciences, USA
Purified influenza vaccines antigen (A/California/07/09 , A/Brisbane/59/07, A/Brisbane/10/07)	Sinovac Biotech Co., Ltd, China

2.1.4 Restriction Enzymes

Product	Catalogue No.	Supplier
NotI	R0189L	New England Biolabs, UK
SmaI	R0141L	New England Biolabs, UK
EcoRV	R0195L	New England Biolabs, UK

2.1.5 Kits and beads

Product	Catalogue No.	Supplier
CD8 antibody-coated magnetic beads (Dynabeads)	11147D	Invitrogen, UK
CD154 MicroBead Kits	130-092-658	Miltenyi Biotec, UK
$CD4^+$ T Cell Isolation Kit II, human	130-046-901	Miltenyi Biotec, UK
CellTrace™CFSE Cell Proliferation Kit - for flow cytometry	C34554	Invitrogen, UK
DETACHaBEAD CD19	12506D	Invitrogen, UK
Dynabeads CD19	11143D	Invitrogen, UK
Effectene Transfection Reagent	301425	Qiagen, UK
Human IgG ELISA kit (ALP)	3850-1AD-6	Mabtech AB, Sweden
Human IgA ELISA kit (ALP)	3860-1AD-6	Mabtech AB, Sweden
Human IgM ELISA kit (ALP)	3840-1AD-6	Mabtech AB, Sweden
Human IFN-γELISpot kit (ALP)	3420-2A	Mabtech AB, Sweden
Human IL-21 ELISA Ready-SET-Go	88-7216-22	eBioscience, UK
Monocyte isloation kit	130-91-153	Miltenyi Biotec, UK
QIAprep Spin Miniprep Kit	27106	Qiagen, UK

2.1.6 Media

Product	Composition/Cat. No.	Supplier
Bronchial Epithelium Growth Media	CC-3170	Lonza, UK
DMEM[2]	32430100	Invitrogen, UK
LB (Luria Bertani) medium	L3022	Sigma Aldrich, UK
RPMI 1640[3]	61870044	Invitrogen, UK
S.O.C. medium[4]	15544-034	Invitrogen, UK
10x MEM	M9288	Sigma Aldrich, UK

[2]Dulbecco's modified Eagle's medium
[3]Roswell Park Memorial Institute medium
[4]Super optimal broth with catabolite repression

2.1.7 Cytokines

Product	Catalogue No.	Supplier
Human recombinant IL-2	187-67	Oxford Radcliffe Pharmacy Services, UK
Human recombinant IL-7	200-07	Peprotech, UK
Human recombinant IL-15	247-IL-005	R&D Systems Europe, UK

2.1.8 Cell lines

Product	Supplier
L-cell lines	Prof. Alain Townsend, WIMM, Oxford
TK-143 cells	Prof. Alain Townsend, WIMM, Oxford

2.1.9 Tissue culture reagents

Product	Catalogue No.	Supplier
Brefeldin A	B6542	Sigma Aldrich, UK
Concanamycin A	27689	Sigma Aldrich, UK
Cyclosporin A	C1832	Sigma Aldrich, UK
FCS (Fetal calf serum)	10106-169	Invitrogen, UK
GolgiPlug	555029	BD Biosciences, UK
GolgiStop	554724	BD Biosciences, UK
Human AB serum	N/A	NHS Blood and Transplant, UK
Penicillin/Streptomycin (Pen/Strep) 100X	15140-114	Invitrogen, UK
Trypan Blue solution	15250-061	Invitrogen, UK

2.1.10 Chemical and biological reagents

Product	Catalogue No.	Supplier
Agarose, LMP (Low-gelling temperature)	A4018	Sigma Aldrich, UK
Ampicillin	A5354	Sigma Aldrich, UK
AP conjugate substrate kit	170-6432	Bio-Rad Laboratories, UK
BD FACS Permeabilization solution 2	340973	BD Biosciences, UK
BUdR (5-bromodeoxyuridine)	B5002	Sigma Aldrich, UK
Cell Lysis Solution	2300720	5 Prime, UK
CytofixCytoperm	554722	BD Biosciences, UK
DNA Hydration Solution	158914	Puregene, Gentra Systems, UK
Ionomycin calcium salt from *Streptomyces conglobatus* - powder, $\geq$98% (HPLC)	I0634	Sigma Chemical, UK
Isopropanol	59080	Sigma Aldrich, UK
Lymphoprep	1114547	Axis-shield, Norway
Phosphate-buffered saline	14190-094	Invitrogen, UK
Proteinase K Solution	2500150	5 Prime, UK
Protein Precipitation Solution	2300720	5 Prime, UK
pNPP tablet (ALP substrate kit)	172-1063	Bio-Rad Laboratories, UK
Phorbol myristate acetate	P8139	Sigma Chemical, UK
RBC Lysis Solution	2301300	5 Prime, UK
SIGMAFAST™3,3-Diaminobenzidine tablets	D4418	Sigma Aldrich, UK
Sodium Bicarbonate Solution (7.5%)	S8761	Sigma Aldrich, UK

Continued...

Product	Catalogue No.	Supplier
Tween-20	P7949	Sigma Aldrich, UK
TrueBlue	50-78-02	KPL, USA
5-Bromo-4-chloro-3-indolyl-β-D-galactoside (X-gal)	7240-906	Melford, UK

2.1.11 Flow cytometry antibodies

Antibodies	Fluorochrome	Clone	Supplier	Catalogue No.
CD3	PerCP	SK7	BD Biosciences, UK	345766
	Pacific blue	UCHT1	Dako, UK	PB982
	PacBlue	S4.1	Invitrogen, UK	MHCD0328
	PE TexasRed	S4.1	Invitrogen, UK	MHCD0317
	PECy7	SK7	BD Biosciences, UK	557851
	APC-H7	SK7	BD Biosciences, UK	641397
	PE	UCHT1	BD Biosciences, UK	555333
CD4	PE	MT310	Dako, UK	R0805
	Pacific blue	MT130	Dako, UK	PB983
	PE-Texa Red	S3.5	Invitrogen, UK	MHCD0417
	PECy5.5	S3.5	Invitrogen, UK	MHCD0418
	PerCP	S3.5	Invitrogen, UK	MHCD0431
	FITC	SK3	BD Biosciences, UK	345768
	PE Cy5	RPA-T4	BD Biosciences, UK	555348
CD8	PerCP	SK1	BD Biosciences, UK	345774
	APC	DK25	Dako, UK	C7227
	APC	DK25	Dako, UK	C7227
	PB	DK25	Dako, UK	C7227
	APC-H7	SK1	BD Biosciences, UK	641400
	PE TexasRed	3B5	Invitrogen, UK	MHCD0817
	QD705	3B5	Invitrogen, UK	Q10059
	APC H7	SK1	BD Biosciences, UK	560179
CD14	QD605	MφP9	Conjugated in-house at NIH	
	V450	MφP9	BD Biosciences, UK	560349
CD19	V450	HIB19	BD Biosciences, UK	560353
	QD655	HIB19	Conjugated in-house at NIH	
CD20	PerCP	L27	BD Biosciences, UK	345794
	APC	2H7	BD Biosciences, UK	559776
CD27	PE	M-T271	BD Biosciences, UK	555441
	PECy5	1A4CD27	Beckman Coulter, UK	6607107
	PE	M-T271	BD Biosciences, UK	555441
	APC H7	M-T271	BD Biosciences, UK	560222
CD38	APC	HIT2	BD Biosciences, UK	555462
	APC	HB7	BD Biosciences, UK	345807
	PE-Cy7	HB7	BD Biosciences, UK	335825
CD45RO	PerCP	UCHL1	BD Biosciences, UK	555494
	PE-TexasRed	UCHL1	Beckman Coulter, UK	IM2712U
	PECy5	UCHL1	BD Biosciences, UK	555494
	PECy7	UCHL1	BD Biosciences, UK	337168

Continued...

Antibodies	Fluorochrome	Clone	Supplier	Catalogue No.
CD57	QD585	NK-1	Conjugated in-house at NIH	
	FITC	NK-1	BD Biosciences, UK	555619
CD69	PE	FN50	BD Biosciences, UK	555531
CD95	FITC	DX2	BD Biosciences, UK	555673
CD107a	PE	H4A3	BD Biosciences, UK	555801
CD127	A647	HIL-7R-M21	BD Biosciences, UK	558598
CD154	FITC	TRAP1	BD Biosciences, UK	555699
	APC	TRAP1	BD Biosciences, UK	555702
Bcl-2	PE	Bcl-2/100	BD Biosciences, UK	340576
Caspase-3 (Active)	FITC	C92-605	BD Biosciences, UK	559341
CXCR5	APC (A647)	RF8B2	BD Biosciences, UK	558113
	A488	RF8B2	BD Biosciences, UK	558112
ICOS	PE	DX29	BD Biosciences, UK	557802
IFN-γ	FITC	25723.11	BD Biosciences, UK	340449
	V450	B27	BD Biosciences, UK	560371
	PE	4S.B3	BD Biosciences, UK	559326
IL-2	APC	MQ1-17H12	BD Biosciences, UK	554567
	APC	5344.111	BD Biosciences, UK	341116
	A700	MQ1-17H12	Biolegend, UK	500319
	PE	5344.111	BD Biosciences, UK	340450
IL-21	A647	3A3-N2	Biolegend, UK	513006
	A647	3A3-N2.1	BD Biosciences, UK	560493
	PE	3A3-N2.1	BD Biosciences, UK	560463
Mouse IgG2a, κ	APC-Cy7	G155-178	BD Biosciences, UK	557751
NP-1	AlexFluor 488 (AF488)	HB-65	3VBiosciences,USA	(Gift)
Ki-67	FITC	B56	BD Biosciences, UK	556026
Live/Dead	Aqua	-	Invitrogen, UK	L34957
	Violet	-	Invitrogen, UK	L34955
HLA-DR	PE	TU36	BD Biosciences, UK	555561
	APC-Cy7	L243 (G46-6)	BD Biosciences, UK	335831
	APC	L243 (G46-6)	BD Biosciences, UK	340549
TNF-α	PE-Cy7	MAb11	BD Biosciences, UK	557647
	A700	MAb11	BD Biosciences, UK	557996
PD-1	PacBlue	EH12.2H7	BioLegend, UK	329916
Perforin	PE	B-D48	Geneprobe, US	854.952.010
Biotin	PE	130-090-756	Mitenyl Biotec, UK	130-090-756

2.1.12 Other antibodies

Antibodies	Clone	Supplier	Cat. No.
anti-CD49d	L25	BD Pharmingen, UK	340976
anti-CD28	L293	BD Pharmingen, UK	340975
Influenza A Matrix protein antibody	GA2B	AbD Serotec, UK	MCA401
BD CompBead	552843	BD Biosciences, UK	
LEAF™Purified anti-human CD3 antibody	OKT-3	BioLegend, UK	317315
Polyclonal Goat anti-Mouse Immunoglobulins/HRP[5]		Dako, UK	P 0447

[5]Horseradish peroxidase

2.2 Methods

2.2.1 Subjects and study cohorts

2.2.1.1 Experimental influenza infection

Study Design

The purpose of this study as detailed in Chapter 3 and 4 was to evaluate cell-mediated immunity in acute influenza infection. Two separate prospective, randomized and double blinded, parallel group clinical studies of experimental human influenza A infection were conducted at a single site in Cambridge, UK. The H3N2 challenge study was carried out between 24th October and 24th November 2008, whereas H1N1 challenge study was carried out between 18th August and 18th September 2009.

Healthy, non-pregnant adults between the age of 18 and 45 were eligible for enrolment. Exclusion criteria included health care workers, history of acute respiratory illness, chronic illness or medications. In the H3N2 challenge study, a total of 17 healthy adult volunteers aged 18-45, with hemagglutination-inhibition (HI) titres less than 1:8 to A/Wisconsin/67/2005 (H3N2) participated in the study. In the H1N1 study, a total of 24 healthy, adult volunteers aged 18-45, with HI titres less than 1:8 to A/Brisbane/59/07 (H1N1) participated in the study.

Both studies were conducted in compliance with Good Clinical Practice guidelines (CPMP/ ICH/135/95) and the Declaration of Helsinki. Additional samples for the immunohistochemistry analysis of human lung biopsies and flow cytometry analysis of cultured respiratory epithelial cells were collected as part of an established protocol at Southampton University Hospitals NHS Trust.

All protocols were approved by East London and City and the Southampton and Southwest Hampshire ethics review committees. Written informed consent was obtained from each participant with an ethics committee approved form. No medication, except acetaminophen for treatment of severe symptoms, was permitted. Subjects were compensated for their participation of the study.

Study Outline

Screening of participants began within 45 days of the scheduled viral inoculation. In both studies, the participants were nasally infected with the virus on day 0 and were quarantined at the study site for a total of 9 days (from day -2 til day 7) (**Fig. 2.1**). They were randomized into 4 groups and each group of the participants were inoculated intra-nasally with different doses of influenza A virus on day 0. The dose of the virus was designated as 1:10 (high), 1:100 (medium-high), 1:1000 (medium-low) and 1:10,000 (low) from the original virus stock. Group 1 received the highest dose, while Group 4 received the lowest. On day 7, participants were given Tamiflu and discharged. 50 ml of blood was taken from participants on day -2 (baseline), day 7, and day 28 (follow-up) using 10 ml BD Vacutainer Heparin Blood Tubes containing 170 IU sodium heparin. An additional time point day 3 was taken for H1N1 study.

Clinical symptoms were recorded throughout the study period. Nasal lavage samples were collected daily until day 7 to determine the viral load. Oral temperatures were measured four times daily and fever was defined as an oral temperature >37.7°C. Symptom assessments were performed by the volunteers twice daily on a four-point scale (0-3 corresponding to absent to severe) (Hayden et al., 1998). The symptoms assessed were nasal stuffiness, runny nose, sore throat, cough, sneezing, earache/pressure, breathing difficulty, muscle aches, fatigue, headache, feverish feeling, hoarseness, chest discomfort, and overall discomfort. The total symptom score for each day was obtained by adding the individual symptoms scores for that particular day. The individual symptoms contributing to the total symptoms scores were divided into three subgroups: systemic symptoms (muscle aches, fatigue, headache, and fever), upper respiratory symptoms (nasal stiffness, ear ache/pressure, runny nose, sore throat, and sneezing) and lower respiratory symptoms (cough, breathing difficulty, hoarseness and chest discomfort).

2.2.1.2 Viruses

Tissue culture grown A/Wisconsin/67/05 (H3N2) virus was used in H3N2 study and egg grown A/Brisbane/59/2007 (H1N1) virus was used in H1N1 study. The stock virus were manufactured and processed by GlaxoSmithKline, UK to a GMP grade. The titre of the stock virus was 10^7 $TCID_{50}$ infectious doses. The stock virus were diluted to four different inoculum titres, prepared in individual aliquots intended for single use and then administered. Subjects were observed for potential allergic reactions for 30 min following inoculation.

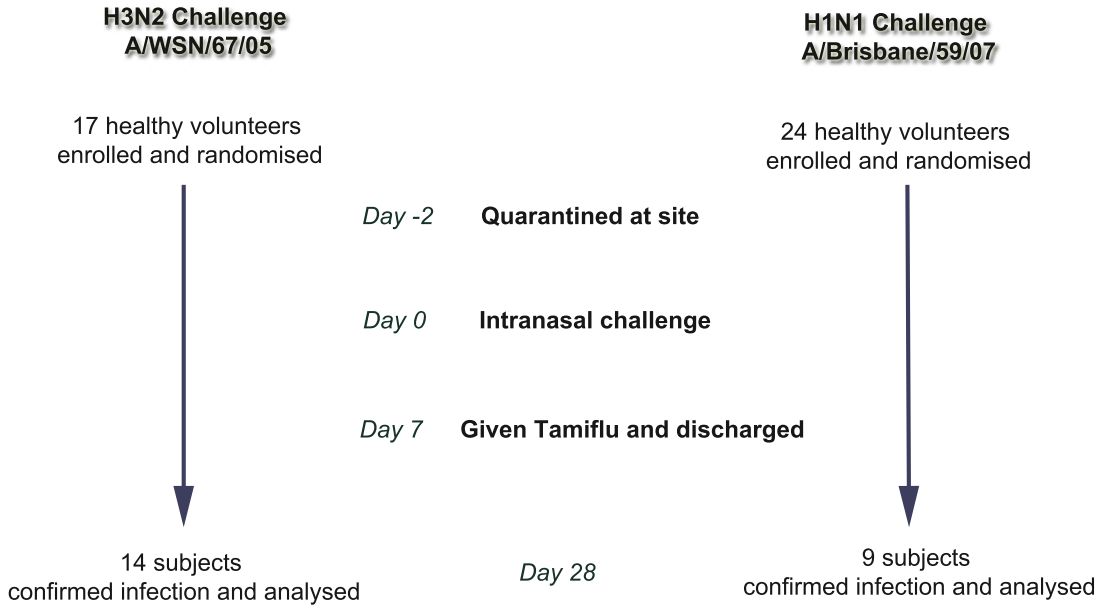

Figure 2.1 Enrolment and outcomes of H3N2 (October 2008) and H1N1 (August 2009) challenge studies.

Apart from the study of T cell responses covered in this thesis, in parallel, roles of B cells and NK cells in these cohorts were investigated by Dr. Arthur Huang, and Dr. Ling-Pei Ho respectively.

2.2.1.3 Experimental H1N1 infection (2010)

Between July and August 2010, an additional prospective, randomized experimental infection of A/Brisbane/59/07 (H1N1) was carried out in Cambridge, UK, following the same protocols and procedures as described in section 2.2.1.1-2.2.1.2. A total of 20 healthy adult volunteers participated, and 3 of them were infected at the end of the study. This cohort was used to further identify H1N1 peptides that elicited memory responses in healthy individuals, and to examine the presence of Tfh in peripheral blood.

2.2.1.4 Pandemic H1N1 vaccine trials

The purpose of the study as detailed in Chapter 5 was to evaluate cell-mediated immunity induced by inactivated influenza vaccines, and the effect of a seasonal influenza vaccine on immunogenicity and safety of the 2009 pandemic H1N1 vaccine in healthy adults in a two-dose regimen. Despite the high amino acid sequence homology (73%) between the HA of pandemic

H1N1 and current circulating seasonal H1N1 (A/Brisbane/59/2007) virus, WHO recommends that seasonal influenza vaccine should be given together with pandemic H1N1 vaccine for highly susceptible populations (**Fig. 1.6c**). Due to the emergence of pandemic H1N1 virus in April 2009, a pandemic H1N1 vaccine trial was conducted at a single site in Chaoyang District, Beijing, China to assess the effectiveness of the new vaccine before the vaccination campaign.

The vaccines used in this study were manufactured by Sinovac Biotech Co., Ltd (Beijing, China). The vaccine was prepared in embryonated chicken eggs using standard procedures as described previously (Liang et al., 2009). The pandemic H1N1 vaccine was a monovalent, unadjuvanted, inactivated, split-virus vaccine. The seed virus was prepared from the reassortant vaccine virus NYMC X-179A (New York Medical College, New York), derived from the A/California/07/2009 (H1N1) virus. The virus strains for the seasonal vaccine were prepared from A/Brisbane/59/2007 (H1N1), A/Uruguay/716/07 (H3N2) (A/Brisbane/10/2007 H3N2-like virus) and B/Brisbane/60/2008 viruses, in accordance with the WHO recommended composition of vaccine virus for use in the 2009-2010 northern hemisphere influenza season.

Healthy, non-pregnant adults between 18 and 60 years of age were eligible for enrolment into this prospective, randomized, observer-blind, parallel-group clinical trial. Exclusion criteria included confirmed or suspected pandemic H1N1 infection and history of pandemic H1N1 or seasonal influenza vaccine during the preceding 6 months. A total of 151 healthy volunteers were enrolled. They were randomized and assigned into three groups. The randomization list was prepared by a statistician employed by Sinovac Biotech Co., Ltd. The vaccine administrator was provided with the randomization code in a sealed enveloped thus all subjects and investigators were masked from the assignments.

All groups received one dose (15 μg haemagglutinin) each of a licensed pandemic H1N1 vaccine and a seasonal trivalent vaccine. Each dose was administered intramuscularly, into the deltoid muscles of one of the arms. Group 1 received the pandemic H1N1 vaccine on day 0, followed by the seasonal flu vaccine on day 21. Group 2 received seasonal vaccine on day 0 and pandemic H1N1 vaccine on day 21. Group 3 received both vaccines simultaneously on day 0. Peripheral blood (20-30 ml) and serum samples (3-5 ml) were collected by venipuncture on day 0, 7, 21, 28 and 42 days after the first immunization. However, Group 3 received no second immunization on day 21 and therefore no 7-day follow-up samples were taken for this group on day 28 (**Fig. 2.2**).

PBMCs were isolated from the blood collected to assay for influenza-specific T cell responses using IFN-γ ELISpot.

In parallel, a similar study of a smaller scale was carried out to examine the phenotype and kinetics of activated T cells using flow cytometry (**Fig. 2.3**). Twenty eight subjects from the Chinese Centre for Disease Control and Prevention (China CDC) were enrolled and separated into two groups: Group A received one dose of pandemic H1N1 vaccine, and Group B received one dose of seasonal vaccine then one dose of pandemic H1N1 vaccine on day 21. Peripheral blood and serum samples were collected on baseline, day 7, 21, 28 and 42. T cell ELISpot and flow cytometry were performed to identify activated memory T cells in this longitudinal study.

The immunogenicity of the pandemic H1N1 and seasonal influenza vaccines was analysed by haemagglutination-inhibition (HI), microneutralization (MN) and B-cell ELISpot assays. These assays were performed with antigens or viruses from A/California/07/2009(H1N1), A/Brisbane/59/2007(H1N1) and A/Brisbane/10/2007(H3N2). Serological assays were performed by investigators not involved with the trial. B-cell assays were performed by Dr. Arthur Huang, who in parallel analysed the role of B cells. All samples were blinded and assays were performed in duplicate using procedures monitored by National Institute for the Control of Pharmaceutical and Biological Products (NICPBP), China.

To monitor the safety of the vaccines, subjects were requested to record underarm body temperature, any injection-site and systemic reaction on diary cards after an on-site safety observation of 30-min duration. Any local adverse event at the injection site and systemic adverse events were recorded for three days following immunization. The diameters of any erythema, swelling, indurations and rashes were determined by investigators. All adverse events were graded using standard scale (http://www3.niaid.nih.gov/LabsAndResources/resources/DMIDClinRsrch/toxtables.html).

These studies were in accordance with both Good Clinical Practice guideline and the Declaration of Helsinki. All subjects in the studies provided written informed consent. The protocol was approved by Beijing Centre for Disease Control and Prevention and the ethics review committee. The study was registered with ClinicalTrials.gov, number NCT01008137.

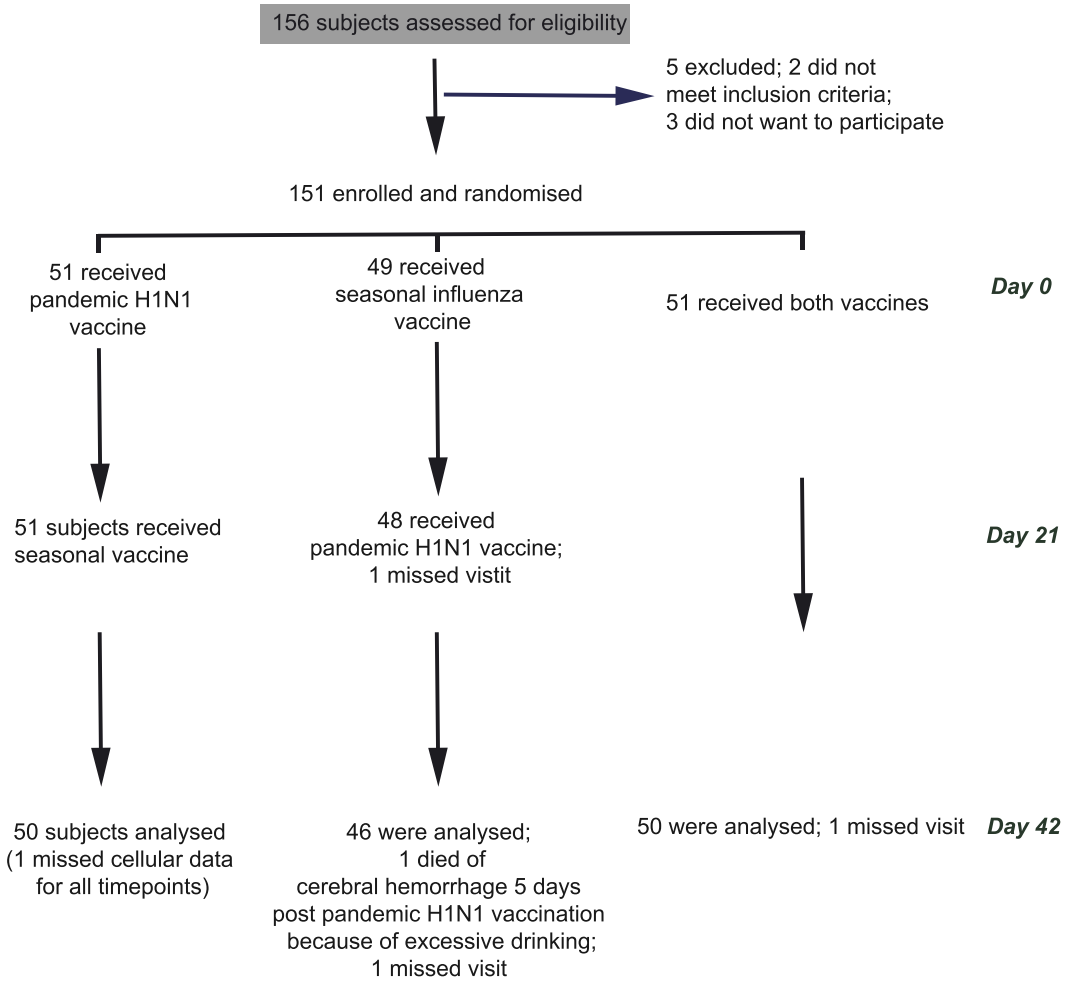

Figure 2.2 Enrolment and outcomes of pandemic H1N1 vaccine studies.

2.2.1.5 Pandemic H1N1 convalescence study (Siren study RHM Med 0914)

A convalescent cohort consisting 18 individuals who had recovered from pandemic H1N1 patients, was collected over two different periods (July 2010 and May 2011) in the UK. The illness onset time of the patients recruited was in January 2010, or January 2011. All patients were hospitalized, suggesting their illness was moderate to severe. Antigen-specific T cell responses against influenza epitopes identified in the challenge and vaccine cohorts were assessed in these subjects. PBMCs isolated from healthy laboratory workers before the pandemic (pre-2009) were used as a control.

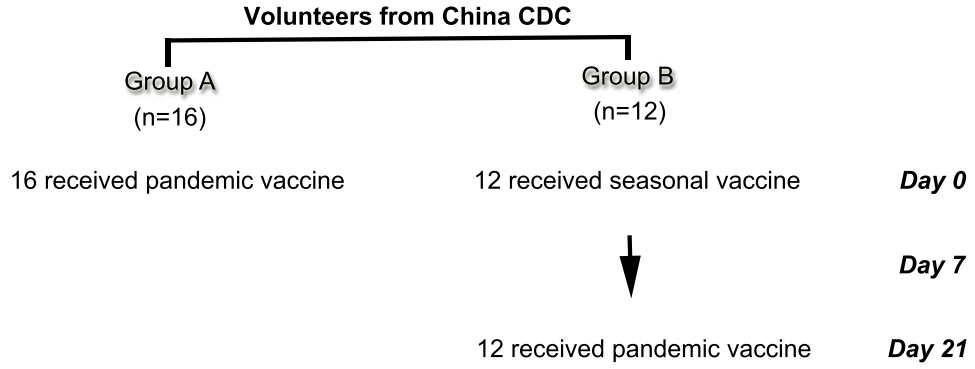

Figure 2.3 Enrolment and outcomes of the China CDC vaccination cohort.

2.2.1.6 Healthy adult donors

Blood specimens from about approximately 70 healthy laboratory volunteers working in Weatherall Institute of Molecular Medicine (W.I.M.M.), Oxford, UK (age 22–50 yr) were collected in order to study their influenza-specific T cell memory responses (Chapter 4, section 4.2.1) or to optimize all the flow cytometry and functional assays described in this thesis. All subjects provided written informed consent. Blood samples were also obtained from buffy coats or cones purchased from Blood Transfusion Service (John Radcliffe Hospital, Oxford).

2.2.2 Cellular immunology

2.2.2.1 Isolation of peripheral blood mononuclear cells (PBMCs)

Heparinised human blood samples were layered on 15 ml of lymphoprep in Leucosep tubes and centrifuged for 20 min, 2000 rpm at 20°C using a Heraeus Multifuge 3SR Plus (Thermo Scientific). After centrifugation, a cloudy white interface that rested above the frit of the Leucosep tube and below the top plasma layer should be present. Plasma was isolated and collected without disturbing the interface; while PBMCs present at the interface were transferred to a separate tube and RPMI medium 1640 (R0) was added to a total volume of 50 ml. The cells were then washed by centrifugation at 1800 rpm for 10 min. The supernatant was discarded and the pellet was washed again in RPMI medium 1640 (supplemented with 2% FCS, 2 mM L-glutamine, 100 μg/ml streptomycin, 100 U/ml penicillin) (R2) at 1000 rpm for 10 min. Finally, the cells

were resuspended in RPMI medium 1640 supplemented with 10 % FCS, 2 mM L-glutamine, 100 μg/ml streptomycin, 100 U/ml penicillin (R10). PBMCs were counted using ABX Pentra 60 cell counter (Horiba Medical) and each sample was adjusted to 1×10^6 cells/ml and used immediately. For cryopreserving of PBMCs, cells were resuspended in cold freezing medium [10% dimethylsulphoxide (DMSO) in FCS], aliquoted in freezing vials at 5×10^6 cells/ml and kept in a Nalgene Cryo 1°C Freezing container (Nunc, U.S.A.) at −80°C overnight to allow the temperature to decrease gradually. The cells were then transferred to liquid nitrogen tank for long-term storage until use.

2.2.2.2 Synthetic peptides

For the challenge studies, 18 amino acids long (18-mers) peptides overlapping by 10 amino acid residues and spanning the full proteome of the H1N1 and H3N2 influenza A viruses were designed using the Los Alamos National Library web-based software PeptGen (http://www.hiv.lanl.gov/content/sequence/PEPTGEN/peptgen.html) and synthesized (purity >70%; PEPscreen; Sigma-Aldrich) using the sequences of the following strains: A/Brisbane/59/2007 (H1N1), A/New York 388/2005 (H3N2) (surface proteins), and A/New York 232/2004 (H3N2) (internal proteins). For the H3N2 peptides, the amino acid sequence homology between challenge Wisconsin strain and New York strain is greater than 99%. The total numbers of peptides used in detecting antigen-specific responses for H1N1 and H3N2 was 554 and 601 respectively. In each IFN-γ ELISpot assay, each individual was simultaneously tested with all overlapping peptides using 2-dimensional matrices with a total of 52 pools (1st D = 25 pools; 2nd D = 27 pools; up to 25 peptides/pool) so that each peptide was present in two different pools (see **Fig. 3.4** for ELISpot layout). For the inactivated influenza vaccine studies, 18 amino acids long (18-mers) peptides overlapping by 10 amino acid residues and spanning the full proteome of the A/California/07/2009 (H1N1) were designed in a similar manner. The total numbers of peptides used in detecting antigen-specific responses for pandemic H1N1 HA and NA was 70 and 58 respectively. Each individual was simultaneously tested with all overlapping peptides using 2-dimensional matrices with a total of 23 pools (1st D = 11 pools; 2nd D = 12 pools; up to 12 peptides/pool) so that each peptide was present in two different pools (see **Fig. 5.1** for ELISpot layout). In all ELISpot assays, peptides were used at a final concentration of 2 μg/ml each. The putative peptide from each positive response well could be deconvoluted from the 2-dimensional matrix system where each peptide only appeared once in each dimension. The putative peptides

were then confirmed individually in a second ELISpot assay with the same input cell number per well (300,000). Additional peptide pools containing overlapping peptides spanning each individual viral protein (e.g. M pool, NP pool) were made.

2.2.2.3 ELISpot assay for human IFN-γ

ELISpot assays are highly sensitive assays for quantifying *ex vivo* antigen-specific T cell responses by measuring cytokine (e.g. IFN-γ) production at a single-cell level. They are performed using either freshly isolated PBMCs or cryopreserved PBMCs. The 96-well Multiscreen Filter Plates were coated by incubating 1:100 dilution of anti-human interferon-γ (IFN-γ) monoclonal antibodies (mAb; 1 mg/ml, 1-D1K) in sterile phosphate-buffered saline (PBS) overnight at 4°C. Plates were then washed with PBS three times and blocked with 250 μl/well of R10 at 37°C for 1 hour (h). PBMCs (300,000) were added to each well in the final volume of 100 μl, and peptide at a final concentration of 2 μg/ml was added. Control wells of cells incubated with media alone in quadruplicate (negative), EC (a mixture of EBV and CMV T cell epitopes), or with 10 μg/ml phytohemagglutinin (PHA) (positive) were also included. All ELISpot assays were performed using a human IFN-γ ELISpot kit (Mabtech AB) according to the manufacturer's instructions. After 18 h at 37°C, 5% CO_2, the plates were washed six times with PBS and incubated with a 1:1000 dilution of detection anti-human IFN-γ mAb (7-B6-1-Biotin) in PBS with 5% BSA at 50 μl/well for 2 h at RT. The plates were then washed six times with PBS and incubated with a 1:1000 dilution of alkaline phosphatase (ALP) conjugated streptavidin in PBS at 50 μl/well for 1 h at RT. Finally, the plates were washed three times with PBS and developed with AP conjugate substrate solution (4% 25x buffer, 1% colour reagent A, and 1% colour reagent B in milliQ water; AP conjugate substrate kit) at 100 μl/well for 30 min. Colour development was terminated by washing the plates with running water. The plates were dried and the spots were counted using automated ELISpot reader and AID ELISPOT 3.1.1 HR software (Autoimmune Diagnostika). One spot formed in a well reflects one IFN-γ- producing cell, while the size of the spot is proportional to how much IFN-γ is produced by that single cell. Values of T cells responses were adjusted by subtracting the mean number of spots in the negative controls of each individual plate, and expressed as Spot Forming Cells per 10^6 PBMCs (SFC/million) PBMC. The threshold values to consider a positive response was that the number of SFCs per well was greater than the mean values + 4 SD found in the three negative control wells (no peptide) in each individual, and that responses had to be greater than 50 SFC/million PBMCs. For single

peptide confirmation assay, responses greater than 10 SFC/million PBMC after background subtraction were considered positive. In all assays, background values of no peptide control wells were determined to be 1.8 ± 4.6 SFC/million PBMC from 150 healthy subjects and 2 ± 5.7 SFC/million PBMC from 150 influenza-exposed subjects.

2.2.2.4 Validation of ELIspot assays

To show that the cell depletion assay is justified to suggest that the responses showed by the CD8 depleted population is proportional to that of total PBMCs, PBMCs were isolated from a healthy subject who has showed memory T cell responses against M and NP proteins, a HLA-A2 restricted matrix specific peptide M1-9 (LTKGILGFVFTLTVPSER) and a peptide H3HA-45 (NVPEKQTRGIFGAIAGFI) that is known to be mediating CD4 response. Total PBMCs, CD4-depleted PBMCs and CD8-depleted PBMCs were stimulated with 2 μg/ml of peptide pools (M and NP), individual peptides M1-9 or H3HA-45, and the level of response (SFC/cells) was determined by *ex vivo* IFN-γ ELIspot. The sum of the responses from the CD4- and CD8- depleted cells in response to peptide stimulations were comparable to the level of response when total PBMCs were used instead. Depletion efficiency and cell purity were determined by flow cytometry.

2.2.2.5 $CD8^+$ T cells depletion

To examine the identity of the IFN-γ producing cells, peptide pools generating positive responses in *ex vivo* ELISpots were characterized by $CD8^+$ T cells depleted from fresh PBMCs using anti-CD8 antibody-coated magnetic beads ($CD8^+$ Dynabeads) according to manufacturer's protocol (Invitrogen). Briefly, PBMCs were resuspended in 1 ml of isolation buffer (0.1% BSA and 2mM EDTA in PBS), mixed with $CD8^+$ Dynabeads at a cell-to-bead ratio of 1:1 in an eppendorf tube. The mixture was incubated for 30 min at 4°C. The cells were then placed into a magnet for 2 min, and the CD8-depleted fraction contained in the supernatant was transferred to a new tube and washed using isolation buffer. The tube containing the beads-bound $CD8^+$ T cells was removed from magnet and cells were washed twice using the isolation buffer. After depletion, both fractions were tested with individual peptides in an ELIspot assay.

2.2.2.6 Generation of antigen-specific CD4+ and CD8+ T cell lines

To increase the sensitivity of ELIspot assays, PBMCs underwent a period of antigen-driven proliferation supported by the addition of IL-2 to enhance for low frequency Th1 responses. The culture period magnifies the responses by allowing T cells to divide and the resting central memory T cell responses to differentiate into effector cells. 1×10^6 PBMCs were pulsed as a pellet for 1 h at 37°C with 10 µl of 100 µM of peptide pools and cultured in H10 (RPMI medium 1640 supplemented with 10% human AB serum, 2 mM L-glutamine, 100 µg/ml streptomycin, 100 U/ml penicillin), together with 25 ng/ml of IL-7 in 48-well flat-bottom plate. IL-2 was added to a final concentration of 1000 U/ml every 3 days. The cells were cultured for 10-14 days at 37°C, 5% CO_2.

2.2.2.7 Generation of B cell lines (BCLs)

1×10^6 PBMCs were incubated with 100 µl of supernatant from an Epstein-Barr virus (EBV)-producing marmoset cell line, B95/8 for 3 h at 37°C in a 96-well U-bottom plate. Then, 1 µg/ml of cyclosporin A in 100 µl R10 was added. Half of the medium was changed every two days and cyclosporin A was replenished until two weeks post-transformation. When cell clumps were observed, the BCLs were expanded in larger volumes in small culture flasks and were tested for mycoplasma.

2.2.2.8 Maintenance of short-term T cell lines

After the establishment of influenza-specific T cell lines, in the subsequent rounds of stimulation and expansion, peptide-pulsed BCLs were used as antigen presenting cells. Autologous BCLs were pulsed with 10 µl of 100 µM of peptides for 1 h, washed and irradiated for 20 min at 40 Gy. Allogeneic PBMCs from 3 donors were also irradiated. Irradiated peptide pulsed BCLs were mixed with the T cell lines and the donor PBMCs at 1:1:4 ratios in H10. The cells were cultured for 10-14 days at 37°C, 5% CO_2. 1000 U/ml IL-2 was added every 3-4 days until day 14.

2.2.2.9 Cytotoxicity assay

The ability of the effector cells to recognize and kill target cells was assayed by a standard 4-h ^{51}Cr-release cytotoxicity assay. The autologous BCL was washed once with R10 and labeled with

3.7 MBq of $Na_2{}^{51}CrO_4$ solution for 45 min - 1 h. ^{51}Cr-labelled BCL was washed 3 times with R10 and then pulsed with 10 µl of 100 µM appropriate peptides at 37°C for 1 h. Peptide-pulsed cells were washed once and counted, and then resuspended in R10 to a concentration of 5×10^4 cells/ml. Inhibition of perforin-mediated cytotoxicity was obtained by incubating the $CD4^+$ T cells for 2 h with 100 nM concanamycin A (CMA) before being incubated with the target cells. Cells were plated out at 100 µl/well in a 96-well U-bottom plate containing 100 µl of peptide specific T cell lines at different effectors to target cell ratios. R10 alone and 5% Triton X-100 was used to measure spontaneous ^{51}Cr -release and maximum lysis of target cells respectively. Plates were incubated at 37°C for a further 4 h. Thereafter, 30 µl of supernatant was carefully removed and mixed with 170 µl of beta-scintillation fluid in a 96-well Beta counter sample plate. The amount of ^{51}Cr release was measured using the MicroBeta JET machine (liquid scintillation and luminescence counter).

The specific cytotoxicity of T cell lines towards autologous targets was measured as a percentage of maximal cytotoxicity (%):

$$\frac{\text{sample release} - \text{spontaneous release}}{\text{maximum release} - \text{spontaneous release}} \times 100$$

2.2.2.10 Isolation of genomic DNA and HLA typing

Genomic DNA was extracted from the red blood cell layers in the Leucosep tubes following PBMCs isolation. Red blood cells were lysed using RBC Lysis Solution. Following centrifugation at 3000 g for 5 min, supernatant was discarded and the pellet was resuspended in Cell Lysis Solution and Proteinase K Solution (final concentration: 20 mg/ml) to initiate cell lysis and protein degradation. The samples were incubated overnight at 55°C. Following incubation, the samples were cooled on ice for 5 min and 0.9 ml Protein Precipitation Solution was added. The samples were then vortexed and centrifuged at 4000 rpm for 10 min, and cooled on ice for 2 min. Subsequently, genomic DNA was precipitated by addition of 100% Isopropanol and centrifuged at 4000 rpm for 3 min. After decanting the supernatant, the pellets were washed with an equal amount of 70% ethanol and centrifuged at 4000 rpm for 1 min. The ethanol was carefully decanted, and the DNA was hydrated using 200 µl of DNA Hydration Solution and sent for typing. All the subsequent processes for HLA typing were carried out by Tim Rostron at the DNA Sequencing Unit at W.I.M.M., Oxford. Briefly, SSP (Sequence Specific Primer) -PCR

was employed to carry out high-solution typing in the following loci: HLA-A, HLA-B, HLA-C, Bw, DRB1, DRB3/4/5 and DQB1.

2.2.2.11 Cultured ELISpot

Cultured ELISpot allows responding T cells to be enriched *in vitro* prior to the assay. T cell lines were washed 4 times using RPMI then rested in H10 for 30 h at 37°C, 5% CO_2. Cells (40 000) were used in each ELISpot well and were stimulated with individual peptides at a concentration of 2 μg/ml.

2.2.2.12 Intracellular cytokine staining (ICS) and flow cytometry

ICS was used to phenotype cytokine-producing T cells upon stimulation. Although less sensitive than ELISpot (limit of detection: 0.05%), it allows multiple properties (function and phenotype) of a single T cell to be analyse simultaneously. Cells (PBMCs or T cell lines) were incubated with peptide antigens in the presence of costimulatory antibodies and a secretion inhibitor [e.g. Brefeldin A (BFA)] to inhibit cytokine release and allow intracellular cytokine accumulation. After stimulation, cells were stained with fluorochrome-conjugated antibodies against markers of interest. In flow cytometry experiments, all fluorochrome-conjugated antibodies were titrated to optimize the volume used for staining. "Fluorescence minus one" (FMO) controls, where cells are stained with all the other antibodies except the one under investigation in a staining experiment, are used to define positive and negative gates for each fluorochrome-conjugated antibody.

ICS for phenotyping influenza-specific T cell lines

T cell lines were washed 4 times using R0 then rested in H10 for 30 h at 37°C, 5% CO_2. Cells ($5X10^5$ cells/stimulation) were incubated with 1 μg/ml each of the co-stimulatory antibodies anti-CD28 and anti-CD49d and peptides (final concentration: 2 μg/ml) volume for 1 h at 37°C. Staphylococcal enterotoxin B (SEB), at 2 μg/ml, stimulation was carried out as a positive control. Appropriate negative controls (PBMC plus no peptide) were included to control for the spontaneous production of cytokines. Cells were then incubated with BFA (final concentration: 10 μg/ml) in a 500 μl for a further 16 h at 37°C.

The FACS buffer was prepared by adding FCS to PBS to a final concentration of 2.5 % (v/v). All cell washes were performed using 2 ml FACS buffer followed by centrifugation (1500 rpm, 5 min). Following stimulation, cells were incubated with 50 nM EDTA for 15 min. Cells were then washed once, and the pellet was resuspended in 500 µl of BD FACS Permeabilization solution 2, vortexed vigorously for 10 seconds and then left for 15 min. After fixation and permeablization, the cells were stained with directly conjugated antibodies specific for surface (e.g. CD3, CD4 and CD8) and intracellular markers (e.g. IFN-γ) for 30 min (section 2.1.11). The cells were washed once and resuspended in FACS wash. Flow cytometry analysis was performed using CyAn ADP flow cytometer (Beckman Coulter) and Flowjo (version 9.4.11, Tree Star). In most experiments at least 100 000 events were acquired. Fluorescence compensation was carried out using cells stained with single fluorochrome of interest on each day of testing. A cytokine response greater than 3 times the negative control was considered positive.

ICS for analysing polyfunctionality of influenza-specific T cells

In analysing the polyfunctionality of influenza-specific T cells, PBMCs from the H3N2 challenge study were stimulated and stained in V-bottomed plates instead of using FACS tubes. This experiment was carried out in Vaccine Research Centre, National Institute of Health (VRC, NIH). The majority of antibodies used are commercially available (section 2.1.11), however, CD57-QD585, CD14-QD605, CD19-QD655 antibodies were conjugated in NIH by Dr. Mario Roederer, Dr. Pratip Chattopadhyay and Joanne Yu, according to standard protocols (http://drmr.com/abcon/index.html).

Frozen PBMCs were thawed and rested for 3.5 h before plating at 100 µl (1×10^6 cells per well). Another 100 µl of R10 containing BFA (10 µg/ml), GolgiStop (0.7 µl/ml) and CD107a-FITC (20 µl/ml), 1 µg/ml of each of the co-stimulatory antibodies anti-CD28 and anti-CD49d, together with peptide pools (2 µg/ml) (M, NP or total H3N2 Flu pool) were used to stimulate cells. In the positive controls, SEB (2 µg/ml) was used instead of peptides. After 6 h at 37°C and 5% CO_2, cells were washed twice with PBS (2000 rpm for 3 min). Live/Dead amine-reactive dye Aqua was diluted 1:40 and added to the plate for 10 min in the dark. Without washing, a surface antibodies master-mix (CD45RO-PE TexasRed, CD27-PECy5, CD4-PECy5.5, CD3-APC-H7, CD57-QD585, CD14-QD605, CD19-QD655, CD8-QD705) of pre-titered amounts was added and incubated for 30 min under foil at 4°C. Cells were then washed twice with PBS by

centrifugation at 2000 rpm for 3 min. Cell permeablization was carried out by resuspending cells in 100 μl of Cytofix/Cytoperm for 30 min under foil at 4°C. Cells were then washed twice by adding Perm/Wash Buffer (1:10 dilution in MilliQ water) and centrifuged for 3 min at 2200 rpm. Cells were then stained with intracellular antibodies mix (Perforin-PE, TNF-α -PECy7, IL-2-APC, IFN-γ-V450) for 1 h under foil at 4°C. Finally, cells were washed twice with Perm/Wash by centrifugation for 3 min at 2200 rpm and were fixed in 250 μl of 1% paraformaldehyde. 14-colour cytometry was performed on a LSRII (BD Immunocytometry Systems). A minimum of 300,000 events was collected per sample. Electronic compensation was conducted using antibody capture beads (BD Compbeads) stained separately with individual monoclonal antibodies.

Data analysis

Data analysis was performed using FlowJo (version 9.4.11; TreeStar). Briefly, I identified lymphocytes based on size and granularity by forward/side scatter. I then gated on singlets based on Forward Scatter Height (FSC-H) and Forward Scatter Area (FSC-A). Then B cells ($CD19^+$), monocytes ($CD14^+$) and non-viable T cells were excluded (Live/Dead $Aqua^+$ $CD3^+$). $CD3^+$ $CD8^-$ $CD4^+$ T cells or $CD3^+$ $CD4^-$ $CD8^+$ T cells versus IFNγ were sequentially selected to account for receptor down-regulation. Non-naïve $CD4^+$ and $CD8^+$ cells were gated using CD45RO and CD27. Naïve T cells (which have never encountered specific antigens) are defined as $CD45RO^-$ $CD27^+$ and were excluded during all analyses; memory cells are defined as $CD45RO^+$ $CD27^+$; while mature effector T cells are defined by the absence of CD27 expression, $CD45RO^+$ $CD27^-$ are effector memory T cells, while $CD45RO^-$ $CD27^-$ are terminally differentiated effector memory RA^+ T cells. Flu-specific responses were analysed by intracellular cytokine production of non-naive cells. Boolean gating analysis was carried out once the positive gates were established for each functional parameter (**Fig. 4.6**). Gates for specific cytokine production were set based on spontaneous release of cytokines by unstimulated controls. This analysis thus resulted in a total of 32 possible functional combinations. Importantly, two combinations were ignored in all analyses: (1) events which are negative for all measured functional parameters ($Perforin^-$ $TNF\text{-}\alpha^-$ $IL\text{-}2^-$ $IFN\text{-}\gamma^-$ $CD107a^-$) and (2) perforin-single and CD107a-single positive cells. In this way, only perforin and CD107a production in response to antigen-specific stimulation was measured and that their expression was considered only within activated flu-specific T cells expressing at least one other functional parameter. Data have been corrected for background based on the unstimulated control (anti-CD28/CD49d only and no peptide). Only response with a total

frequency above 0.01% of total $CD4^+$ and $CD8^+$ memory T cells (after background subtraction) were considered to be positive. Negative values (where response frequency in the unstimulated control was greater than the peptide-stimulated sample) and values below the threshold were set to zero. The threshold was used to avoid a systemic bias incurred by zeroing only negative values. Graphs were made using Pestle (version 1.6.2, provided by Mario Roederer) and SPICE (version 5.22, provided by Dr. Mario Roederer). Pie graphs were analysed by SPICE in-built permutation test.

2.2.2.13 Immunophenotyping of activated cells

Activated ($CD38^+$) and proliferating (Ki-67^+) cells in PBMC samples were stained with mAbs against Ki-67-FITC, CD38-APC, CD8-PECy5 and CD4-Pacific Blue. The results were analysed on a CyAn ADP flow cytometer (Beckman Coulter) and by using Flow Jo (version 9.4.11, Tree Star).

2.2.2.14 Epithelial Cell MHC Class II Expression

Immunohistochemistry

Lung explants were harvested from lung tissue recovered from patients undergoing routine thoracic surgery under additional consent. Prior to embedding in GMA resin, human parenchymal and bronchial tissue was fixed in acetone. Two millimetre sections were cut sequentially and immunostained using isotype control monoclonal antibodies or antibodies specific for MHC II (HLA-DR) at the same concentration. Avidin-Biotin Complex (ABC) system was used to amplify the signals, and 3,3′-Diaminobenzidine (DAB) stain was used to develop colour. This experiment was performed by Dr. Tom Wilkinson, Southampton University.

Flow cytometry

Primary bronchial epithelial cells (PBECs) were obtained from subjects undergoing research bronchoscopies in the Wellcome Trust Clinical Research Facility at Southampton General Hospital. Bronchial brushings were cultured in Bronchial Epithelium Growth Media (BEGM), in collagen coated flasks (PureCol™) and incubated in a humidified atmosphere at 37°C, 5% CO_2. The collection and use of these samples were approved by the Southampton and South West Hampshire Research Ethics Committee (REC No: 06/Q1701/98 & 08/H0504/138).

Influenza A virus strain X31 was provided at a concentration of 4×10^7 pfu/ml. Inactivated virus (UVX31) was prepared by exposure to an ultra-violet (UV) light source for 2 h. PBECs were seeded at 1×10^5 cells per well onto a collagen-coated 24 well plate and left at 37°C, 5 % CO_2 for 24 h. Cells were then growth media starved for 24 h in 0.5 ml Bronchial Epithelium Basal Media (BEBM) supplemented with 1 mg/ml BSA, insulin, transferrin and selenium (BEBM+ITS). Cells were incubated for 2 h with no virus, or 2×10^3 pfu of X31 or UVX31. Cells were then washed three times with BEBM+ITS and incubated for a further 20 h at 37 °C, 5% CO_2 in 0.5 ml of BEBM+ITS. Cells were treated with trypsin and prepared for flow cytometry analysis.

Samples were incubated on ice in the dark for 30 min with either anti-HLA-DR APC-Cy7 or the appropriate isotype control (IgG2a). After washing, intracellular staining for viral nucleoprotein (NP)-1 was performed using BD Cytofix/Cytoperm kit according to manufacturer's instructions, and AlexFluor 488 (AF488)-conjugated anti-NP-1 antibody. Flow cytometry analysis was performed on a FACSAria using FACSDiva software v5.0.3 (BD Biosciences). This experiment was performed by Dr. Tom Wilkinson, Southampton University.

2.2.2.15 Virology and Serology Assays

Virus titration by $TCID_{50}$

$TCID_{50}$ assay (Tissue Culture Infectious Dose 50%) assay is an end-point dilution assay measuring viral titers. It assesses the virus dilution where 50% of the cell cultures were infected. Viral load in the nasal lavage samples were determined by $TCID_{50}$ assay as described by the WHO manual of Animal Influenza Diagnosis and Surveillance (World Health Organization Global Surveillance Network, 2011). Serial ten-fold dilutions of virus-containing samples were inoculated into 96-well microtitre plates seeded with Madin-Darby canine kidney (MDCK) cells, and incubated for 5–6 days at 37°C. Cytopathic effects in individual wells were determined by light microscopy. A titre greater than 1:5 was considered positive. This work was carried out by collaborators at Retroscreen Virology Ltd.

Hemagglutination Inhibition (HI) Assay

The HI assay measures antibody responses to influenza HA proteins. HA can agglutinate erythrocytes and antibodies specific to the viral HA can interfere with the binding between HA and its receptors on erythrocytes. Hemagglutinin-specific antibody titers (HI titers) against H1N1

(A/Brisbane/59/2007) or H3N2 (A/Wisconsin/67/05) in the serum samples were determined by HI assay using chicken erythrocytes as described in the WHO manual (World Health Organization Global Surveillance Network, 2011). Briefly, serum samples were pre-treated with receptor destroying enzyme (RDE) to prevent non-specific hemagglutination for 16 h at 37°C, and were subsequently tested in a standard hemagglutination inhibition test using red blood cell solution and 4 HA units of virus antigens. Treated serum samples were serially diluted by 2-fold from 1:10 dilution. Red blood cells that are not bound by the virus (hemagglutination inhibited) will sink to the bottom of the round-bottom well and a tear-shaped streaming can be observed when the plate is tilted. The reciprocal of the highest dilution of serum that showed complete inhibition hemagglutination was expressed as HI titers. This work was carried out by collaborators at Retroscreen Virology Ltd (Chapter 3 and 4) and at China CDC (Chapter 5 and 6).

Microneutralisation (MN) Assay

MN assay is used to determine the level of influenza-neutralizing antibodies. In MN assay, heat-inactivated serum samples of serial dilution were first mixed with live vaccine virus for 1 h at 37°C. It is followed by incubating the mixture with Madin-Darby canine kidney cells for 5 days to check for cytopathogenicity. The titre was calculated by the Reed-Muench method, as described by the WHO manual (World Health Organization Global Surveillance Network, 2011). This work was carried out by collaborators at China CDC (Chapter 5 and 6).

2.2.3 Molecular Biology

2.2.3.1 Construction of recombinant vaccinia viruses (rVACVs)

Construction of rVACVs plasmids

Plasmids for rVACVs were kindly constructed by China CDC, Beijing. The M1 open reading frames of the cDNA copy of RNA segment 7 from A/California/07/2009 (H1N1) and A/Brisbane/59/07 (H1N1) were amplified by PCR using the following primers designed to introduce a Kozak sequence around the initiating methionine codon (shown in bold) and unique NotI and SmaI restriction sites (underlined) for subcloning:

5′-ATAAGAAT <u>GCG**GCCGC**</u> **CACC atga**gtcttc taaccgaggt cgaaacgta-3′ (5′ primer);

5′- CTAGGCCTT CCCGGG tcacttgaatcgctgcatctgcactccc -3′ (3′ primer).

The PCR product was digested with EcoRV and SmaI, and cloned into a SmaI site of the VACV expression vector pSC11 downstream of the 7.5k promoter. The resultant plasmid was termed pSC11-H1N1 M1 and pSC11-H1N109 M1. The fidelity of the DNA sequence was confirmed by sequencing. This plasmid was used to construct rVACV-expressing M1.

Transformation of DH5α cells

To increase the quantity of the DNA, vaccinia plasmids containing M proteins (pSC11-H1N1 M1 and pSC11-H1N109 M1) were transformed into competent DH5α cells. Plasmid DNA (1-10 ng) was added into 50 μl of thawed DH5α cells, and incubated for 30 min on ice. Cells were heat shocked in a 42°C water bath for 30s, then placed on ice for 2 min. 250 μl of pre-warmed S.O.C. medium was added to the cells, then was incubated for 1 h at 37°C shaking at 225 rpm. The transformation reaction was then plated on a LB (Luria-Bertani) plate containing 100 μg/ml ampicillin and was incubated overnight at 37°C. Colonies were picked and incubated on 5 ml of LB medium at 37°C overnight shaking at 225 rpm. Plasmid DNA was extracted and purified using a QIAprep Spin Miniprep Kit. All plasmids were sent for sequencing at WIMM.

Transfection of TK-143 cells infected with wild-type vaccinia

A thymidine kinase–negative rVACV expressing the H1N1 M1 was constructed by transfecting pSC11-H1N1 M1 or pSC11-H1N109 M1 together with wild type vaccinia into TK-143 cells. Confluent TK-143 cells were grown in 75cc flask in D10 (DMEM supplemented with 10% FCS, 2 mM L-glutamine, 100 μg/ml streptomycin, 100 U/ml penicillin). The evening before the transfection, the cells were treated with 0.125% trypsin for 1 min at RT and were harvested. One third of the cells in 10 ml were then seeded in 10 ml in 25cc flask, while the remaining were discarded. The following day, the cells were infected with wild-type vaccinia. The medium was removed from the monolayer, and 1 ml of vaccinia virus [final concentration: 5×10^5 plaques forming unit (pfu)/ml] diluted in VDM (virus dilution medium, 0.1% BSA in RPMI) was added and incubated for 2 h at 37°C with intermittent redistribution of virus by gentle tilting. While infecting the TK-143 cells, the plasmid DNA (pSC11-H1N1 M1 or pSC11-H1N109 M1) to be transfected was prepared using Effectene Transfection Reagent (Qiagen), according the manufacturer's instruction. Briefly, 2 μg of miniprep purified plasmid DNA was added to 150 μl of buffer EC and 16 μl of enhancer, then incubated for 5 min at room temperature (RT). 20

μl of effectene was then added and the mixture was incubated for a further 10 min, then 1 ml of D10 buffer was added. After the infection of TK-143 cells, the medium was removed from the monolayer. The DNA mixture was added together with 3 ml of D10. The cells were then incubated at 37°C, 5% CO_2 for 2 days, until the characteristic cytopathic effect was evident throughout the monolayer. The infected cells were then harvested by scraping them off the plastic into the medium. The medium was then decanted into a 15 ml tube, centrifuged at 1500 rpm for 5 min and the cells were resuspended in 0.5 ml of VDM. The mixture was vortexed and freeze-thawed for three times. The supernatant containing the crude recombinant virus was subsequently decanted into sterilized eppendorf tubes then was stored at −80°C.

Purification of plaque

Three 6-well plates were prepared from a confluent flask of TK-143 cells and incubated overnight at 37°C, 5% CO_2. All medium from the cells was drained off carefully, without disturbing the monolayer. 0.5 ml of crude virus (1: 100 dilution from stock) was added to each of the 18 wells. The viruses were evenly distributed by tilting, and were incubated at 37°C, 5% CO_2 for 2 h with intermittent redistribution.

i) Selection of recombinant virus in 5-bromodeoxyuridine (BUdR)

At the end of infection, the virus was removed from the monolayer and an Agarose/MEM/BUdR overlay was prepared. 2% LMP Agarose was sterilized by autoclaving. Briefly, warm 2×MEM was added to FCS, BUdR and 2% LMP Agarose. The mixture was then drawn up in a 20 ml syringe through a straw, and 3 ml of mixture was gently dispensed onto each of the 6 wells without disturbing the monolayer. The plate was left for 30 min at RT to allow the mixture to set. The cells were then incubated at 37°C, 5% CO_2 for 2-3 days, depending on the appearance of the plaques.

To make 200 ml 2×MEM (filtered through a 0.22 μm syringe filter):

	(ml)
7.5% Sodium Bicarbonate	10
100×Pen/Strep	4
Sterile water	146
10×MEM	40

To prepare Agarose/MEM/BUdR overlay for one 6-well plate:

	(ml)
Warm 2×MEM	9
FCS	0.45
BUdR (5 mg/ml in PBS)	0.09
2% LMP Agarose (at 37-45°C)	9

ii) Visualizing recombinant plaques

On the second or third day of incubation, a 5-Bromo-4-chloro-3-indolyl-β-D-galactoside (X-gal) overlay was prepared using 2×MEM, 2% LMP Agarose and X-gal. The mixture was then drawn up in a 20 ml syringe through a straw, and 3 ml of mixture was gently dispensed onto each of the six well without disturbing the monolayer. The plate was left for 30 min at RT to allow the mixture to set. The cells were then incubated at 37°C, 5% CO_2 overnight.

To prepare X-gal overlay for one 6-well plate:

	(ml)
Warm 2×MEM	9
2% LMP Agarose (at 37-45°C)	9
X-gal (30 mg/ml in Dimethylformaide)	0.18

iii) Pick plaques

The next day, using an inverted microscope, at least 6 blue plaques that were well separated from any other blue plaques were picked by using a sterile Pasteur pipette to core out the plaque through the agarose, ensuring the infected cells of the plaque have been collected. The plaques were washed into 0.5 ml of VDM in a sterile eppendorf tube. The mixture was vortexed and freeze-thawed for three times. The supernatant containing the crude recombinant viruses were then decanted into sterilized eppendorf tubes and stored at −20°C.

At least three of the collected plaques were purified. Three 6-plates (one of each plaque) were prepared from a confluent flask of TK-143 cells. The following day, 0.3 ml of 0.5 ml plaque viruses were diluted into 3ml of VDM. 0.5 ml of the diluted viruses was then placed into 6 wells of confluent TK-143 cells each. The viruses were spreaded by tilting, and incubated at 37°C for 2 h with intermittent redistribution. The overlaying steps were repeated for another two times to further purify the plaques. The resulting purified viruses were termed H1N1 M1-VACV and H1N1 2009 M1-VACV.

Propagation of vaccinia virus

Vaccinia or recombinant viruses were propagated by infecting TK-143 cells with the virus. The cell-associated viruses were released by three cycles of freezing and thawing. Monolayers of TK-143 cells were infected with lysates of vaccinia virus at the multiplicity of 1 to 2 pfu per cell. Incubation at 37°C, 5% CO_2 was continued for 2-3 days, until the characteristic cytopathic effect was evident throughout the monolayer.

Plaque assay for virus

A plaque assay is used to measure the titer of recombinant virus. Viruses at different $\log_{10}$ dilutions were allowed to adsorb to the monolayers of TK-143 cells for 2 h. 3 ml of complete D10 was added to the monolayers and incubated at 37°C, 5% CO_2 for 2 days. The medium was then removed and washed gently with PBS once. The monolayers were stained with 1 ml of crystal violet for 5 min. Excess stain was washed away with PBS and the dish was allowed to airdry at RT. Plaques appeared as unstained areas of the well and could be counted easily.

Antibodies staining for plaques

To check for expression of the recombinant proteins upon infection with the rVACVs within plaques, monolayers of TK-143 cells in 6-well plate were infected with the virus for 2 h then 3 ml of complete D10 was then added to the monolayers and cultured at 37°C, 5% CO_2 for 2-3 days. The monolayers were washed once with PBS and then fixed with 4% formaldehyde for 30 min at 4°C. The cells were then washed once with PBS/20 mM glycine, and incubated with PBS/20 mM glycine/0.5% Triton X-100 for 20 min to block residual aldehyde group. The monolayers were washed twice with staining buffer (PBS/0.1% BSA/0.05% sodium azide), followed by staining with 0.3 ml of primary antibodies against influenza matrix protein (diluted 1:1000) with occasional shaking for 1 h at RT. The monolayers were then washed with staining buffer twice, and incubated with 0.3 ml of the secondary antibodies (Goat anti-mouse immunoglobulin HRP, 1:1000) for 1 h at RT. The monolayers were then washed by PBS/0.05% Tween-20. 0.3 ml of the peroxidase substrate TrueBlue was added for 20 min to allow visualization of the plaques expressing recombinant proteins. The reaction was stopped by washing the plates twice with distilled water.

Antibodies staining for virally infected L-cells

To check for expression of the recombinant proteins upon infection with the rVACVs (H1N1 M1-VACV and H1N1 2009 M1-VACV), 5×10^4 L-cells were treated with trypsin and plated on glass slides at a volume of 50 µl overnight. The next day, medium was removed and 50 µl of virus was used to infect the cells for 1.5 h. The medium was then removed and was replaced with 50 µl of R10 and was incubated for a further 6 h (2-3h minimum). The slides were then fixed in acetone for 5 min and left to airdry overnight. The next day, the slide was marked properly with a hydrophobic barrier pen. Either 40 µl of primary antibodies against influenza matrix protein (diluted 1:1000) or Tris-buffered saline (TBS) at pH 7.5 was added to the wells and incubated for 1 h at RT. The slides were then washed twice in TBS. Goat anti-mouse immunoglobulin HRP (diluted 1:100) was added to the cells and incubated for 30 min at RT. The slides were washed with TBS twice. SIGMAFAST 3,3′-Diaminobenzidine tablets made up in distilled water was added to the cells for a maximum of 20 min. Slides were washed twice in tap water and soaked in counterstain haematoxylin for 1.5 min. The slides were then washed again with tap water and were mounted under cover slips. Infected cells were visualized under a microscope.

Similarly, the concentration of vaccinia virus used in infecting B cell lines was determined by infecting B cell lines with rVACVs. B cells were infected with different dilutions of rVACV-M1 in R0 for 1.5 h and were fixed onto a microscopy slide by cytocentrifugation (cytospin), as B cells are not adherent. The slides were then fixed in acetone for 5 min and left to air-dry overnight. Staining procedures were carried out as described above to optimize the concentration of virus used for infection.

Cytotoxicity assay

To assay the ability of the effector cells to recognize processed antigens of virally infected target cells, a standard 4-h ^{51}Cr -release cytotoxicity assay was carried out. The autologous BCL was washed once with R10 and labeled with 3.7 MBq of $Na_2{}^{51}CrO_4$ solution for 45 min to 1 h. ^{51}Cr -labelled BCLs were washed 3 times with R10 and then infected with either 10 pfu/cell of H1N1 M1-VACV and H1N1 2009 M1-VACV in RPMI+BSA for 90 min. Infected BCL were washed once and rested in R10 for 2.5 h to allow expression of the viral proteins. They were then counted, and resuspended in R10 at a concentration of 5×10^4 cells/ml. Cells were plated out at 100 µl/well in a 96-well U-bottom plate containing 100 µl of peptide specific T cell lines at different effectors to target cell ratios. R10 alone and 5% TritonX-100 treated controls were used to measure spontaneous ^{51}Cr -release and maximum lysis of target cells respectively. Plates were incubated for a further 4 h at 37°C. Thereafter, 30 µl of supernatant was carefully removed and mixed with 170 µl of beta-scintillation fluid in a 96-well Beta counter sample plate. The amount of ^{51}Cr release was measured using the MicroBeta JET machine (liquid scintillation and luminescence counter).

The specific cytotoxicity of T cell lines towards autologous targets was measured as a percentage as follows:

$$\frac{\text{sample release} - \text{spontaneous release}}{\text{maximum release} - \text{spontaneous release}} \times 100$$

2.2.4 Assays for circulating follicular T helper cells

2.2.4.1 T cell proliferation assay

The ability of the T cell to proliferate in response to antigen is assayed using Carboxyfluorescein diacetate succinimidyl ester (CFSE). CFSE is a fluorescent green dye which binds to cytoplasmic components of cells covalently. Upon the cell division, the concentration of the dye of the CFSE- labeled cells is halved; by analysing the mean fluorescence intensity of CFSE using a flow cytometer, one can determine the number of cell division undergone by cells in culture over a period of time.

Freshly sorted $CXCR5^+$ and $CXCR5^-$ $CD4^+$ T cells were washed once with PBS before resuspending in PBS/0.1% FCS in a final concentration of $1x10^6$ cells/ml, whilst vortexing (to ensure the equal uptake of the dye), CFSE was added at a final concentration of 10 μM. Cells were incubated with the dye for 10 min at 37°C followed by quenching by the addition of 5 volumes of ice-cold R10. Cells were then incubated for 5 more min on ice. Cells were pelleted and washed three times with fresh R10. Labeled $CD4^+$ T cells were then cultured with autologous monocytes pre-incubated for 15 h with purified inactivated influenza vaccine antigens at 37°C, 5% CO_2. On day 5, cells were washed once with FACS wash then stained with fluorochrome labeled antibodies (anti-CD4 and anti-CD14) for 30 min at 4°C, washed and the proliferation of $CD4^+$ T cells were analysed on a CyAn ADP flow cytometer (Beckman Coulter).

2.2.4.2 Phenotyping of blood and tonsillar follicular helper cells

Frozen human tonsillar cells were kindly provided by Prof. Nick Willcox (WIMM, Oxford). Fresh PBMCs were isolated from healthy human volunteers. Both PBMCs and tonsillar cells were stained for antibodies against CD3, CD4, CD45RO, CXCR5, ICOS, CD57 and PD-1 for 30min at RT, and analysed on CyAn ADP flow cytometer (Beckman Coulter). Blood follicular T helper cells were defined as $CD4^+$ T cells that were $CD45RO^+$ and $CXCR5^+$.

2.2.4.3 Isolation of B cells

B cells were positively selected from PBMCs of healthy donors using $CD19^+$ Dynabeads. Briefly, PBMCs were resuspended in buffer (0.1% BSA and 20 mM EDTA in PBS). $CD19^+$ Dynabeads

were added to the cell suspension using a target-to-bead ratio of 1:10. The cell-bead mixture was transferred to sterile eppendorfs and incubated for 20-30 min at 4°C on a rotator. Bound cells were then captured using a magnet. The CD19 depleted population was subsequently used to isolate for $CD4^+$ T cells (section 2.2.4.4). To detach B cell population from the beads, DETACHaBEAD was added at a volume ratio of 1:2.5 of Dynabeads added for isolation. The eppendorfs were rotated for 45 min at RT on a rotator. After incubation the eppendorf was placed in the magnet and the cells were collected. The remaining beads were washed twice by pipetting, in order to maximize cell recovery. The total B cells were then stained with antibodies against CD3, CD19 and CD27 to sort by flow cytometry using cell sorter MoFlo (Beckman Coulter) into naïve B cells ($CD3^-$ $CD19^+$ $CD27^-$) and memory B cells ($CD3^-$ $CD19^+$ $CD27^+$).

2.2.4.4 Isolation of $CD4^+$ T cells

To isolate a pure population of $CD4^+$ T cells for coculture, $CD4^+$ T cells were negatively enriched from CD19-depleted PBMCs using $CD4^+$ T Cell Isolation Kit II (Miltenyi Biotec) and a magnetic cell sorter according to the manufacturer's instructions. Briefly, PBMCs were incubated with a $CD4^+$ T-cell isolation cocktail containing biotin-conjugated anti-human CD8, CD14, CD16, CD19, CD36, CD56, CD123, TCR$\gamma\delta$, and glycophorin-A antibodies for 10 min at 4°C and then labelled with magnetic bead-conjugated streptavidin. Subsequently, the cells were washed and subjected to separation on MS (up to 10^7 magnetically labeled cells) or LS (up to 10^8 magnetically labeled cells) columns (Miltenyi Biotec). Untouched $CD4^+$ T cells in the pass-through fraction were resuspended in R10. The total $CD4^+$ T cells were then stained with antibodies against CD3, CD4, CD45RO and CXCR5 and to sort by flow cytometry using cell sorter MoFlo (Beckman Coulter) into memory $CXCR5^+$ cells ($CD3^+CD4^+CD45RO^+CXCR5^+$) and memory $CXCR5^-$ cells ($CD3^+$ $CD4^+$ $CD45RO^+$ $CXCR5^-$).

2.2.4.5 Co-culture of $CD4^+$ T cells and B cells

3×10^4 of naïve B cells were co-cultured with equal numbers of either sorted memory $CXCR5^+$ cells or memory $CXCR5^-$cells in 96-well U-bottomed plate, in the presence of 1 μg/ml SEB for 15 days at 37°C, 5% CO_2. Subsequently, the culture supernatants were collected and immediately stored at −20°C. The enzyme-linked immunosorbent assay (ELISA) was performed to analyse antibodies levels in the culture supernatant. Frequency of plasmablasts was analysed by staining the harvested cells with CD38, CD20 and CD3 at the end of the culture period.

2.2.4.6 ELISA for IgA, IgM and IgG

The production of antibodies (IgA, IgM and IgG) by B cells was determined using commercial ELISA kits (Mabtech). ELISA plates were coated with mouse monoclonal anti-human IgG (2 μg/ml) at 100 μl/well and left overnight at 4°C. The plate was washed five times in PBS, and blocked with incubation buffer [PBS with 3% bovine serum albumin (BSA) and 0.05% Tween-20] at 200 μl/well for 1 h at RT on a shaker. The plate was then washed another five times with wash buffer (0.05% Tween-20 in PBS). After washing, the supernatants from tissue culture were diluted accordingly (1:1, 1:25 and 1:50) with incubation buffer, and were added at 50 μl/well and incubated for 2 h at RT. All the samples and standards were simultaneously tested in duplicates. For a standard IgG curve, human IgG standards were prepared in the range of 0.5-100 ng/ml. The plate was then washed six times with wash buffer, and the goat anti-human IgG antibody conjugated with alkaline phosphatase (diluted 1:1000 in incubation buffer) was added at 100 μl/well and incubated for 1 h at 37°C. After washing five times with wash buffer, the plates were developed with p-nitrophenyl-phosphate solution (pNPP) at 100 μl/well for 10 min at RT. pNPP solution was prepared by mixing together 1 ml of 5×diethanolamine buffer and 4 ml of water for each pNPP tablet. A yellow colour results when pNPP solution reacts with alkaline phosphatase-labeled conjugates, and the optical density (OD) can be measured at 405 nm on a microplate reader with Microplate Manager software version 6 (MPM6, Bio-Rad Laboratories, Netherlands). Sample was considered to be positive if the OD reading was higher than the mean OD value +2 standard deviation (SD) of the negative controls. ELISA for IgA and IgM were carried out similarly but using separate kits from Mabtech. For a standard IgM curve, human IgM was prepared in the range of 0.1-500 ng/ml; while for a standard IgA curve, human IgA was prepared in the range of 0.2-100 ng/ml. No extrapolated OD values outside standard curve were used.

2.2.4.7 ELISA for IL-21

The concentrations of IL-21 in culture supernatants or serum were determined using a commercial ELISA kit (eBioscience). Briefly, plates were coated with 100 μl of capture Ab (1:250 dilution) overnight at 4°C, washed five times with wash buffer (PBS + 0.05% Tween 20), and blocked with assay diluent (1:5 dilution) for 1 h. Standards and samples were added at 100 μl/well in duplicate and plates were left for 2 h at RT. Plates were washed again for six times followed by

addition of 100 µl/well enzyme conjugate to HRP (1:250 dilution in assay diluent) for 1 h at RT. The plates were washed six times and 100 µl/well substrate was added for 15 min at RT. The reaction was stopped by adding 50 µl/well of stop solution (2N sulphuric acid). Plates were then read at 450 nm and mean values of IL-21 were reported as ng per ml. All samples were analysed in duplicates using the mean OD values to calculate concentrations. A sample with an OD value which was at least two SD away from mean OD values of the negative controls was considered to be positive. The minimum detection limit was 16 pg/ml for IL-21. No extrapolated OD values outside standard curve were used. OD values below the cutoff were assigned the cutoff value.

2.2.4.8 Cell stimulation

Isolated $CXCR5^+$ and $CXCR5^-CD4^+$ T cells were stimulated with either phorbol myristate acetate (PMA) (final concentration: 10 ng/ml) plus ionomycin HCl (ION) (final concentration: 500 ng/ml) for cytokine assays, or with monoclonal anti-human CD3 antibody 5 µg/ml (OKT3) for the analysis of cell surface molecules. For cytokine assays, $CD4^+$ T-cells were plated at 1×10^6/ml in a 24-well plate and stimulated with plate-bounded OKT3 for 48 h at 37°C.

2.2.4.9 Intracellular staining for IL-21

The antibody used for this assay was IL-21 A647. PBMCs or sorted cells were stimulated with PMA and ION in the presence of 1 µg/ml costimulatory antibodies (anti-CD28/CD49d) and secretion inhibitor (monensin and brefeldin A) for 5 h. Cells were then fixed with Cytofix/Cytoperm on ice for 20 min, washed twice with perm buffer. Cells were subsequently resuspended in perm buffer and left for 15 min on ice. Antibodies conjugated to CD3, CD4, IL-21, IFN-γ, and IL-2 were added to the cells to incubate for 30 min on ice. The cells were washed twice and resuspended in 1% paraformaldehyde.

2.2.4.10 $CD154^+$ assay for antigen-specific cells

Freshly isolated PBMCs were resupsended in H5 (RPMI medium 1640 supplemented with 5% human AB serum, 2 mM L-glutamine, 100 µg/ml streptomycin, 100 U/ml penicillin) at a concentration of 10^7 cells/ml. For instance 3×10^7 PBMCs were resupended in 3 ml of H5 and were cultured in 12 well plate, along with 1 µg/ml anti-CD40 antibodies and 2 µg/ml of peptide pools (M or NP) for 6-16 h at 37°C. Cells were then harvested and stained with anti-CD154

biotin for 15 min at 4°C. Antigen-specific cells were enriched by the selection of CD154$^+$ cells via streptavidin magnetic bead cell separation. CD154$^+$ cells were cultured in the presence of 50:1 irradiated (30 Gy) autologous feeder cells and 10 ng/ml IL-7 and IL-15 in H10 for 21 days. Cultures were supplemented with cytokines every other day. Cells were starved for 5 days before restimulation.

2.2.4.11 Co-culture of CD154 $^+$ cells and autologous B cells

To assess the ability of antigen-specific CD154$^+$ CD4$^+$ cells to help B cells in the production of antibodies and class-switching, expanded CD154$^+$ cell lines were restimulated with 2 μg/ml of peptides pools (M or NP) for 6-16 h at 37°C in the presence of 1 μg/ml anti-CD40 antibodies. CD154$^+$ cells were isolated by streptavidin magnetic bead cell separation. Cells were then washed and resuspended in R10, counted, and 3×10^4 of CD154$^+$ cells were added to sorted naïve B cells or memory B cells at a 1:2 ratio in the presence of 1 μg/ml SEB for 10 days at 37°C, 5% CO_2. Culture supernatants were collected and immediately stored at −20°C. ELISAs (IgA, IgM and IgG) were performed to analyse antibody levels in the culture supernatant.

2.2.5 Statistical Analysis

All graphing and statistical analysis was carried out using GraphPad Prism (version 5.0a). Spearman rank correlation analysis was run between clinical parameters such as the number of responding T cells, measures of infection and illness or serological responses, as detailed in the corresponding result chapters. Differences between groups or timepoints were compared using nonparametric tests: Mann-Whitney *U*-test was used for comparing differences between values of two groups; and in comparing three or more groups, datasets were analysed using one-way analysis of variance (ANOVA), using non-parametric Kruskal–Wallis's test followed by Dunn's test for multiple comparisons. To evaluate differences between groups with normally distributed data, one-way ANOVA test with Bonferroni correction was used. The statistical significance of differences between two groups was analysed by two-tailed paired t-test. *P* values less than 0.05 were considered statistically significant, and marked with one asterisk. *P* values less than 0.01 were marked with two asterisks. Error bars represent the standard deviation (s.d.) unless otherwise noted.

Chapter 3

Experimental human acute influenza challenge

3.1 Introduction

Host responses are crucial in defence against influenza infection. Protective immunity against influenza is mediated by neutralizing antibodies, while cross-reactive $CD4^+$ and $CD8^+$ T memory cells established by previous influenza infection and vaccination provide protection against a variant subtype of virus by clearing virus from infected lungs. Extensive research in mice has shown that viral clearance is mediated by antigen-specific $CD8^+$ T cells, and memory $CD4^+$ T cells are important in maintaining $CD8^+$ and B cell responses (Belz et al., 2002; Bevan, 2004; Mozdzanowska et al., 1997; Topham and Doherty, 1998; Topham et al., 1997; Topham et al., 1996).

Knowledge of T cell epitopes is important for our understanding of the nature of the T cell responses. The majority of T cell studies in influenza A infection have been done with mice, however mice are not a natural host of influenza viruses and most viruses replicate poorly in them (Bouvier and Lowen, 2010). Studies in humans have mainly examined responses induced in volunteers vaccinated with influenza vaccines, or surveillance of the circulating strains which are essential in identifying outbreaks early. Experimental human challenge studies are useful to study the host response to influenza infection, as serologically susceptible individuals can be infected at specific times, and conditions such as virus dosage and environmental conditions can be controlled. Briefly, susceptible healthy adult volunteers are selected according to their low or absent serum antibody titers, and are infected intransally with a well characterized, less virulent wildtype virus subtype. The majority of the subjects will be infected and developed mild illness

similar to that of natural infection; and virus can be recovered from nasopharynx (Carrat et al., 2008a; Killingley et al., 2011).

In humans, pre-existing memory T cell responses have been shown to limit disease severity (McMichael et al., 1983) but the roles of protective cell-mediated immunity (CMI) in sero-negative individuals to a particular strain is not well understood. Here I investigate the role of cell-mediated immunity in humans using an experimental infection model in healthy volunteers who lack humoral immunity to the challenge strain. Peptides for the internal influenza proteins, which are highly conserved across strains are of special interest; by mapping the epitopes that generate responses across different strains of virus, this study provides a direction for the development of broadly protective T cell responses.

Techniques to determine the frequency of antigen-specific T cells involve enumeration of memory T cells by the enzyme-linked immunospot (ELISpot) assay and intracellular cytokine staining. The IFN-γELISpot assay detects IFN-γ secreted by a single cell upon stimulation with antigen, without the need for prior *in vitro* expansion. The secreted IFN-γ is captured on the membrane coated with cytokine-specific monoclonal antibodies, and is detected by enzyme-conjugated secondary antibodies. The spot size and intensity is also related to the amount of IFN-γ secreted by each cell. It is highly sensitive for quantifying antigen-specific T cell responses. Production of IFN-γ is an important anti-viral defence in influenza infection (Morris et al., 1982), and is readily detectable within 6-12 hours of peptide stimulations. Influenza-specific T cells measured by *ex vivo* IFN-γ ELISpot are a subset of circulating memory T cells capable of mediating effector function immediately upon antigen encounter, without differentiation or proliferation (Lalvani et al., 1997).

The aims of this chapter are as follows:

1) To use an experimental human infection model for studies of anti-viral immunity.

2) To measure the breadth and magnitude of T cell responses against two seasonal strains of influenza A viruses.

3.2 Results

3.2.1 Validation of experimental approach

To validate the use of cell depletion to identify $CD4^+$ and $CD8^+$ responses, a validation assay was conducted using PBMCs from a healthy volunteer who had been infected by seasonal influenza and exhibited memory CD8 and CD4 responses to both M and NP peptide pools, a HLA-A2 restricted matrix-specific epitope M-9 (LTKGILGFVFTLTVPSER) and a CD4 epitope peptide H3HA-45 (NVPEKQTRGIFGAIAGFI) in an IFN-γ ELISpot. In ELISpot, magnitude of T cell responses was presented by SFC/million PBMCs. $CD8^+$ T cells were depleted from PBMCs using magnetic beads, over 90% of purity of the depleted populations was obtained (**Fig. 3.1a**). $CD8^+$ T cell responses were calculated by subtracting the level of $CD4^+$responses from that of the total T cell response. When PBMCs were stimulated with peptides pool containing both CD4 and CD8 responding epitopes, the sum of responses (Spots Forming Cells/M; SFC/M) of $CD4^+$ and $CD8^+$ depleted PBMCs in response to the peptides were comparable to undepleted PBMC control, thus responses obtained from that depleted population were proportional to total PBMCs (**Fig. 3.1b-d**). This approach has been used in a number of studies (Kaufhold et al., 2005; Lee et al., 2008; Tobery and Caulfield, 2004).

3.2.2 Experimental influenza infection and symptom pattern of the study groups

To examine human memory T cell responses following an acute infection, two experimental infection cohorts were established (Oxford et al., 2005). A total of 41 healthy volunteers aged between 18 and 45 were inoculated intra-nasally with serial tenfold dilution of influenza A viruses: a cell-grown H3N2 WS/67/05 or an egg-grown H1N1 BR/59/07. Volunteers were then followed longitudinally in isolation for viral shedding, symptom development and measurement of cellular and humoral immune responses for the first 7 days. All volunteers were seronegative to the challenge strain and PCR (Polymerase Chain Reaction) negative for the virus in nasal lavage at the time of challenge. The overall infection rate is defined by evidence of virus shedding by quantitative PCR and/or seroconversion on day 28.

Demography, virus shedding and antibody titre of the study groups and the infected subjects are summarized in **Table 3.1** and **3.2** respectively. Infection rate was higher in subjects challenged

	H3N2 challenge group				H1N1 challenge group			
	Group 1	Group 2	Group 3	Group 4	Group 1	Group 2	Group 3	Group 4
N	4	4	4	5	6	6	6	6
Age-yr								
Mean±SD	26±3	28±5	25±2	29±8	25±5	25±5	27±4	23±3
Median	26	27	25	28	24	24	26	22
Range	23-29	25-35	22-27	22-41	20-32	22-35	23-31	19-27
Sex-no.(%)								
Female	2(50)	2(50)	2(50)	2(40)	2(33)	1(17)	2(33)	2(33)
Male	2(50)	2(50)	2(50)	3(60)	4(67)	5(83)	4(67)	4(67)
Virus shedding no. (%)								
	1(25)	4(100)	2(50)	2(40)	1(17)	3(50)	1(17)	1(17)
HAI titre on Day 28								
Positive	3(75)	2(50)*	1(25)**	1 (25)	2 (33)	2 (33)	2 (33)	1(17)
GMT	96	33	0.6	0	1	5	0	0
Mean symptom scores								
Mean±SD	10.5±19.7	60.8±10.7	13.8±14	4.6±5.5	11.2±7.7	39±23.2	14.5±14.1	8.3±15.2
Median	1	57.5	7.7	1	11.5	44.5	14.5	0.5
Range	0-40	52-76	5-22	0-9	0-22	3-65	0-31	0-38

Table 3.1 Demography, virus shedding and antibody titre of the study groups. *One subject was unavailable for D28 visit.**Two subjects were unavailable for D28 visit.

with H3N2 WS/67/05 virus (14/17, 82%) than subjects challenged with H1N1 BR/59/07 virus (9/24, 38%). In the H3N2 challenge group, virus was recovered from 50% of (7/14) of infected subjects by day 2 post challenge. Most subjects (8/14, 57%) cleared the virus completely by day 4, but virus shedding persisted in some individuals as long as 7 days. In H1N1 challenge group, however, low virus titre (1.75-2.5 log $TCID_{50}$) was recovered from all infected volunteers. This may be due to a phenomenon that has been described previously with egg-grown virus when first passaged through mammalian cells (Ho et al., 1976) (**Fig. 3.2a**).

Occurrence of a set of defined systemic and local symptoms were semi-quantified as symptom scores. A similar symptom pattern was observed between both studies and were comparable to natural infections (Newton et al., 2000). In H3N2 challenge group, total symptoms tracked with peak viral load (**Fig. 3.2b**, r= 0.6977, p= 0.0055, Spearman coefficient). Mean symptom scores that peaked on day 3 and returned to zero by day 7 after viral inoculation. 11 out of 14 (79%) infected volunteers developed one or more symptoms (**Fig. 3.2c**). In H1N1 challenge group, 8 out of 9 (89%) infected volunteers developed one or more symptoms and showed mean symptom scored that peaked on day 4 and returned to zero by day 7 after viral inoculation (**Fig. 3.2d**).

Total symptoms were dominated by upper respiratory illness such as runny nose and sore throat, which occurred in 10/14 (71%) in H3N2 group and 2/9 (22%) of H1N1 group. Fever was

observed in 3/14 (21%) of volunteers in the H3N2 group and 1/9 (11%) volunteer in the H1N1 group (**Fig. 3.3**).

	Subject	Lab. ID	Viral Load (Log_{10} TCID50)[1]							Pre-existing T cell responses	HI titre		Flu-like illness[2]
			D1	D2	D3	D4	D5	D6	D7	(SFC/M)	D-2	D28	
H3N2 Challenge (Oct 2008)	FLU001	15	4.25	4.25	-	-	-	-	-	77	NDA[3]	320	Yes
	FLU002	7	-	-	-	-	1.75	-	1.75	271	NDA	40	Yes
	FLU003	8	-	-	-	-	-	-	-	487	NDA	160	No
	FLU004	10	-	-	-	1.5	-	-	1.75	160	NDA	NDA	No
	FLU005	2	-	4.5	3.5	-	-	-	1.75	166	NDA	320	Yes
	FLU006	9	3.75	5	3.25	-	-	1.75	1.75	43	NDA	57	Yes
	FLU007	4	-	6.25	2.75	-	-	-	1.75	0	NDA	<20	Yes
	FLU008	3	-	4.75	1.75	-	-	-	-	668	NDA	N/A	Yes
	FLU010	5	-	-	3.75	-	2.75	-	-	0	NDA	N/A	Yes
	FLU012	16	-	5.01	5.01	-	-	2.75	1.75	193	NDA	80	Yes
	FLU013	18	-	3.51	5.5	2.5	-	-	-	113	NDA	40	Yes
	FLU014	14	-	-	-	-	-	1.75	-	100	NDA	NDA	Yes
	FLU015	17	-	-	-	3.75	4.5	4	-	0	NDA	20	Yes
	FLU016	11	-	-	-	-	-	1.75	-	414	NDA	<20	Yes
H1N1 Challenge (Aug 2009)	B004	19	-	-	-	-	-	-	-	240	NDA	20	No
	B005	15	-	-	-	-	2.5	-	-	155	NDA	40	Yes
	B006	14	-	-	-	-	-	-	-	0	NDA	40	Yes
	B008	23	-	2.25	-	-	-	-	-	45	NDA	160	Yes
	B009	20	-	-	1.75	-	-	-	-	34	NDA	10	Yes
	B012	16	-	2.25	-	-	-	-	-	60	NDA	40	Yes
	B015	7	-	-	2.5	-	2.25	3	-	267	NDA	20	Yes
	B017	2	-	-	-	-	-	-	-	45	NDA	40	Yes
	B021	8	-	-	-	-	-	-	-	70	NDA	160	Yes

1 Viral Load ≤1.50 was marked as "-".

2 Influenza-like illness was defined as headache, muscle pain, plus respiratory symptoms e.g. rhinorrhea/cough/sore throat

3 No Detectable Activity

Table 3.2 Summary of infected subjects in the H3N2 and H1N1 challenge studies.

3.2.3 T cell responses of infected volunteers

Influenza-specific T cell responses during the course of acute infection were measured in breadth and magnitude against the entire influenza proteome. Homology based on the amino acid sequence between H1N1 and H3N2 is 40% (surface antigen HA and NA) and 90% (internal proteins M1, M2, NP, PB2, PB1, and PA) respectively. The library of overlapping peptides (18-mers) used to stimulate an antigen specific response covered the entire influenza virus proteome (**Fig. 3.4ab**). The magnitude of the memory T cell response was measured by the number of IFN-γ -producing cells upon stimulation (**Fig. 3.4c**). Breadth of T cell response was defined by the number of proteins recognized by each subject.

Antibodies against the challenge virus were absent in all subjects in both study groups prior to challenge. Antibody responses (HI titer) were not detectable at 7d when the viruses were completely cleared, but antibody responses were detected at day 28 (**Fig. 3.5a**).

The nature of pre-existing T cell memory prior to viral challenge was determined. Although the volunteers were seronegative for the challenge virus strains, pre-existing memory T cells specific to the proteins expressed by the challenge virus were present in both groups. At baseline, the size of the total T cell responses was below 1000 spot-forming cells (SFCs) per million PBMCs in all subjects studied, as shown by *ex vivo* ELISpot. In H3N2 challenge group, 11 out of 14 (79%) of the infected subjects displayed memory T cell responses to one or more H3N2 protein, with a median of two proteins recognized (range 1-5). Nucleoprotein (8/14, 57%), and matrix protein (7/14 50%) are immunodominant, as determined by the number of responders and magnitude of IFN-γ response. In the H1N1 challenge study, 7 out of 9 (78%) of the infected subjects showed baseline memory T cell response direct against one or more proteins, with M being the most immunodominant protein (6/9, 67%) (**Fig. 3.5b**).

On day 7 post-challenge, the breadth and magnitude of T cells responding to influenza peptides increased in the peripheral blood by an average of tenfold. Following an acute H3N2 infection, all infected subjects (14/14, 100%) showed an antigen-specific T cell response, with a median of five proteins recognized (range 1-8), thus the responses were polyclonal. In the H1N1 group, further T cell responses were not induced by day 3 post-challenge (results not included). Similar to my observation in an acute H3N2 infection, antigen-specific T cells had rapidly expanded in both breadth and magnitude by Day 7. All H1N1 infected subjects (9/9, 100%) had a T cell

response, with a mean of 5 proteins being recognized (range 2-7) (**Fig. 3.5b**). No significant change was found from baseline in the day 7 T cell responses against known $CD8^+$ epitopes of cytomegalovirus and Epstein-Barr virus in control wells, indicating no bystander activation (**Fig. 3.6**).

On day 28, after the study was truncated following the use of Tamiflu, the total memory T cell responses returned to baseline level (<1000 SFCs per million PBMCs) in both groups. Immunodominant responses to proteins such as nucleoprotein and matrix persisted at a baseline level, whereas most newly generated responses against other proteins disappeared after the acute phase of infection. In the H3N2 group, 7 out of 10 (70%) infected subjects possess a T cell response that recognizes an average number of just one protein (range 1-2). NP and M remained immunodominant while responses to other viral proteins disappeared following the expansion. In the H1N1 group, 8/9 (89%) of infected subjects recognized just 2 different viral proteins (range 2-4). Moreover, 4/9 (44%) had newly generated HA responses that persisted at low level (average 60 SFC/million PBMC) (**Fig. 3.5b**).

3.2.4 Phenotypes of the pre-existing T cell responses

Correlates of protection against influenza involved pre-existing memory T cells from previous exposure of the virus. To characterize the role and quality of pre-existing T cells in an acute H3N2 infection, T cell lines were established by pulsing cyropreserved PBMCs from the baseline (day -2 timepoint) with H3N2 peptide pools. These cells were stimulated with individual candidate peptides in an *in vitro* cultured ELIspot assay to confirm the positive responses shown from *ex vivo* ELIspot. The cultured ELIspot assay is able to enhance the specific T cell responses by allowing T cells present to expand, and the resting central memory T cells to differentiate into effector T cells (**Fig. 3.7a**). After narrowing down the number of candidate peptides, intracellular staining (ICS) was carried out to phenotype antigen-specific cells by stimulating the cells with individual peptide overnight (**Fig. 3.7bc**).

In the H3N2 group, 9 subjects had responses to NP and M at baseline, and 8 out of these 9 subjects had their responding peptides identified at single peptide level. CD4 dependent responses that were direct against surface protein HA, internal proteins NP and M were found to be most common. 7 out of 10 (70%) peptides within M protein and 8 out of 11 (73%) peptides within NP, that elicited a response, were CD4 dependent (**Table 3.3**).

To assess the specificity of T cells in the pre-existing memory pool in the H1N1 challenge study, I carried out epitope mapping on baseline PBMCs using 2-D matrix. Identified individual peptides were then confirmed in a second ELISpot assay (**Fig. 3.7a**). On day 3, as well as assessing total T cell responses using the 2-D matrix, $CD8^+$ cells were depleted from PBMCs. The depleted cells, undepleted cells and the $CD8^+$ cells (attached to beads) were stimulated with the confirmed individual peptides to identify the subset of the IFN-γ-responding T cells. In addition, T cell lines were established by pulsing fresh PBMCs from day -2 and day 7 with H1N1 peptide pools. ICS was carried out to phenotype the antigen-specific cells by stimulating the cells with individual peptides, confirmed previously by cell depletion (**Fig. 3.7bc**).

At baseline, 7 subjects had positive responses to NP and M, all of which were identified at the individual peptide level. 5 out of 5 of these peptides identified within M protein, and 3 out of 6 (50%) peptides identified within NP proteins, are CD4 dependent (**Table 3.4**). Responses to these individual peptides also expanded on day 7 (not shown). Taken together, responses to the immunodominant proteins (nucleoprotein and matrix) were predominantly mediated by $CD4^+$ T cells in both groups (56% CD4 versus 44% CD8 for H3N2, and 72% CD4 versus 28% CD8 for H1N1, consistent with a previous report (Lee et al., 2008) (**Fig. 3.7d**).

Protein	Peptide ID	Amino acid position	Amino acid sequence	CD4 or CD8 dependency	SFC/million PBMC (range)	Number positive (%)
HA	HA31	233-250	IGSRPRVRDIPSRISIYW	4	299	1 (13)
	HA32	241-258	DIPSRISIYWTIVKPGDI	4	114 (19-269)	3 (38)
	HA42	317-333	TYGACPRYVKQNTLKLA	4	48	1 (13)
	HA45	338-355	NVPEKQTRGIFGAIAGFI	4	70	1 (13)
	HA46	346-363	GIFGAIAGFIENGWEGMV	4	20 (19-20)	3 (38)
	HA58	432-447	TKIDLWSYNAELLVAL	4	35	1 (13)
	HA68	507-524	YRDEALNNRFQIKGVELK	4	79	1 (13)
	HA69	515-532	RFQIKGVELKSGYKDWIL	4	70	1 (13)
	HA70	522-538	LKSGYKDWILWISFAI	4	321	1 (13)
	HA71	529-546	DWILWISFAISCFLLCVA	4	261	1 (13)
NA	NA01	1-17	MNPNQKIITIGSVSLTI	4	63	1 (13)
M	M01	1-15	MSLLTEVETYVLSIV	8	21	1 (13)
	M02	6-22	EVETYVLSIVPSGPLKA	4	33 (26-39)	2 (26)
	M07	40-57	EALMEWLKTRPILSPLTK	8	58 (24-91)	2 (26)
	M08	48-64	TRPILSPLTKGILGFVF	4	60	1 (13)
	M09	55-72	LTKGILGFVFTLTVPSER	8	78	1 (13)
	M15	103-119	LKREITFHGAKEIALSY	4	67 (35-96)	3 (38)
	M23	159-175	HRSHRQMVATTNPLIKH	4	158	1 (13)
	M25	173-189	IKHENRMVLASTTAKAM	4	118	1 (13)
NP	NP05	24-41	EIRASVGKMIDGIGRFYI	4	141.5 (35-248)	2 (26)
	NP08	48-65	KLSDHEGRLIQNSLTIEK	4	26	1 (13)
	NP14	95-111	PIYRRVDGKWMRELVLY	4	113 (45-181)	2 (26)
	NP15	102-119	GKWMRELVLYDKEEIRRI	4	93 (45-141)	2 (26)
	NP16	110-29	LYDKEEIRRIWRQANNGEDA	4	18	1 (13)
	NP20	141-156	SNLNDATYQRTRALVR	8	391	1 (13)
	NP21	147-163	TYQRTRALVRTGMDPRM	8	331	1 (13)
	NP27	192-208	ELIRMVKRGINDRNFWR	4	29	1 (13)
	NP31	221-238	RMCNILKGKFQTAAQRAM	4	134	1 (13)
	NP32	229-246	KFQTAAQRAMVDQVRESR	8	104	1 (13)
	NP57	404-420	GQTSVQPTFSVQRNLPF	4	10	1 (13)
	NP58	411-428	TFSVQRNLPFEKSTIMAA	4	10	1 (13)
PB1	PB1-19	131-147	WTLNRNQPAATALANTI	4	16	1 (13)
	PB1-55	402-419	SLSPGMMMGMFNMLSTVL	4	40	1 (13)
	PB1-56	410-426	GMFNMLSTVLGVSILNL	4	35 (16-55)	2 (26)
PA	PA68	495-512	RRKTNLYGFIIKGRSHLR	4	66	1 (13)
NS	NS02	5-23	VSSFQVDCFLWHIRKQVV	4	21	1 (13)
	NS14	97-112	ELSRNWFMLMPKQKVE	4	19	1 (13)

Table 3.3 T cell peptides in H3N2 challenge study (Published epitopes were underlined).

3.2.5 Role of T cell in viral control and symptom development

I subsequently analysed the relationship between pre-existing T cells and measures of infection and illness (virus shedding, total symptom scores and illness duration) (La Gruta et al., 2007; Li et al., 2010). Spearman rank correlation analysis was based on data collected from all infected individuals (culture positive or 4 fold or more increase in HI antibody titre). In the H3N2 challenge studies, total symptoms strongly correlated with peak viral load (**Fig. 3.2b**, r=0.6977, p=0.0055, Spearman coefficient). The magnitude of total pre-existing T cell responses strongly correlated with illness duration in H3N2 challenge study (**Fig. 3.8a**, r=-0.5740, p=0.0318, Spearman coefficient) and total symptom scores in H1N1 challenge (**Fig. 3.8b**, r=-0.7113, p=0.0369, Spearman coefficient).

When T cell responses to immunodominant NP and M proteins were examined, I observed that these protective T cell responses were mediated by pre-existing $CD4^+$ but not $CD8^+$ T cells. In both studies, pre-existing $CD4^+$ but not $CD8^+$ cells against internal proteins NP and M strongly correlated with total symptom scores (**Fig. 3.8**). Peak virus shedding strongly correlated with pre-existing $CD4^+$ T cell responses against internal proteins NP and M (**Fig. 3.8a**, r=-0.6087, p=0.0209 Spearman coefficient), but not with $CD8^+$ T cells. Total virus shredding (summation of the amount of viral shredding measured daily in the seven-day period) also correlated with pre-existing $CD4^+$ T cells against NP and M, but not with $CD8^+$ T cells (**Appendix III**).

On the other hand, when I analyse the relationship between T cell responses at day 7 with viral shedding and symptom severity, a positive correlation was found in both studies. This suggests that the pre-existing memory $CD4^+$ T cells are the main player in the cell-mediated immunity in limiting the illness. Once the illness is established, acutely expanding T cells tracked peak viral load and thus symptoms (**Fig. 3.9**).

3.2.6 Kinetics of T cells during influenza infection

To understand the generation of activated T cells and their functional status, I assessed proliferation of $CD4^+$ and $CD8^+$ T cells using Ki-67, a marker expressed only in cycling but not in resting T cells (Scholzen and Gerdes, 2000) (**Fig. 3.10a**). Activated ($CD38^+$) and proliferating ($Ki\text{-}67^+$) $CD4^+$ and $CD8^+$ cells were undetectable at baseline, but an expansion of activated and proliferating $CD4^+$ and $CD8^+$ T cells was observed by day 7. These cells contracted by day 28

Protein	Peptide ID	Amino acid position	Amino acid sequence	CD4 or CD8 dependency	SFC/million PBMC (range)	Number positive (%)
HA	HA46	336-353	NIPSIQSR**GLFGAIAGFI**	4	86	1 (14)
	HA47	344-361	**GLFGAIAGFI**EGGWTGMV	4	74	1 (14)
M	M08	57-74	K**GILGFVFTL**TVPSERGL	4	15	1 (14)
	M12	89-106	DPNNMDRAVKLYRKLKRE	4	38 (30-46)	2 (28)
	M13	97-114	VK**LYRKLKREITF**HGAKE	4	41 (30-52)	2 (28)
	M14	105-122	REITFHGAKEIALSYSAG	4	22 (10-34)	2 (28)
	M27	209-226	ARQMVQAMRAIGTHPSSS	4	37 (28-48)	2 (28)
NP	NP09	65-82	**RMVLSAFDER**RNKYLEEH	4	38	1 (14)
	NP14	105-122	VRELVLYDKEEIRRIWRQ	4	15	1 (14)
	NP22	169-186	GSTLPRRSGAAGAAVKGV	8	28	1 (14)
	NP27	209-226	GENGRKTRIAYERMCNIL	8	30	1 (14)
	NP28	217-234	IA**YERMCNILKG**KFQTAA	8	40	1 (14)
	NP52	409-426	QPTFSVQRNLPFDKTTIM	4	26	1 (14)
PB1	PB1-52	409-426	MGMF**NMLSTVLGV**SILNL	4	59	1 (14)
PA	PA-71	561-578	MFLYVRTNGTSKIKMKWG	8	29	1 (14)

Table 3.4 T cell peptides in H1N1 challenge study

(**Fig. 3.10b**). Size of proliferation of activated T cells (expressing activation marker CD38) was found to correlate with the size of antigen specific T cell responses on day 7 by IFN-γ ELISpot (**Fig. 3.10c**). I also evaluated whether these activated cells were susceptible to apoptosis by looking at Caspase-3 and Fas-L expression. T cells did not express or upregulate either Caspase-3 and Fas-L on day 3, day 7 or day 28 in this longitudinal study, showing that the T cells did not undergo apoptosis in any of the timepoint analysed (not shown).

3.2.7 HLA-DR was expressed in the respiratory epithelium

Respiratory epithelial cells are the major cell type that becomes productively infected by most influenza strains, thus are the primary targets of the immune responses (Hammad and Lambrecht, 2008). For $CD4^+$ T cells to recognize infected cells and to exhibit direct effector function, MHC Class II (HLA-DR) has to be expressed in the respiratory epithelium. It is not possible to assess this requirement in the infected subjects directly; thus the constitutive expression of HLA-DR in explanted lung tissue and primary bronchial epithelial cells (PBECs) in culture and the effect of *in vitro* influenza infection on the expression level were analysed. It was found that HLA-DR was expressed in both lung tissue (parenchymal and bronchial tissue) and cultured PBECs, and the expression is enhanced after PBECs were infected with X31 H3N2 *in vitro*, compared to cells treated with ultraviolet light-inactivated virus. This confirms that respiratory epithelial cells are potential target cells for $CD4^+$ T cells (**Fig. 3.11**). This experiment was carried out by Dr. Tom Wilkinson at University of Southampton.

3.3 Discussion

3.3.1 Experimental infection of influenza A viruses

My approach was to infect healthy volunteers with a virulent strain of influenza A virus and then assess the T cell responses of these volunteers in the periphery longitudinally from the onset of infection. Multiple parameters, including viral titers in nasal washes, symptom scores, serological conversion to neutralizing antibody, were also monitored over time. It allowed me to more accurately describe the natural history of the infection, as the date of infection was known, plus the dose and type of inoculum was controlled. Volunteers in the studies were selected based on their HI antibody titer to eliminate pre-existing homosubtypic immunity. However, heterosubtypic immunity was not excluded and immunity to internal proteins of the virus may explain the milder disease observed in some volunteers.

The dynamics of viral shedding of the study was consistent with previously reported experimental infections, where viral loads of the subjects increased during the first day following inoculation, peaked at 2-3 day, and returned to baseline values by day 6 or 7 (Carrat et al., 2008b; Hayden et al., 1998; Nicholson et al., 2003). Shedding usually lasted for less than 6 days (Leekha et al., 2007). In naturally acquired seasonal and pandemic H1N1 infection of healthy adults, viral loads have been shown to peak at around 1 to 2 days post-symptom onset [reviewed in (Carrat et al., 2008b)], thus leaving a narrow window for antiviral treatment. Poor virus shedding was observed in the subjects of the H1N1 challenge group. Several reasons may account for this. Previous reports have suggested that A/H3N2 infections sustain higher viral titers compared to A/H1N1 (Carrat et al., 2008b), and that the H3N2 subtype gives more severe illness as shown by higher mortality and hospitalization rates (Thompson et al., 2004; Thompson et al., 2003). Secondly, it may be also be related to the procedure of virus stocks preparation. Tissue culture-grown H3N2 viruses may resemble originally clinical isolates more closely than the egg-grown H1N1 viruses used in the studies. Despite the low virus titres recovered, volunteers were considered to be infected if they had seroconverted by day 28.

In both study groups, the dynamics of symptoms were consistent with previous experimental studies, where total symptom scores peaked around day 2 or 3 and returned to baseline values by day 7 (Carrat et al., 2008b). Dynamics of viral shedding, which equated to influenza

infectiousness, largely overlapped with systemic symptoms, and viral clearance correlated with symptom resolution. A previous study also suggested that duration of shedding was proportional to the intranasal dose (Keitel et al., 1990). However no such correlation was observed in our study; indeed, infection rate and mean symptom scores was highest in the medium high dose (1:100) group in the H3N2 challenge group (**Table 3.1**).

3.3.2 Roles of CD4$^+$ T cells in protection

Cellular immunity plays a crucial role in controlling influenza A virus during an infection. T cells cannot prevent virus infection but can see epitopes derived from the viral proteins of the influenza virus complexed to HLA on the surface of the infected epithelial cells or APCs. Data from the two independent challenge cohorts suggest that pre-existing memory CD4$^+$ T cell responses play a more important role in the control of infection than previously reported in humans. Pre-existing virus-specific CD4$^+$ T cell counts, rather than CD8$^+$, correlated with lower virus shedding in response to H3N2 viruses, and with lower symptom scores to both H3N2 and H1N1 viruses. Priming of this memory response is presumably from previous live infection or vaccination, although all subjects were seronegative to the challenge strain prior to the studies, suggesting they have not been recently exposed to this subtype. Antigen-specific T cells increased in both breadth and magnitude on day 7 post challenge and declined thereafter.

In mice studies, CD4$^+$ T cells are believed to function mainly to promote antibody responses (Doherty et al., 2006). However, conserved CD4$^+$ T cell epitopes, some of which are shown to be naturally generated in infected cells, have been identified in the internal and surface proteins of human and avian influenza viruses (Assarsson et al., 2008; Greenbaum et al., 2009; Lee et al., 2008; Richards et al., 2010). Regarding the CD4$^+$ T-cell specificities in the two challenge studies, it is not surprising that the internal viral proteins M and NP appeared to be the most immunogenic upon challenge. Although M and NP are expressed in the cytosol and nucleus of the infected cells, their abundance within antigen-presenting cells may allow them to efficiently access the MHC class II loading compartment via autophagy (Dengjel et al., 2005; Richards et al., 2009). On the other hand, T cells specific for HA and NA epitopes in the vaccination cohorts (to be discussed in Chapter 5) were predominantly CD4$^+$. Membrane associated HA and NA are likely to readily accessible to endosomally localized MHC class II molecules and more efficiently presented, leading to the priming of CD4$^+$ T cells. If the viral specificity of CD4$^+$ T

cells and antigen-specific B cells were shared, as reported for some viruses (Sette et al., 2008), these HA- and NA-specific $CD4^+$ cells may contribute by facilitating antibodies responses.

In employing a challenge model to study immune responses, although care was taken to ensure that all subjects were seronegative to the challenge strain, it is still possible that heterosubtypic and cross-reactive antibodies to the challenge subtype may have contributed to the protective effects seen, as antibodies to the alternative subtype or the pandemic H1N1 viruses were not measured. Although there was a possibility that subclinical infections from pandemic H1N1 could have an impact on the A/Brisbane/59/07 (H1N1) study, the chance of a substantial effect on the overall findings is minimal. The key observations were seen in both study cohorts, and the first study was performed in 2008, well before the occurrence of the pandemic. In addition, both the incidence of pandemic H1N1 infections described in field studies of this age group at the time, and the incidence of subclinical infections, were low (Riley et al., 2011). Moreover, care is required in comparing the results of a human study based on readouts in the periphery compared to animal studies where cellular immunity at the site of infection can be readily examined. Importantly, a major concern about human challenge studies is whether experimental infection can be comparable with natural influenza infection. Firstly, symptom severity with challenge studies using nasal inoculation is generally lower than those with natural infection, thus may result in lower viral shredding. The strains used for infection in the studies are closely related to circulating strains, although during their passage they may have lost some of their virulence. Secondly, questions may be raised about whether the profile of viral shredding in experimental infection is comparable to natural infection, however it has been shown recently that the pattern is largely similar (Lau et al., 2010). Other factors such as the relative contribution of different forms of transmission (droplets/aerosols/contacts etc). might impact differently in experimental and natural transmission. Finally, given the small number of subject in this study, the contribution of pre-existing, cross-reactive $CD8^+$ T cells must not be discounted entirely. These virus-specific memory $CD8^+$ T cells may reside predominately in the respiratory tract rather than in the circulation, thus a relationship between symptoms and cell numbers were not observed based on readouts in the blood.

To conclude, my data suggest a role of $CD4^+$ T cells in protective heterosubtypic immunity in influenza. Pre-existing memory $CD4^+$ T cells are associated with increased virus clearance and reduced symptom score. Activated and proliferating T cells expand in response to the virus, and

return to baseline level as the virus is cleared. In the subsequent result chapters, the functions of these influenza-specific $CD4^+$ T cells, and their relationship with antibody responses are further examined. Future studies are required to determine whether future vaccines that generate $CD4^+$ T cell responses to conserved viral proteins may limit disease severity for a range of influenza viruses.

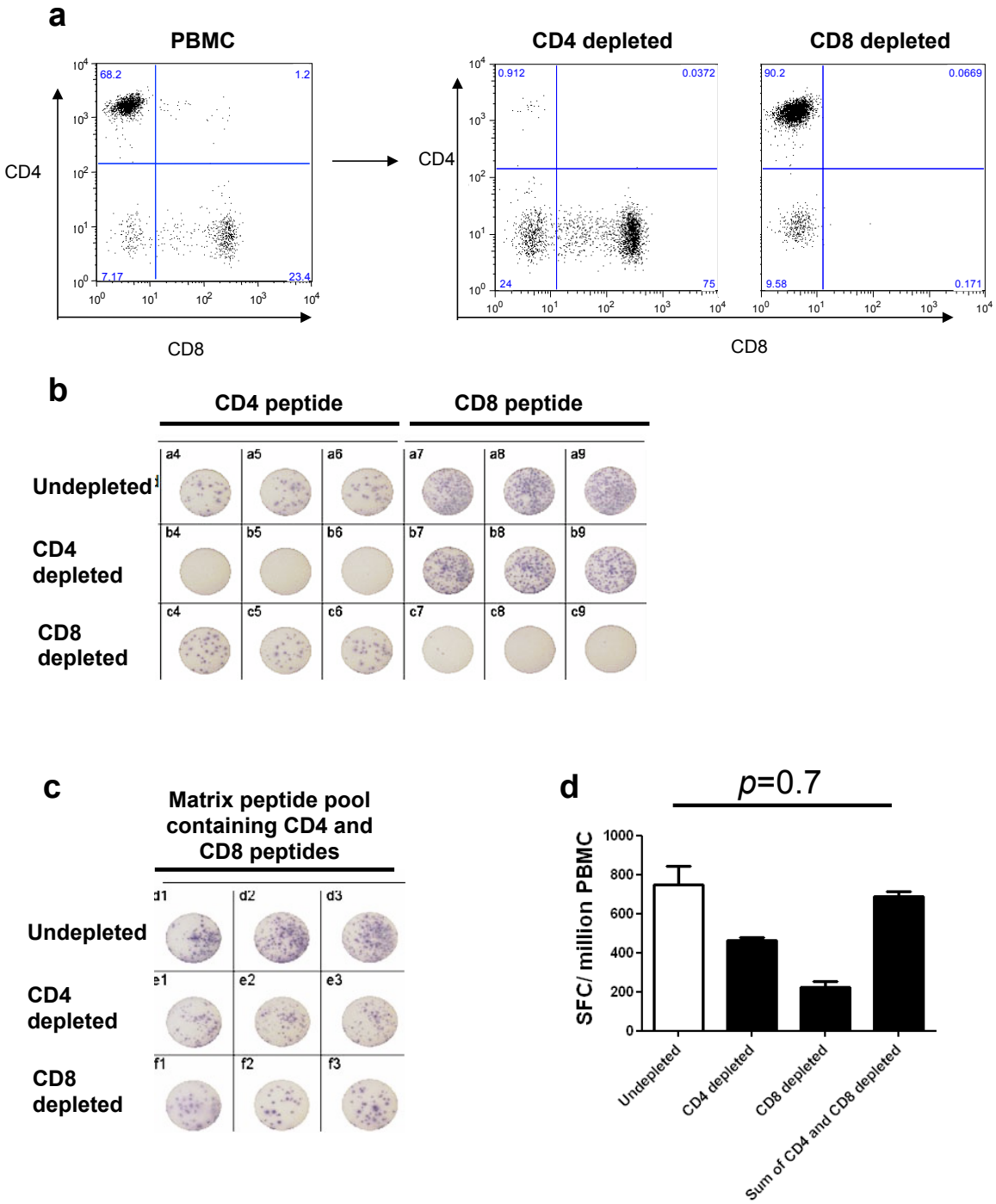

Figure 3.1 ***Ex vivo*** **IFN-γ ELISpot with cell depletion.** **(a)** Purity of the PBMCs upon depletion using positive selection of $CD8^+$ cells ($CD8^+$ Dynabeads). PBMCs were stained with CD4-APC and CD8-PB after depletion to check for purity. Over 90% of depletion efficiency is achieved. **(b)** Undepleted PBMC, $CD4^+$ depleted and $CD8^+$ depleted PBMC from one subject were stimulated with either flu $CD4^+$ or $CD8^+$ peptides and the response was measured by IFN-γ ELISpot. **(c)** Undepleted PBMC, $CD4^+$ depleted and $CD8^+$ depleted PBMC from the same subject were stimulated with flu matrix peptide pools containing a mixure of $CD4^+$ and $CD8^+$ peptides and the response was measured by IFN-γ ELISpot. **(d)** IFN-γ ELISpot response in undepleted, $CD4^+$ depleted, $CD8^+$ depleted fractions. Comparisons between groups were determined by Mann-Whitney *U* test.

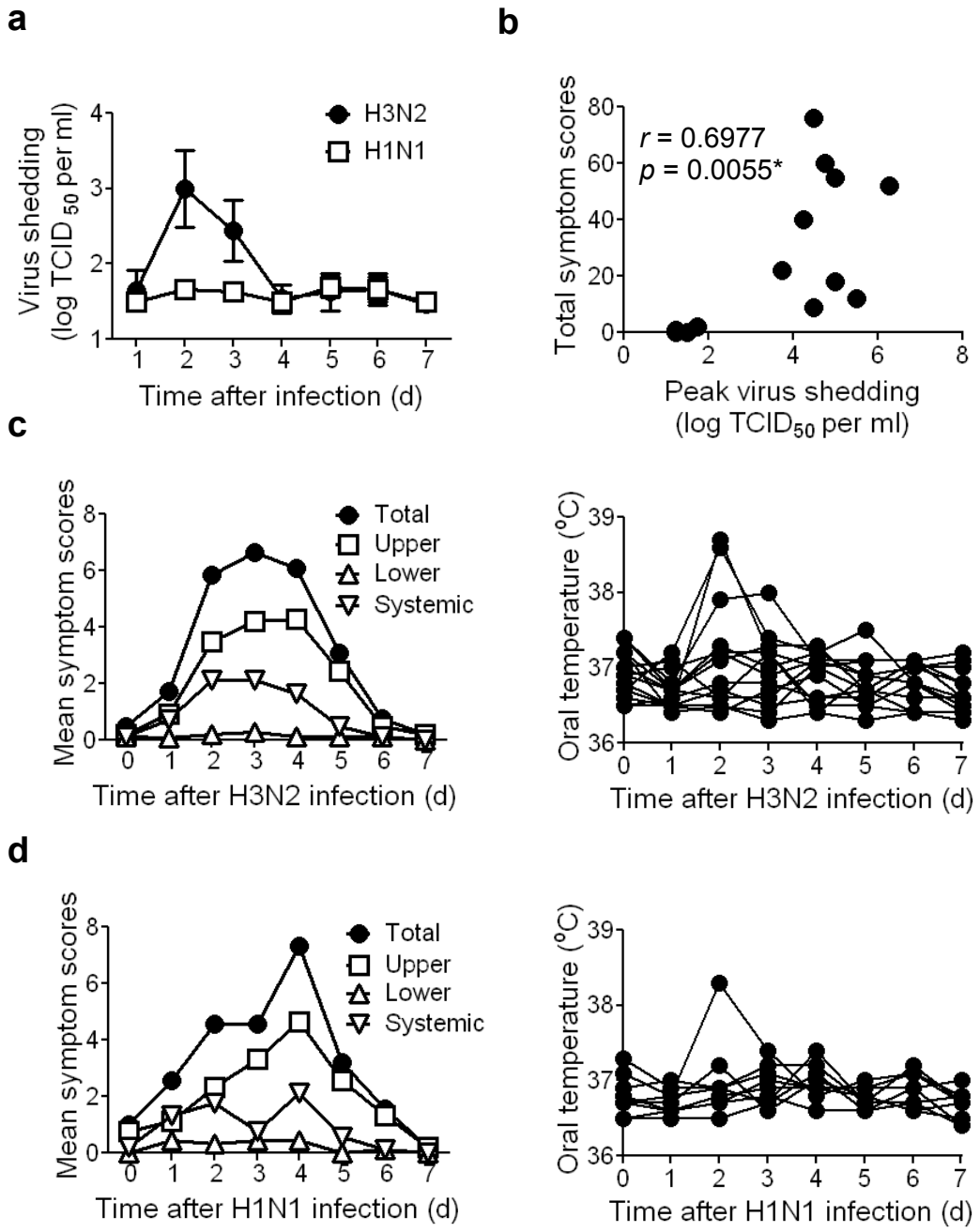

Figure 3.2 Viral shedding in nasal wash, seroconversion and symptom development in seronegative healthy volunteers experimentally challenged with influenza A viruses. (a) Volunteers infected with cell-grown H3N2 (WS/67/05) or egg-grown H1N1 (BR/59/07) viruses. The virus was titrated by $TCID_{50}$ assay. Presence of flu-specific antibody was measured by hemagglutination inhibition assay. **(b)** Correlation of total symptom scores against nasal virus shedding in each infected subject by Spearman rank correlation test. **(c)** Mean symptom scores and oral temperatures of volunteers infected with H3N2 virus. **(d)** Mean symptom scores and oral temperatures of volunteers infected with H1N1 virus.

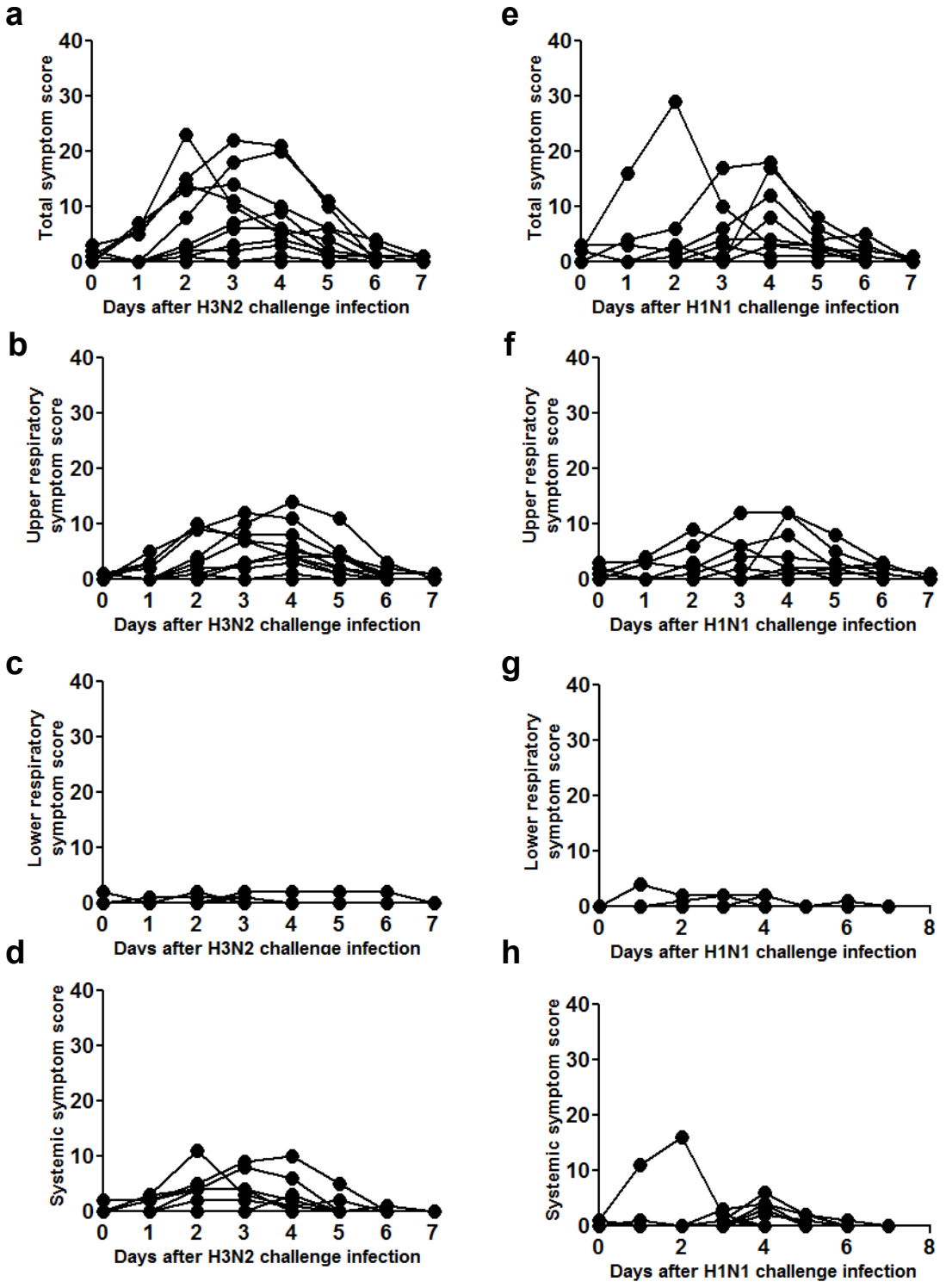

Figure 3.3 Symptom scores in each volunteer infected with influenza virus. (a) Total symptom scores in volunteers infected with H3N2 (WS/67/05). **(b)** Upper symptom scores in volunteers infected with H3N2 (WS/67/05). **(c)** Lower symptom scores in volunteers infected with H3N2 (WS/67/05). **(d)** Systemic symptom scores in volunteers infected with H3N2 (WS/67/05). **(e)** Total symptom scores in volunteers infected with H1N1 (BR/59/07) virus. **(f)** Upper symptom scores in volunteers infected with H1N1 (BR/59/07) virus. **(g)** Lower symptom scores in volunteers infected with H1N1 (BR/59/07) virus. **(h)** Systemic symptom scores in volunteers infected with H1N1 (BR/59/07) virus.

a

H3N2 Challenge Study (A/Wisconsin/67/05) T cell Elispot layout

	1	2	3	4	5	6	7	8	9	10	11	12
A	HA			NA			NP			Matrix		NS
	Pool 1	Pool 2	Pool 3	Pool 4	Pool 5	Pool 6	Pool 7	Pool 8	Pool 9	Pool 10	Pool 11	Pool 12
B	NS	PB2					PB1					PA
	Pool 13	Pool 14	Pool 15	Pool 16	Pool 17	Pool 18	Pool 19	Pool 20	Pool 21	Pool 22	Pool 23	Pool 24
C	PA			Second dimension								
	Pool 25	Pool 26	Pool 27	Pool 28	Pool 29	Pool 30	Pool 31	Pool 32	Pool 33	Pool 34	Pool 35	Pool 36
D	Second dimension											
	Pool 37	Pool 38	Pool 39	Pool 40	Pool 41	Pool 42	Pool 43	Pool 44	Pool 45	Pool 46	Pool 47	Pool 48
E	2nd				No peptide control x 4				Flu CD8	EBV + CMV (CD8)		PHA
	Pool 49	Pool 50	Pool 51	Pool 52								

b

H1N1 Challenge Study (A/Brisbane/59/07) T cell Elispot layout

	1	2	3	4	5	6	7	8	9	10	11	12
A	HA			NA			NP			Matrix		NS
	Pool 1	Pool 2	Pool 3	Pool 4	Pool 5	Pool 6	Pool 7	Pool 8	Pool 9	Pool 10	Pool 11	Pool 12
B	NS	PB2				PB1				PA		
	Pool 13	Pool 14	Pool 15	Pool 16	Pool 17	Pool 18	Pool 19	Pool 20	Pool 21	Pool 22	Pool 23	Pool 24
C	PA	PB1-F2	Second dimension									
	Pool 25	Pool 26	Pool 27	Pool 28	Pool 29	Pool 30	Pool 31	Pool 32	Pool 33	Pool 34	Pool 35	Pool 36
D	Second dimension											
	Pool 37	Pool 38	Pool 39	Pool 40	Pool 41	Pool 42	Pool 43	Pool 44	Pool 45	Pool 46	Pool 47	Pool 48
E	2nd			No peptide control x 4				Flu CD8		EBV + CMV (CD8)		PHA
	Pool 49	Pool 50	Pool 51									

c

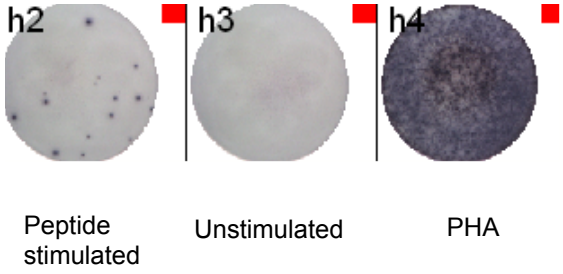

Figure 3.4 IFN-γ- ELISpot layout of experimental infection in humans. (a) H3N2 challenge study. **(b)** H1N1 challenge study. 300 000 of fresh PBMCs were stimulated with 2 μg/ml of peptide pool for 18 hours in each well. **(c)** Representative example of one donor is shown. IFN-γ spots were visible when PBMCs were incubated with a responsive peptide. Unstimulated PBMCs were used as a negative control, while PHA-stimulated PBMCs were used as positive control in all experiments.

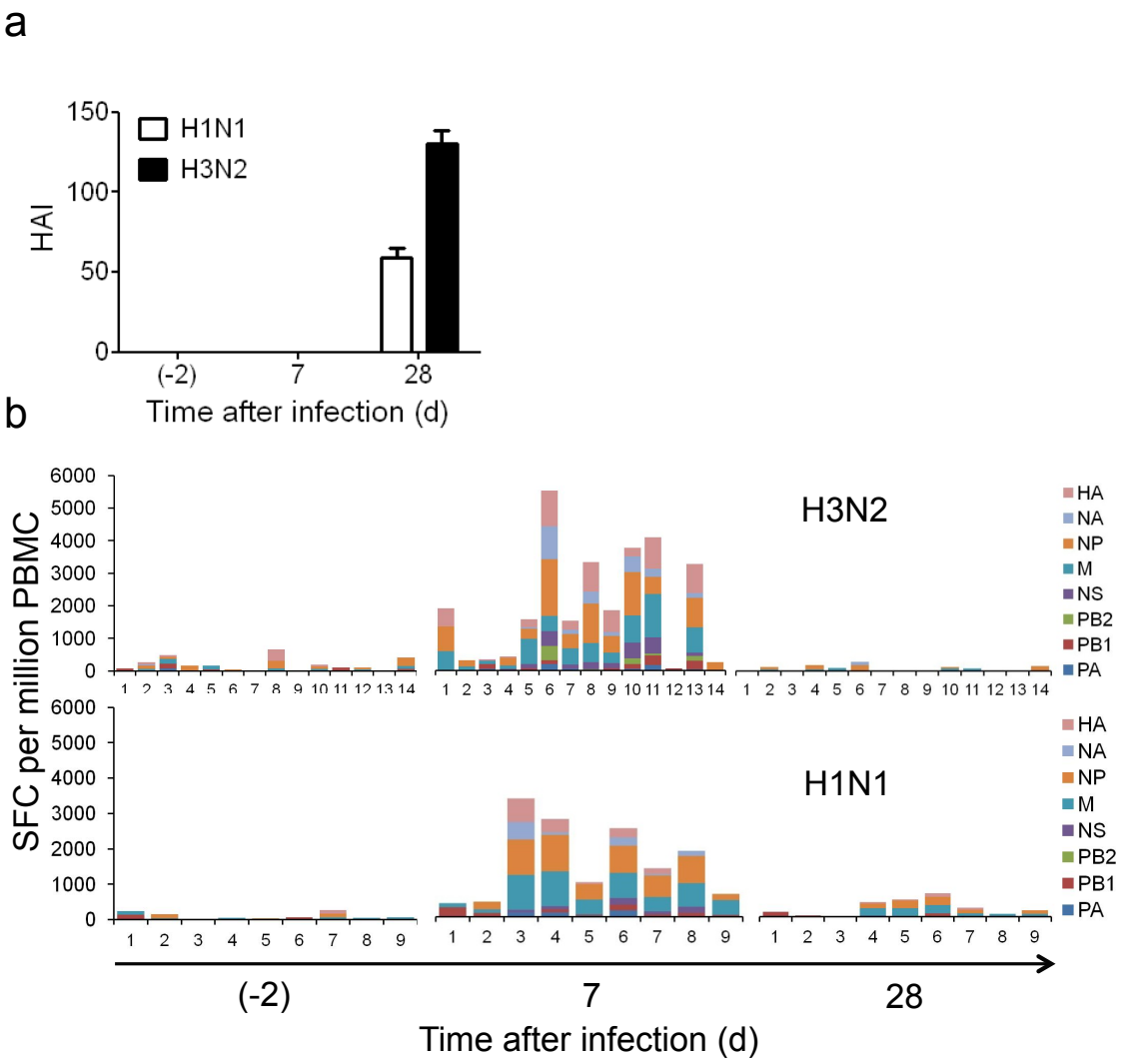

Figure 3.5 T cell responses in seronegative healthy volunteers experimentally infected with influenza A viruses. (a) Presence of flu-specific antibody was measured by hemagglutination inhibition assay. **(b)** *Ex vivo* flu-specific T cell responses were measured by stimulating fresh PBMCs with peptide pools spanning the entire proteome of the challenge strains. Each bar represent the proportion of total T cell responses per million PBMCs to the entire influenza proteome and each colour box represents T cell response to each viral protein. X axes denote subject number. HA, hemagglutinin; NA, neuraminidase; NP, nucleoprotein; M, matrix; NS, nonstructural proteins; PB1, PB2, PA, RNA polymerase complex.

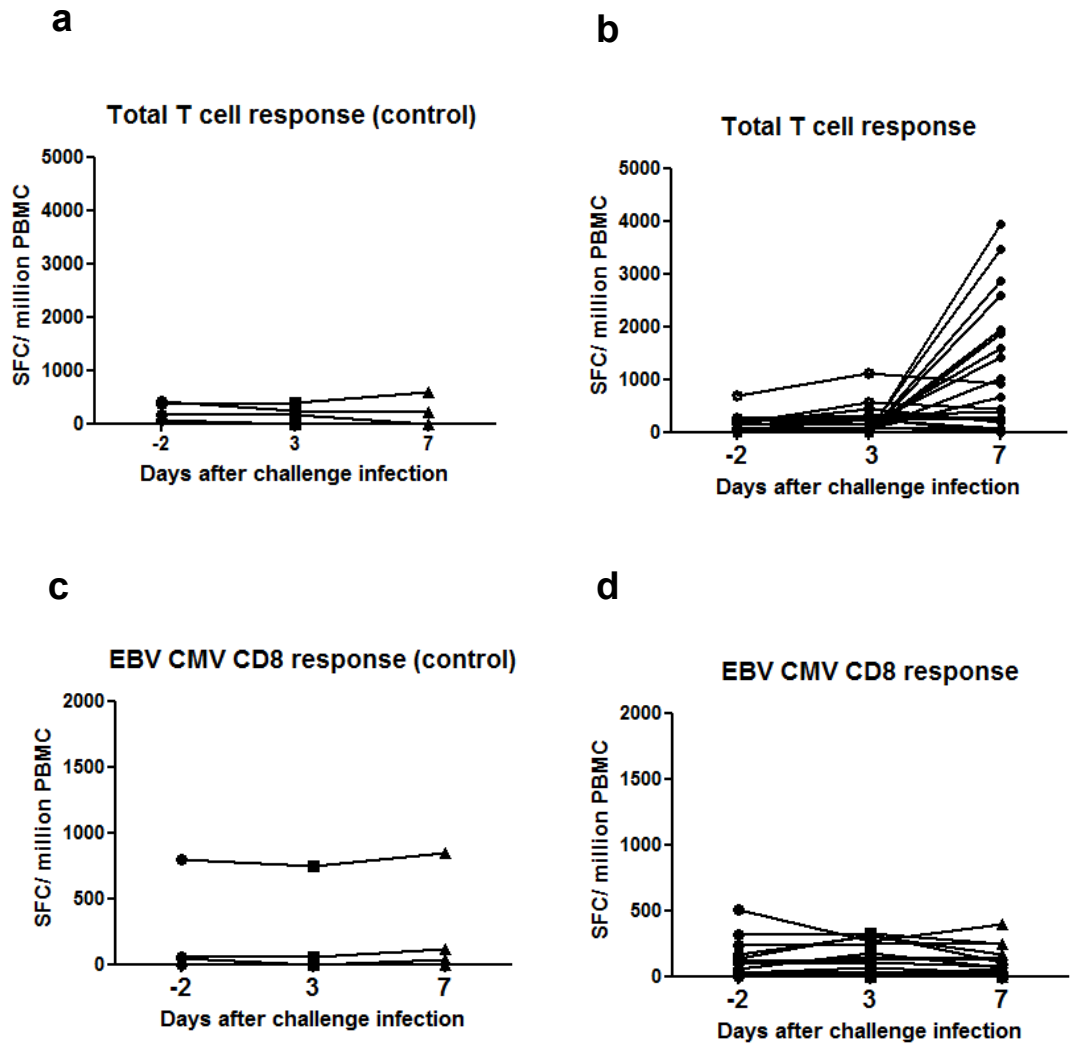

Figure 3.6 T cell responses to *ex vivo* stimulation in the H1N1 group. **(a)** Control (negative) in uninfected subjects. **(b)** Influenza peptide stimulation demonstrating expansion of responders by day 7. **(c)** CD8 responses to CMV and EBV peptide stimulation in uninfected subjects. **(d)** CD8 responses to CMV and EBV peptide stimulation in uninfected subjects. The lack of expanded response to CMV and EBV during acute influenza infection demonstrates that the T cell response is pathogen specific and bystander activation is minimal in PBMCs.

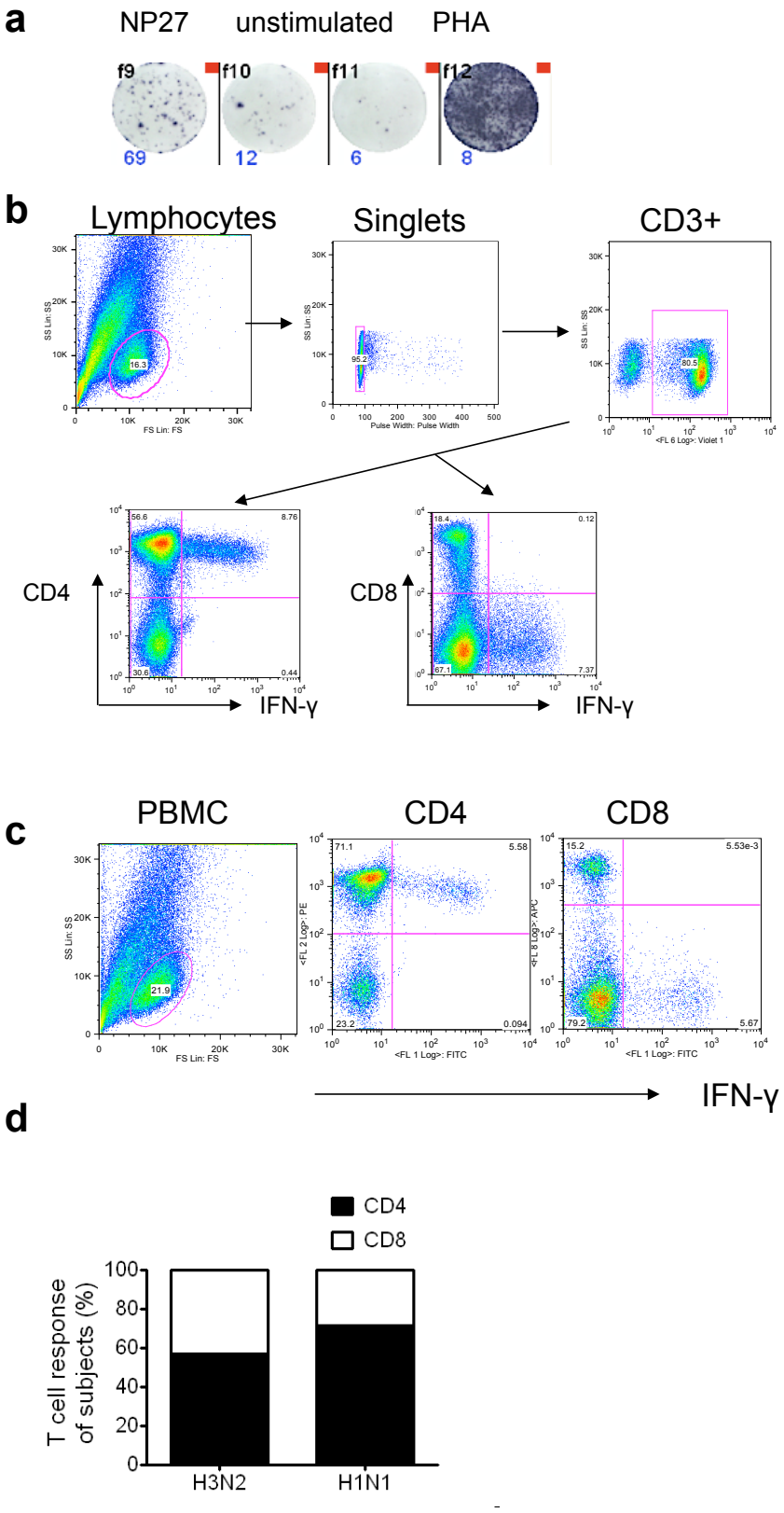

Figure 3.7 Antigen-specific responses to viral peptides in infected subjects. Baseline responses of infected subjects were mapped to individual peptide by **(a)** cultured ELISpot. Representative example where cells responded to NP27. **(b)** Gating strategy for intracellular cytokine staining. **(c)** Representative example where T cell lines stimulated by NP-27 showed a response mediated by $CD4^+$ cells. **(d)** Plot of relative proportion of $CD4^+$ and $CD8^+$ contribution to T cell responses to influenza peptides NP and M at baseline for each cohort. Data from *ex vivo* stimulation and intracellular staining.

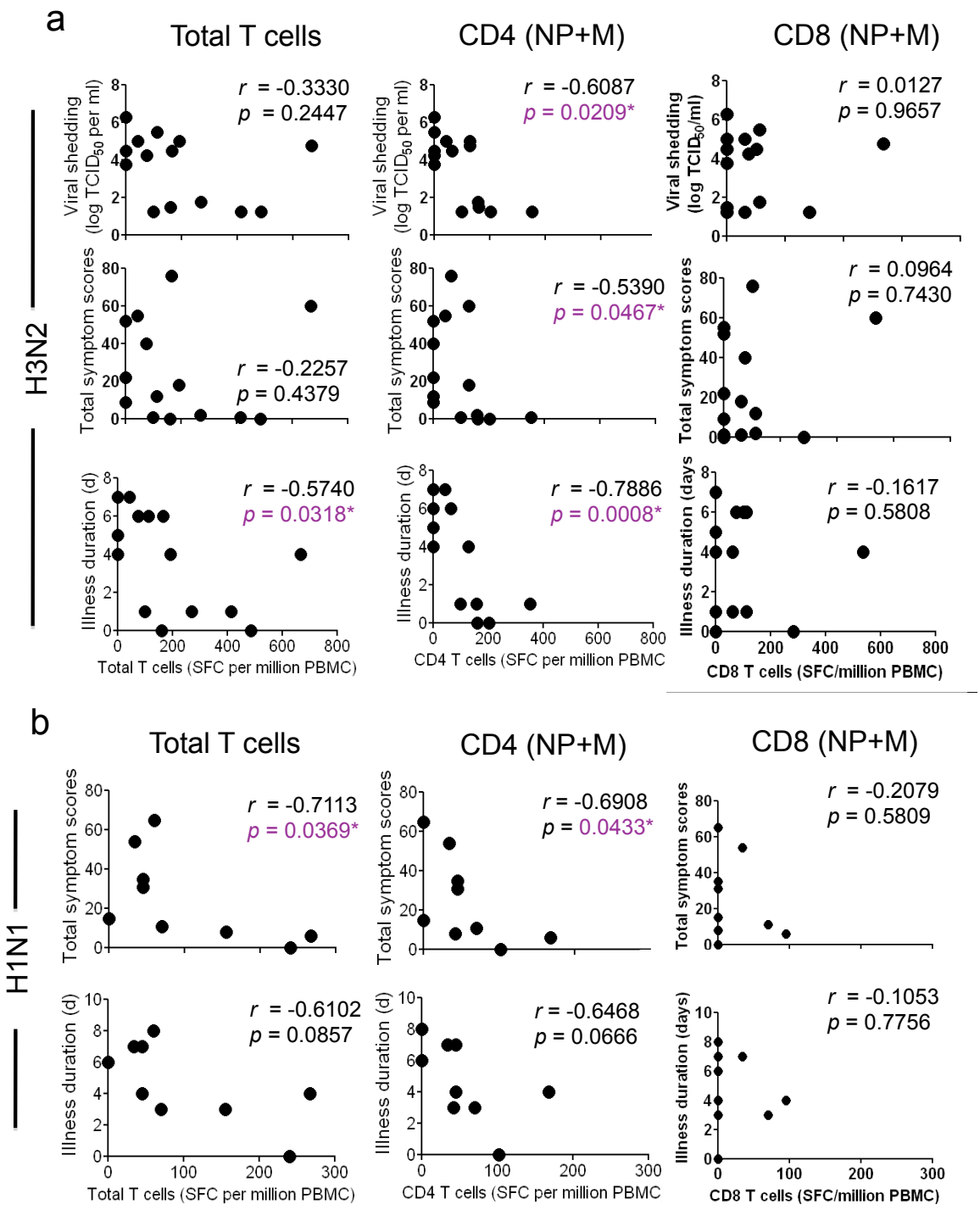

Figure 3.8 Relationship between influenza-specific T cell responses and illness severity. Correlations between influenza-specific total, $CD4^+$ and $CD8^+$ T cell responses to internal proteins (NP and M) and measures of influenza severity (viral shedding, symptom severity or illness duration) in volunteers infected with **(a)** H3N2 (WS/67/05) or **(b)** H1N1 (BR/59/07). All tests were run by Spearman rank correlation test. A *p* value of less than 0.05 was considered significant (*$p < 0.05$) and was highlighted in purple.

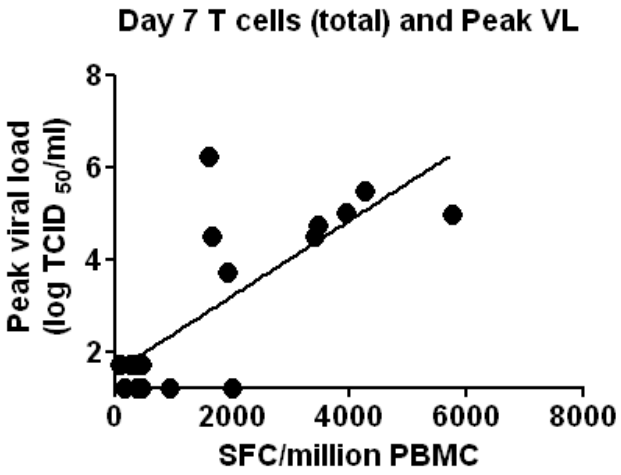

r^2=0.5898,
p=0.0003

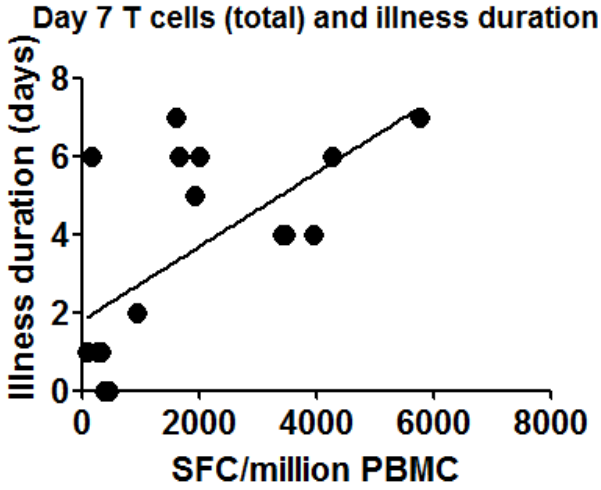

r^2=0.3932,
p=0.0071

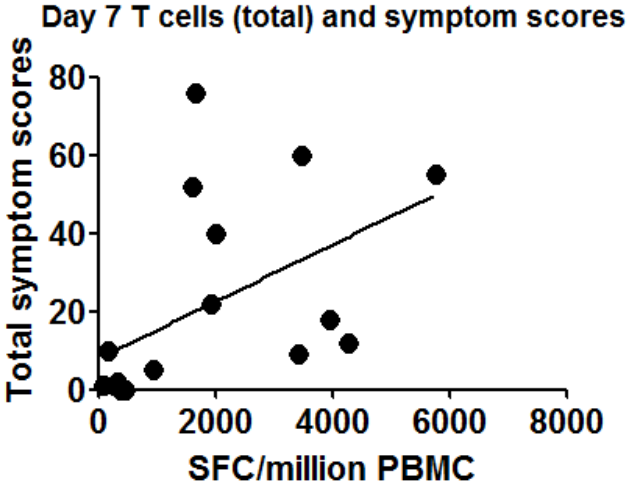

r^2=0.2546,
p=0.0389

Figure 3.9 Relationship between viral shedding, total symptom score and illness duration against total T cells responsive to influenza proteins in H3N2 group on day 7.

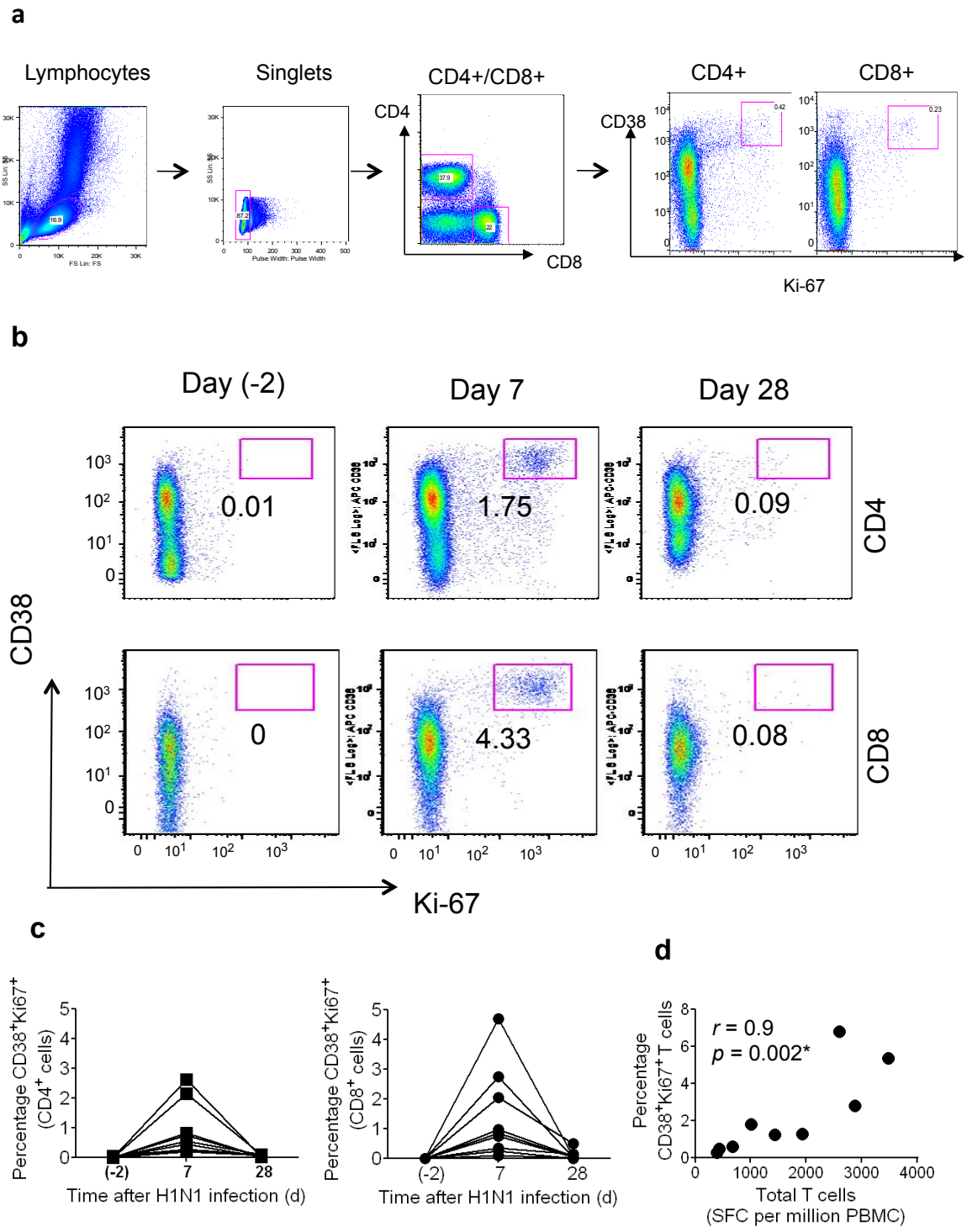

Figure 3.10 Kinetics of T cells in influenza infection. (a) Gating strategy. Activation status ($CD38^+$) and proliferating ($Ki\text{-}67^+$) abilities of T cells subsets were measured as depicted. **(b and c)** Dynamics in the proportion of activated and proliferating T cells in fresh PBMCs isolated from volunteers infected with H1N1 virus by flow cytometry. **(d)** Correlation between proportion of $CD38^+$ $Ki\text{-}67^+$ T cells on day 7 of H1N1 infected subjects with their magnitude of ELIspot response by Spearman rank correlation test. A *p* value of less than 0.05 was considered significant (*$p< 0.05$).

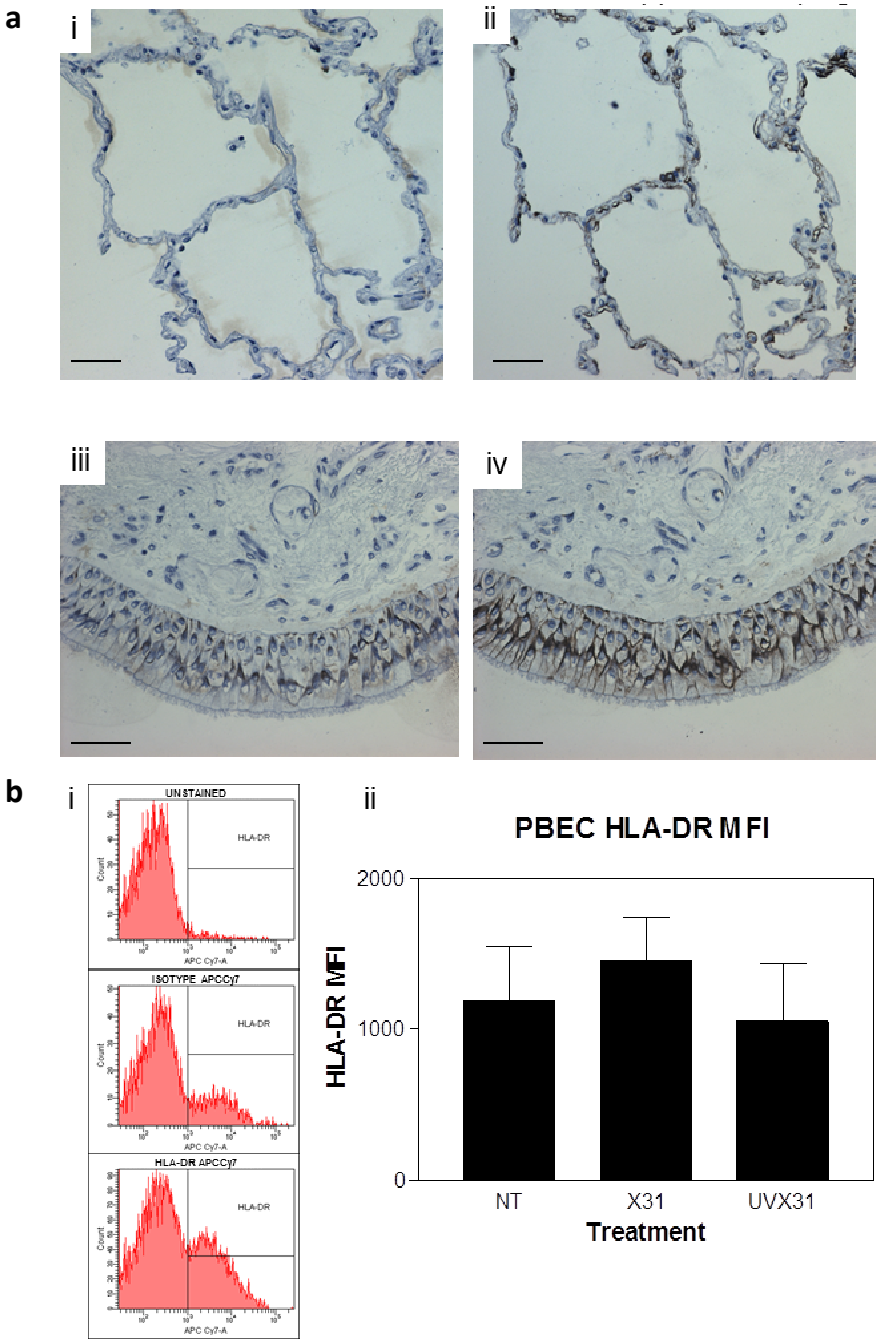

Figure 3.11 Expression of MHC Class II on the respiratory epithelium. (a) Human parenchymal (i) and (ii) and bronchial tissue stained (iii and iv) for MHC II (HLA-DR) 2mm sequentially cut sections and immunostained using isotype control monoclonal antibodies (i) and (iii) or antibodies specific for HLA-DR (ii) and (iv) at the same concentration. Signal was amplified using the ABC system, and colour developed using DAB stain. Specific staining is shown in brown, haematoxylin counterstain is shown in blue. Size bar represents 50 µm. **(b)** (i) Representative histograms showing specific staining of HLA-DR expression on primary bronchial epithelial cells (PBECs) by flow cytometry using cells incubated in the presence or absence of HLA-DR APC-Cy7 or IgG2a APC-Cy7 (isotype). (ii) Mean fluorescence intensity of HLA-DR expression on PBECs using flow cytometry. NT- non treated control, X31 influenza infected cells, UVX31- UV inactivated viral control. HLA-DR is constitutively expressed on primary respiratory epithelial cells, there is a small rise in expression following *in vitro* infection of these cells with influenza virus which was significant in comparison to stimulation with UV-treated (inactivated) virus. *This experiment was carried out by Dr. Tom Wilkinson.*

Chapter 4

Functional studies of influenza-specific CD4$^+$ T cells

4.1 Introduction

Anti-viral CD4$^+$ T cells play a crucial role in controlling influenza A virus during an infection. Understanding the mechanisms by which T cells mediate control is critical for us to be able to harness aspects of immunity that protect against the virus in vaccine design. Identifying the immune correlates of protection is not definitive and is difficult for any given pathogen. Different functional studies have been developed to dissect the immune response underlying acute infection in humans, which can then lead to a better understanding of the mechanisms that control the differentiation and maintenance of memory T cells (Makedonas and Betts, 2006), and thus protection.

Studies from the two experimental infection models suggested that pre-existing memory CD4$^+$ T cell responses play a more important role in the control of infection than previously reported in humans [(Wilkinson et al., 2012) and Chapter 3]. Through the secretion of cytokines to activate dendritic cells, CD4$^+$ T cells provide help for the maintenance and expansion of CD8$^+$ T cells by licensing antigen-presenting cells (Bevan, 2004; Brown et al., 2006; Doherty et al., 2006; Sun et al., 2004). CD4$^+$ T cells are thought to have more of a regulatory role in resolving an infection. The role of CD4$^+$ T cells in the clearance of influenza viruses has been shown through promotion of antibody production and/or cytokine-based mechanisms, and/or direct cytotoxicity (McKinstry et al., 2011; Swain et al., 2012).

Disease severity in influenza infection may also be correlated with functional exhaustion of antigen- specific T cells, which has been shown for other symptomatic infectious diseases such

as HIV, CMV and active tuberculosis (Wherry, 2011). However, the functional properties of influenza-specific T cells in the control for infection have not been extensively studied. It is important to understand the functional nature and protective attributes of T cells induced by natural infection; and by comparing those to that of a vaccine candidate we can assess whether protective or irrelevant responses have been generated.

Intracellular cytokine staining effectively detects antigen-specific T cells and allows their functions (cytokine production) and phenotype to be analysed simultaneously. PBMCs are stimulated for a short period of time in the presence of protein transport inhibitors such as brefeldin A and monensin, thus the induced cytokines accumulate inside the cells and can be readily detected by staining with fluorochrome conjugated antibodies after permeabilization. The overall immune response to influenza is best assessed by examining the response to the peptide pools made from the viral proteome, without taking immunodominance into account, as we aim to give an accurate representation of the total influenza-specific response. Previous studies have indicated that multifunctionality of antigen-specific T cells correlate with viral control, and changes in cytokine secretion profiles and phenotypic markers are associated with acute viral or bacterial infections (Sester et al., 2011). By measuring different T-cell functions, the quality and the possible breadth of influenza-induced responses in addition to simple magnitude can be assessed. The current dogma is that the higher number of effector functions in the overall response, the more protective the response (Makedonas and Betts, 2006; Seder et al., 2008). To assess the polyfunctional nature of the T cell response, I simultaneously quantified the upregulation of IFN-γ, interleukin-2 (IL-2) and tumor necrosis factor (TNF)-α. IFN-γ is often used as a readout for antigen-specific cell anti-viral activity because T cells release IFN-γ immediately after stimulation with antigens and it is readily detectable by flow cytometry (Liu and Whitton, 2005). IFN-γ is a Type II interferon, one of the protein families that were discovered to interfere with viral replication. IFN-γ has an important role in antiviral protection in influenza infection (Morris et al., 1982). IL-2 is a cytokine that is secreted by T cells to enhance proliferation and differentiation of antigen-specific T cells. TNF-α is released by T cells after engagement of TCR, and amplifies Th1 responses by inducing synthesis of IL-12 and IL-18 from antigen presenting cells(Feldmann et al., 1995), in turn augmenting IFN-γ production. TNF-α also acts by binding to its receptor on the cell surfaces of the virally infected cells, inducing apoptosis (Pfeffer, 2003). *De novo* synthesis of perforin was also assayed to give an indication of the cytotoxic response. Recent studies have

shown that when CD8$^+$ T cells from healthy humans were stimulated flu peptides, they seldom upregulate perforin and the polyfunctional responses are led by IL-2 (Makedonas et al., 2010).

The aims of this chapter are as follows:

1) To assess the ability of influenza- specific CD4$^+$ T cells to induce heterosubtypic responses.

2) To examine the cytotoxic functions of influenza-specific CD4$^+$ T cells.

3) To analyse cytokine expression profiles of antigen-specific T cells induced after influenza infection, and their relationship with viral control.

4.2 Results

4.2.1 Pre-existing T cell immunity in healthy individuals against seasonal H3N2 and H1N1

I first examined the virus-specific $CD4^+$ and $CD8^+$ memory T cell responses to the proteomes of human influenza A virus, H3N2 WS/67/05 and H1N1 BR/59/07, in healthy individuals. Before the occurrence of H1N1 pandemic in April 2009, H3N2 and H1N1 were the circulating strains within the population. A number of adult volunteers (n=55) in the laboratory were tested for their pre-existing T cell responses against the H1N1 (n=55) and H3N2 (n=24), by stimulating PBMCs with peptide pools containing overlapping peptides spanning the proteomes of the respective strains in an IFN-γ ELISpot. Positive responses detected during peptide pool screening were subsequently confirmed at a single-peptide level in a second round of *ex vivo* IFN-γ ELISpot. The majority of donors (96% for H1N1, 92% for H3N2) exhibited influenza-specific memory T cell responses. The magnitude and breadth of responses varied between individuals (**Fig. 4.1**), with the median number of one protein recognized (range 1-3) in both the H1N1 and H3N2 group. T cell responses specifically targeted the internal regions of the virus (**Fig. 4.1cd**). Therefore it would seem reasonable to suggest that T cells that are specific for highly conserved internal protein regions of the influenza virus exist in the majority of healthy adults.

4.2.2 Functional avidity of seasonal H1N1-specific T cells that cross-react with pandemic H1N1 epitopes

I then asked whether memory $CD4^+$ T cell responses are heterosubtypic. Influenza viruses escape detection by immune system through selection for amino acid substitutions that are disadvantageous for immune recognition. Such mutations within the immune epitopes may inhibit MHC binding or alter T-cell recognition, though the immune system may still be able to elicit a response if the viruses retain the immune epitope identity. Memory $CD4^+$ T cells from H1N1 challenge subjects were tested to determine if they could cross- recognize equivalent peptides from pandemic H1N1 (A/CA/07/2009) proteins using *ex vivo* ELISpot. Given the homology between the M1, NP proteins among the different influenza A subtypes (**Fig. 1.6**), a certain degree of cross-recognition by T cells was expected. I examined whether amino acid differences in pandemic H1N1 peptides affect the quality of the T cell responses. Peptides for

each responder were mapped at individual peptide level by 2-D ELISpot (as described in Chapter 3). PBMCs from each responder were then stimulated with the mapped H1N1 peptides and the equivalent peptides from pandemic H1N1 (A/CA/07/2009) at decreasing concentrations in an *ex vivo* IFN-γ ELISpot. **Fig. 4.2** shows T cell responses against matrix peptides, while **Fig. 4.3** shows T cell responses against nucleoprotein peptides. For epitopes M1-01, M1-12, M1-14 and M1-29, the dose-response curves for pandemic H1N1 overlap with that of seasonal H1N1. As their maximal SFC values essentially overlapped, this implied that the majority of seasonal H1N1 specific T cells respond to pandemic H1N1 homologues as well. Finally, M1-13 specific T cells did not respond to their pandemic H1N1 counterpart, despite only a single amino acid difference between the two, suggesting they were the key anchor positions to bind corresponding HLA molecules. M1-26 and M1-27 specific T cells also did not respond to heterologous pandemic peptides (**Fig. 4.2**).

As for NP peptides, dose-response curves of NP-28 and NP-38 completely overlapped with their pandemic H1N1 homologues (**Fig. 4.3**). Seasonal H1N1-specific T cells also cross-reacted with pNP-14, pNP-15, pNP-27, pNP-36 and pNP-39 (pandemic H1N1 sequences). However, across the Ag concentrations, the curves for pandemic H1N1 peptides followed but did not overlap those of seasonal H1N1 peptides, suggesting the presence of only a partial cross-reactivity. Responses to pandemic H1N1 were weaker than that of their seasonal H1N1 counterparts (**Fig. 4.3**).

4.2.3 Cytotoxic ability of flu-specific T cells

Increasing evidence has shown that CD4$^+$ T cells can act directly as effectors through secretion of antiviral cytokines or through direct cytotoxicity (Swain et al., 2012). To investigate further the effector functions including cytotoxicity displayed by these CD4$^+$ T cells, autologous EBV-transformed B cell lines (BCLs) were pulsed with the corresponding H3N2 peptides and were used as targets. The ability of T cell lines derived from PBMCs, which were collected on the baseline of the H3N2 challenge study, to recognize and lyse target cells were evaluated by ^{51}Cr release assay and CD107a (a marker of degranulation) staining. A CD8$^+$ T cell clone specific for cytomegalovirus (CMV) HLA-A2 binding epitope NLV (NLVPMVATV) was used as a control (**Fig. 4.4a**). All T cell lines specific to the mapped peptides were successfully made, while B cell lines from 7 out of 9 subjects were made successfully. Cytotoxic responses were observed in four out of the ten CD4$^+$ T cell lines tested. As shown in **Fig. 4.4a**, T cell line specific for

$CD8^+$ peptide NP-21 also displayed cytolytic ability when recognizing pulsed targets, although a certain degree of non-specificity was observed. T cell lines specific for NP-14, M-2 or HA-45 (all CD4-dependent) were also able to recognize and lyse autologous targets (**Fig. 4.4a**). Specific ^{51}Cr release showed a marked decrease (50-80% of reduction) in response upon addition of Concanamycin A (CMA), which accelerated the degradation of perforin by increasing the pH in the lytic granules, indicating the $CD4^+$ killing activity was largely perforin dependent (**Fig. 4.4b**). These cell lines expressed IFN-γ and upregulated CD107a simultaneously (**Fig. 4.4c**).

4.2.4 Recognition of target cells infected with rVACVs expressing seasonal or pandemic H1N1 M protein

To eliminate misleading results due to relatively high peptide concentration (2 μg/ml) used in *ex vivo* ELIspot assay, I investigated whether T cell responses to H1N1 peptides were functional against naturally processed seasonal or pandemic H1N1 virus proteins. Recombinant vaccinia viruses (rVACVs) expressing M1 of seasonal or pandemic H1N1 were generated (H1N1 M1-VACV and H1N1 2009 M1-VACV) (**Fig. 4.5a**). Briefly, vaccinia expression vectors (pSC11) containing the M1 proteins were constructed, and were transfected into TK-143 cells infected with wild type vaccinia virus. The supernatant containing the crude recombinant virus was purified for three rounds using 5-bromodeoxyuridine (BUdR) and 5-bromo-4-chloro-3-indolyl-β-D-galactoside (X-gal) selection. The titers of the purified viruses were measured using plaque assays. Monolayers of TK-143 cells, L- cells and B cells were infected with different concentrations of rVACVs and were stained for the M1 proteins to check for expression of the recombinant proteins upon infection. Subsequently, autologous B cell lines were infected by the rVACVs, and the extent of cross-recognition of target cells infected with rVACVs by T cell lines were evaluated by ^{51}Cr release assay. B cell lines infected with wild-type VACVs were not recognized. Specific lysis was displayed by 2 out of 10 T-cell lines tested (M-26 and M-12 $CD4^+$ T cell lines), even at low effector to target ratios (**Fig. 4.5b**).

4.2.5 Polyfunctionality of T cells in an acute influenza infection

4.2.5.1 Cytokine profile of flu-specific T cells

As T cells are capable of exerting many functions simultaneously, I next assessed the ability of flu –specific $CD4^+$ and $CD8^+$ T cells to upregulate IFN-γ, TNF-α, IL-2 and/or perforin, or to

degranulate by multicolour flow cytometry. PBMCs from the 10 of the 14 infected subjects of the H3N2 challenge studies were stimulated by H3N2 peptides pools together with secretion inhibitors and costimulatory antibodies for six hours, followed by intracellular cytokine staining. These peptides pools contained overlapping peptides spanning the sequence of the viral M or NP protein (M or NP pool), or contained all the overlapping peptides spanning the entire H3N2 proteome (total flu pool). I identified which peptide pools to use based on prior epitope mapping experiments (detailed in Chapter 3) (**Table 4.1**). Gating strategy and staining of a representative subject (stimulated by SEB) is shown in **Fig. 4.6**. Doublets and dead cells were excluded to reduce background noise. For both non-naïve CD8$^+$ and CD4$^+$ cells, positive responses for each individual function (IFN-γ, TNF-α, IL-2 and/or perforin and CD107a) were selected. Boolean gates were then generated from these individual 5 gates to produce 2^5 (=32) different functional categories, encompassing all possible combinations of these five functions. In **Fig. 4.7a**, flu-specific responses were calculated based on the summation of all the individual functional response patterns. Both memory CD4$^+$ and CD8$^+$ T cell responses to flu peptide pools could be detected (**Fig. 4.7ab**). No significant difference was found between the three timepoints when stimulated with either Flu, M or NP peptide pools. Comparing the difference between stimulations at the same time point, it was found that at baseline, the magnitude of total flu-specific CD4$^+$ T cells (median = 0.34%) were higher than that of M-specific and NP-specific CD4$^+$ T cells (median = 0.04% and 0.05% respectively) ($p< 0.01$). No difference in magnitude was found in other timepoints.

IFN-γ is the standard parameter by which T cell responses to influenza virus are assessed, due to the high detection limit by most cytokine assays. As shown in **Fig. 4.7b and 4.8a**, SEB stimulation was used as a positive control for IFN-γ production, and all subjects produced strong CD8$^+$ and CD4$^+$ IFN-γ responses after polyclonal SEB stimulation. Flu-specific, M-specific and NP-specific IFN-γ production in CD8$^+$ and CD4$^+$ T cells was readily detectable (**Fig. 4.7b**). No significant difference was found between the three timepoints when stimulated with either entire influenza proteome (flu), M or NP peptide pools, and no difference was also found in comparing different stimulations at the same timepoint (**Fig. 4.8bc**). As M and NP peptide pools contained most of the immunodominant epitopes that could elicit a response, the responses elicited by total flu peptides or with just M or NP pools were comparable.

Subjects	Timepoint	Stimulation	Timepoint	Stimulation	Timepoint	Stimulation
2	0	M	7	M	28	M
3	0	Flu, M, NP	7	Flu, M, NP		
4			7	Flu, M, NP	28	Flu, M, NP
5	0	Flu, M, NP	7	Flu, M, NP		
7	0	M, NP	7	M, NP	28	Flu, M, NP
8	0	Flu, M, NP	7	Flu, M, NP	28	Flu, M, NP
11	0	Flu, M, NP	7	Flu, M, NP	28	Flu, M, NP
14	0	Flu, M, NP	7	Flu, M, NP	28	Flu, M, NP
15	0	Flu, M, NP	7	Flu, M, NP		
18	0	Flu, M, NP	7	Flu, M, NP	28	Flu, M, NP

Stimulation	Flu			M			NP		
Days post infection	0	7	28	0	7	28	0	7	28
Total no. of subjects	7	8	6	9	10	7	8	9	6

Table 4.1 Summary of stimulations used for each subject. PBMCs from one subject (no. 2) were only stimulated by M pool due to limited number of cells. Data from subject (no. 4) on day 0 were removed from analysis, as the data file of the unstimulated control of that subject was lost during acquisition. Samples for three subjects on day 28 (no. 3, 5 and 15) were not available for this experiment.

4.2.5.2 Flu-specific T cells expressed other cytokines in addition to IFN-γ

Influenza-specific CD4+ and CD8+ T cell responses were further broken down into individual functions (IFN-γ, TNF-α, IL-2 and/or perforin and CD107a). Stimulation with peptide pools resulted in production of TNF-α and IL-2, and mobilization of degranulation marker CD107a. The functional hierarchy was dominated by the production of TNF-α and IL-2 in CD4+ cells. As shown in **Fig. 4.9a**, at baseline, frequency of CD4+ cells expressing TNF-α (median = 0.23%) was significantly higher than CD4+ cells expressing perforin (median = 0.02%) and CD107a (median = 0.06%) ($p< 0.005$ and $p< 0.05$ respectively). Frequency of CD4+ cells expressing IL-2 (median = 0.17%) was also significantly higher than CD4+ cells expressing perforin ($p< 0.05$). Difference between frequency of CD8+ cells expressing CD107a (median = 0.32%) and CD8+ cells expressing IL-2 and IFN-γ at baseline were not significant. Differences in magnitude between production of each cytokine on day 7 and 28 were insignificant. There was also no significant difference between production of each cytokine across different timepoints (**Fig. 4.9bc**). Therefore, when each of the cytokines was quantified in isolation, none of the cytokines were significantly changed throughout the study.

4.2.5.3 IFN-γ -producing flu-specific T cells differentially expressed other functions

As flu-specific CD4$^+$ T cell lines were shown to be cytotoxic, the ability of memory CD4$^+$ T cells to upregulate IFN-γ and degranulate by CD107a expression *ex vivo* was further examined following stimulation of peptide pools with entire influenza proteome, NP or M peptide pools. Frozen PBMCs were thawed and rested, stimulated by peptides pools together with secretion inhibitors and costimulatory antibodies for six hours, followed by intracellular cytokine staining. Prior to influenza challenge and seven days after challenge, memory CD4$^+$ T cells specific for NP or M at baseline and day 7 in infected subjects expressed IFN-γ; in addition, IFN-γ$^+$ CD4$^+$ cells also upregulated CD107a, indicating that these CD4$^+$ cells can degranulate (**Fig. 4.10**).

It is unclear whether IFN-γ-producing virus-specific T cells represent a true correlate of immune protection for influenza. I therefore assessed the capacity of IFN-γ-producing virus-specific T cells to perform other functions which might be associated with effective viral control. In assessing perforin responses, D48 anti-perforin antibody was used, to enable the measurement of both pre-formed and new perforin that were rapidly upregulated in response to antigenic stimulation. By quantifying perforin with the D48 antibody together with another function, it was then possible to identify the new perforin from pre-formed perforin in activated T cells (Makedonas et al., 2010).

For CD4$^+$ T cells, IFN-γ$^+$ cells that upregulated perforin in response to flu peptides were low at baseline (median = 0%), day 7 (median = 8%) and day 28 (median = 12%). For the degranulation marker CD107a, the expression level was also low at baseline (median = 24.8 %), day 7 (median = 18.8%) and day 28 (median = 39%). In contrast, IFN-γ$^+$ cells that upregulated IL-2 in response to flu peptides were elevated at baseline (median = 55.4%), day 7 (median = 50.5%) and day 28 (median = 31.3%). A high percentage of IFN-γ-producing CD4$^+$ cells also produced TNF-α at baseline (median = 80.2%), day 7 (median = 73%) and day 28 (median = 59.3%) (**Fig. 4.11a**).

For CD8$^+$ cells, IFN-γ$^+$ cells that upregulated perforin in response to flu peptides were also low at baseline (median = 0%), day 7 (median = 10.9%) and day 28 (median = 24.7%). The surface mobilization of CD107a was higher compared to that of CD4$^+$ cells (median = 61.9 % at baseline, median = 46.7% at day 7 and median = 43.1 % at day 28). IL-2 production of IFN-γ producing cells was also less elevated compared to that of CD4$^+$ cells (median = 14.7 %

at baseline, median = 22.9% at day 7 and median = 0% at day 28). Lastly, IFN-γ-producing CD8+ cells also produced TNF-α at baseline (median = 38%), day 7 (median = 60%) and day 28 (median = 61%) (**Fig. 4.11b**).

Taken together, these results suggested that flu-specific CD4+ and CD8+ cells are capable of eliciting multiple functions after stimulation; however, perforin production by activated T cells appeared to be minimal.

4.2.6 Memory phenotype of responding CD4+ and CD8+ cells

I characterized flu-specific CD4+ and CD8+ T cells by examining the expression of memory and maturation phenotypic markers CD27 and CD45RO. CD45RO is an isoform of CD45 associated with the transition from naïve to memory cells. CD27 is a costimulatory marker, which is irreversibly lost when continuously exposed to cognate epitopes (Hintzen et al., 1993). **Fig. 4.12a** shows an overlay of flu-specific cells positive for IL-2, IFN-γ, TNF-α and CD107a over density plots for CD27 versus CD45RO expression. Flu-specific CD4+ cells have primarily a central memory-like (CD27+ CD45RO+) phenotype. Flu-specific CD8+ cells are primarily effector-like (CD27- CD45RO-) and central memory-like (CD27+ CD45RO+).

In addition, surface expression of CD57 was used as a marker of terminally differentiated effector cells which are replication incompetent. While overlaying flu-specific cells positive for IL-2, IFN-γ, TNF-α and CD107a onto density plots showing CD27 versus CD57 expression, both flu-specific CD4+ and CD8+ T cells expressed less CD57 as compared to T cells being stimulated by SEB, showing the cells have strong homeostatic potential (**Fig. 4.12b**).

4.2.7 Polyfunctional analysis of influenza-specific CD4+ and CD8+ T cell responses

I next characterized the complexity of influenza-specific CD4+ and CD8+ T cell response by looking at all five functional parameters in various combinations. The total frequency of responding antigen-specific T cells was set to 100%, thus the contribution of each functional group was expressed as a percentage of total response. For both CD4+ and CD8+ cells, when stimulated by SEB, a broad repertoire of functional response was seen, indicating that there was no impairment of the cells' abilities to produce cytokines. The cytokine expression profiles of

SEB stimulated cells did not differ between timepoints (**Fig. 4.13**). This indicated that there is not some intrinsic difference in capacity for the cells to produce cytokines upon infection.

For CD4$^+$ T cells (**Fig. 4.14**), flu-specific responses displayed a functional profile consisting of one, two, three or four functions. When summing all the flu-specific responses together, monofunctional CD4$^+$ T cells that produced either IL-2 or TNF-α dominated the total response, although there were also polyfunctional responses (two or more functions simultaneously). The CD4$^+$ response profile was dominated by TNF-α production, and the primarily multifunctional population was the IL-2$^+$ CD107a$^+$ IFN-γ^+ TNF-α^+ subset. No difference in the overall functionality of the flu-specific CD4$^+$ T cell response was found between the three timepoints (day 0, 7 and 28). Stimulation with M or NP peptide pools induced a similar cytokine pattern, with responses skewed towards single or dual functions. Functionality of M-specific CD4$^+$ T cells was significantly different between day 7 and day 28 (**Fig. 4.15**), with a higher proportion of responding cells producing two or more functions on day 28.

For CD8$^+$ T cells (**Fig. 4.16**), the functional responses consisted of mainly CD107a expression in combination with another function. Flu-specific CD8$^+$ T cells tended to have a higher level of functionality than the CD4$^+$ T cell responses, expressing two or more functions. Similar to flu-specific CD4$^+$ cells, the functional profile of the flu-specific CD8$^+$ T cells was not different between timepoints. When stimulated by M or NP peptide pool, the CD8$^+$ T cells produced a combination of CD107a, TNF-α and perforin. Functionality of NP-specific CD8$^+$ T cells was significantly different between day 7 and day 28, with responses skewed towards the single or dual functions on day 28 (**Fig. 4.17**).

4.2.8 Relationship between polyfunctional T cell responses and clinical parameter

No significant relationship was found between frequency of each functional subset and clinical parameters of the H3N2 challenge study, including peak viral load, total symptom scores and antibodies level.

4.3 Discussion

During an influenza challenge, virus-specific memory CD4$^+$ T cells are primed and increased in number. The role of CD4$^+$ T cells in helping B cells and the licensing of antigen-presenting cells to promote the expansion of functional CD8$^+$ cytotoxic T cells is well established. They might also produce or induce mediators that facilitate innate immune response and contribute to viral clearance (Strutt et al., 2010). Alternatively, they might exert direct cytotoxic activity against virally infected cells (Strutt et al., 2009). Less is known about their roles in the direct control of influenza infection in humans. Here I demonstrated that CD4$^+$ T cells, specific for influenza peptides, are capable of mediating antiviral effector functions.

Firstly, I highlighted a potential benefit of generating CD4$^+$ T cell memory with recognition of peptides from core viral proteins that are conserved across strains. My results were consistent with previous studies, where responses to pandemic H1N1 were seen in previously unexposed individuals (Scheible et al., 2011), and peptides derived from pandemic H1N1 virus were able to induce responses in seasonal influenza virus- specific T cells from pandemic H1N1-naïve individuals (Ge et al., 2010). Harnessing this robust cross-reactive response may present a promising approach for the development of more broadly protective vaccines.

My studies suggest that CD4$^+$ T cells may have a more direct role in coordinating an effector T cell response during an infection. In mice it is thought that viral clearance depends on cytotoxic CD8$^+$ T cells [reviewed in (Thomas et al., 2006)], while CD4$^+$ cells have more of a regulatory role in resolving an infection. The role of CD4$^+$ T cells as cytotoxic effectors is less certain. Through secretion of cytokines to activate dendritic cells, CD4$^+$ T cells provide help for the maintenance and expansion of CD8$^+$ T cells by licensing of antigen-presenting cells (Bevan, 2004; Brown et al., 2006; Doherty et al., 2006; Sun et al., 2004). A mouse model of herpes simplex infection recently showed that CD4$^+$ T cells are essential in recruiting cytotoxic CD8$^+$ T cells into virally infected tissues (Nakanishi et al., 2009). Memory CD4$^+$ T cells have been shown to clear influenza virus through synergy with naïve B cells and CD8$^+$ T cells in mice (McKinstry et al., 2012). CD4$^+$ T cells arrive at the site of infection, secrete IFN-γ and induce expression of chemokines to attract CD8$^+$ T cells (Nakanishi et al., 2009). Cytotoxic CD4$^+$ T cells that can exert a cytolytic effect on virally infected cells are positive for both granzyme and perforin. They are Th1 polarized and are found in low frequencies in healthy individuals,

but increase in numbers during viral infections (Appay et al., 2002). Cytotoxic CD4$^+$ T cells have been reported in infections such as CMV and HIV (Casazza et al., 2006; Soghoian et al., 2012; Swain et al., 2012), and are involved in viral clearance (Appay, 2004; Soghoian and Streeck, 2010). Whether influenza-specific CD4$^+$ T cells are able to act as cytotoxic cells *in vivo* is controversial, early evidence (Lukacher et al., 1985) showed that a panel of CD4$^+$ T cell clones had direct cytolytic activity towards target cells expressing MHC Class II which was inhibited with the addition of CD4 blocking antibodies. Several murine studies have suggested roles for CD4$^+$ T cells in viral clearance (Alexander et al., 2010; Hogan et al., 2001), including a recent study which showed CD4$^+$ T cell-mediated cytotoxicity protects against lethal influenza infection (Brown et al., 2012). It has also been demonstrated that cytotoxic CD4$^+$ T cells utilize both perforin and the Fas:FasL pathway to lyse target cells (Brown, 2010; Brown et al., 2009). A large number of influenza-specific CD4$^+$ effector T cells accumulate in the lung and produce IFN-γ prior to viral clearance, indicating that CD4$^+$ T cells may play more of a role in viral control other than their classical roles which are to augment CD8$^+$ memory T cells and B cells responses (Roman et al., 2002). Indeed, my results showed that influenza-specific CD4$^+$ T cell lines are cytotoxic, and this cytolytic pathway is likely to be perforin-based, similar to CD4$^+$ CTL reported in other viral infections (Appay et al., 2002). It is unclear whether this cytotoxicity is relevant *in vivo* but it will be difficult to evaluate directly in humans.

Secondly, my findings also indicated that pre-existing influenza-specific CD4$^+$ or CD8$^+$ cells are polyfunctional. Multifunctional T cell responses in mouse and human are associated with superior antiviral protection and vaccine efficacy (Betts et al., 2006; Darrah et al., 2007; Duvall et al., 2008). Production of IFN-γ, TNF-α and IL-2 were observed in both influenza-specific CD4$^+$ and CD8$^+$ T cells. Expression of IL-2 indicated the ability of the influenza-specific T cells to expand in response to viral antigens. Previous reports have shown that CD8$^+$ T cell responses to influenza is led by IL-2, and IL-2 production and perforin upregulation are not co-expressed in any polyfunctional population (Makedonas et al., 2010). In agreement, perforin upregulation was not commonly observed in this study. It is thought that continual antigen exposure may be required to induce perforin upregulation (Makedonas et al., 2010), thus as viral antigens were cleared rapidly upon influenza infection, perforin upregulation were not observed in influenza-specific T cells. In this study, correlation between clinical outcome and polyfunctionality of influenza-specific T cells was not found. However, care has to be taken in

interpreting the analyses done here based on the peripheral blood as it has been reported that characteristics of influenza-specific T cells in the blood differ from those in the lung, with the lung containing pools of differentiated respiratory virus-specific T cells (de Bree et al., 2007; de Bree et al., 2005).

The present analysis also showed that influenza-specific CD4$^+$ T cells maintained a central memory phenotype, while both effector-like memory and central memory phenotype are maintained by a proportion of influenza-specific CD8$^+$ T cells. Previous studies have also showed that influenza-specific CD4$^+$ cells in the peripheral blood have a central memory phenotype (Lucas et al., 2004). This may imply that upon acute infection, influenza- specific T cells occupy different niches: CD8$^+$ T cells located in periphery act as immediate effectors provide immediate protection; whereas central memory CD4$^+$ cells proliferate in a greater capacity upon reactivation. However, an important issue in understanding T cell immunity to influenza in humans is whether virus-specific T cells residing in the lungs are locally reactivated upon infection, or whether circulating virus-specific T cells are recruited from the circulation. In mice, a majority of CD4$^+$ cells isolated from the lungs after primary influenza infection were CCR7$^+$, which would allow these cells to recirculate back into lymphoid tissues (Debes et al., 2004). In another study where lung-residing T cells were isolated from tissue specimens from patients undergoing surgery for lung cancer, all lung-residing T cells lacked CCR7, and thus may use other chemokine receptors to migrate to the lung (de Bree et al., 2005). Therefore, future studies are required to be done to examine the capacity of T cells to migrate to peripheral effector sites, such as the lungs and the airways, by looking at their expression for chemokine receptors during the course of infection.

Taken together, this chapter indicates that flu-specific CD4$^+$ T cell responses are cross-reactive and are capable of inducing heterosubtypic responses. They are also cytotoxic and polyfunctional, thus may be helpful in generating protective immunity.

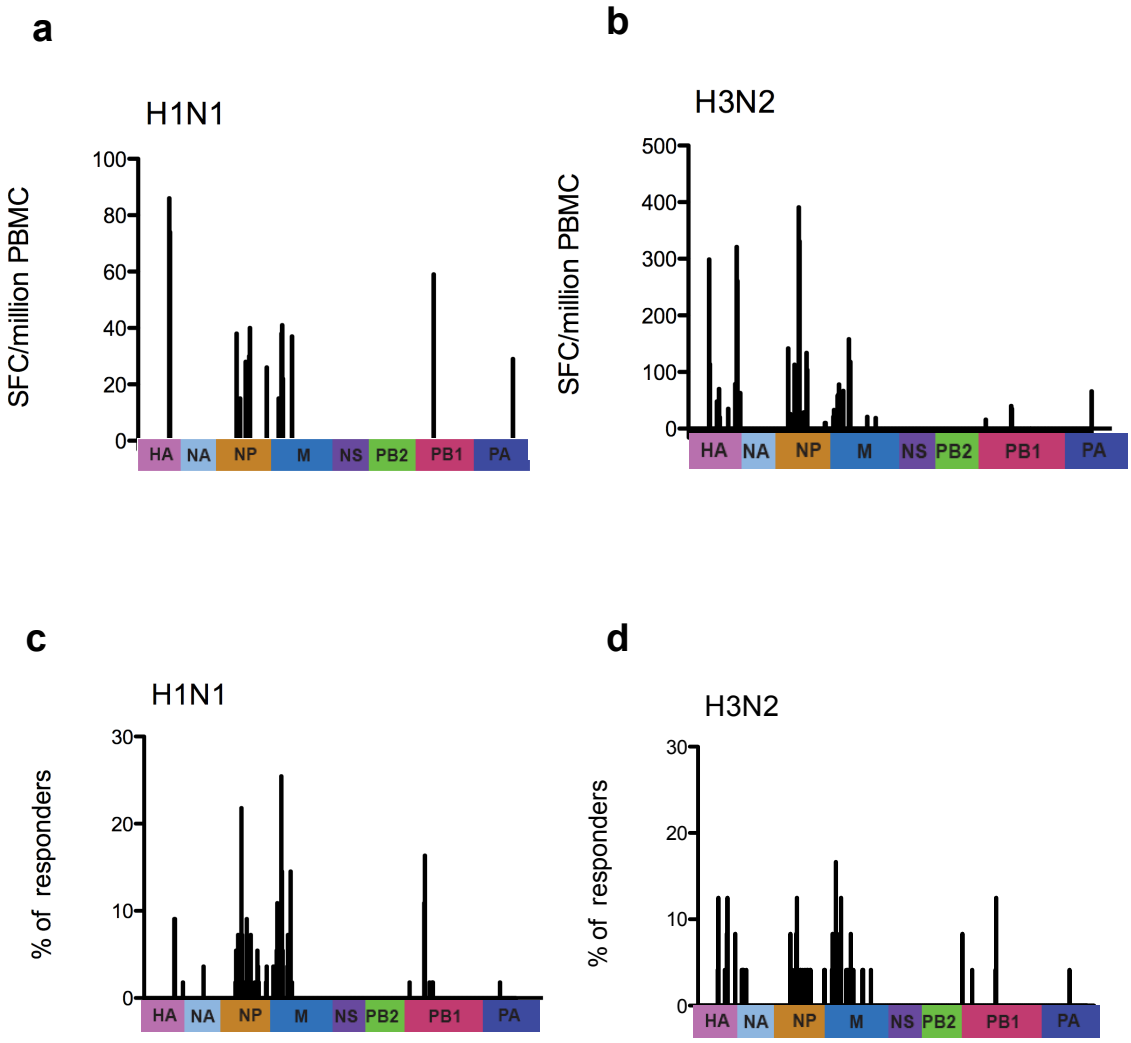

Figure 4.1 Flu-specific T cell responses of healthy individuals. *Ex vivo* IFN-γ production as measured by stimulating PBMCs from healthy individuals with overlapping peptides spanning the entire proteome of H1N1 (BR/59/07) (n=55) or H3N2 (WS/67/05) viruses (n=24). Magnitude of responses against H1N1 (BR/59/07) or H3N2 (WS/67/05) as measured by SFC per million PBMC of donors is shown in **(a)** and **(b)** respectively. Breadth of T cell response as measured by the percentage of recognition of the peptide response across **(c)** H1N1 and **(d)** H3N2 proteome. Most responses were directed towards the conserved NP and M proteins. For this single peptide ELISpot assay, responses greater than 10 SFC/million PBMC after background subtraction were considered positive.

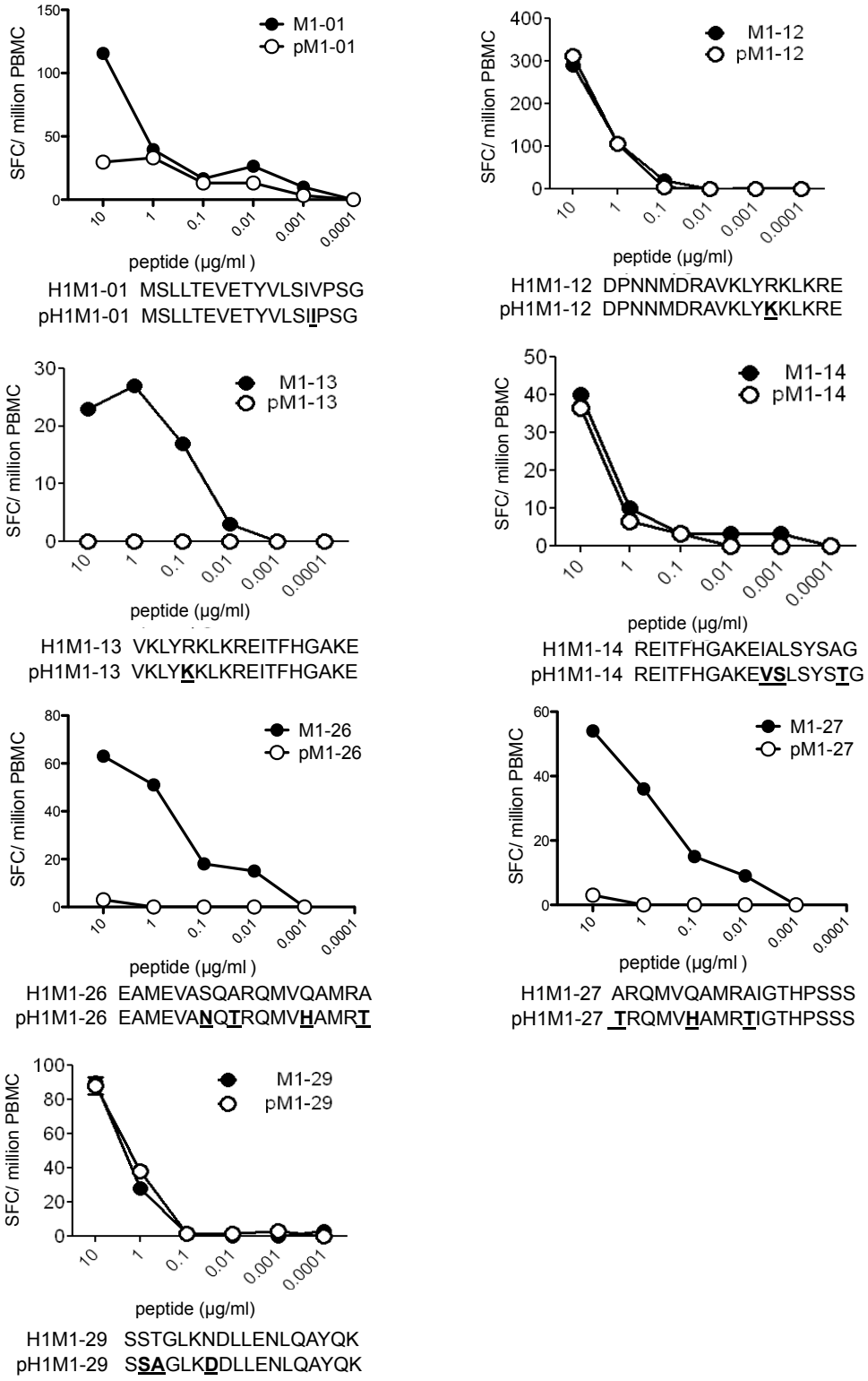

Figure 4.2 Cross- reactivity study of CD4 memory cells from H1N1 infected subjects to matrix peptides from pandemic H1N1. PBMCs from different subjects were stimulated with decreasing dosage of M peptides, and responses were measured by IFN-γ ELISpot. Each plot represents result from one donor to homologous seasonal (closed circles) and heterologous pandemic peptides (open circles). Differences in peptide sequences between seasonal H1N1 (A/Brisbane/59/07) and pandemic H1N1 (pH1N1) (A/California/07/09) are highlighted in bold, underlined text.

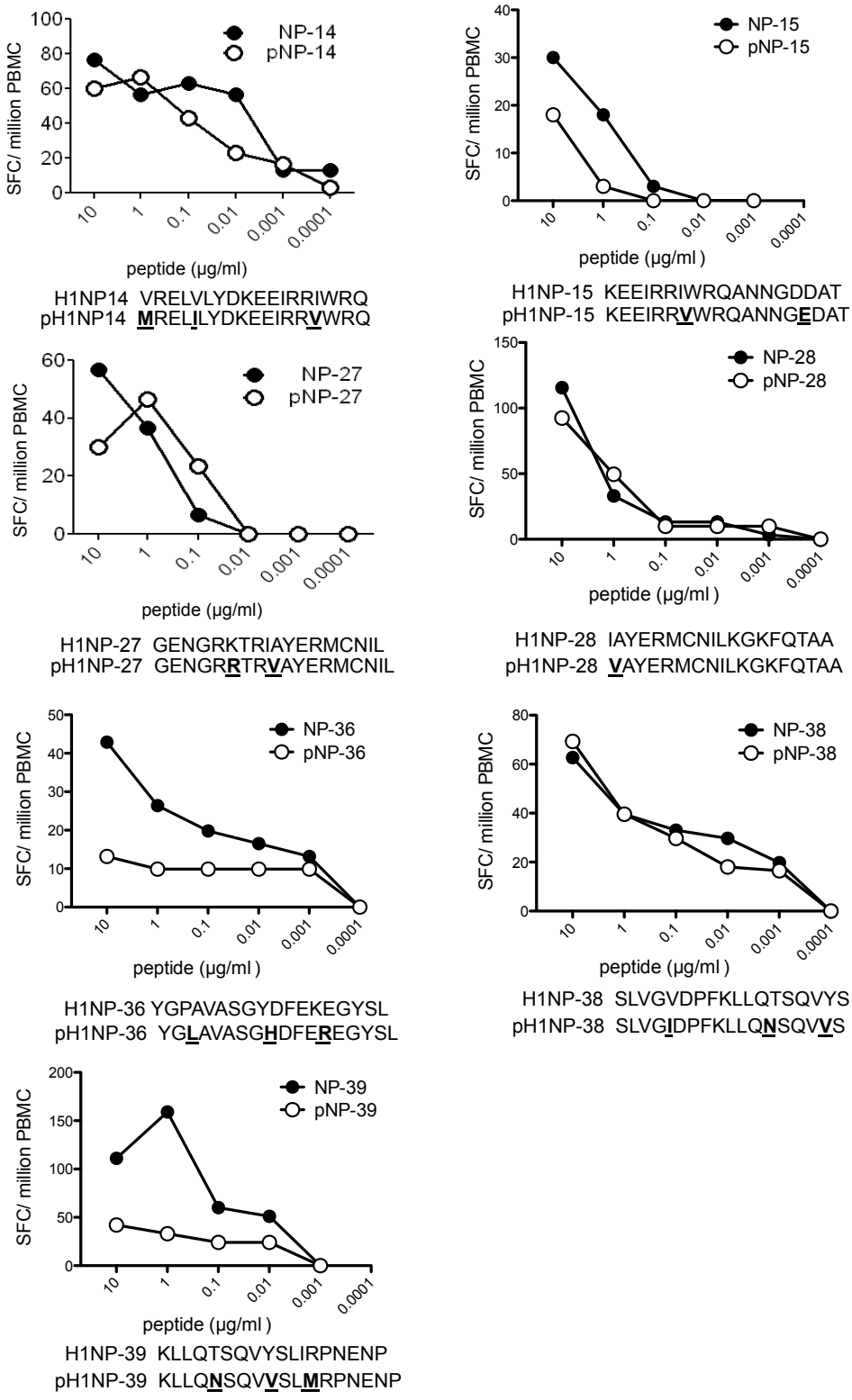

Figure 4.3 Cross- reactivity study of CD4 memory cells from H1N1 infected subjects to nucleoprotein peptides from pandemic H1N1. PBMCs from different subjects were stimulated with decreasing dosage of NP peptides, and responses were measured by IFN-γ ELISpot. Each plot represents result form one donor to homologous seasonal (closed circles) and heterologous pandemic peptides (open circles). Differences in peptide sequences between seasonal H1N1 (A/Brisbane/59/07) and pandemic H1N1 (pH1N1) (A/California/07/09) are highlighted in bold, underlined text.

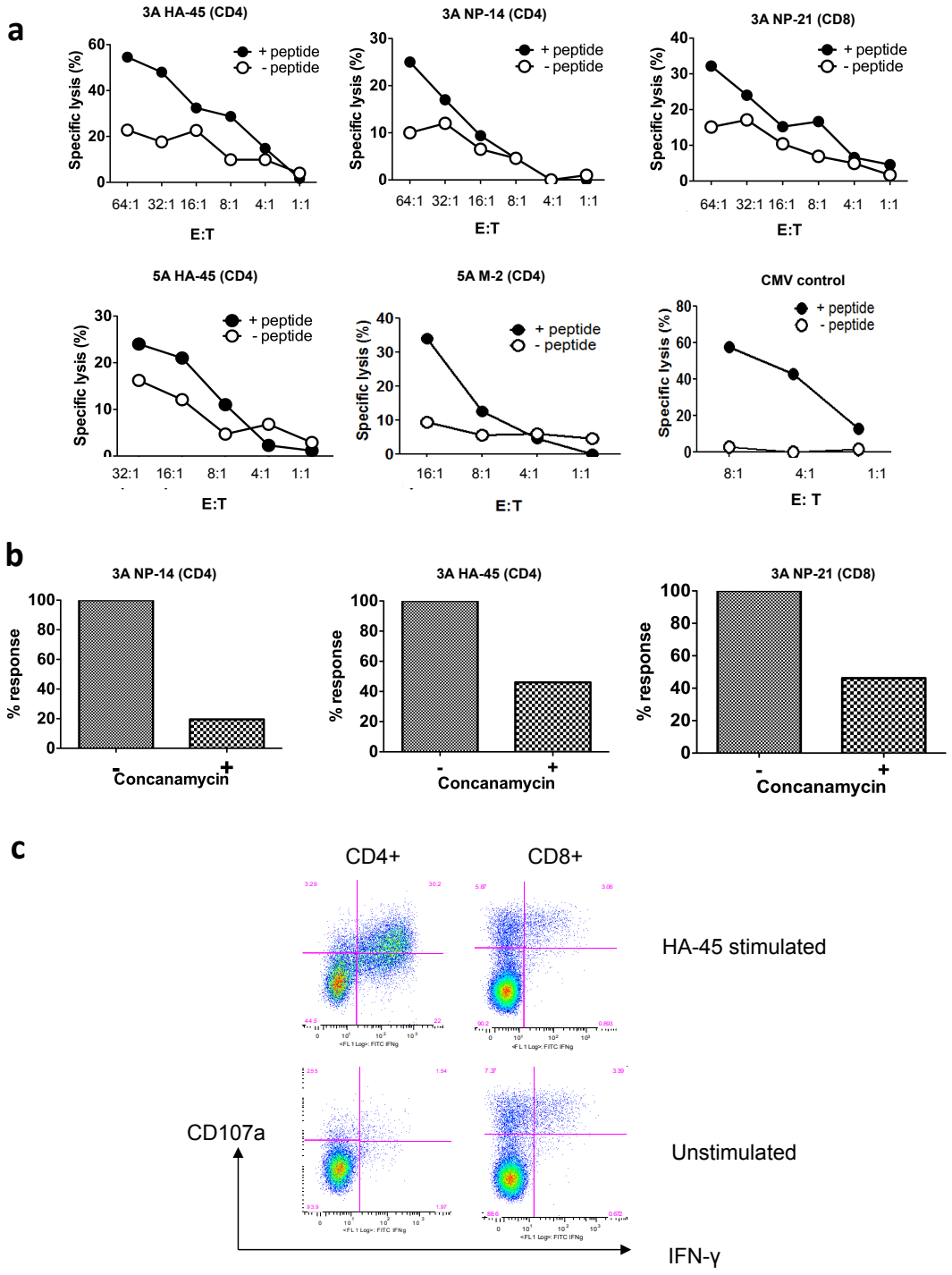

Figure 4.4 Killing activities displayed by T cell lines generated from H3N2 infected volunteers upon recognition of target cells by chromium release assay. (a) T cell lines were generated by stimulating PBMCs from two donors with identified peptides. Each plot represents lysis of chromium-loaded autologous target cells (B cell lines) pulsed with or without peptides in the presence of T cell lines at several E:T cell ratios for 4 h. **(b)** Perforin-dependent cytotoxicity was measured by sensitivity to concanamycin. **(c)** HA-45 specific T cell lines (CD4 dependent) were analysed for their IFN-γ and degranulation marker CD107a expression. T cells were stimulated with peptide-pulsed target cells overnight in an intracellular cytokine staining assay. E:T represents the effector to target cell ratio. 5A and 3A are individual subject identification numbers. HA-45, NP-14, NP-21 and M-2 are the influenza peptide identification numbers. CMV represents a CD8$^+$ T cell clone used as a control.

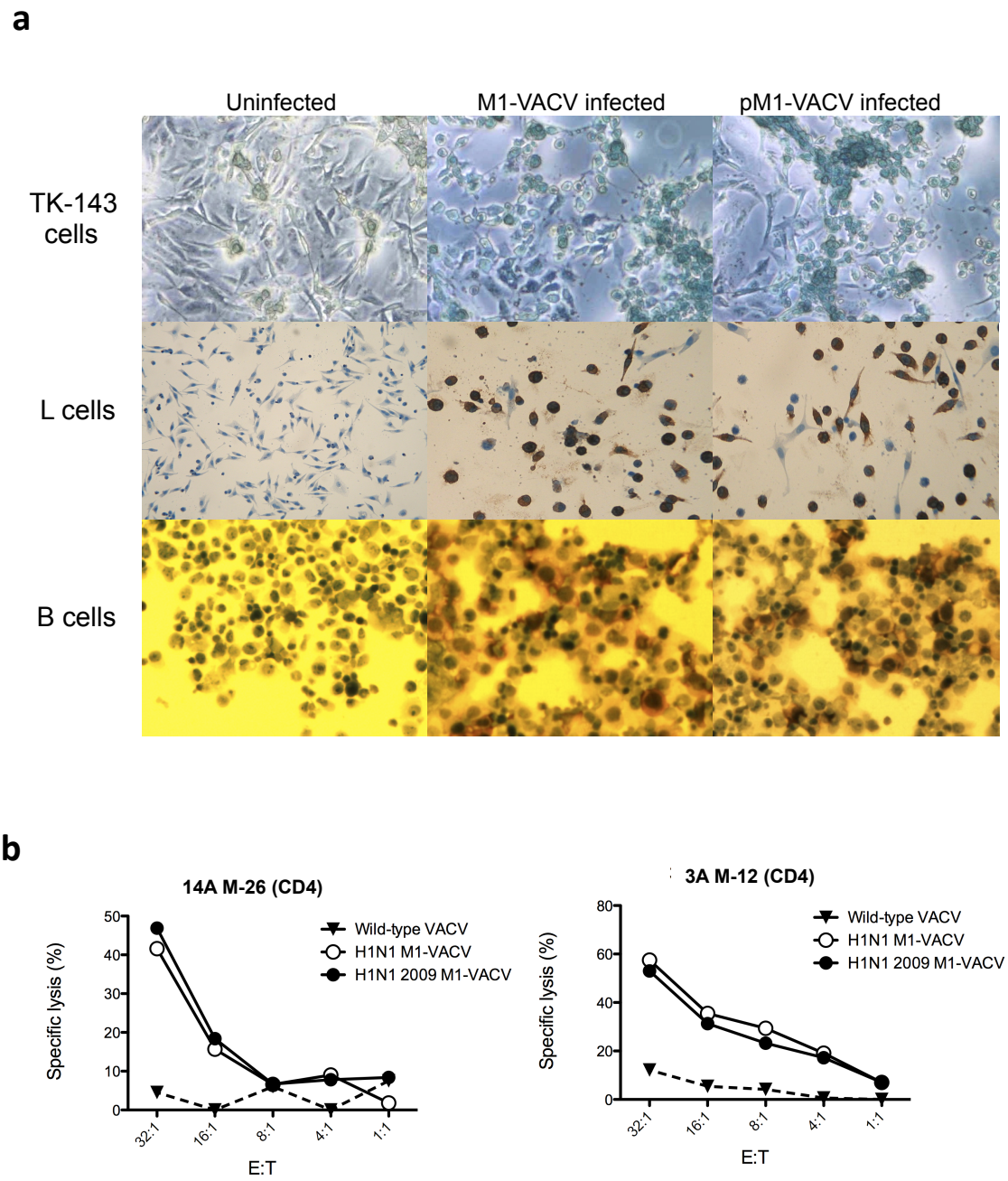

Figure 4.5 Killing activities displayed by T cell lines generated from subjects with a memory responses to H1N1, upon recognition of target cells infected by recombinant vaccinia virus by chromium release assay. (a) Infection of different cell lines (TK-143 cells, L-cells and B cells) with recombinant vaccinia virus M1-VACV and pM1-VACV. The expression of flu matrix protein in infected cells was confirmed by immunocytochemistry. Infected TK-143 cells were used to propagate the virus. To check expression of M proteins in plaques, monolayers of TK-143 cells were infected with VACVs then immunostained with antibodies against M proteins in a 6-well plate assay. Staining of the infected cells is visualised with TrueBlue peroxidase substrate. Infected cells display cytopathic effects. L-cells and B cells were plated on glass slides and infected with VACVs, followed by immunostaining with antibodies against M proteins. Staining of the infected cells is visualised with DAB. Specific staining is shown in brown, haematoxylin counterstain is shown in blue. **(b)** T cell lines were generated by stimulating PBMCs with peptides. Each plot represents lysis of chromium-loaded autologous target cells (B cell lines) infected with VACVs at several E:T cell ratios for 4 h. E:T represents the effector to target cell ratio. 14A and 3A are individual subject identification numbers. M-26 and M-12 are the influenza peptide identification numbers.

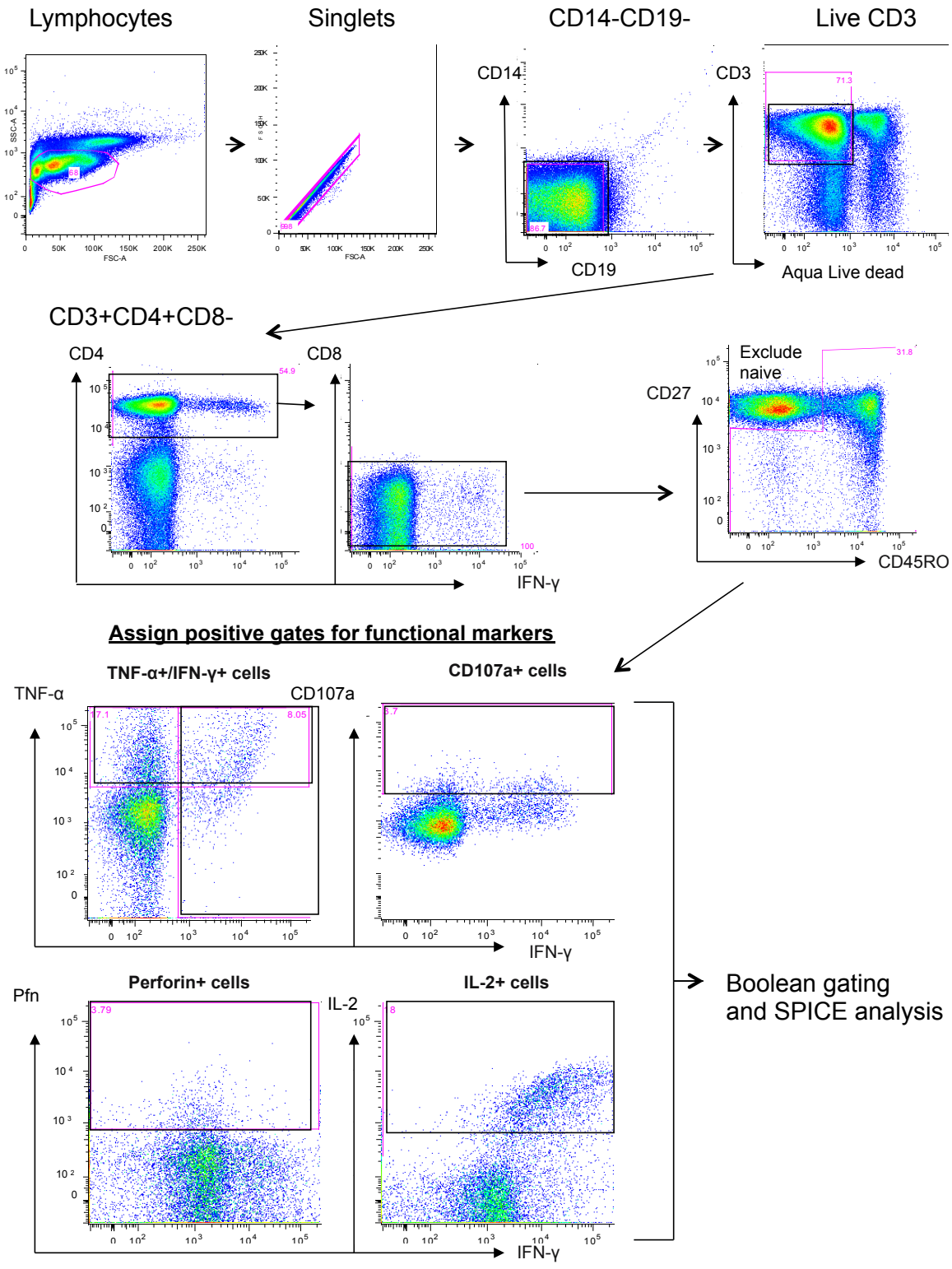

Figure 4.6 Gating Strategy of determining influenza-specific polyfunctional analysis of CD8+ and CD4+ T cells producing IL-2, IFN-γ, TNF-α , perforin and CD107a. Representative staining of a subject stimulated with SEB is shown.

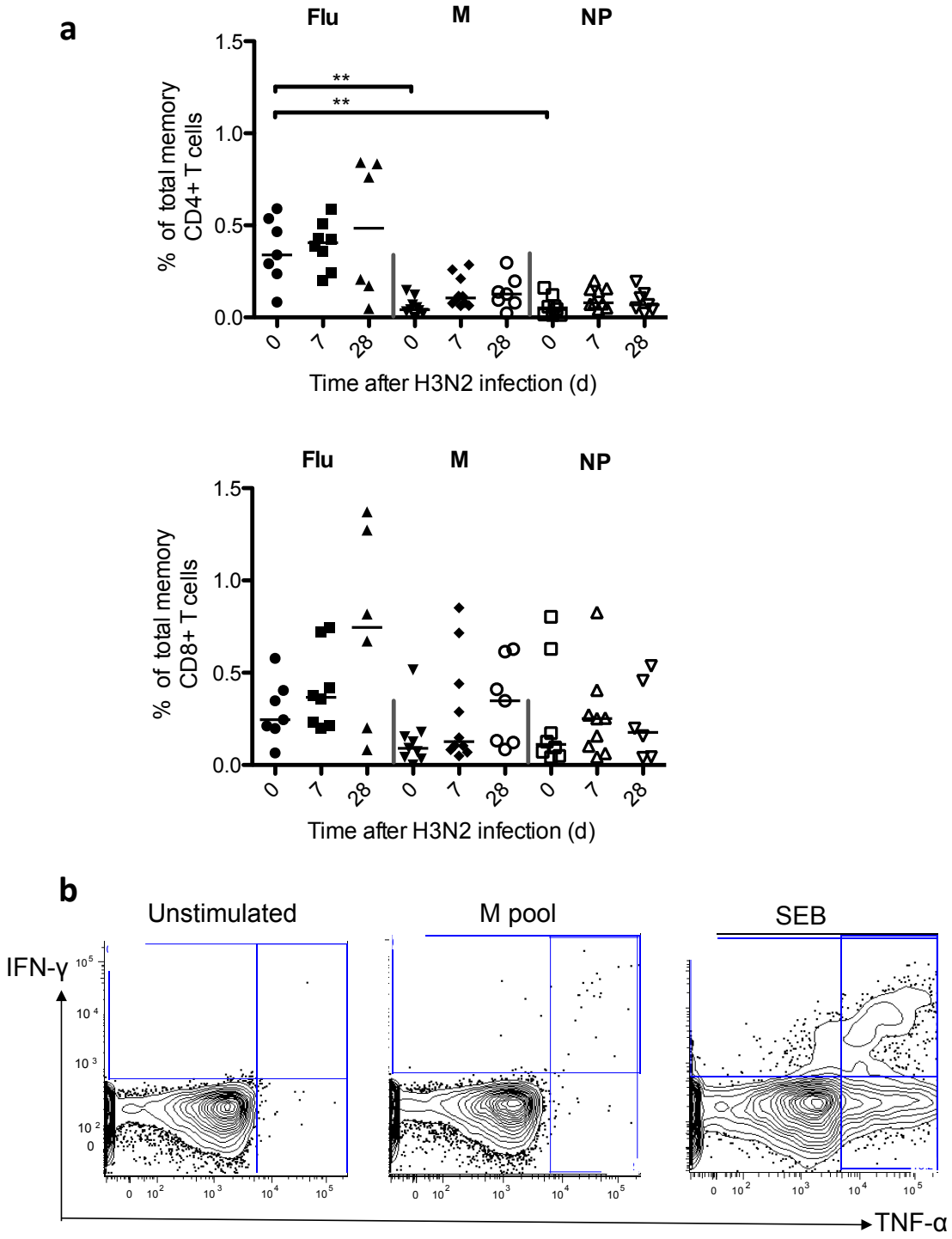

Figure 4.7 Influenza-specific T cells express multiple effector functions. PBMCs were stimulated with 2 μg/ml peptide pools (M, NP or flu pool) for 6 h, and five functional parameters (IFN-γ, IL-2, TNF-α, perforin and CD107a) were measured. **(a)** The magnitude of the total influenza, M-specific, or NP-specific memory $CD4^+$ and $CD8^+$ T cell response was calculated based on the summation of all individual functional response patterns. Small horizontal bars indicate median. Differences between stimulations were tested using non-parametric Kruskal–Wallis's test with post hoc Dunn's test for multiple comparisons. A p value of less than 0.05 is considered to be significant (**p< 0.01). **(b)** A representative $CD4^+$ T cell IFN-γ response, after stimulation with a M pool. Unstimulated and SEB-stimulated cells are shown as negative and positive controls respectively. Cells were gated on non-naïve $CD4^+$ T cells.

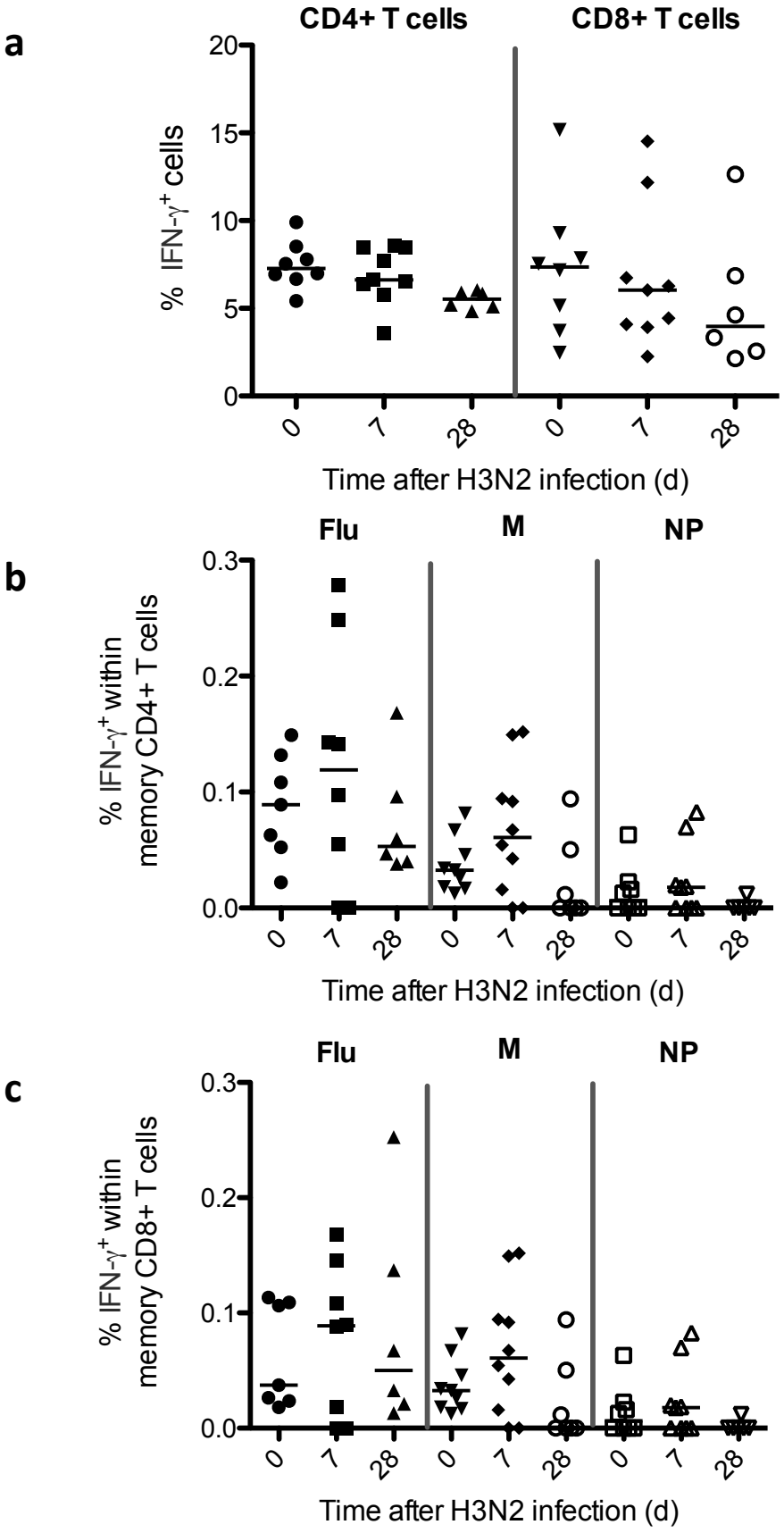

Figure 4.8 Frequency of IFN-γ producing CD4+ and CD8+ T cells as measured by intracellular cytokine staining. (a) Frequency of IFN-γ producing CD4+ and CD8+ T cells in response to SEB stimulation. Frequency of IFN-γ producing **(b)** CD4+ and **(c)** CD8+ T cells in response to peptide pool stimulation (total flu pool, M pool or NP pool). Small horizontal bars indicate median.

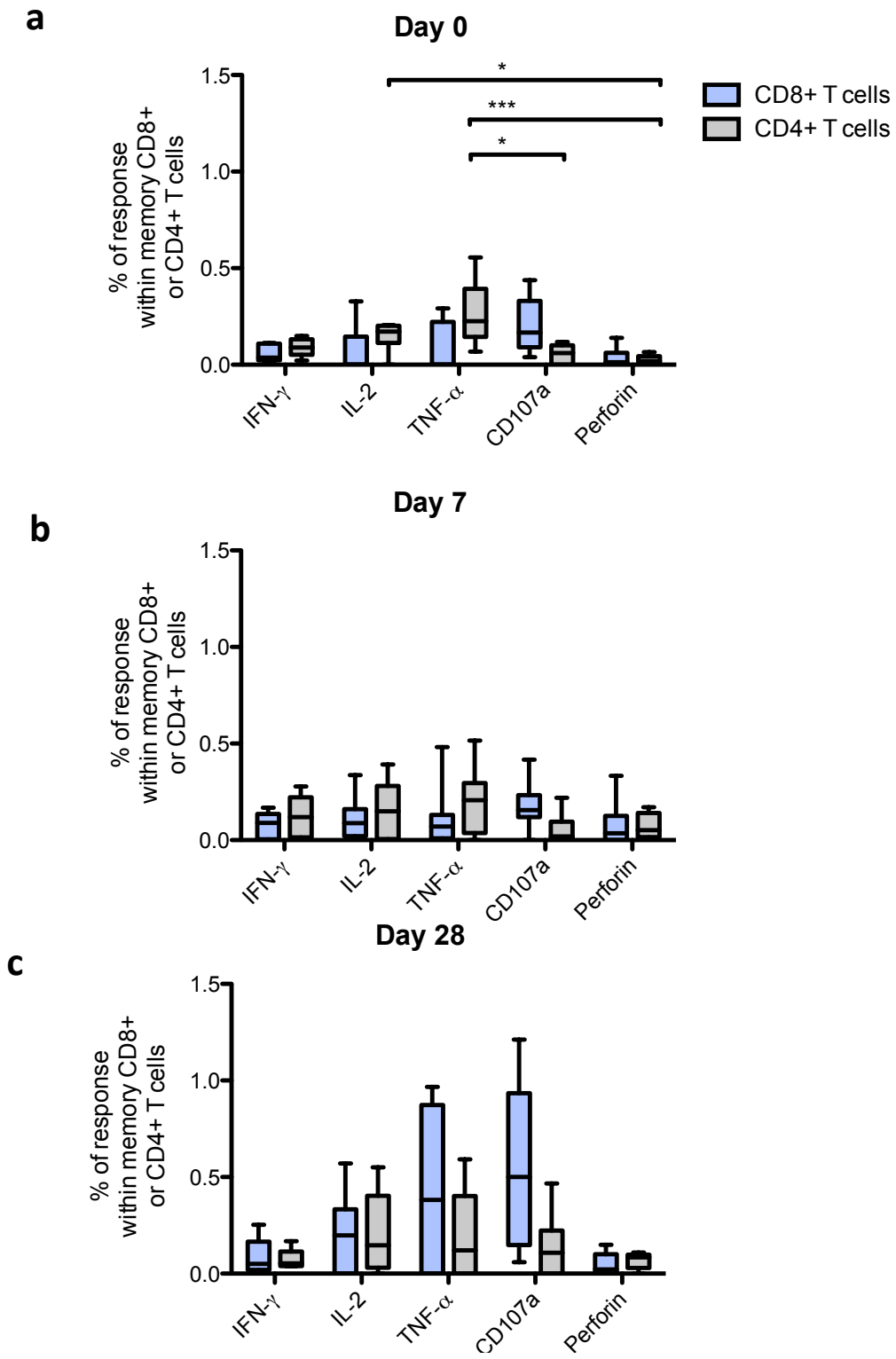

Figure 4.9 Cytokine responses of flu-specific CD4+ and CD8+ T cells. Percentage of memory CD4+ and CD8+ T cells responding to the total influenza peptide pools were analysed on **(a)** day 0, **(b)** day 7 and **(c)** day 28. Percentage of cells staining positive for IL-2, IFN-γ, TNF-α, perforin and CD107 within memory CD8+ or CD4+ T cells were summed to compute the total percentage of responding cells. CD8+ responses are depicted in light blue bars and CD4+ responses in grey. Center line represents the median, the boundaries of the box represent the upper and lower quartiles, and whiskers depict the max and min. Differences between cytokines were tested using non-parametric Kruskal–Wallis's test with post hoc Dunn's test for multiple comparisons. A p value of less than 0.05 is considered to be significant (*$p < 0.05$, ***< 0.005).

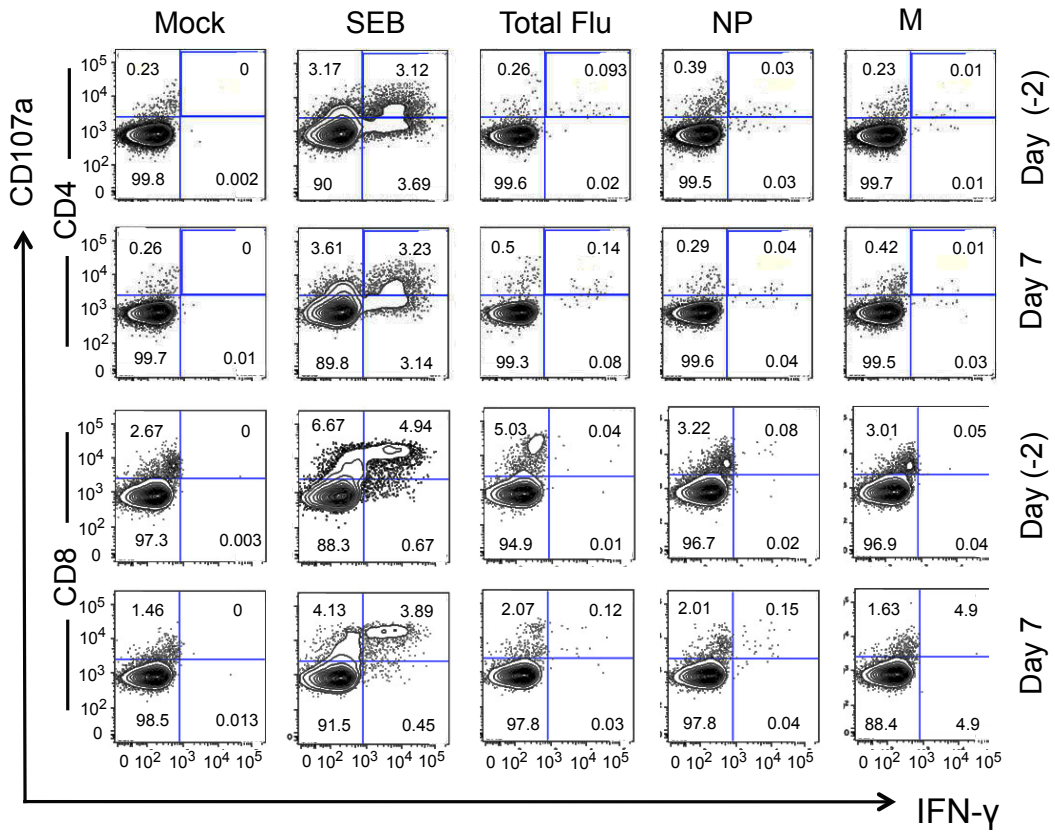

Figure 4.10 IFN-γ and CD107a production of Flu-, M- or NP- specific CD4+ and CD8+ T cells on baseline and day 7. IFN-γ and CD107a expression of memory T cells of a representative H3N2 infected subject. PBMCs from baseline and day 7 post infection were stimulated with NP, M peptides pool, or total flu pools containing all the peptides spanning H3N2 proteome for 6 hours. *Ex vivo* responses were measured by flow cytometry. Mock indicates non-stimulated negative control. SEB was used as a positive control.

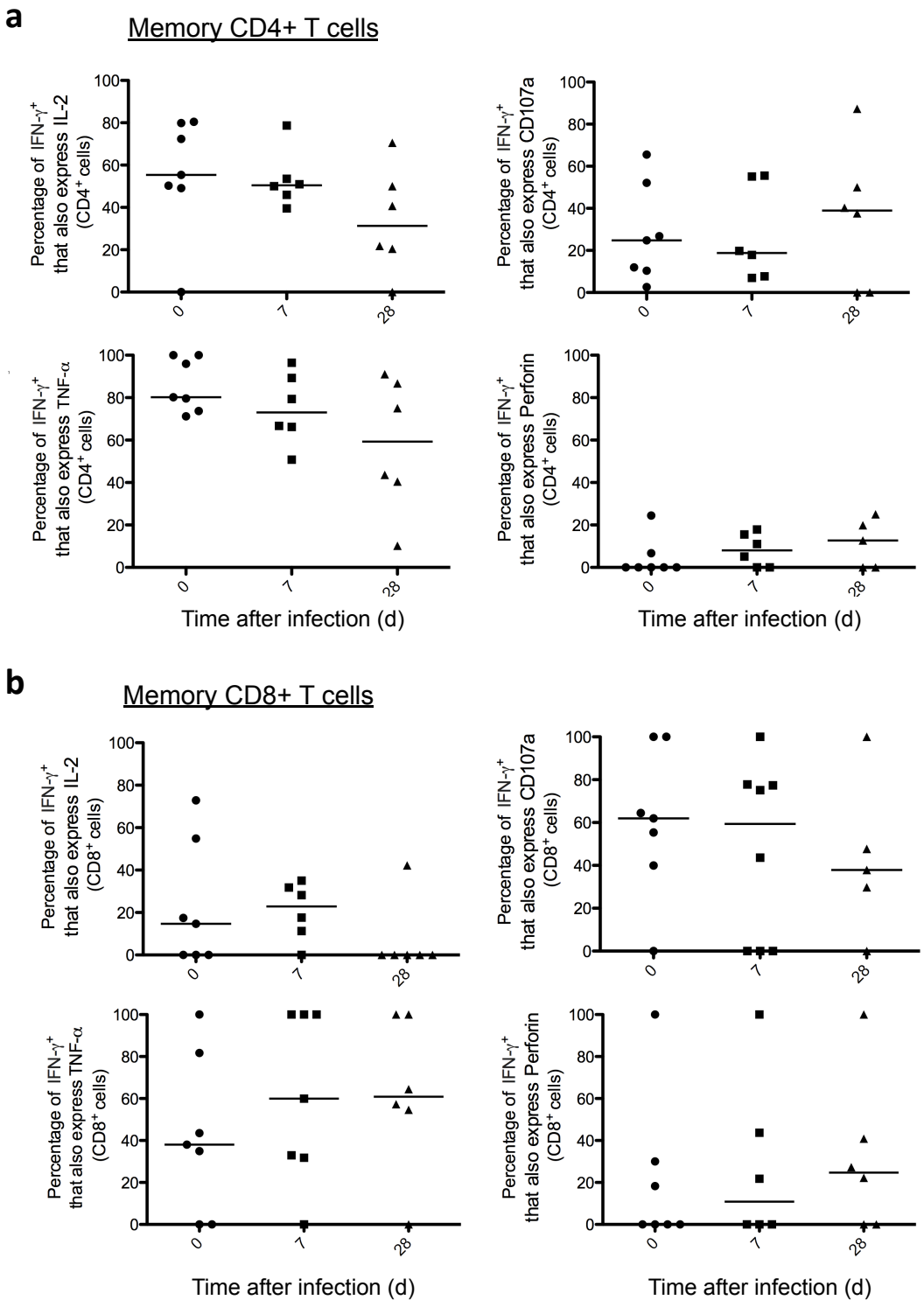

Figure 4.11 Percentage of IFN-γ^+ CD4$^+$ and CD8$^+$ T cells performing different functions were analysed on day 0, 7 and 28. PBMCs were stimulated with 2 μg/ml peptide pools spanning the entire H3N2 proteome for 6 hours, and ability of IFN-γ producing cells to upregulate IL-2, TNF-α , CD107a and perforin was measured. **(a)** Percentage of IFN-γ^+ CD4$^+$ T cells that were also expressing IL-2, TNF-α, CD107a or perforin. **(b)** Percentage of IFN-γ^+ CD8$^+$ T cells that were also expressing IL-2, TNF-α, CD107a and perforin. Small horizontal bars indicate median.

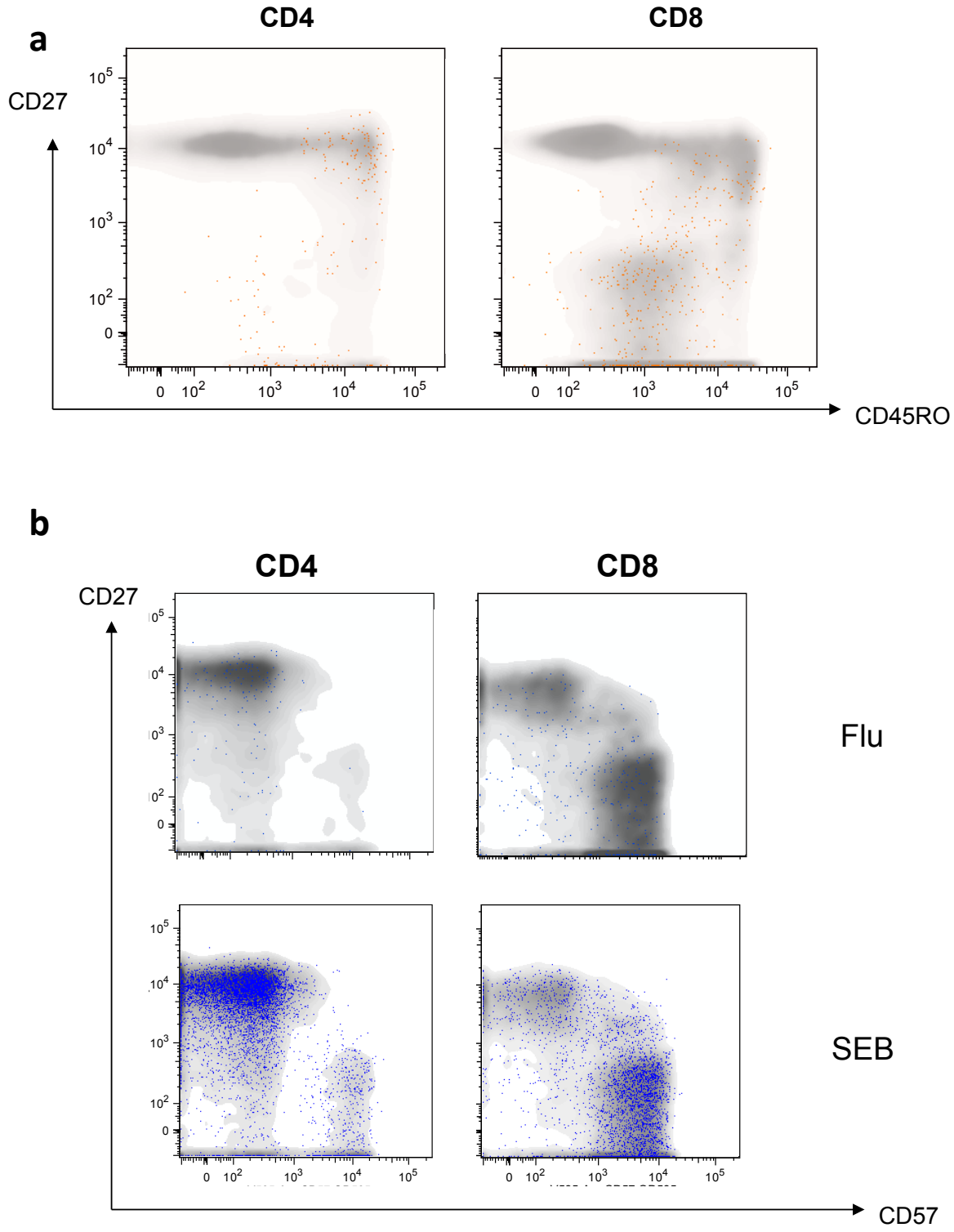

Figure 4.12 Memory phenotype of flu-specific CD4+ and CD8+ cells. (a) Memory phenotype of all CD4+ and CD8+ cells is shown in grey. Red dots represent cells positive for IL-2, IFN-γ, TNF-α and CD107a after stimulation with total flu peptides. **(b)** Expression of CD27 and CD57. Blue dots represent cells positive for IL-2, IFN-γ, TNF-α and CD107a after total flu pool or SEB stimulation. Representative data from one of the subjects is shown.

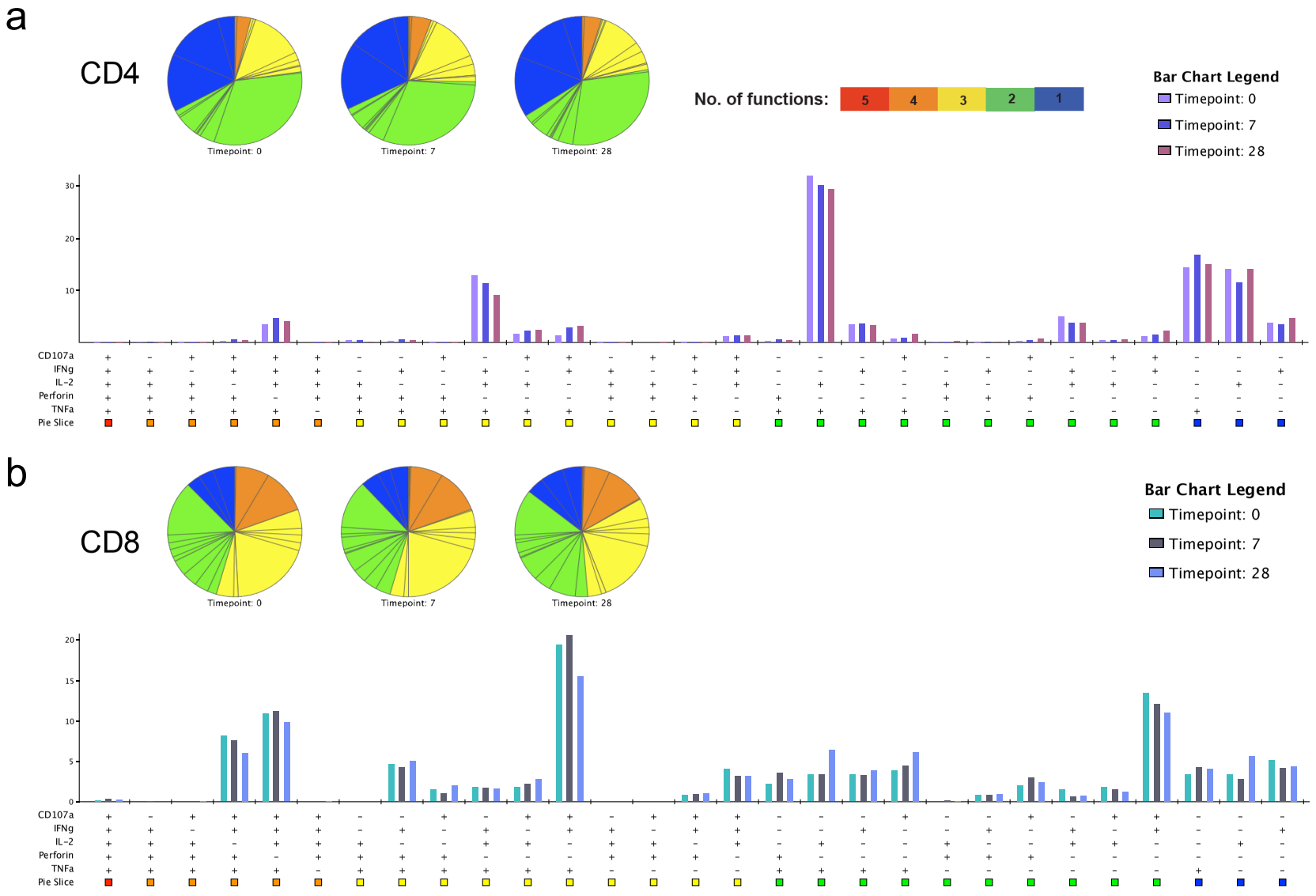

Figure 4.13 Functional profile of SEB- stimulated T cells of infected volunteers. Multiparametric analyses were performed with SPICE 5.22 software (M. Roederer, NIH). Average functional response profile of infected volunteers is symbolised as a pie chart. PBMCs were assayed for perforin, IFN-γ, IL-2, TNF-α, and CD107a upregulation. Pie slices represent the proportion of responding **(a)** $CD4^+$ and **(b)** $CD8^+$ T cells that upregulated all 5 (red), 4 (orange), 3 (yellow), 2 (green) and 1 (blue) functions while stimulating by SEB on day 0,7 and 28. Bar chart represents the mean and the distribution of responding $CD4^+$ and $CD8^+$ T cells across different functional subsets when stimulated by SEB. The y-axis denotes the proportion of the total T cell response that produces a specific function.

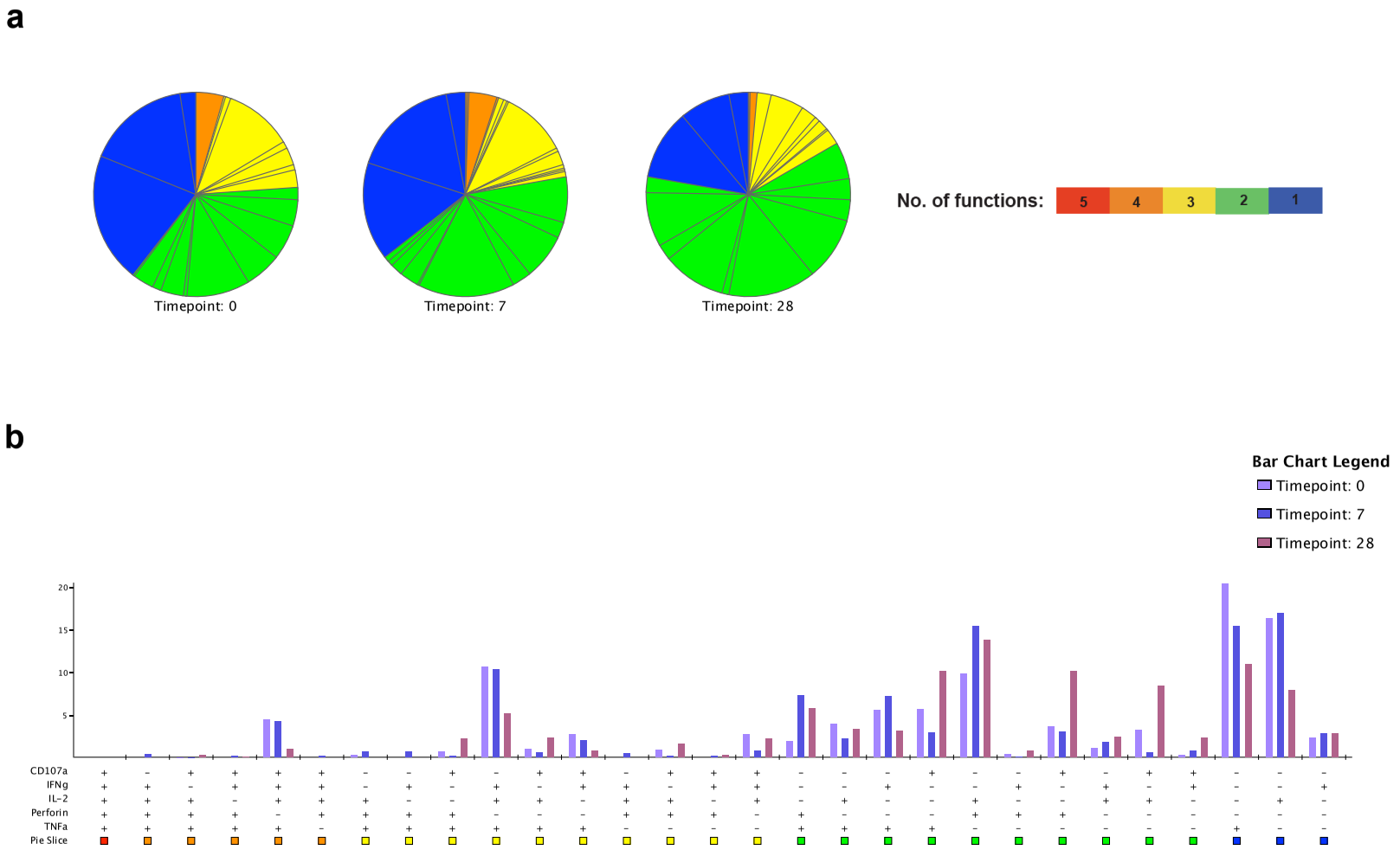

Figure 4.14 Functional repertoire of CD4⁺ T cells in response to flu peptides stimulation. Multiparametric analyses were performed with SPICE 5.22 software (M. Roederer, NIH). Average functional response profile of infected volunteers is symbolized as a pie chart. PBMCs were assayed for perforin, IFN-γ, IL-2, TNF-α, and CD107a upregulation. **(a)** Pie slices represent the proportion of responding CD4⁺ T cells that upregulated all 5 (red), 4 (orange), 3 (yellow), 2 (green) and 1 (blue) functions while stimulated by flu peptides on day 0,7 and 28. **(b)** The bar chart represents the mean and the distribution of responding CD4⁺ T cells across different functional subsets at three timepoints (day 0, 7 and 28). The y-axis denotes the proportion of the total CD4⁺ T cell response that produces a specific function.

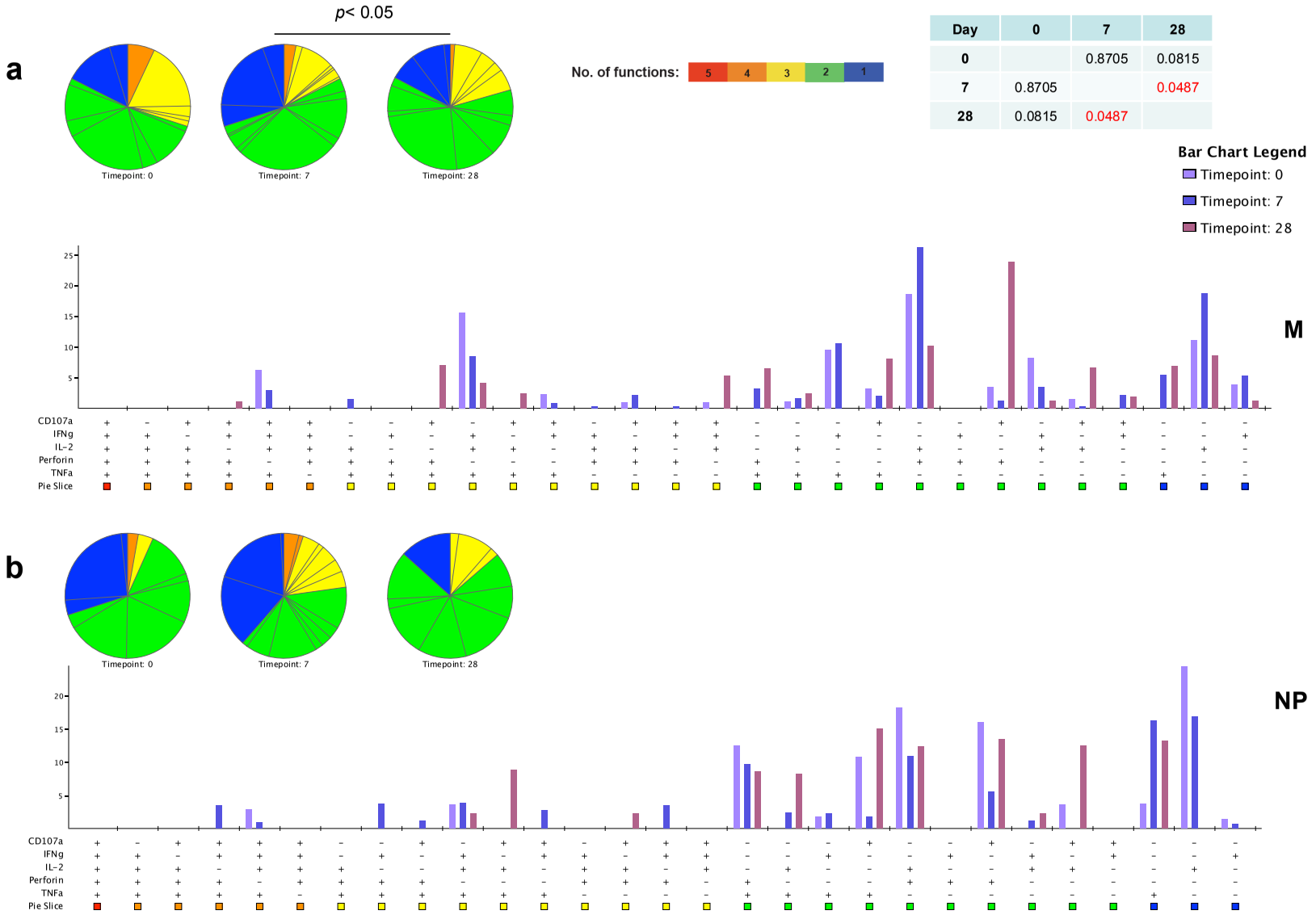

Figure 4.15 Functional repertoire of CD4⁺ T cells of in response to M or NP peptide pools. Average functional response profile of infected volunteers is symbolised as a pie chart. PBMCs were assayed for perforin, IFN-γ, IL-2, TNF-α, and CD107a upregulation. Pie slices represent the proportion of responding CD4⁺ T cells that upregulated all 5 (red), 4 (orange), 3 (yellow), 2 (green) and 1 (blue) functions while stimulated by either **(a)** M or **(b)** NP peptide pools on day 0,7 and 28. The bar chart represents the mean and the distribution of responding CD4⁺ T cells across different functional subsets when stimulated by either **(a)** M or **(b)** NP peptide pools. The y-axis denotes the proportion of the total CD4⁺ T cell response that produces a specific function. Table shows the results of one-sided permutation tests comparing pies segments at each timepoint with each other as analysed by SPICE; *p* values of <0.05 are considered significant and are highlighted.

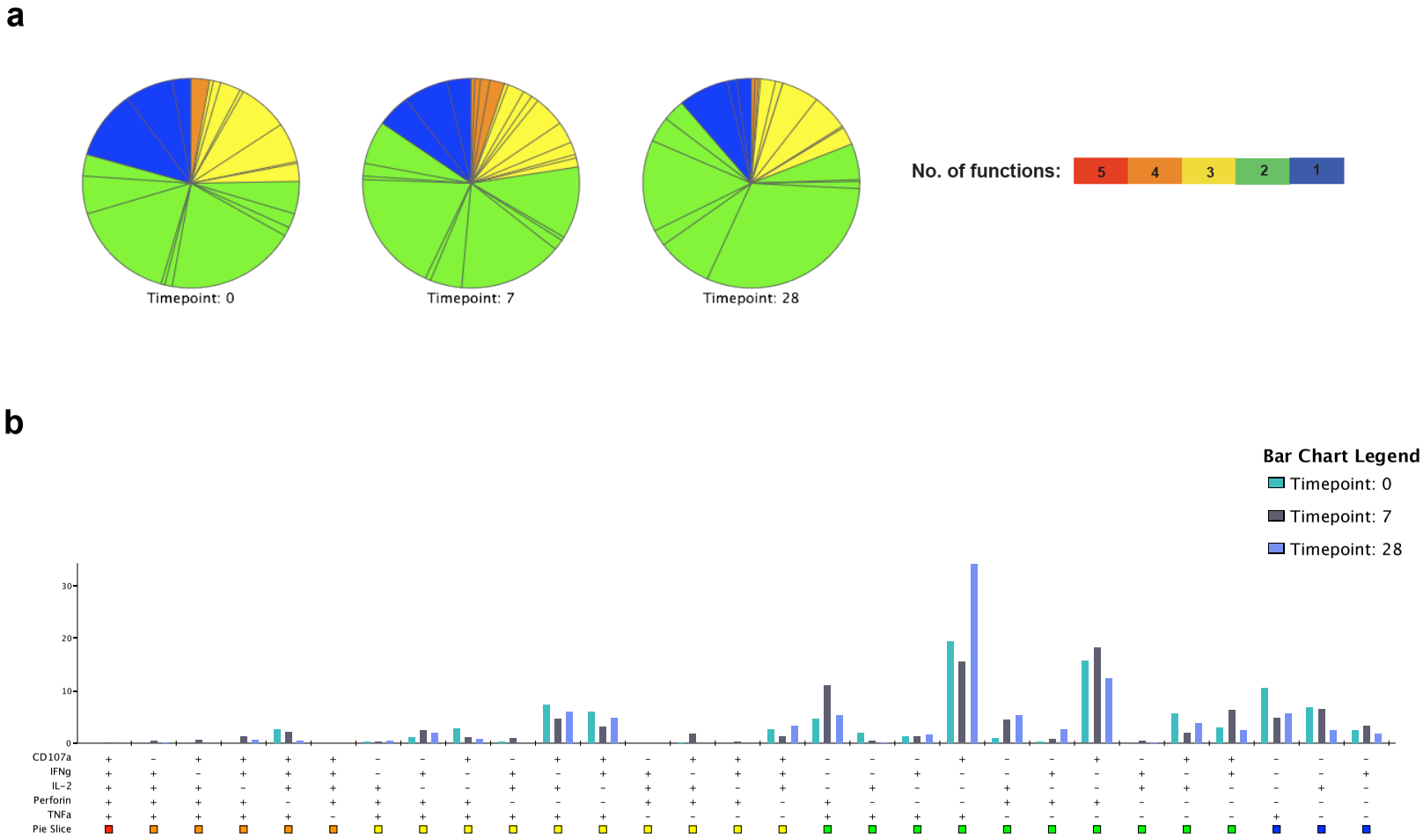

Figure 4.16 Functional repertoire of CD8⁺ T cells in response to flu peptides stimulation. Multiparametric analyses were performed with SPICE 5.22 software (M. Roederer, NIH). Average functional response profile of infected volunteers is symbolized as a pie chart. PBMCs were assayed for perforin, IFN-γ, IL-2, TNF-α, and CD107a upregulation. **(a)** Pie slices represent the proportion of responding CD8⁺ T cells that upregulated all 5 (red), 4 (orange), 3 (yellow), 2(green) and 1 (blue) functions while stimulated by flu peptides on day 0,7 and 28. **(b)** The bar chart represents the mean and the distribution of responding CD8⁺ T cells across different functional subsets. The y-axis denotes the proportion of the total CD8⁺ T cell response that produces a specific function.

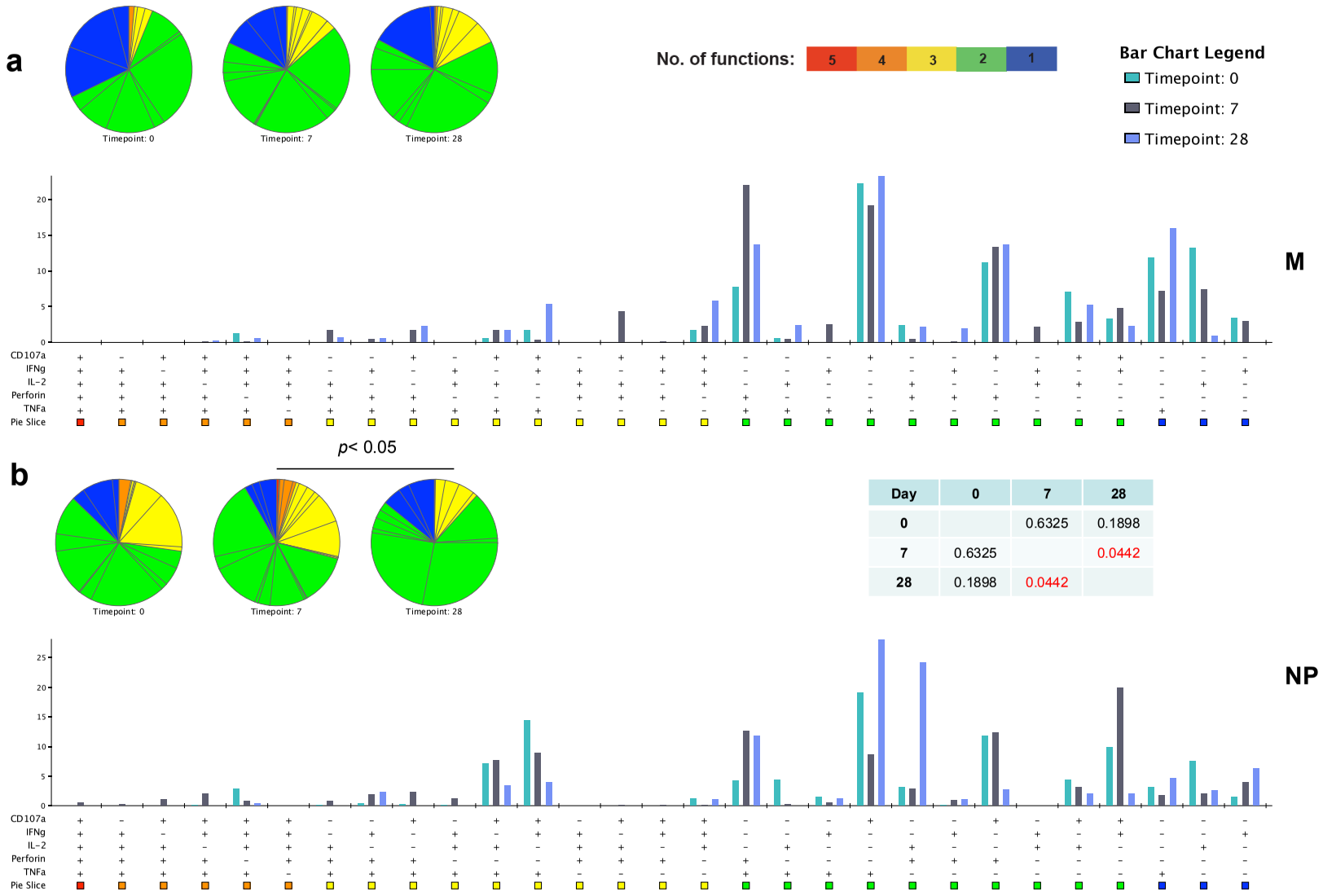

Figure 4.17 Functional repertoire of CD8⁺ T cells in response to M or NP peptide pools. Average functional response profile of infected volunteers is symbolised as a pie chart. PBMCs were assayed for perforin, IFN-γ, IL-2, TNF-α, and CD107a upregulation. Pie slices represent the proportion of responding CD8⁺ T cells that upregulated all 5 (red), 4 (orange), 3 (yellow), 2 (green) and 1 (blue) functions while stimulated by either **(a)** M or **(b)** NP peptide pools on day 0,7 and 28. The bar chart represents the mean and the distribution of responding CD8⁺ T cells across different functional subsets when stimulated by either **(a)** M or **(b)** NP peptide pools. The y-axis denotes the proportion of the total CD8⁺ T cell response that produces a specific function. Table shows the results of one-sided permutation tests comparing pies segments at each timepoint with each other as analysed by SPICE; *p* values of <0.05 are considered significant and are highlighted.

Chapter 5

T cell responses to an inactivated influenza vaccine

5.1 Introduction

In 2009, a novel swine-origin influenza A (H1N1) 2009 virus emerged and caused a pandemic. With little pre-existing immunity in the population, mass vaccination campaigns were required to control influenza and to elicit protective memory response worldwide. Several vaccine trials against the pandemic strain have been carried out around the world, and it is generally agreed that one dose containing 15 µg hemagglutinin without adjuvant is enough to elicit the immune responses required of licensing for use in population of 3-60 years old (Clark et al., 2009; Greenberg et al., 2009; Liang et al., 2010; Zhu et al., 2009).

In addition to the pandemic H1N1 virus, a seasonal H1N1 virus has been circulating in the population since 2008. The need to vaccinate against the seasonal virus remains as vaccines produced against the pandemic virus do not induce broad protective immunity against the seasonal virus. The components of the seasonal influenza vaccine were decided upon in advance of the season, and the vaccine production was in progress by the time the new 2009 H1N1 virus emerged (Lambert and Fauci, 2010). Therefore, the vaccine against the new virus was produced separately, and it was recommended that both the pandemic vaccine and seasonal vaccine be given together for the susceptible population in the 2009-2010 season, which was the time of this study (Fiore et al., 2009 ; National Center for Immunization and Respiratory Diseases, 2009).

It is well characterized that the correlate of protection in inactivated influenza vaccine is antigen-specific antibody production after vaccination with pandemic H1N1 or seasonal influenza vaccines (Davies and Grilli, 1989; Plotkin, 2008). However, knowledge on the induction and

function of cellular immunity in response to the pandemic vaccine, and its potential cross-reactivity with seasonal antigens and on the influence of previous exposure with seasonal strains is limited.

In this study, a randomized, observer-blinded clinical trial was carried out in healthy adults to compare three possible immunization strategies using a licensed pandemic split vaccine and a seasonal trivalent split influenza vaccine recommended for the 2009-2010 season. The pandemic vaccine was administrated before, after or at the same time as the seasonal vaccine. The safety and immunogenicity of both vaccines were evaluated. A parallel study was carried out by Dr. Arthur Huang to analyse serological responses to pandemic H1N1 and seasonal influenza vaccines using HI and MN assays, and the frequency of influenza-specific ASC in the peripheral blood using B-cell ELIspot [Dr. A. Huang's thesis and (Wu et al., 2010)]. In this chapter, in particular, the induction and functional characteristics of antigen-specific T cells in response to influenza vaccination, and the cross-reactivity with seasonal antigens was analysed.

5.2 Results

5.2.1 Study subjects

A total of 156 eligible healthy adult volunteers aged from 18 to 60 years old were recruited in the study, conducted at a single site in Chaoyang District, Beijing, China, from 24th October to 6th December, 2009. The study complied with Good Clinical Practice guidelines and the Declaration of Helsinki. The protocol was approved by Beijing Centre for Disease Control and Prevention and the ethics review committee. All subjects provided written informed consent. Five were excluded between enrolment and randomization, thus 151 subjects were randomized into three groups at a 1:1:1 ratio (see below and chapter 2, **Fig. 2.2**), and were immunized in a pre-designated order provided by a statistician who was not involved in the rest of the trial. Across all three groups, the mean age ranged from 34.7 to 41.4 years. There was a statistically significant difference in age between the three groups (p = 0.028, Fisher's exact test), which is a chance result of random stratification. On the other hand, no difference was found in height, weight and sex (**Table 5.1a**).

The pandemic H1N1 vaccine was a monovalent, unadjuvanted, inactivated, split vaccine, which was prepared from the reassortant vaccine virus NYMC X-179A derived from A/California/7/2009 (H1N1) virus and contained 15 μg/0.5ml HA per vial. The seasonal vaccine was prepared from high growth reassortants of A/Brisbane/59/2007 (H1N1), A/Uruguay/716/07 (H3N2) (A/Brisbane/10/2007 H3N2-like virus) and B/Brisbane/60/2008 viruses, according to the WHO recommended composition of influenza virus vaccines for use in the 2009–2010 northern hemisphere influenza season (http://www.who.int/csr/disease/influenza/recommendations2009_10north/en/index.html). Both vaccines were manufactured by Sinovac Biotech Co., Ltd (Beijing, China).

Group 1 received the pandemic H1N1 vaccine first, and received the seasonal flu vaccine on day 21. Group 2 received seasonal vaccine on day 0 and pandemic H1N1 vaccine on day 21. Group 3 received both vaccines simultaneously on day 0. All provided blood samples before receiving first dose on day 0. In Group 2 and 3, one subject from each group missed their day 21 visit due to travelling and failed to provide blood samples (and missed second dose in the case of Group 2). One subject from Group 2 died five days after the second dose, and the cause of death was

confirmed as cerebral haemorrhage due to factors unrelated to the vaccination. Another subject in Group 2 missed day 42 follow-up due to traveling and was excluded from analyses.

5.2.2 Safety of the vaccines evaluated

All three immunization strategies were safe and well tolerated. No serious adverse event or event of special interests was reported in the three study groups. The proportion of subjects reporting an adverse event did not differ between three groups ($p = 0.375$). Most of the adverse events were mild in intensity, pain at the injection site was the most common reaction reported after the first dose. The main systemic reactions were headache, angina and fatigue, but no difference was found between the three groups.

5.2.3 Immunogenicity of the vaccines evaluated

Immunogenicity of the vaccines was evaluated in detail in a parallel study analysed by Dr. A Huang (Wu et al., 2010). All three immunization strategies were immunogenic, capable of inducing antibody responses that met the criteria for licensing. At baseline, 15 out of 151 of the subjects (10%) had antibody titres of 1:40 or more against pandemic H1N1 in haemagglutination-inhibition (HI) assay. In contrast, the proportion of subjects with a baseline titres 1:40 or more was higher for seasonal H1N1 (63/151, 42%), H3N2 (28/151, 19%) and influenza B (70%). Seroconversion or significant increase in Geometric Mean Titre (GMT) in HI assay occurred in all 3 groups (94%-100%) on day 42 (study end-point) (**Table 5.1b**). Seroconversion was defined as a titre of less than 1:10 prior to vaccination and a titre of 1:40 post vaccination; or a titre of 1:10 or more pre-vaccination and at least a four-fold increase after vaccination.

(a)

	Group 1 (n=51) *(Pandemic vaccine, Day 0 Seasonal vaccine, Day 21)*	***Group 2 (n=49)*** *(Seasonal vaccine, Day 0 Pandemic vaccine, Day 21)*	***Group 3 (n=51)*** *(Pandemic vaccine and Seasonal vaccine, Day 0)*
Age — yr			
Mean ± SD	41.1±13.1	34.7±11.0	37.2±11.8
Median	44	34	37
Range	19-59	18-59	18-59
Height — cm			
Mean ± SD	165.9±7.1	167.0±7.2	164.4±6.8
Median	165.0	169.0	164.5
Range	150-180	152-178	146-181
Weight — kg			
Mean ± SD	67.5±11.6	69.6±12.4	65.4±9.8
Median	68.0	70.0	65.0
Range	42.0-99.0	49.0-100.0	48.0-90.0
Sex — no. (%)			
Female	26 (51.0)	28 (57.1)	23 (45.1)
Male	25 (49.0)	21 (42.9)	28 (54.9)

(b)

	Group 1				***Group 2***				***Group 3***			
Day and antigen	GMT (95%CI)	GMT ratio (95%CI)	Seroconversion (95%CI)	Seropositivity (95%CI)	GMT (95%CI)	GMT ratio (95%CI)	Seroconversion (95%CI)	Seropositivity (95%CI)	GMT (95%CI)	GMT ratio (95%CI)	Seroconversion (95%CI)	Seropositivity (95%CI)
Day 0			*N* = 51				*N* = 49				*N* = 51	
Pandemic H1N1	9.1 (7.2–11.5)	–	–	13.7 (6.2–27.0)	8.1 (6.5–10.1)	–	–	10.2 (3.8–23.1)	7.1 (6.0–8.4)	–	–	5.9 (1.5–17.3)
Seasonal H1N1	30.9 (23.6–40.5)	–	–	45.1 (31.4–59.8)	25.4 (19.6–33.0)	–	–	32.7 (20.4–47.8)	28.1 (21.4–36.8)	–	–	49 (35.0–63.5)
Seasonal H3N2	12.4 (9.1–17.0)	–	–	25.5 (14.8–40.1)	9.9 (7.5–13.0)	–	–	14.3 (6.4–28.0)	9.9 (7.5–13.0)	—	–	13.7 (6.2–27.0)
Seasonal B	33.5 (28.8–39.0)	–	–	70.6 (56.0–82.5)	36.7 (31.0–43.6)	–	–	71.4 (56.5–83.4)	31.7 (26.9–37.4)	–	–	66.7 (52.0–79.2)
Day 42			*N* = 51				*N* = 46				*N* = 50	
Pandemic H1N1	622.8 (422.6–918.0)	68.5 (47.8–98.2)	96.1 (85.4–100.0)	98 (88.2–100.0)	296.8 (217.5–404.9)	36.3 (26.2–51.2)	100 (90.4–100.0)	100 (90.4–100.0)	220.1 (158.8–305.0)	30.7 (22.0–42.8)	94.1 (82.5–99.3)	94 (82.5–99.3)
Seasonal H1N1	606.1 (466.8–787.0)	19.6 (13.3–29.0)	92.2 (80.3–98.2)	100 (91.3–100.0)	466.4 (348.9–623.4)	17.5 (12.2–25.2)	93.5 (81.1–99.3)	100 (90.4–100.0)	541.9 (380.8–771.1)	20 (12.9–30.9)	92 (79.9–98.2)	100 (91.1–100.0)
Seasonal H3N2	342.5 (223.3–525.2)	27.6 (17.9–42.4)	92.2 (80.3–98.2)	96.1 (85.4–100.0)	263.1 (159.9–432.8)	26.3 (16.3–42.4)	84.8 (70.5–93.8)	89.1 (75.6–96.7)	239.2 (162.2–352.6)	23.9 (15.9–35.9)	86 (72.6–94.3)	94 (82.5–99.3)
Seasonal B	147.5 (117.6–184.9)	4.4 (3.4–5.6)	62.7 (48.1–75.8)	100 (91.3–100.0)	135.6 (107.2–171.4)	3.7 (2.8–4.8)	65.2 (49.7–78.6)	97.8 (87.0–100.0)	147.2 (119.0–182.2)	4.7 (3.7–6.1)	68 (53.2–80.4)	100 (91.1–100.0)

Table 5.1 Demography and antibody titre of the study groups. (a) Demographic characteristics of the study population. **(b)** Hemagglutination-inhibition antibody response before and after immunization in the three groups. Proportions of subjects are based on the total number of subjects tested at each time point. Seroconversion was defined as a titre of less than 1:10 before vaccination and a titre of 1:40 or more after vaccination, or a titre of 1:10 or more before vaccination and at least a fourfold increase after vaccination. Seropositivity was defined as HI titre ≥ 1:40. GMT, geometric mean titres. *This experiment was carried out and analysed by China CDC and Dr. Arthur Huang.*

5.2.4 Antigen-specific T cell responses in 2009 pandemic H1N1 and seasonal vaccine trials

Influenza-specific T cell responses to surface antigens HA and NA were measured by *ex vivo* IFN-γ -ELIspot during the course of vaccination (**Fig. 5.1**). 50 subjects were analysed in Group 1, 46 subjects were analysed in Group 2, and 50 subjects were analysed in Group 3 (**Fig. 2.2**). **Fig. 5.2** showed that T cell responses were induced at day 7 of the study, but no boosting effect on day 21 was observed. T cell responses to the vaccines were mapped at individual peptide level in all groups. As both vaccine strains were generated by reverse genetics viruses, manufactured through a reassortment between RNA segments encoding the surface antigens HA and NA plus the PR/8 backbone, only antigen-specific responses to HA and NA proteins were mapped. Values of T cell responses were adjusted by subtracting the mean values of negative controls, and expressed as SFC/million PBMCs. Background values of no peptide control wells were determined to be 1.11 ± 0.95 SFC/million PBMC. Wells containing spot number greater than the mean +4 SD of negative control wells, provided the total was greater than 50 SFC/million, were considered to be positive. Prior to vaccination, 71% (92/146) of all subjects had influenza-specific T cell responses. Total T cell responses were dominated by responses directed against internal proteins M and NP, which are highly conserved within influenza A virus. Seasonal H1N1 HA-specific responses, and pandemic H1N1 HA-specific responses elicited by the three groups are shown in **Table 5.2 and 5.3**. Assessing pandemic H1N1- specific HA and NA responses, before vaccination, 14% (21/146) of all subjects responded to pandemic H1N1 HA antigens and 2% (3/146) of the subjects responded to pandemic H1N1 NA antigens.

On day 7, when a transient boosting of influenza-specific T cells was observed, over half of the subjects in all three groups had T cell responses to pandemic H1N1 and seasonal H1N1 HA antigens (**Table 5.2 and 5.3**). On the final timepoint (i.e. day 42), 70% (35/50) of subjects in Group 1, 65% (30/46) of subjects in Group 2, 70% (35/50) of subjects in Group 3 had influenza-specific T cell responses. Assessing T cell responses to pandemic H1N1 HA antigens, 16% (8/50) of subjects in Group 1, 24% (11/46) of subjects in Group 2, 16% (8/50) of subjects in Group 3 had pandemic H1HA-specific T cell responses. 6% (3/50) of subjects in Group 1, 8% (4/46) of subjects in Group 2, and 2% (1/50) of subjects in Group 3 responded to pandemic H1N1 NA antigens after vaccination. The increase in the number of positive subjects before

and after vaccination was found to be insignificant (p> 0.5 for all three groups, analysed by chi-squared tests).

In a parallel investigation of the same cohort, pre- or co-vaccination with the seasonal flu vaccine (Group 2 and 3) has been found to lead to a significant reduction by up to 50% in HI titer to pandemic H1N1 virus after pandemic vaccination, thus vaccination with pandemic H1N1 vaccine first is recommended to avoid an associated inhibitory effect by the seasonal vaccine (Wu et al., 2010). The current data suggest that the overall number of seasonal HA and pandemic HA –specific T cells does not alter significantly before and after vaccination, regardless of the order of vaccine administrated. In all three groups, the vaccine induces an expansion of seasonal HA and pandemic HA –specific T cells, followed by a rapid contraction phase, resulting in minimal change in magnitude and number of responders (**Table 5.2 and 5.3**). The inhibitory effects observed in serological studies thus should not be related to the T cells that were activated by the vaccines.

5.2.5 CD4 dependent responses of vaccine-induced flu-specific T cells

To understand the phenotype and specificity of T cell responses induced by vaccination, pandemic H1HA- and pandemic H1NA-specific T cell responses were mapped based on IFNγ-ELISpot results on day 21 and day 28 (7 days post second dose) in a 2-D matrix of peptides. Other responses were not mapped as the internal genes came from the vaccine strain PR8. The positive responses detected during the peptide pool screening were confirmed subsequently in a second round of *ex vivo* IFNγ-ELISpot using PBMCs depleted of $CD8^+$ T cells. Briefly, on day 42, PBMCs were mixed with $CD8^+$ Dynabeads, which bound to $CD8^+$ cells within a short incubation. The bead bound $CD8^+$ cells were then isolated using a magnet. The $CD8^+$ depleted PBMCs, undepleted cells and the sorted $CD8^+$ cells were stimulated with individual peptides corresponding to the known responses on day 21 and day 28 in order to look at the phenotype of responding cells. **Fig. 5.3a** shows a representative response in one subject.

The responses detected against positive peptide pools and individual peptides confirmed by cell depletion were characterized further for $CD4^+$ or $CD8^+$ dependency using intracellular cytokine staining. T cell lines were established by pulsing PBMCs collected on day 42 with pandemic H1N1 peptide pools, cultured with IL-2 for 10 to 15 days, restimulated with individual peptides and assayed for IFN-γ response (**Fig. 5.3b**). It revealed that responses to pandemic H1N1

SFC/M cells	All subjects (N=146)	Group 1 (N=50)	Group 2 (N=46)	Group 3 (N=50)
Day 0	Pre-vaccination	Pre-vaccination	Pre-vaccination	Pre-vaccination
Median (range)	73.8 (50.5 - 142.6)	69.1 (50.5-131.5)	74.1 (52.7-142.6)	91.6 (56.6 - 107.1)
Mean ± s.d.	82.93 ± 28.47	77.7 ± 27.6	87.34 ± 32.78	85.1 ± 25.87
% of subjects with a positive HA response	13% (19/146)	16% (8/50)	17% (8/46)	6% (3/50)
Day 7				
Median (range)		87.4 (51.6-249.2)	108.8 (51.1-272)	129.9 (52.2 - 394.6)
Mean ± s.d.	-	109.1 ± 56.6	127 ± 67.3	163 ± 104
% of subjects with a positive HA response		44% (22/50)	63% (29/46)	62% (31/50)
Day 21				
Median (range)		59.1 (54.9-63.3)	67.15 (58.3- 228.7)	93 (53.3 - 141.5)
Mean ± s.d.	-	59.1 ± 5.9	90.75 ± 57.98	97.83 ± 37.71
% of subjects with a positive HA response		4% (2/50)	17% (8/46)	16% (8/50)
Day 28				
Median (range)		77.7 (52.2-132.6)	108.5 (72.7-156.5)	
Mean ± s.d.	-	80.34 ± 26.9	111.6 ± 34.4	-
% of subjects with a positive HA response		16% (8/50)	9% (4/46)	
Day 42	Post-vaccination	Post-vaccination	Post-vaccination	Post-vaccination
Median (range)	72.2 (50.5- 143.7)	72.2 (65.5-104.3)	79.65 (61.1-143.7)	69.95 (50.5- 95.5)
Mean ± s.d.	80.28 ± 23.56	77.94 ± 16.04	91.85 ± 31.4	70.76 ± 16.61
% of subjects with a positive HA response	16% (23/146)	14% (7/50)	17% (8/46)	16% (8/50)

Table 5.2 Seasonal H1N1 HA-specific T cell responses elicited by the three groups

SFC/M cells	All subjects (N=146)	Group 1 (N=50)	Group 2 (N=46)	Group 3 (N=50)
Day 0	Pre-vaccination	Pre-vaccination	Pre-vaccination	Pre-vaccination
Median (range)	94.4 (51.6- 364.4)	79.4 (61.1- 334.6)	95.2 (59.4-159.3)	138.5(51.6- 364.6)
Mean ± s.d.	131.4 ±96.08	120.5±98.3	100.9±36.86	184.9±135.4
% of subjects with a positive pHA response	14% (21/146)	14% (7/50)	17% (8/46)	12% (6/50)
Day 7				
Median (range)		106.7 (51.1-264.2)	106.4 (52.2-267.5)	116 (51.1-977.9)
Mean ± s.d.	-	127.2 ± 62.7	83.5 ± 62.2	171.5 ± 184.8
% of subjects with a positive pHA response		50% (25/50)	48% (22/46)	58% (29/50)
Day 21				
Median (range)		102.1 (53.3-134.3)	133.6 (62.7-278.8)	81.85 (53.3-601.6)
Mean ± s.d.	-	93.68 ± 31.7	96.6 ± 98.3	139.5± 164.3
% of subjects with a positive pHA response		10% (5/50)	9% (4/46)	20% (10/50)
Day 28				
Median (range)		82.7 (62.2-89.9)	112.3 (52. -157.1)	
Mean ± s.d.	-	78.73 ± 11.18	119.6 ± 47.5	-
% of subjects with a positive pHA response		14% (7/50)	9% (4/46)	
Day 42	Post-vaccination	Post-vaccination	Post-vaccination	Post-vaccination
Median (range)	86 (51.6 - 494.5)	86 (58.8- 321.3)	81.6 (51.6- 220.3)	151 (59.9- 494.5)
Mean ± s.d.	145.2± 122	138.5±107.2	91.66±48	225.4±169
% of subjects with a positive pHA response	18% (27/146)	16% (8/50)	24% (11/46)	16% (8/50)

Table 5.3 Pandemic H1N1 HA-specific T cell responses elicited by the three groups.

vaccine were predominately mediated by HA-specific $CD4^+$ T cells. 8 out of 10 of the pandemic H1N1 specific HA peptides that elicited a response, and 5 out of 6 of the NA peptides, were mediated by $CD4^+$ T cells (**Table 5.4**). This may be because the inactivated vaccine antigens are presented by antigen-presenting cells to $CD4^+$ T cells in the context of MHC Class II molecules, while only a small proportion of antigen is presented to $CD8^+$ T cells via MHC class I by cross-presentation.

I next examined the possible relationship between T cell responses and antibody responses following influenza vaccination. Evaluation by Spearman rank correlation revealed no statistically significant correlation between HI and MN antibody titers on day 21 and T cell responses against surface HA post vaccination on day 7 post vaccination in all three groups ($p > 0.05$ for all analyses) (**Fig. 5.4**). Therefore antibody responses were not predictive of ELIspot results. Similar to reports described earlier (Co et al., 2008; McElhaney et al., 2006), antibody responses post-vaccination with T cell responses were found not to correlate with each other.

Protein	Peptide ID	Amino acid position	Amino acid sequence	CD4 or CD8 dependency	SFC/million PBMC (range)	Number positive (%)
HA	pH1HA13	97-104	VETPSSDNGTCYPGDFID	8	73 (36-96)	2 (1.3)
	pH1HA16	121-138	QLSSVSSFERFEIFPKTS	4	26	1 (0.7)
	pH1HA21	161-178	FYKNLIWLVKKGNSYPKL	4	30	1 (0.7)
	pH1HA33	257-274	ITFEATGNLVVPRYAFAM	4	53	1 (0.7)
	pH1HA39	305-322	TSLPFQNIHPITIGKCPK	4	72 (30-119)	6 (4)
	pH1HA40	313-330	HPITIGKCPKYVKSTKLR	4	56 (23-89)	8 (5.4)
	pH1HA43	337-354	NIPSIQSRGLFGAIAGFI	4	43 (36-50)	1 (0.7)
	pH1HA54	425-442	NKKVDDGFLDIWTYNAEL	8	102 (40-165)	3 (2)
	pH1HA55	433-450	LDIWTYNAELLVLLENER	4	75.9 (13-33)	2 (1.3)
	pH1NA13	97-114	WAIYSKDNSVRIGSKGDV	4	33	1 (0.7)
NA	pH1NA15	113-130	DVFVIREPFISCSPLECR	4	81 (26-172)	4 (2.7)
	pH1NA27	209-226	NGIITDTIKSWRNNILRT	4	41 (30-53)	2 (1.3)
	pH1NA28	217-234	KSWRNNILRTQESECACV	4	30	1 (0.7)
	pH1NA52	409-426	HPELTGLDCIRPCFWVEL	8	58 (23-92)	2 (1.3)
	pH1NA55	433-450	ENTIWTSGSSISFCGVNS	4	17	1 (0.7)
	pH1NA57	449-466	NSDTVGWSWPDGAELPFT	4	23	1 (0.7)

Table 5.4 T cell peptides in pandemic H1N1 vaccine study (Published epitopes were underlined).

5.2.6 Inverse correlation between baseline cell-mediated immune response and fold increase in influenza-specific response post vaccination

Next I looked at the impact of pre-existing influenza-specific T cells on induction of T cell responses post vaccination. The limited ability of vaccination to significantly increase influenza-specific T cell responses has been reported (He et al., 2008; van Assen et al., 2011). An inverse correlation was found between influenza-specific T cell responses at baseline and the fold increase in spot-forming cells in IFNγ-ELISpot post-vaccination **(Fig. 5.5)**. Almost all correlation-coefficients analysed pre- and post- vaccination were negative (not shown); the inverse correlations between total flu-specific T cell response in the baseline and fold-change post-vaccination were strongly statistically significant after the first dose in both Group 1 and Group 2 **(Fig. 5.5)**. No significant correlation was found between baseline and fold-change post-vaccination in Group 3 (p= 0.0527, r= - 0.3767), and post second dose of immunization in all three groups.

5.2.7 Phenotype of memory T cells in vaccination

A parallel, smaller cohort (n=28) was set up within volunteers from China CDC to analyse phenotype of T cells [activation ($CD38^+$), proliferative ($Ki\text{-}67^+$) and memory status] during the course of vaccination. Volunteers either received one dose of pandemic vaccine on day 0 only (Group A, n=16), or received one dose of seasonal vaccine on day 0 and an additional dose of pandemic H1N1 vaccine on day 21 (Group B, n=12). In this cohort, T cell responses followed similar kinetics to the larger vaccination cohort as described earlier, with a boosting effect observed on day 7 post vaccination but not on day 28 (**Fig. 5.6**). Correlation analyses were not carried out in this cohort due to the small number of subjects.

Immune activation and proliferation as assessed by CD38 and Ki-67 expression was analysed within $CD4^+$ and $CD8^+$ T cells (**Fig. 5.7a**). The proportion of activated and proliferating T cells increased after inactivated influenza immunization are within the $CD4^+$ $CD45RO^+$ $CD27^+$ central memory population, but not the $CD45RO^+$ $CD27^-$ effector memory population (**Fig. 5.7b**).

The percentage of activated proliferating $CD8^+$ and $CD4^+$ cells did not change significantly during the course of vaccination. Some subjects exhibited exceptional high frequency of activated

T cells at the baseline or two weeks post vaccination (**Fig. 5.8a**). It might be because subjects were not quarantined and thus may have been exposed to infections that were not documented. In Group A, the proportion of Ki-67$^+$ CD38$^+$ cells within CD4$^+$ T cells correlated with the sum of pandemic H1 HA and NA-specific SFCs assayed by ELISpot on day 7 (**Fig. 5.8b**, r = 0.56, p = 0.02). No such correlation was found in Group B.

The frequency of T cell subsets within the total T cell population was examined by flow cytometry during the course of vaccination. The memory status of T cells was defined by their expression of CD45RO and CD27. The frequencies of naïve T cells (CD45RO$^-$ CD27$^+$) and non-naive T cells (CD45RO$^+$ CD27$^+$, CD45RO$^+$ CD27$^-$ and CD45RO$^-$ CD27$^-$) were analysed within the T cell population (CD3$^+$CD4$^+$). It was found that the frequency of both populations did not change significantly during the course of vaccination (**Fig. 5.9 and 5.10**). The distribution of subsets within both the CD4$^+$ and CD8$^+$ T cell populations did not alter after vaccine administration, indicating that influenza-specific responses represent a small portion of the entire T cell repertoire.

5.2.8 Antigen-specific T cell responses in pandemic H1N1 convalescent patients

The HA of pandemic H1N1 virus shared over 70% of amino acid sequence homology with that of seasonal H1N1 virus (Ikonen et al., 2010). In order to examine for the presence of cross-reactive T cells, I analysed T cell responses in a group of convalescent pH1N1 virus infected individuals. Ag-specific responses of these individuals were analysed by IFN-γ- ELIspot. All patients had been diagnosed with pandemic H1N1 infection by PCR about half year before sample collection. PBMCs were tested for their responses against a panel of 16 pandemic H1N1 HA and NA peptides (**Table 5.4**), and 33 H1N1 peptides (**Table 5.5**), that were identified as epitopes in the H1N1 challenge studies (section 2.1.1) and vaccine studies described here. 12 out of 18 (66%) patients responded to at least one peptide. All of these subjects responded to at least one H1N1 peptide, but only 5 out of 18 patients (27%) responded to one or more pandemic H1N1 HA or NA peptides, suggesting that many pandemic H1N1-specific responses might become undetectable after half a year. CD4$^+$ T responses dominated the response. 12 out of 17 H1N1 peptides, and 5 out of 6 of the pandemic H1N1 peptides that elicited responses in at least one of the subject, were mediated by CD4$^+$ T cells (**Fig. 5.11ac**).

Cryopreserved PBMC of healthy volunteers collected before 2009 were also tested against the same panel of peptides to examine the presence of cross-reactive T cells against pandemic H1N1 (**Fig. 5.11bd**). 5 out of 12 (42%) subjects responded to at least one H1N1 or pandemic H1N1 HA or NA peptide. Out of the 12 subjects tested, 3 subjects (25%) responded to at least one pandemic H1N1 HA or NA peptides, even they had never been exposed to the pandemic H1N1 virus. However, the H1 peptides that elicited responses, i.e. M05, M06, M07 and M08, had identical sequences to that of their pandemic H1 homologues (**Table 5.5**).

Protein	Peptide ID	A/BR/59/07(H1N1)	Pandemic H1N1 equivalent regions	CD4 or CD8 dependency	SFC/million PBMC (range)	Number positive (%)
M	M01	MSLLTEVETYVLSIVPSG	MSLLTEVETYVLSIIPSG	CD4	30 (27-32)	2 (11)
	M05	AGKNTDL**EALMEWLKTRP**	Identical to *H1N1*	CD4	26	1 (6)
	M06	ALMEWLKTRPILSPLTKG	Identical to *H1N1*	CD4	39 (24-54)	2 (11)
	M07	RPILSPLTK**GILGFVFTL**	Identical to *H1N1*	CD8	86	1 (6)
	M08	K**GILGFVFTLTVPSERGL**	Identical to *H1N1*	CD4	116	1 (6)
	M12	DPNNMDRAVKLYRKLKRE	DPNNMDRAVKLYKKLKRE	CD4	32	1 (6)
	M13	VKLYRKLKREITFHGAKE	VKLYKKLKREITFHGAKE	CD4	35 (12-106)	8 (44)
	M14	REITFHGAKEIALSYSAG	REITFHGAKEVSLSYSTG	CD4	59 (18-90)	6 (33)
	M15	KEIALSYSAGALASCMGL	KEVSLSYSTGALASCMGL	CD4	57 (32-82)	3 (17)
	M23	N**RMVLASTTAK**AMEQMAG	Identical to *H1N1*	CD4	60 (54-110)	2 (11)
	M24	TAKAMEQMAGSSEQAAEA	Identical to *H1N1*	CD4	46	1 (6)
	M26	EAMEVASQARQMVQAMRA	EAMEVANQTRQMVHAMRT	CD4	66	1 (6)
	M27	A**RQMVQAMRAIGTHPSSS**	TRQMVHAMRTIGTHPSSS	CD4	26 (20-30)	3 (17)
NP	NP05	IGGIGRFYIQMCTELKLN	Identical to *H1N1*	CD8	58	1 (6)
	NP06	IQM**CTELKLNDY**EGRLIQ	IQM**CTELKLSDY**DGRLIQ	CD4	18 (16-19)	2 (11)
	NP09	**RMVLSAFDER**RNKYLEEH	Identical to *H1N1*	CD8	62	1 (6)
	NP13	YKRVDGKWVRELVLYDKE	YRRVDGKWMRELILYDKE	CD4	30	1 (6)
	NP14	VRELVLYDKEEIRRIWRQ	MRELILYDKEEIRRVWRQ	CD4	43 (16-86)	7 (39)
	NP15	KE**EIRRIWRQANNG**DDAT	KEEIRRVWRQANNGEDAT	CD4	35 (16-54)	2 (11)
	NP24	GVG**TMVLELIRMIK**RGIN	GVG**TIAMELIRMIK**RGIN	CD4	22	1 (6)
	NP27	GENGRKTRIAYERMCNIL	GENGRRTRVAYERMCNIL	CD8	50	1 (6)
	NP28	IA**YERMCNILKG**KFQTAA	VA**YERMCNILKG**KFQTAA	CD4/8	42	1 (6)
	NP34	**ILRGSVAHK**SCLPACVYG	Identical to *H1N1*	CD4	50	1 (6)
	NP38	SLVGVDPFKLLQTSQVYS	SLVGIDPFKLLQNSQVVS	CD4	18 (15-20)	2 (11)
	NP39	KLLQTSQVYSLIRPNENP	KLLQNSQVVSLMRPNENP	CD4	15 (10-20)	2 (11)
	NP40	YSLIRPNENPAHKSQLVW	VSLMRPNENPAHKSQLVW	CD8	82	1 (6)
	NP52	QPTFSVQRNLPFDKTTIM	QPTFSVQRNLPFERATVM	CD4	56	1 (6)

Table 5.5 List of H1N1 T cell peptides identified. Previously reported peptide regions are in bold; amino acids variations between the two sequences are underlined.

5.3 Discussion

This study was set up to understand the induction of cellular immune responses to inactivated vaccine and potential T-cell cross-reactivity against other strains. Serum antibody titers to influenza virus, whether elicited by naturally acquired infection or through vaccination, have been considered as a correlate of protection against influenza. In live attenuated vaccine, serum antibodies have been found not to associate with protection (Belshe et al., 1998; Beyer et al., 2002; Forrest et al., 2008; Treanor et al., 1999). Hence, it is important to define the role of cell-mediated immunity in influenza immunity, and to compare the response to influenza infection, for the development of next generation of influenza vaccine.

Both pandemic and seasonal vaccines studied have proven to be highly immunogenic, as shown by their abilities to induce protective antibodies. A detailed quantitative and qualitative characterization of T-cell immunity was performed against pandemic H1N1 and seasonal antigens in healthy individuals before and after vaccination. This study showed that an inactivated vaccine i) induced influenza-specific T cells against both surface and internal influenza antigens, without the use of any adjuvant. ii) Vaccination with the pandemic vaccine also led to an increase in T cells specific to seasonal antigens, and vice-versa, indicating cross-reactivity. iii) Moreover, pre-existing T cell memory to influenza leads to a less pronounced induction of T cell responses post-vaccination, and minimal effect on cellular immunity was found when volunteers were immunized by a heterologous vaccine three weeks after first immunization. iv) T cell responses to pandemic H1N1 vaccine are mainly mediated by $CD4^+$ T cells. v) Finally, the distribution of memory subsets within both $CD4^+$ and $CD8^+$ T cell populations remained constant during the course of immunization.

Pre-existing immunity towards H1N1 antigens may be due to exposure to the pandemic H1N1 virus or the seasonal H1N1 viruses, although none of the participants have clinical history of H1N1 2009 infection prior to the study. The existence of cross-reactivity is supported by the fact that induction of pandemic H1N1 specific T cells was accompanied by an induction of seasonal H1N1 specific T cells. Assessment of T cell immunity in both individuals recovering from severe pandemic H1N1, and in PBMCs collected from healthy volunteers prior to the pandemic, further emphasized the fact that memory responses are directed towards epitopes of both seasonal and pandemic strains, consistent to previous studies (Richards et al., 2010; Xu et

al., 2010). Therefore, the extent of T-cell cross reactivity with seasonal antigens may protect an individual without any prior exposure to the pandemic virus and cross-protective antibody response.

In subjects of Group 1 and 2, pre-existing immunity led to a lower fold increase in influenza-specific response. This is consistent with previous studies which showed antigen-specific T cells induced by vaccination with live seasonal influenza viruses were lower in individuals that had higher baseline level of influenza specific T cell responses compared to those with lower baseline levels (Subbramanian et al., 2010). Although continuous exposure to similar antigens can lead to T-cell exhaustion, as seen in infectious diseases such as HIV, hepatitis C or active tuberculosis (Sester et al., 2011; Wherry, 2011), no change in functionality of influenza specific T cells post- or pre- vaccination was observed in this cohort. Limited boosting of cellular responses can also be related to the presence of pre-existing neutralizing antibodies, especially for those against seasonal H1N1 (as nearly half of the volunteers had neutralizing antibodies against H1N1), which could reduce the amount of antigen available for boosting. It may explain why in Group 3 where the individuals were vaccinated with both vaccines at the same time, a higher availability of antigens allow a more pronounced boosting of influenza-specific T cells. Indeed, a study done in mice has found that treatment with HA-specific Igs after infection with influenza A virus can interfere with the generation of cellular immune responses (Greenspan and Doherty, 1982). Similarly, when volunteers were vaccinated by heterologous vaccines on day 21 in both Group 1 and 2, no increase in the magnitude of influenza-specific T cells were observed. These are consistent with previous studies looking at cell-mediated response to inactivated influenza vaccination in healthy children, in which boosting effects were not observed in T cell IFN-γ secretion (He et al., 2006b; Madan et al., 2008).

Unlike serological responses, it has not been established whether an ELIspot value or fold change from baseline can be predictive of the cell-mediated immune response to the virus. Given the evidence in the previous human challenge studies that protection against influenza virus may occur in the absence of a detectable antibody response (Mcmichael et al., 1983; Treanor J, 2003), and the results from the challenge models (Chapters 3), subjects may still be protected despite a lack of correlation between measurable antibody response and T cell response. Comparing influenza infection to vaccination, T cell responses induced by experimental challenge were seen to be 4- to 6- fold higher than the T cell responses induced by the inactivated vaccine. This can be

related to how T cells recognize viral antigens. As the vaccine antigens cannot reach the cytosol and thus cannot be processed and presented as MHC-peptide complexes for T cell recognition, inactivated vaccines are inefficient at priming strong influenza-specific CTL responses. Split vaccine may not be taken up and processed efficiently by DCs since it is not a particulate antigen, and lacks intact immunostimulatory viral ssRNA to act as an adjuvant to stimulate TLR7 on DCs (Wagner et al., 2004). Effective priming of CTL activity requires the coupling of the vaccine to an alternative TLR-ligand, CpG (Wagner, 2009). In mouse models, it was reported in 1980 that an HA-NA subunit vaccine was not able to prime CTL responses (Webster and Askonas, 1980). Whether the inactivated vaccine is able to induce T cell responses should not be of importance if the vaccine strains and the circulating strains match, however if the two do not match well, the $CD8^+$ and $CD4^+$ T cell responses induced against internal/surface antigens may make a difference to the disease outcome. It should be emphasized that only 1-2% of total T cells in the entire body are present in peripheral blood, thus influenza-specific T cells detected in the periphery post vaccination contributes to only a small subset of the overall influenza-specific T cell population, thus the frequency and phenotype of such cells may differ from those in the lymphoid organs or sites of infections (de Bree et al., 2005).

In this study, activated proliferating cells ($CD38^+$ Ki-67^+) detected in the course of vaccination were found to be of a central memory phenotype. It is thought that T cell responses generated by central memory cells are delayed compared with that mediated by effector memory cells already present in the lung, because $CD4^+$ memory cells take 2-3 days after restimulation to become effectors and migrate to the lung (Swain et al., 2006). However, even if such response is delayed, the pathological effects of an infection can be minimized if the induced response is robust enough. In a recent study, one dose of an MF59-adjuvanted A/H1N1 pandemic vaccine was found to induce rapid expansion of pre-existing $CD4^+$ T cells in healthy adults (Faenzi et al., 2012). Expression of Ki-67 was monitored using *ex vivo* staining and no change in kinetics was found in this study. In contrast, trivalent inactivated vaccine was found to induce Ki-67 expression transiently (at 4-6 days after vaccination) in influenza-specific T cells that produced cytokines in response to influenza vaccine or peptide *in vitro*. Measuring intracellular Ki-67 expression directly *ex vivo* has been employed in our challenge studies (Chapter 3, section 3.2.6), and in other studies to measure specific T cell responses induced by vaccination and acute viral infection (Akondy et al., 2009; Querec et al., 2009). *Ex vivo* staining may not be sensitive enough

to detect the relatively low magnitude of the short-lived proliferative burst of antigen-specific T cells induced by an inactivated vaccine, thus in future studies, an *in vitro* restimulation should be used instead to detect the response from influenza-specific cells but not from the bulk memory $CD4^+$ or $CD8^+$ populations.

It would be interesting to compare the results of this study with those of a live attenuated vaccine (LAIV), which should be capable of enhancing the pool size of T cells that are directed against multiple internal viral proteins of variant strains. LAIV is shown to elicit significantly higher magnitude of T cell responses against H3N2 HA antigens than inactivated vaccine (Basha et al., 2011). Mean percentage of influenza-specific IFN-γ^+ $CD4^+$ and $CD8^+$ T cells also increased significantly after LAIV immunization in children (He et al., 2006a). It has also been shown in animal models that LAIV induce broad, protective immune responses (Fan et al., 2009; Suguitan et al., 2006). More comprehensive studies can then be used to elucidate the phenotype and function of influenza-specific T cells following vaccination.

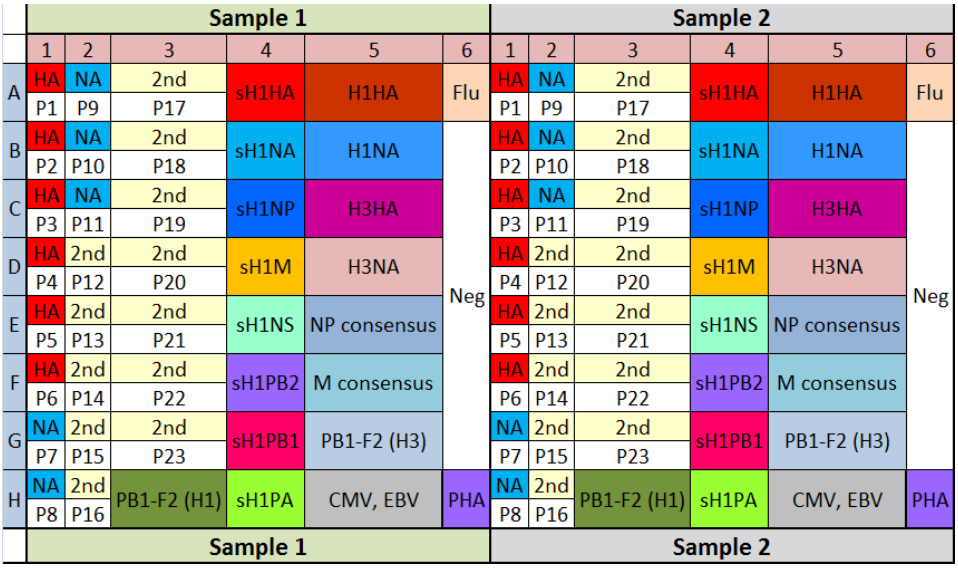

Figure 5.1 IFN-γ ELISpot layout of pandemic H1N1 vaccine trials. 300 000 of fresh PBMCs were stimulated with 2 μg/ml of peptide pool for 18 hours in each well. PHA-stimulated PBMCs were used as a positive control. Overlapping peptides spanning the pandemic H1N1 HA and NA proteins were included in a total of 23 pools (column 1, 2 and 3), with each peptide presented in two of the pools. The responses were mapped in such a way that for each peptide that made a response, there would be two wells that appeared positive. Overlapping peptides spanning other viral proteins (HA, NA, NP, M, NS, PB2, PB1 and PA) of pandemic H1N1, and also peptide pools of seasonal H3 and H1 HA, NA and PB1-F2 proteins, peptide pools of the conserved regions of the M and NP proteins, were also included. Epitopes of CMV and EBV were used as bystander controls. Known flu epitopes (well 6A) and PHA-stimulated PBMCs were used as positive controls. Unstimulated PBMCs were used as negative controls.

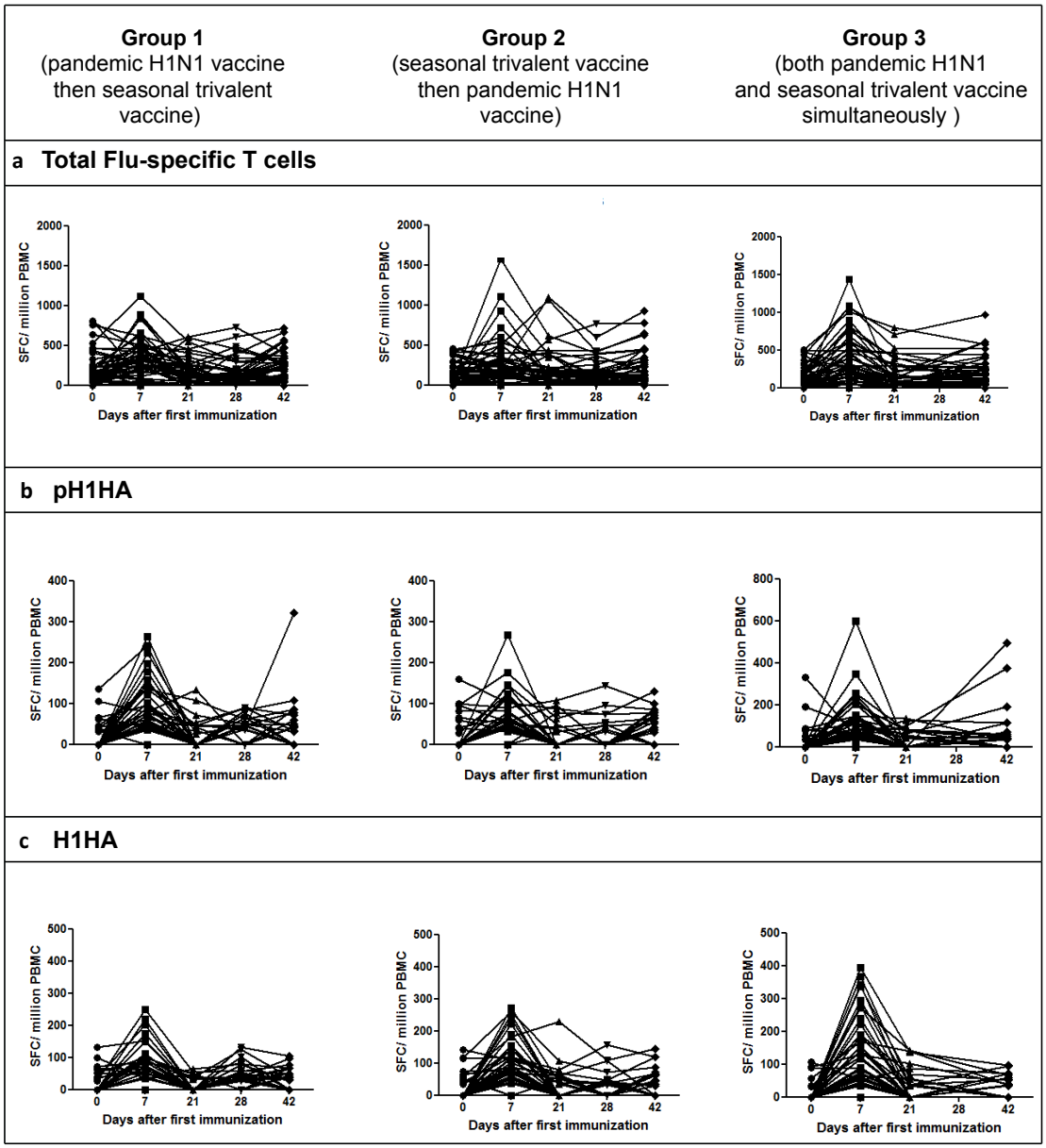

Figure 5.2 T cell responses in volunteers vaccinated with inactivated influenza vaccines. Group 1 received pandemic vaccine on day 0 followed by seasonal flu vaccine on day 21. Group 2 received seasonal vaccine on day 0 and then pandemic vaccine on day 21. Group 3 received both vaccines simultaneously on day 0. **(a)** Total flu-specific T cell responses as measured by *ex vivo* IFN-γ ELISpot of each responding subject. **(b)** T cell responses to pandemic H1 HA peptides. **(c)** T cell responses to seasonal H1 HA peptide.

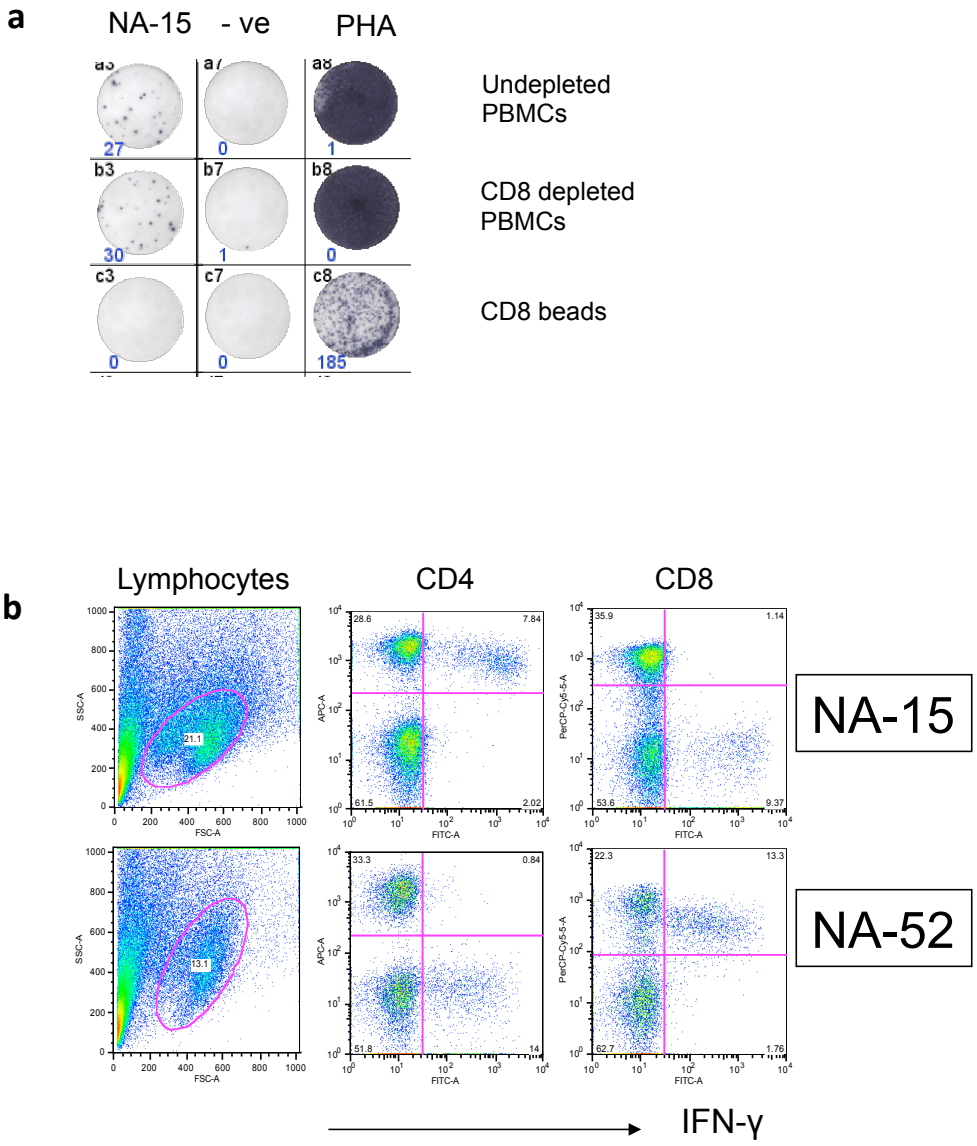

Figure 5.3 Antigen-specific responses to viral peptides in vaccinated subjects. Responses of vaccinated subjects to flu surface antigens were mapped to individual peptide by **(a)** cell depletion and *ex vivo* ELIspot, and **(b)** intracellular cytokine staining. Representative example showing $CD8^+$ T cells were depleted from PBMCs, and were stimulated with peptides (e.g. NA-15) in an ELISpot assay. NA-15 elicited a $CD4^+$ T cell-mediated response; while NA-52 elicited a $CD8^+$ T cell-mediated response.

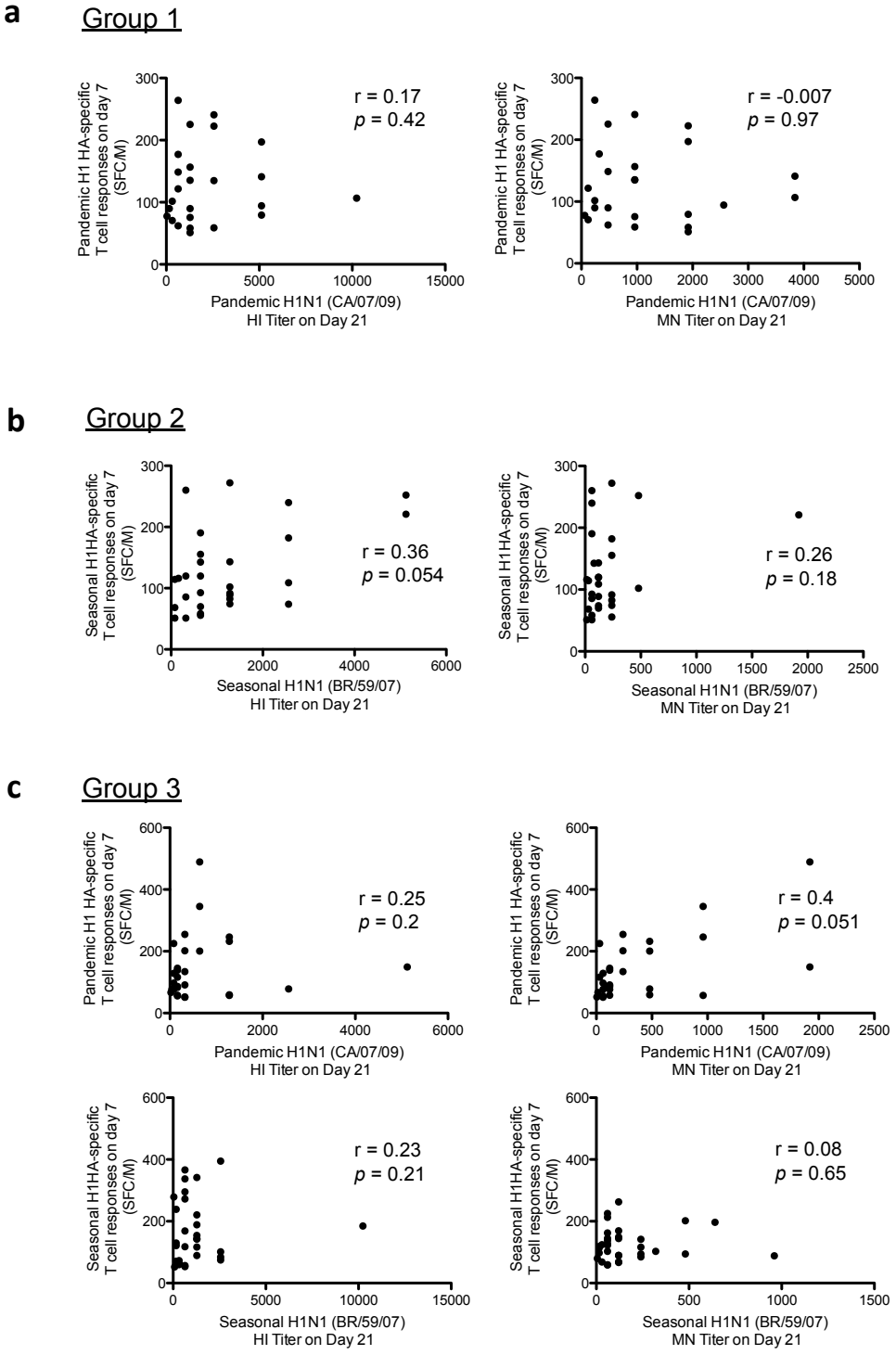

Figure 5.4 Correlation between humoral and cellular immune responses in vaccinated subjects. **(a)** Relationship between HI and MN titers on day 21 and pandemic H1N1 HA-specific T cell responses on day 7 in Group 1. **(b)** Relationship between HI and MN titers on day 21 and seasonal H1N1 HA-specific T cell responses on day 7 in Group 2. **(c)** Relationship between HI and MN titers on day 21 and pandemic H1N1 HA-specific T cell responses on day 7, and between HI and MN titers on day 21 and seasonal H1N1 HA-specific T cell responses on day 7 in Group 3.

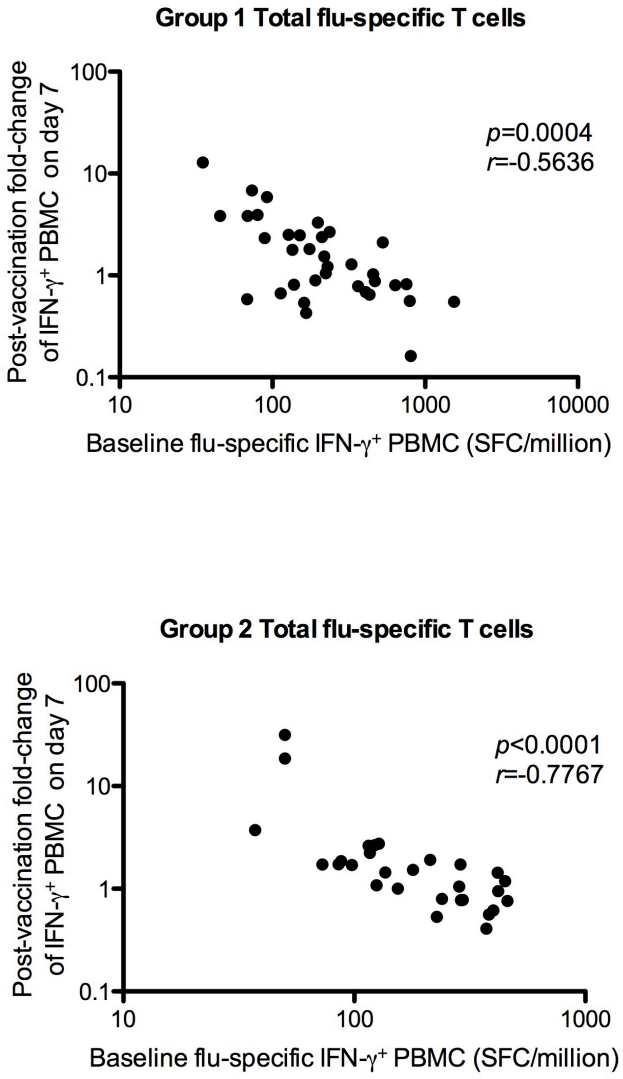

Figure 5.5 Relationship between influenza-specific T cell responses at baseline and the fold-increase in spot-forming cells in IFN-γ ELISpot on day 7 post-vaccination. Correlation (Spearman rank correlation) was found between influenza-specific T cells of Group 1 and 2, and the corresponding fold-change post vaccination. A *p* value of less than 0.05 was considered significant (*$p < 0.05$).

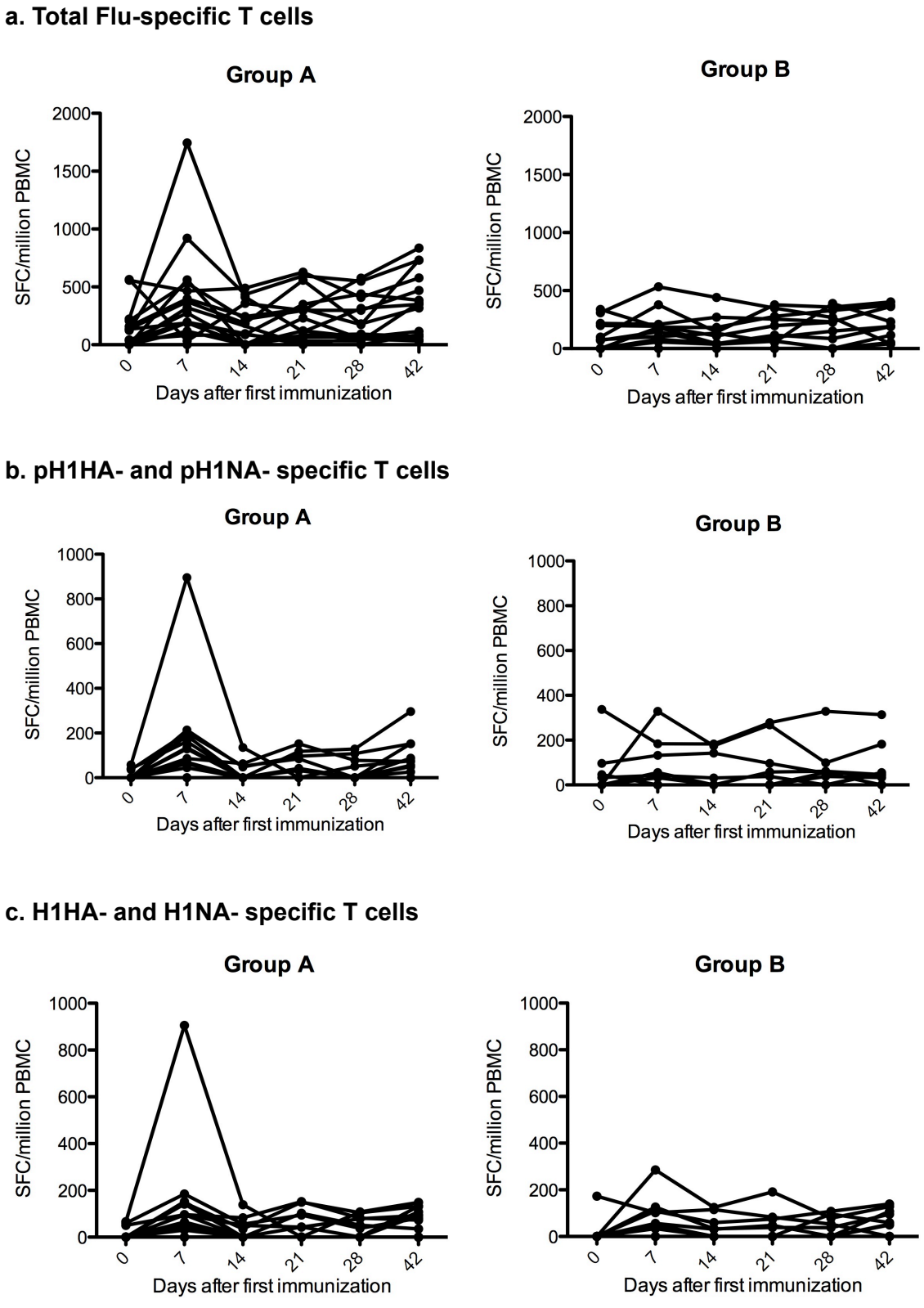

Figure 5.6 T cell responses in a group of volunteers from China CDC vaccinated with seasonal and pandemic H1N1 vaccine. Group A (n=16) received pandemic vaccine on day 0; and group B (n=12) received seasonal vaccine on day 0 then pandemic vaccine on day 21. PBMCs were stimulated with overlapping peptides in an IFNγ-ELISpot as shown in the layout in Fig. 5.1. **(a)** Total flu-specific T cell responses; **(b)** pandemic H1N1 HA- and NA- specific T cell responses; **(c)** seasonal H1N1 HA- and NA –specific T cell responses in Group A and B.

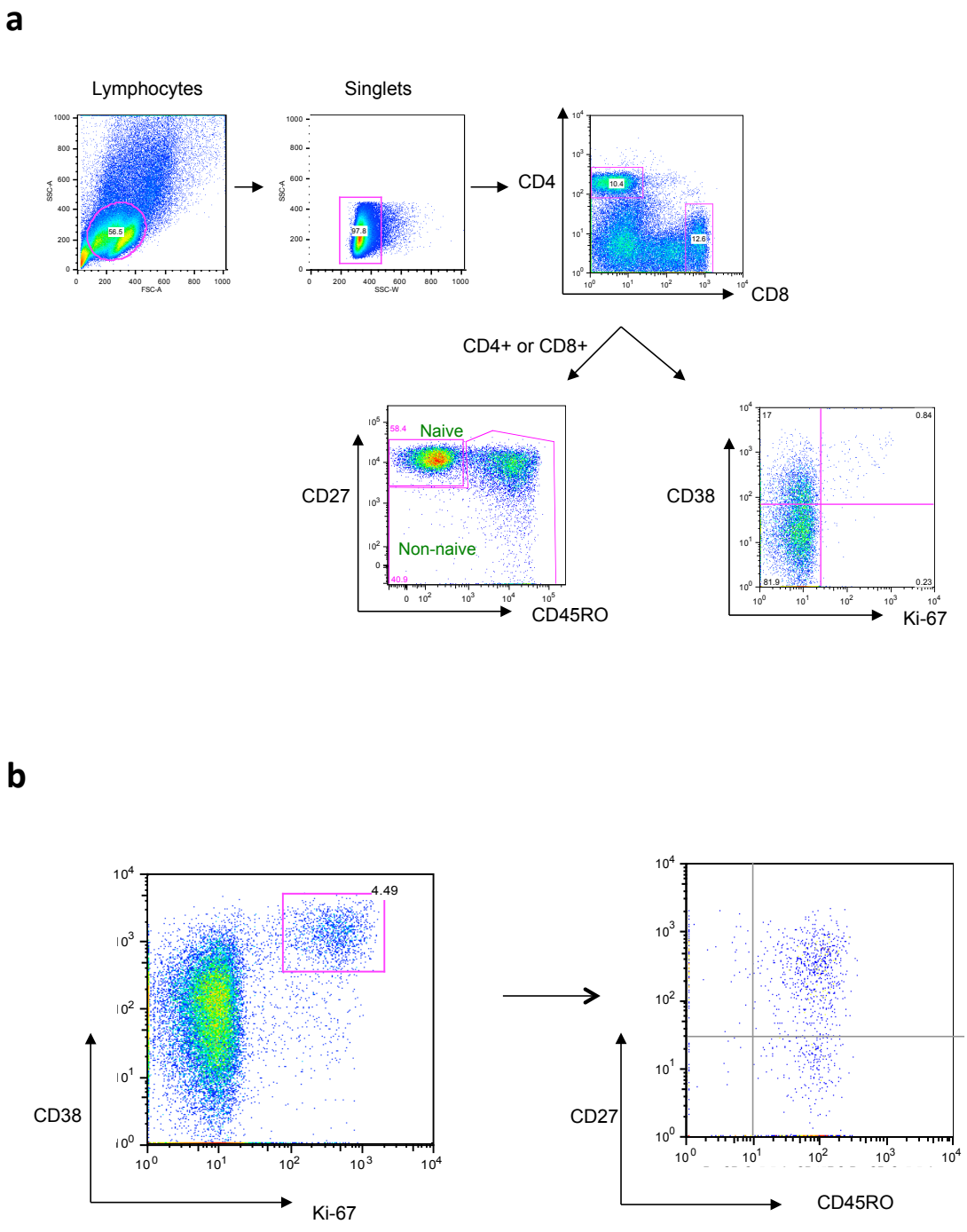

Figure 5.7 Memory phenotype of activated proliferating T cells. **(a)** Gating strategy for analysing activation and proliferation. **(b)** Memory phenotype of activated and proliferating ($CD38^+$ $Ki\text{-}67^+$) $CD4^+$ T cells in fresh PBMCs isolated from vaccinated subjects were analysed by flow cytometry. Representative staining from one subject.

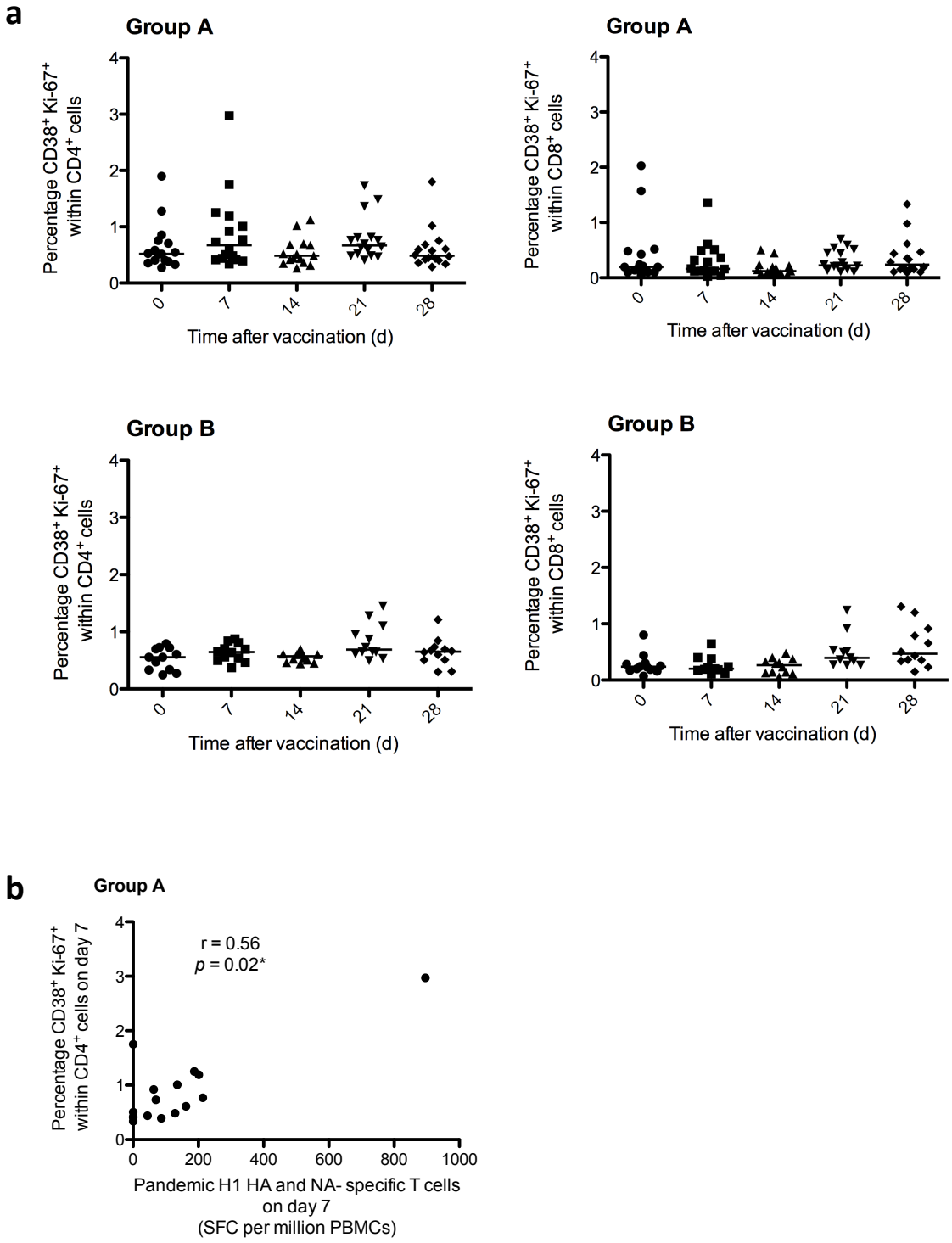

Figure 5.8 Activated and proliferative (CD38$^+$ Ki-67$^+$) CD4$^+$ and CD8$^+$ T cells in vaccination. (a) Frequency of activated proliferative (CD38$^+$ Ki-67$^+$) CD4$^+$ and CD8$^+$ T cells in the course of vaccination in both Group A and Group B. Bar indicates median value. Differences between timepoints were tested using non-parametric Kruskal–Wallis's test with post hoc Dunn's test for multiple comparisons. A *p* value of less than 0.05 was considered significant (*p< 0.05). **(b)** Correlation between proportion of CD38$^+$ Ki-67$^+$ CD4$^+$ T cells on day 7 of the subjects in Group A with the sum of magnitude of pandemic HA and NA- specific T cell response on day 7 in ELISpot, analysed by Spearman rank correlation test.

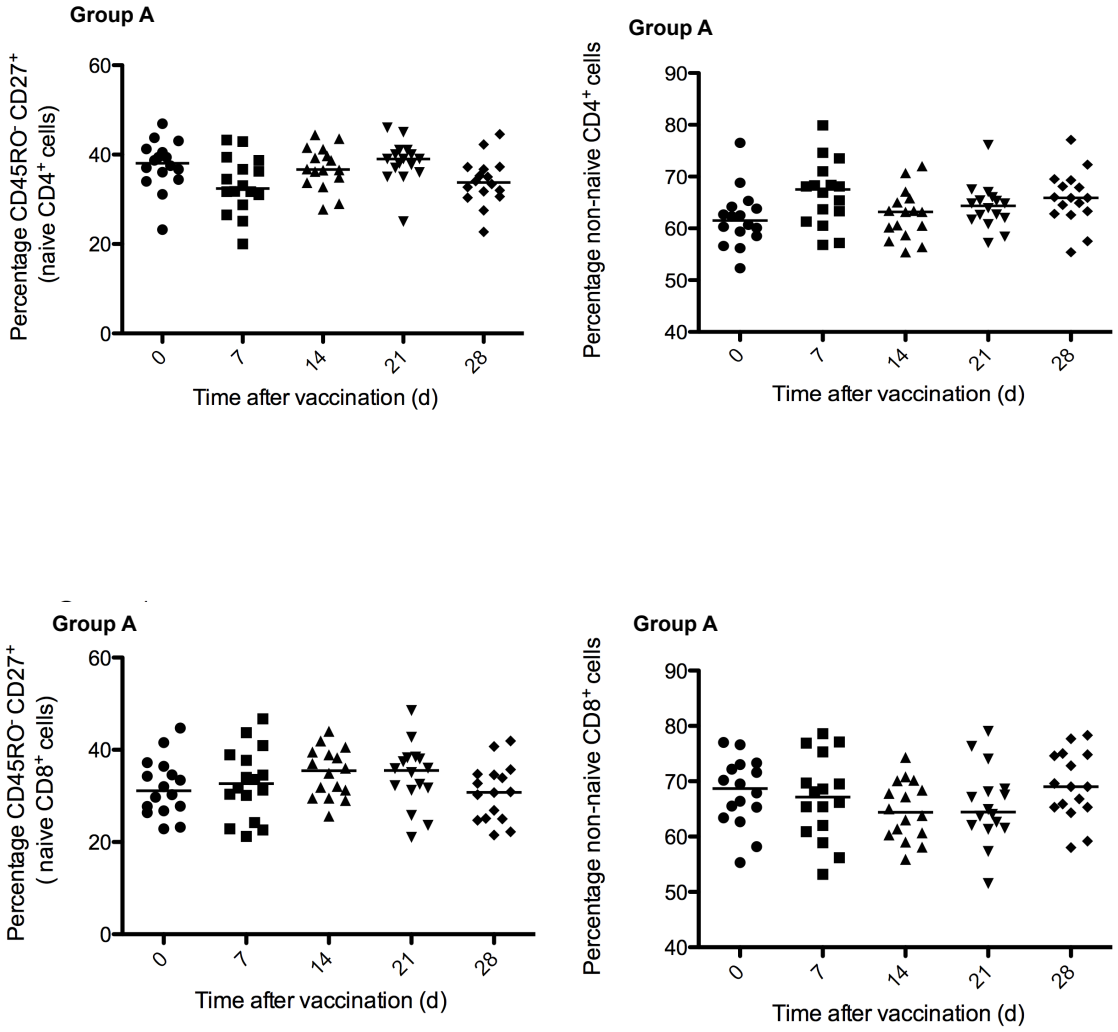

Figure 5.9 Frequency of naïve and non-naïve CD4⁺ and CD8⁺ T cells in the course of vaccination. Phenotype of CD4⁺ and CD8⁺ T cells in Group A. Bar indicates median value. Differences between timepoints were tested using non-parametric Kruskal–Wallis's test with post hoc Dunn's test for multiple comparisons.

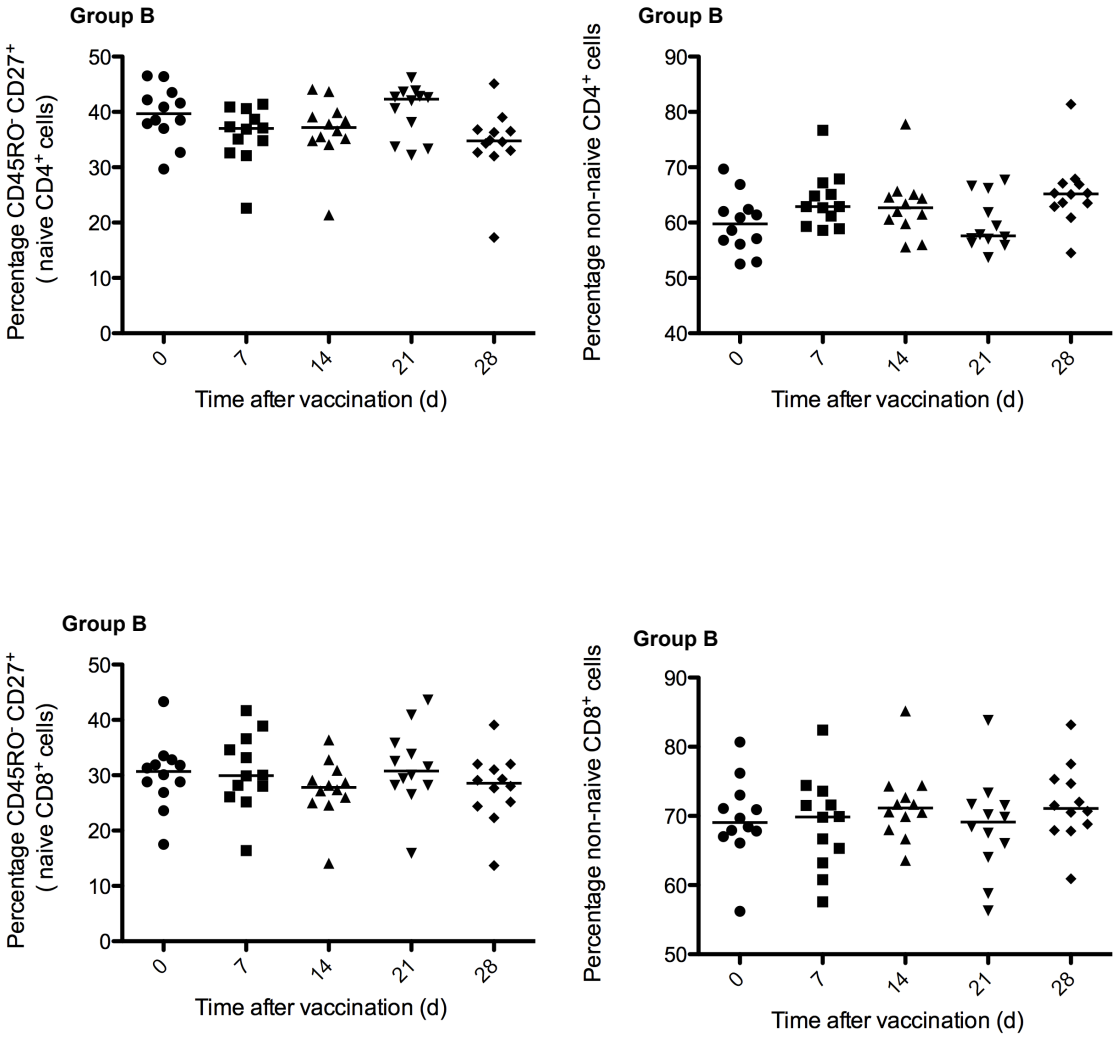

Figure 5.10 Frequency of naïve and non-naïve CD4⁺ and CD8⁺ T cells in the course of vaccination. Phenotype of CD4⁺ and CD8⁺ T cells in Group B. Bar indicates median value. Differences between timepoints were tested using non-parametric Kruskal–Wallis's test with post hoc Dunn's test for multiple comparisons.

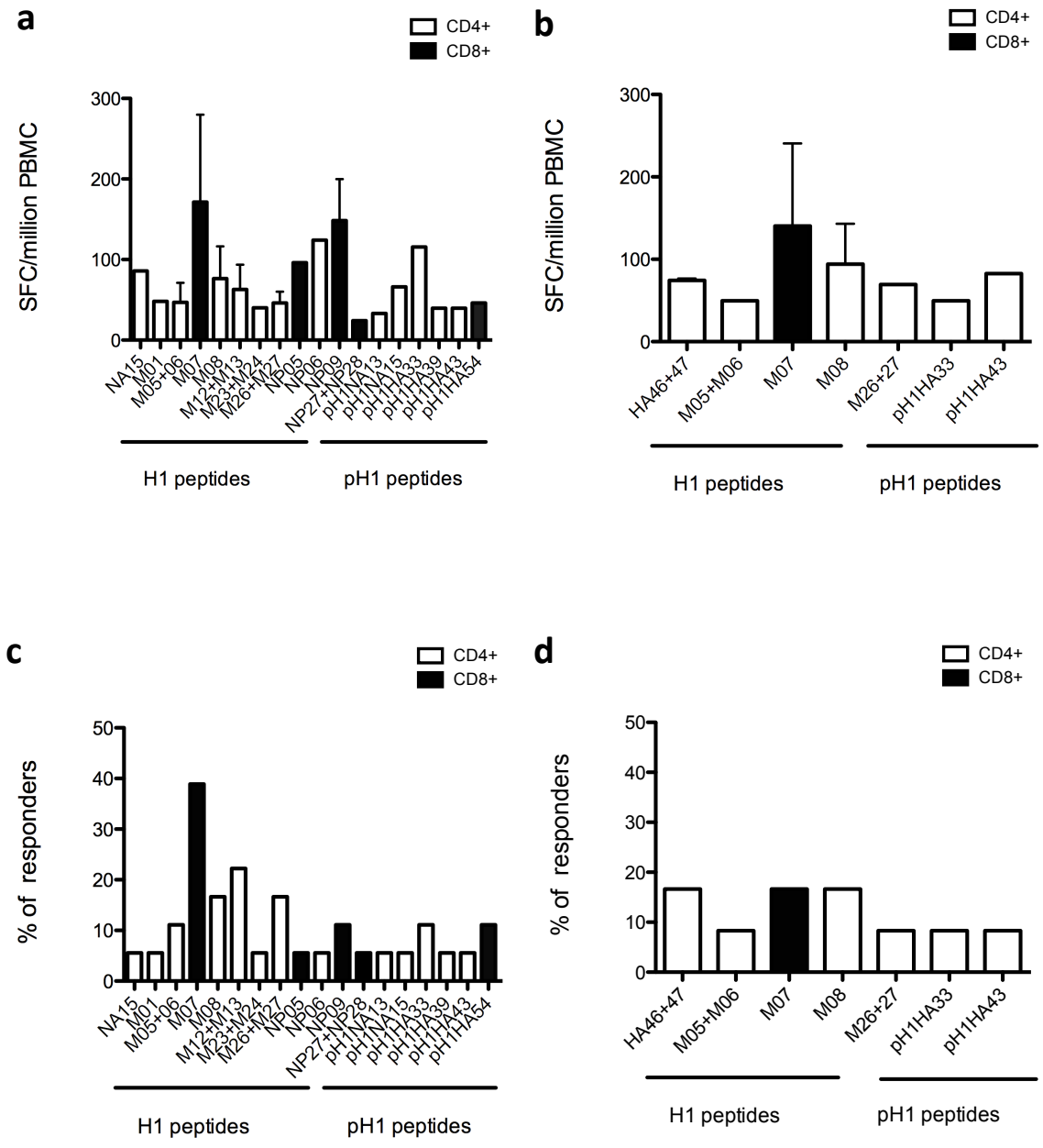

Figure 5.11 Flu-specific T cell responses of pandemic H1N1 convalescent subjects and healthy PBMCs collected before 2009. Magnitude of T cell responses of **(a)** pandemic H1N1 convalescent subjects and **(b)** healthy PBMCs collected before 2009, as measured by stimulating PBMCs with individual peptides, of which specificity were identified in the H1N1 challenge and pandemic H1N1 vaccine cohorts. Breadth of T cell response of **(c)** pandemic H1N1 convalescent subjects and **(d)** healthy PBMCs collected before 2009 as measured by percentage of responders to the range of peptides identified. Bars depict mean values and s.d.. White bar indicates that a response is mediated by $CD4^+$ T cells, while black bar indicates that a response is mediated by $CD8^+$ T cells.

Chapter 6

Circulating T follicular helper cells and their capacity to provide B cell help

6.1 Introduction

Current influenza vaccines aim at inducing potent neutralizing antibodies. Such antibodies protect the host against invading pathogens by, for example, neutralizing the virus. The generation of a humoral immune response requires the help of T follicular helper cells (Tfh) in germinal centres (GC) within the secondary lymphoid organs. Tfh in humans were first described as $CD4^+$ T cells in tonsils that express high levels of chemokine receptor CXCR5 (Breitfeld et al., 2000; Kim et al., 2001; Schaerli et al., 2000). Expression of CXCR5 drives Tfh cells to migrate out of the T cell zone of the lymphoid tissue into the B cell follicle (Ansel et al., 1999; Hardtke et al., 2005; Haynes et al., 2007). Tfh cells also express high levels of other surface markers, including the inducible T cell costimulator (ICOS), CD40 ligand (CD40L or CD154) and the T cell inhibitory receptor programmed death 1 (PD-1), which are important for their development and function (Crotty, 2011). ICOS is a CD28 family costimulatory molecule that induces the production of helper cytokines such as IL-10 and IL-21 when it binds to its ligand (ICOS-L) (Greenwald et al., 2005; Lohning et al., 2003; Vogelzang et al., 2008). PD-1 and its ligands are involved in the maintenance of peripheral tolerance through the modulation of costimulation in activated T cells (Gomez-Martin et al., 2011). The interaction between CD40L and CD40 on B cells stimulates B cell activation and isotype switching (van Kooten and Banchereau, 2000). The generation of Tfh cells is controlled by the expression of transcription factor B cell lymphoma 6 (Bcl-6) (Johnston et al., 2009; Nurieva et al., 2009; Yu et al., 2009). They also express cytokines such as interleukin-21 (IL-21) which are implicated in B cell differentiation and antibody production.

IL-21 is involved in promoting B cell differentiation and somatic hypermutation (Avery et al., 2008; Bryant et al., 2007; Ettinger et al., 2008).

The analysis of Tfh cells in humans has involved the utilization of tonsillar tissues, where a large number of Tfh cells are present in the germinal centres, and their presence in other compartments such as the peripheral blood was, until very recently, unexplored. $CXCR5^+$ $CD4^+$ T cells are present within the memory $CD4^+$ T cell compartment in human peripheral blood, but their relationship with Tfh is unclear. As CXCR5 is a general activation marker, the relationship between blood $CXCR5^+$ $CD4^+$ T cells and Tfh is controversial as the former are resting while the latter are highly activated (Schaerli et al., 2000). Secondly, microarray-based gene expression analysis shows distinct gene expression patterns between the two cell types (Rasheed et al., 2006). Lastly, blood $CXCR5^+$ $CD4^+$ T cells do not express increased levels of Bcl-6 protein (Crotty, 2011). Recently, however, blood $CXCR5^+$ $CD4^+$ T cells have been shown to provide better help to naïve B cells than their $CXCR5^-$ counterparts, at least in the presence of superantigens (Chevalier et al., 2011; Morita et al., 2011). In addition to blood $CXCR5^+$ $CD4^+$ T cells, the majority of which do not express phenotypic markers characteristic of GC Tfh cells (Chevalier et al., 2011; Morita et al., 2011), rare blood Tfh cells with a more similar phenotype to that of GC Tfhs have been observed. Studies have demonstrated that such circulating Tfh-like cells can be found in the peripheral blood of patients with autoimmune diseases such as systemic lupus erythematosus (SLE) and Sjögren's syndrome (SS) (Linterman et al., 2009; Simpson et al., 2010). One-third of these patients have an increase in otherwise rare circulating Tfh-like (cTfh) cells with a $CXCR5^{high}ICOS^{high}PD\text{-}1^{high}$ $CD4^+$ phenotype. These markers were also found on the Tfh subset in secondary lymphoid organs. These circulating Tfh could be a subset distinct from the Tfh resident in the secondary lymphoid organs, or they may represent a subset of Tfh which, upon maturation and trafficking from the spleen and lymph nodes, have downregulated the molecules crucial for their effector functions in the lymphoid organs. The substantial presence of these circulating Tfh closely correlated with disease severity (Simpson et al., 2010). Also, a comparable increase in the circulating Tfh population in sanroque mice (which display a lupus-like phenotype with a number of autoimmune characteristics) correlated with the increase in resident Tfh cells in the secondary lymphoid organs (Linterman et al., 2009).

The nature of influenza infection is completely different to that of an autoimmune disease, in which expansion of Tfh is related to the production of autoantibodies, and it has not been

examined whether there is any change in the proportion of blood Tfh subsets during the course of an acute viral infection in humans. Studying Tfh cells in humans is difficult as it is not easy to access secondary lymphoid organs where their functions are exerted. Therefore studies to evaluate human Tfh functions are mainly restricted to flow cytometry analysis of $CXCR5^+$ $CD4^+$ T cells in the peripheral blood (Feng et al., 2011), or *in vitro* assays of their response to stimuli leading to the upregulation of molecules (e.g. CD154 and ICOS) involved in T-B cell interaction and cytokines necessary for a mature humoral response (Chevalier et al., 2011; Morita et al., 2011). In mice acutely infected with LCMV, Tfh differentiation and B cell development are the result of the combined effects of IL-6 and IL-21 (Eto et al., 2011). Other studies have shown that HIV-specific IL-21 producing cells that expressed CXCR5 were found in blood in HIV infected patients, and these cells correlated with viral control (Yue et al., 2010). However the relationship between IL-21 producing cells and disease severity in influenza infection is currently unknown.

Another important question is how well Tfh cells are induced by vaccination. A recent study in mice showed that vaccines that expanded Tfh cells and promoted GC induction were associated with strong antibody responses to a malaria antigen, supporting the need for antibody-inducing vaccines to prime good Tfh responses (Moon et al., 2012). It has also been shown in studies in mice that memory $CD4^+$ T cells that express CXCR5 have an intrinsic ability to provide help to responding naïve B cells (MacLeod et al., 2011). Thus it is likely to be particularly important to prime and maintain $CXCR5^+$ memory T cells when developing vaccines against influenza virus.

Given the predominant role of CXCR5-expressing $CD4^+$ T cells with Tfh activity in antibody-mediated immune responses, the aims of this chapter were as follows:

1) To determine whether blood $CXCR5^+$ $CD4^+$ T cells can provide help to naïve B cells in the presence of superantigen.

2) To examine the presence of antigen-specific cells within blood $CXCR5^+$ $CD4^+$ T cells.

3) To examine the production of IL-21 in blood $CXCR5^+$ $CD4^+$ T cells.

4) To describe the kinetics of blood Tfh during acute influenza infection and vaccination.

5) To determine whether flu-specific $CD4^+$ T cells in the peripheral blood can provide help to B cells.

6.2 Results

6.2.1 Phenotype of CD4$^+$ CXCR5$^+$ cells in human blood

Initial experiments addressed the frequency and phenotype of CD4$^+$ CXCR5$^+$ cells in the peripheral blood of healthy adult donors, and compared this to findings made with tonsillar cells. The CXCR5$^+$ population of CD4$^+$ memory T cells in the blood was identified as shown in **Fig. 6.1a**. In healthy adult blood, CXCR5 was expressed by a minority of CD4$^+$ T cells, making up 9.12 ± 2.26% of memory (CD45RO$^+$) CD4 T cells (mean ± s.d., n= 7), consistent with what was previously reported **(Fig. 6.1b)**. CXCR5$^+$ CD4$^+$ T cells were central memory T cells (CD27$^+$ CD45RO$^+$) **(Fig. 6.2a)**. Few blood CXCR5$^+$ CD4$^+$ cells expressed activation molecules expressed by Tfh cells, such as ICOS and PD-1, in contrast to CXCR5 cells present in the tonsils. In blood, 10.32 ± 2.87% of CXCR5 -expressing memory CD4$^+$ cells expressed PD-1, 1.08 ± 0.65% expressed ICOS, and 4.46 ± 1.96% expressed CD57 (mean ± s.d., n= 7) **(Fig. 6.2b and c)**. In contrast these markers were highly enriched in tonsillar T cells. In tonsils, CXCR5$^+$ cells made up 42 ± 5.66% of memory (CD45RO$^+$) CD4 T cells (mean ± s.d., n= 2) **(Fig. 6.3a)**. Tonsillar CXCR5$^+$ CD4$^+$ cells were highly activated. 77.8 ± 0.57% of CXCR5 -expressing memory CD4$^+$ cells expressed PD-1, 64.9 ± 2.07% expressed ICOS, and 32.3 ± 1.47% expressed CD57 (mean ± s.d., n= 2) **(Fig. 6.3b)**.

6.2.2 Human blood CD4$^+$ CXCR5$^+$ cells induce differentiation of the naïve B cells towards plasmablasts that produce class-switched antibodies

The CXCR5$^+$ subset of CD4$^+$ T cells in peripheral blood has been suggested to be resting memory Tfh cells. Next I looked at whether this population of cells are Tfh cells that circulate in the blood, and mediate similar functions to their tonsillar counterparts. To determine the capacity of blood CXCR5$^+$ cells to help B cells, memory (CD45RO) CXCR5$^+$ CD4$^+$ cells were sorted and cultured with autologous naïve (CD19$^+$ CD27$^-$) B cells **(Fig. 6.4)**. Memory CXCR5$^-$ CD4$^+$ cells were also sorted for comparison. The purity of CXCR5$^+$ and CXCR5$^-$ exceeded 90% after sorting. Staphylococcal enterotoxin B (SEB), a superantigen, was used in the cultures to mimic antigen-specific interaction between T and B cells. In agreement with previous studies (Chevalier et al., 2011; Morita et al., 2011), CXCR5$^+$ CD4$^+$ cells were found to be able to induce

naïve B cells to produce IgM, IgG and IgA at the end of the culture period. In contrast, $CXCR5^-$ $CD4^+$ T cells were unable to induce a similar antibody response. Naïve B cells co-cultured with $CXCR5^+$ $CD4^+$ T cells did not produce Igs in the absence of SEB, indicating that Ig production is dependent on cognate interactions between T and B cells **(Fig. 6.5 and 6.6)**.

$CXCR5^+$ $CD4^+$ T cells induced naïve B cells to produce Igs by day 7 of culture **(Fig. 6.5a)**. The number of viable plasmablasts recovered at the end of the culture was significantly higher when naïve B cells were co-cultured with $CXCR5^+$ cells than with $CXCR5^-$ cells ($p < 0.05$) **(Fig. 6.6b)**. Importantly, culturing naïve B cells with $CXCR5^+$ $CD4^+$ T cells yielded a higher percentage of $CD38^+CD19^{lo}$ cells compared to $CXCR5^-$ $CD4^+$ T cells, indicating that naïve B cells had differentiated into plasmablasts *in vitro* **(Fig. 6.7a)**.

Previous reports demonstrated that expansion and plasma cell differentiation of co-cultured B cells required IL-21 secreted by tonsillar Tfh cells (Bryant et al., 2007). Here, I found that blood $CXCR5^+$ $CD4^+$ cells secreted IL-21 when co-cultured with naïve B cells, as early as 24h after interaction **(Fig. 6.7b)**. The average amount of IL-21 produced was higher in $CXCR5^+$ $CD4^+$ cells than in $CXCR5^-$ $CD4^+$ cells, although the difference between the two was not statistically significant **(Fig. 6.7bc)**.

Taken together, these results show that blood $CXCR5^+$ $CD4^+$ T cells were more efficient than their $CXCR5^-$ counterparts at providing help for naïve B cells, inducing them to differentiate into plasmablasts and produce class-switched antibodies.

6.2.3 The human blood $CD4^+$ $CXCR5^+$ subset can contain influenza virus-specific cells

Previous reports have suggested that the pool of circulating $CXCR5^+$ memory $CD4^+$ T cells represent T cells undergoing recent or on-going immune activation, while $CXCR5^-$ $CD4^+$ T cells represent a pool of "old" memory cells (Schaerli et al., 2000). Blood $CXCR5^+$ $CD4^+$ T cells have also been found to have a nonpolarized phenotype and lack prototypic effector functions (Breitfeld et al., 2000; Kim et al., 2001; Rivino et al., 2004; Schaerli et al., 2000). To assess the response of the circulating $CD4^+$ $CXCR5^+$ population to stimulation, purified memory ($CD45RO^+$) $CXCR5^+$ $CD4^+$ cells and $CXCR5^-$ $CD4^+$ cells were stimulated with PMA and ionomycin (PMA/ION) for 5 hours and analysed for intracellular production of cytokines by flow

cytometry. Both CXCR5$^+$ CD4$^+$ cells and CXCR5$^-$ CD4$^+$ cells produced IFN-γ, suggesting that some of these cells had differentiated into early stage effector T cells. Comparing the two subsets, production of IL-2 was significantly greater in CXCR5$^-$ CD4$^+$ cells ($p< 0.05$). However, the ratio of IL-2- producing cells to IFN-γ - producing cells is higher for the CXCR5$^+$ CD4$^+$ cells than the CXCR5$^-$ CD4$^+$ cells (9.5 and 3.7 respectively). Overall, a lower proportion of CXCR5$^+$ cells responded to stimulation by production of either of the cytokine analysed **(Fig. 6.8ab)**. This may imply that CXCR5$^+$ cells comprise a more unpolarized population than CXCR5$^-$ cells, and may function to support humoral responses rather than being specialized into a cytokine-producing Th subset.

I also assessed the expression of the co-stimulatory molecules ICOS and CD154, co-stimulation via which is of importance in GC reactions and T-B interaction, on purified CXCR5$^+$ CD4$^+$ cells and CXCR5$^-$ CD4$^+$ cells after *in vitro* stimulation by plate- bound anti-CD3 and soluble anti-CD28 antibodies for 48 hours. Both subsets upregulated ICOS and CD154 upon stimulation, and differences were insignificant **(Fig. 6.9ab)**. It shows that the two markers do not distinguish cells capable of mediating Tfh activity, but rather may be upregulated on all CD4$^+$ cells that have been recently activated.

To investigate whether blood CXCR5$^+$ CD4$^+$ T cells contain antigen-specific memory cells, isolated CXCR5$^+$ and CXCR5$^-$ CD4$^+$ T cells were co-cultured with autologous monocytes that had been pulsed with influenza vaccine antigens, and proliferation of T cells was analysed on day 5. Both CXCR5$^+$ and CXCR5$^-$ cells proliferated robustly in response to stimulation with monocytes pulsed with the virus **(Fig. 6.10)**.

Taken together, these observations show that the peripheral blood CXCR5$^+$ CD4$^+$ T cells shared some functional properties of Tfh cells in the GCs, although none of the cytokines and costimulatory markers analysed were uniquely expressed by cells in the CXCR5$^+$ subset. The circulating CXCR5$^+$ CD4$^+$ T cells also contained antigen-specific memory cells.

6.2.4 IL-21 production by influenza virus-specific CD4$^+$ T cells

In the generation of a primary antibody response to a vaccine, naïve B cells are activated by the vaccine antigen and undergo a process of maturation, differentiation, and proliferation to generate Ab-secreting cells, memory B cells and long-lived plasma cells. This process is regulated by a

variety of factors including the pleiotropic cytokine IL-21. IL-21 is an acute phase cytokine of the IL-2 cytokine family and is responsible for early pro-inflammatory immune responses during autoimmune and infectious diseases. IL-21 is mainly produced by $CD4^+$ T cells, in particular Tfh cells, Th17 cells and NK cells. A wider range of cells express the IL-21 receptor (IL-21R), e.g. T cells, B cells, NK cells, NKT cells, dendritic cells, macrophages, keratinocytes and intestinal fibroblasts, thus IL-21 is involved in the regulation of both innate and adaptive immune responses. IL-21 induces the proliferation of B cells, NK cells and T cells. Most importantly, IL-21, in addition to signals provided by CD40 ligation and IL-4, induces the differentiation of human B cells into plasma cells in the $CD4^+$ T helper cell response (Leonard and Spolski, 2005; Spolski and Leonard, 2009).

To characterize IL-21 production by $CD4^+$ T cells, I optimized an intracellular staining assay for IL-21. I examined the capacity of $CD4^+$ $CD45RO^+$ T cells to produce IL-21, by stimulating them at maximal strength with PMA plus ionomycin (PMA/ION) **(Fig. 6.11ab)**. I then attempted to address IL-21 production by influenza virus-specific $CD4^+$ T cells by stimulating PBMCs with influenza M or NP peptides and reading out the frequency of cells induced to produce IL-21, but the frequency of antigen-specific IL-21 producing cells in the peripheral blood was too low to permit their analysis by this method (not shown). In light of this, PBMCs were stimulated with peptides (M pool and NP pool) and short-term T cell lines were generated. When the T cell lines were restimulated with flu peptides at the end of the culture, the percentage of flu-specific $CD4^+$ T cells was higher, increasing the sensitivity of the assay and allowing the detection of flu-specific IL-21-producing cells (**Fig. 6.11c**). These results showed that, at least after a period of *in vitro* expansion, a proportion of the influenza-specific $CD4^+$ T cells in the peripheral blood are capable of producing IL-21. When looking at production of IL-21 during influenza infection, the level of IL-21 in the plasma of the volunteers during acute influenza infection was hardly detectable by ELISA (not shown).

6.2.5 Analysis of the expression of Tfh markers on peripheral blood $CD4^+$ T cells during acute influenza infection

Given that Tfh cells are important in generating serological responses, it is likely that these $CD4^+$ T cells are involved in the regulation of infection or vaccine-induced Ab responses. Therefore I wanted to look at whether $CD4^+$ T cells expressing Tfh markers were present at

increased frequencies in the circulation during an immune response to influenza infection. Before addressing this question, I looked for their presence during an acute influenza challenge (section 2.2.1.3). Briefly, a total of 17 healthy adult volunteers aged 18-45, who had hemagglutination-inhibition (HI) titres less than 1:8 to A/Brisbane/59/07 (H1N1), were nasally infected with H1N1 virus on day 0 and were quarantined at the study site for 9 days (from day −2 to day 7). Volunteers were considered to be infected if they had seroconverted by day 28. To investigate the expression of Tfh markers on peripheral blood $CD4^+$ T cells during acute influenza infection, the frequency of peripheral blood memory ($CD45RO^+$) $CD4^+$ T cells expressing CXCR5, CD57 or ICOS, or co-expressing CXCR5 and PD-1 was analysed by flow cytometry in the three infected volunteers **(Fig. 6.12)**. H1N1- specific IgG antigen secreting cells (ASC) in these subjects were measured by an *ex vivo* B cell ELIspot assay, as described (Clutterbuck et al., 2008) (conducted by Dr. A. Huang). The frequency of $CXCR5^+$ memory $CD4^+$ T cells (**Fig. 6.12a**), $CD57^+$ memory $CD4^+$ T cells **(Fig. 6.12b)** and the proportion of CD4 memory cells co-expressing PD-1 and CXCR5 **(Fig. 6.12d)** remained unchanged during the course of infection. The frequency of ICOS-expressing memory $CD4^+$ T cells and that of $ICOS^+$ $CXCR5^+$ $CD4^+$ T cells appeared to increase in the three infected volunteers on day 7 post infection **(Fig. 6.12c and e)**, and the higher the frequency of this population of cells, the higher the frequency of H1N1-specific ASC that was found in the same volunteer **(Fig. 6.12f)**. The frequency of flu-specific IFN-γ producing $CD4^+$ T cells was found not to correlate with the frequency of ASC (Chapter 5). These results suggest that the increase in $ICOS^+CXCR5^+$ $CD4^+$ T cells in the circulation provides a correlate of the magnitude of the influenza-specific Tfh response. Although the observations made here do not show that these cells are Tfh cells, and they may simply be activated $CD4^+$ T cells, it could be that during the infection the extent of total $CD4^+$ T cell activation is related to the magnitude of the GC reaction in lymph nodes, providing an indirect measure of the latter.

6.2.6 Relationship between circulating memory $CXCR5^+$ $CD4^+$ T cells and antibody responses after immunization with inactivated influenza vaccine

There is limited information on the role of $CXCR5^+$ $CD4^+$ Tfh cells in the response to vaccination. My epitope mapping studies suggested that there is induction of a $CD4^+$ T cell response post vaccination (Chapter 5). I next sought to characterize the peripheral $CXCR5^+$ $CD4^+$ T cell recall

response induced by trivalent inactivated vaccine in my cohorts (detailed in Chapter 5) and to examine whether this may serve as a useful biomarker to examine vaccination strategies.

Volunteers were immunized with unadjuvanted, inactivated, split-virus influenza vaccine [immunogenicity was detailed in Chapter 5 and (Wu et al., 2010)]. The first group (Group A) received one dose of pandemic H1N1 vaccine at baseline, and the second group (Group B) received one dose of seasonal vaccine at baseline then one dose of pandemic H1N1 vaccine on day 21. Frozen PBMCs were thawed and analysed by multiparameter flow cytometry on day 0 (baseline; pre-vaccination), 7, 14 and 21. I analysed the frequency of $CD4^+$ cells expressing $CXCR5^+$ and $CD45RO^+$ and assessed the proportion of these cells expressing ICOS. Serum antibody titers were measured by microneutralization assays (MN) on day 42 after immunization, and H1N1- or H3N2- specific IgG ASCs were measured by B cell ELIspot (both conducted by Dr. A. Huang). ICOS expression on $CD4^+$ $CXCR5^+$ $CD45RO^+$ cells remained low or negative throughout the study (not shown). No significant difference was observed in the frequency of $CXCR5^+CD45RO^+$ cells within the $CD4^+$ T cell population at pre- and post vaccination timepoints **(Fig. 6.13a)**. A positive correlation was observed between the percentage of $CXCR5^+CD45RO^+$ $CD4^+$ T cells on day 7 and serum antibody titres at the trial endpoint (day 42) as determined by MN, and with the frequency of pandemic H1N1-specific IgG ASC on day 7 in group A vaccinees **(Fig. 6.13b)**, but not in group B vaccinees (not shown). It is unclear why no relationship was observed between the serological responses on day 42 and percentage of $CXCR5^+$ memory $CD4^+$ T cells on day 7 in these subjects, apart from an extra vaccination was given to the group B vaccinees on day 21; further investigation is required to confirm the observation in group A and to better understand the precise relationship between circulating $CXCR5^+$ $CD4^+$ T cells and antibody response.

6.2.7 Influenza-specific cells from peripheral blood are able to help memory but not naive B cells

The circulating $CXCR5^+$ $CD4^+$ T cell population contained antigen-specific memory cells, and also contained cells capable of providing help to naïve B cells. In the final set of experiments in this chapter, I wanted to directly investigate the capacity of antigen-specific $CD4^+$ T cells to provide help for B cells. Initially, I used the T-B coculture method employed in **Fig. 6.5**, but instead of using the superantigen SEB, flu peptides or activated influenza virus (H1N1 and

H3N2) were added to the T-B co-cultures. However, no production of Ig was detected (not shown). This could have been because no cognate interaction occurred between T cells and B cells when these antigens were used, or because the frequency of influenza-specific cells in the memory $CXCR5^+$ cell population was too low to provide help for B cell activation.

Further experiments were then carried out using influenza-specific $CD4^+$ T cells rather than total $CXCR5^+$ memory $CD4^+$ T cells. To enable the isolation of rare, flu specific memory cells that are not necessarily cytokine producing, I made use of CD154 to isolate antigen-specific T cells. CD154 is an activation marker that is transiently expressed on activated $CD4^+$ T cells and to a lesser extent on activated $CD8^+$ cells after antigen exposure, thus enabling the identification of $CD4^+$ T cells responding to an antigenic stimulus (Chattopadhyay et al., 2006; Cohen et al., 2005; van Kooten and Banchereau, 2000). In contrast to other activation markers such as CD25, CD69 and CD71, which can be induced by TCR-independent stimuli and are also expressed by certain T cell subsets without any stimulation, CD154 expression is highly specific to short-term antigen-activated T cells (Chattopadhyay et al., 2005; Frentsch et al., 2005; Frentsch et al., 2004).

After T cell stimulation, CD154 is rapidly removed from the cell surface by internalization or proteolytic shedding following interaction with its receptor CD40 on APC (Graf et al., 1995; Henn et al., 2001; Yellin et al., 1994). Therefore to detect surface expression of CD154 in a live cell assay, blocking of CD154/CD40 interaction by anti-CD40 antibodies is required for stably visualizing $CD154^+$ cells for sorting and subsequent analysis **(Fig. 6.14a)**. The sorted $CD154^+$ cells remained fully functional, as they could be expanded and responded to antigen restimulation **(Fig. 6.14b)**. Therefore this isolation strategy, which was based on activation-dependent expression of CD154, enabled enrichment and expansion of $CD4^+$ cells specific for flu antigens within a short time period, regardless of the precursor frequency in the peripheral blood.

The T cell lines expanded from a healthy donor contained a high population of cells that were specific for flu peptides **(Fig. 6.14b)**. Although flu-specific T cell frequencies in the peripheral blood were barely detectable when cells from this donor were stimulated with flu peptides and flu-specific cells read out by IFN-γ staining, the generation of T cell lines with a high frequency of antigen-specific cells was achieved by addition of IL-7 and IL-15. These cytokines reduce activation induced cell death of antigen-specific T cells, and thus increase the frequency of responding cells.

Fresh PBMCs from two healthy donors were stimulated with flu peptide pools (M or NP), and $CD154^+$ cells were sorted and expanded in vitro with IL-7 and IL-15 for 21 days. The short-term cell lines generated were then restimulated again with flu peptides, and $CD154^+$ cells were sorted to co-culture with either autologous naïve B cells or memory B cells (isolated as shown in **Fig. 6.15a**). T cells were added at a 1:2 ratio with B cells in the presence of 1 μg/ml SEB. Supernatants from cultures were collected on day 0, 3, 7 and 10. Ig production was measured by ELISA. The results showed that $CD154^+$ flu- specific $CD4^+$ T cells could help both naïve and memory B cells to produce IgM, but supported class switching to IgG and IgA in memory B cells only (**Fig. 6.15b**). The total blood $CXCR5^+$ memory CD4 cells used in the experiments in **Fig. 6.5** were able to support naïve B cell differentiation into plasmablasts that made IgM and also support class-switching to IgA and IgG. However, when influenza-specific CD4 cells were used instead, they only supported IgA and IgG production by memory B cells but not naïve B cells. This may reflect the presence of a lower frequency of Tfh cells in the flu-specific $CD4^+$ T cell populations used here than in the total peripheral blood $CXCR5^+$ memory $CD4^+$ T cell population used in the experiments in **Fig. 6.5**, and/or differences in the functional properties of the two $CD4^+$ T cell populations.

6.3 Discussion

Tfh cells promote long-lived antibody responses in GCs. Recently some reports have shown that the circulating CXCR5$^+$ CD4$^+$ T cell population contains cells that may be memory Tfh cells, providing a potential surrogate strategy to assess the quality of Tfh responses in humans (Chevalier et al., 2011; Morita et al., 2011; Simpson et al., 2010). Circulating CXCR5$^+$ CD4$^+$ T cells are reported to be resting and migrate weakly to chemokines (Schaerli et al., 2000), thus may represent a subset of memory T cells that have left secondary lymphoid tissues before clonal expansion. They require activation in order to provide help to B cells via cognate interaction.

In line with published data, I found that blood CXCR5$^+$CD4$^+$ T cells did not exhibit a phenotype typical of Tfh cells (expressing high levels of ICOS, PD-1 or CD57) *ex vivo*, and were unable to upregulate these markers to high levels upon *in vitro* stimulation with PMA/ION or anti-CD3/CD28. However, I confirmed the published reports (Chevalier et al., 2011; Morita et al., 2011) that blood CXCR5$^+$ CD4$^+$ T cells efficiently support the production of Igs during co-culture with B cells, in contrast to CXCR5$^-$ CD4$^+$ T cells, therefore sharing similar functional properties with their tonsillar counterparts. Given the predominant role of CXCR5-expressing memory T cells in Ab-mediated responses, several recent studies have used CXCR5$^+$ CD4$^+$ cells as a biomarker to examine and monitor treatment of certain autoimmune or chronic infections (Feng et al., 2011). In light of this, I examined the kinetics of CXCR5$^+$ CD4$^+$ T cells during an acute influenza infection and after vaccination. I found that the frequency of CXCR5$^+$ CD4$^+$ T cells did not increase during the course of infection or vaccination, although the proportion of CXCR5$^+$ ICOS$^+$ CD4$^+$ T cells increased after infection, peaking on day 7 post infection. ICOS is an activation marker expressed by activated T cells, and I have shown that T cells are highly activated on day 7 post infection (Chapter 3), so this increase in CXCR5$^+$ ICOS$^+$ CD4$^+$ T cells may well reflect CD4$^+$ T cell activation rather than the presence of Tfh cells in the circulation. However infected individuals with a high frequency of CXCR5$^+$ ICOS$^+$ CD4$^+$ T cells also had a high frequency of influenza-specific antibody-producing cells, and I also found a positive correlation between the frequency of CXCR5$^+$ memory CD4$^+$ T cells in the circulation and serum neutralizing H1N1 antibody titres or the frequency of flu-specific IgG ASC in vaccine recipients. This suggests that these recently activated memory cells may be relevant for the humoral response.

Although the extent of $CD4^+$ T cell activation after influenza virus infection or vaccination may give some insights into the magnitude of the concurrent humoral response, it would be preferable to have more specific readouts for evaluating antigen-specific Tfh responses. IL-21 is a key effector cytokine produced by Tfh cells (Spolski and Leonard, 2009). I thus tried to address IL-21 production by flu-specific $CD4^+$ T cells. Intracellular staining for IL-21 showed that PBMCs from individuals who have memory response to flu barely expressed any IL-21 when stimulated with flu peptide pools. Stimulation of PBMCs from healthy individuals with PMA/Ionomycin resulted in some IL-21 production by $CD4^+$ T cells, but IL-21 responses were much lower than those observed in patients chronically infected with HIV (personal communication from Dr. Andrea Stacey). In line with this, studies in LCMV infected mice have shown that Tfh responses do develop during acute LCMV infection (Eto et al., 2011), but $CD4^+$ T cell differentiation is progressively redirected towards Tfh cells during virus persistence via an IL-6- dependent mechanism (Fahey et al., 2011; Harker et al., 2011). The relatively low frequency of IL-21-producing $CD4^+$ T cells generated during acute virus infections compared to chronic infections could reflect a greater requirement for IL-21 in the maintenance of immune responses during chronic infection (Elsaesser et al., 2009; Frohlich et al., 2009). As IL-21 production is regulated by the balance between IL-2 and IL-6, IL-21 producing $CD4^+$ T cells may develop preferentially in chronic infection, where elevated IL-6 production and impaired IL-2 production are observed, (Ciuffreda et al., 2008; Falasca et al., 2006; Nixon and Landay, 2010).

I also used other functional assays to address whether there are antigen-specific Tfh cells in peripheral blood, and whether they support B cell differentiation into Ab-producing cells. I showed that flu-specific T cells were present in both the $CXCR5^+$ and $CXCR5^-$ $CD4^+$ T cell subsets. However, attempts to induce Ab production in T-B co-cultures using flu antigens as a stimulus instead of SEB failed to induce antibody production, which could due either to the frequency of antigen-specific cells in the peripheral blood being too low to initiate a response, or the system not having been optimized to provide the right co-stimulatory stimuli to enable cognate interaction between the T and B cells. Therefore, an expansion method was used (Frentsch et al., 2005) to first isolate antigen-specific cells from the blood and then increase their frequency by culturing with cytokines. The expanded flu-specific cells were capable of helping both naïve and memory B cells to produce IgM, but only helped memory B cells to class switch to IgG and IgA. Failure of these antigen-specific cells to cause naïve B cells to undergo class

switching could be due to their inadequate expression of molecules such as ICOS which are essential for providing help. Had time permitted it would have been interesting to address how expression of such co-stimulatory molecules alters during the course of culture. Also, this could be related to the particular culture conditions I used, which may have selectively maintained memory $CD4^+$ T cells polarized to a particular effector phenotype. It has been reported that within the $CXCR5^+$ $CD4^+$ T cell population, the capacity of differently-polarized cell subsets to induce naïve B cells to differentiate into Ig-producing cells is different. Th1 $CXCR5^+$ cells were unable to induce Ab production by both naïve and memory B cells, while Th2 and Th17 $CXCR5^+$ induced differentiation of naïve B cells into ASCs, but differentially promoted class-switching (Morita et al., 2011).

The origins of human blood $CXCR5^+$ $CD4^+$ T cells are currently unclear: they may originate from cells that migrate out of GCs or from Tfh-committed extrafollicular helper cells. Based on the data from patients with ICOS deficiency, whose GC responses are severely reduced (Warnatz et al., 2006) and in whom blood $CXCR5^+$ $CD4^+$ T cells are absent (Bossaller et al., 2006), it seems that blood $CXCR5^+$ $CD4^+$ T cells are probably memory Tfh that have passed through a GC reaction. As I showed that antigen-specific cells in the peripheral blood are capable of helping memory B cells in the presence of SEB, it implies that there exist memory $CD4^+$ T cells in the blood that are capable of Tfh function. However how these cells are related to $CXCR5^+$ $CD4^+$ T cells requires further investigation. Future work will need to be carried out to measure the functional capacity of $CXCR5^+$ $CD4^+$ T cells that are antigen-specific. This could be done by setting up quantitative assays to measure the helper functions of antigen-specific T cells, with stimuli that mimic T-B cell interactions.

To conclude, I have shown in this chapter that blood $CXCR5^+$ cells represent a population of memory $CD4^+$ cells with helper functions. In addition, I demonstrated that antigen-specific Tfh cells could be found in the peripheral blood of healthy volunteers who have memory T cell responses to influenza. Influenza-specific T cells were isolated from these donors and expanded into cell lines, and these cells were able to support antibody production of autologous memory B cells. I also found that markers of $CD4^+$ T cell activation are associated with the magnitude of the humoral response induced during acute influenza infection and after vaccination. These results suggest that evaluation of the induction of flu-specific Tfh may provide a useful readout

for analysis of vaccine efficacy, and indicate that it may be possible to develop PBMC-based assays that enable quantification of antigen-specific $CD4^+$ Tfh responses in the future.

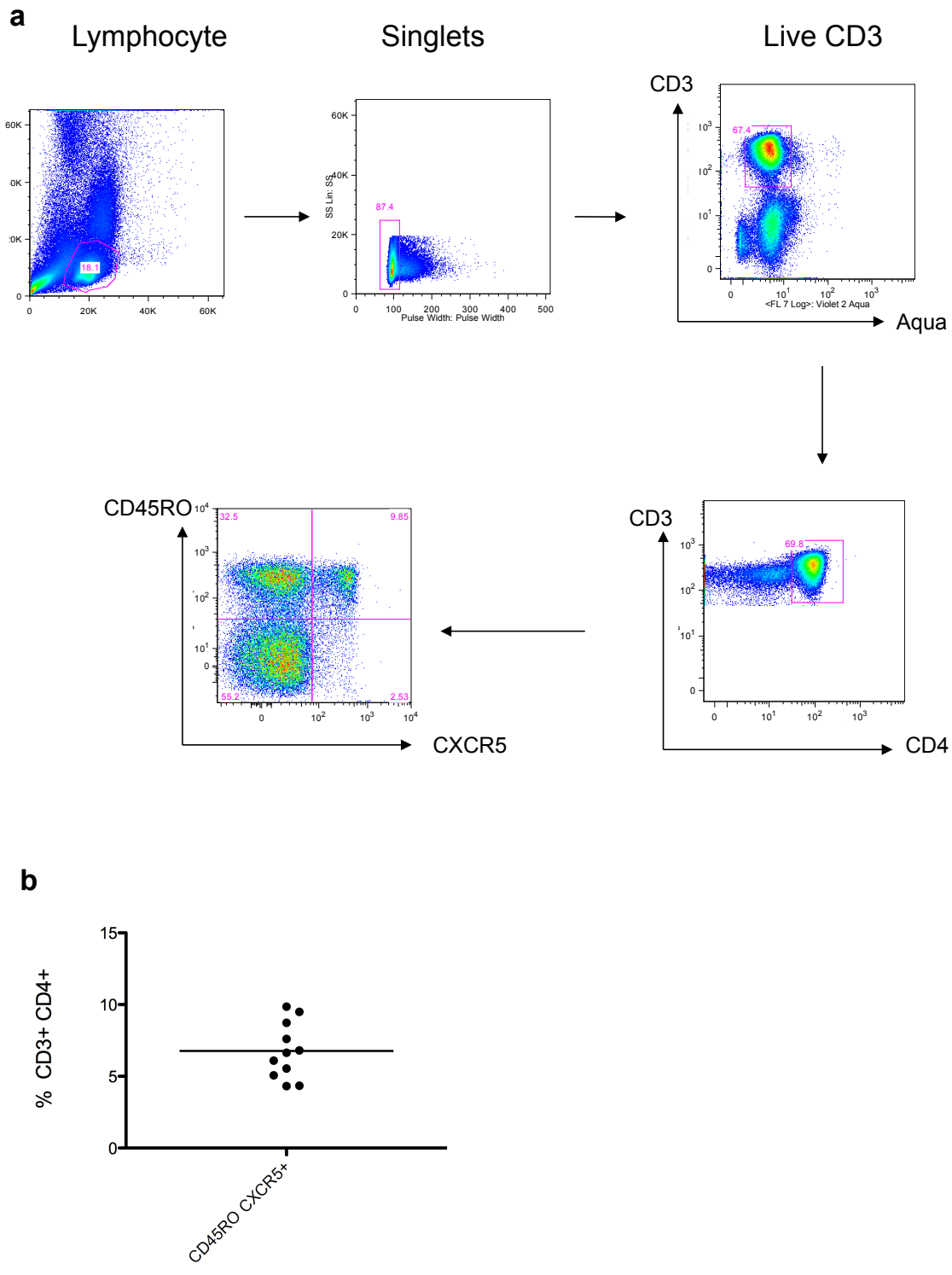

Figure 6.1 Expression of CXCR5 by circulating CD4⁺ T cells from blood. (a) Gating strategy showing CXCR5 expression by blood CD4⁺ T cells. **(b)** Frequency of memory CXCR5⁺ cells in the blood. Small horizontal bars indicate mean.

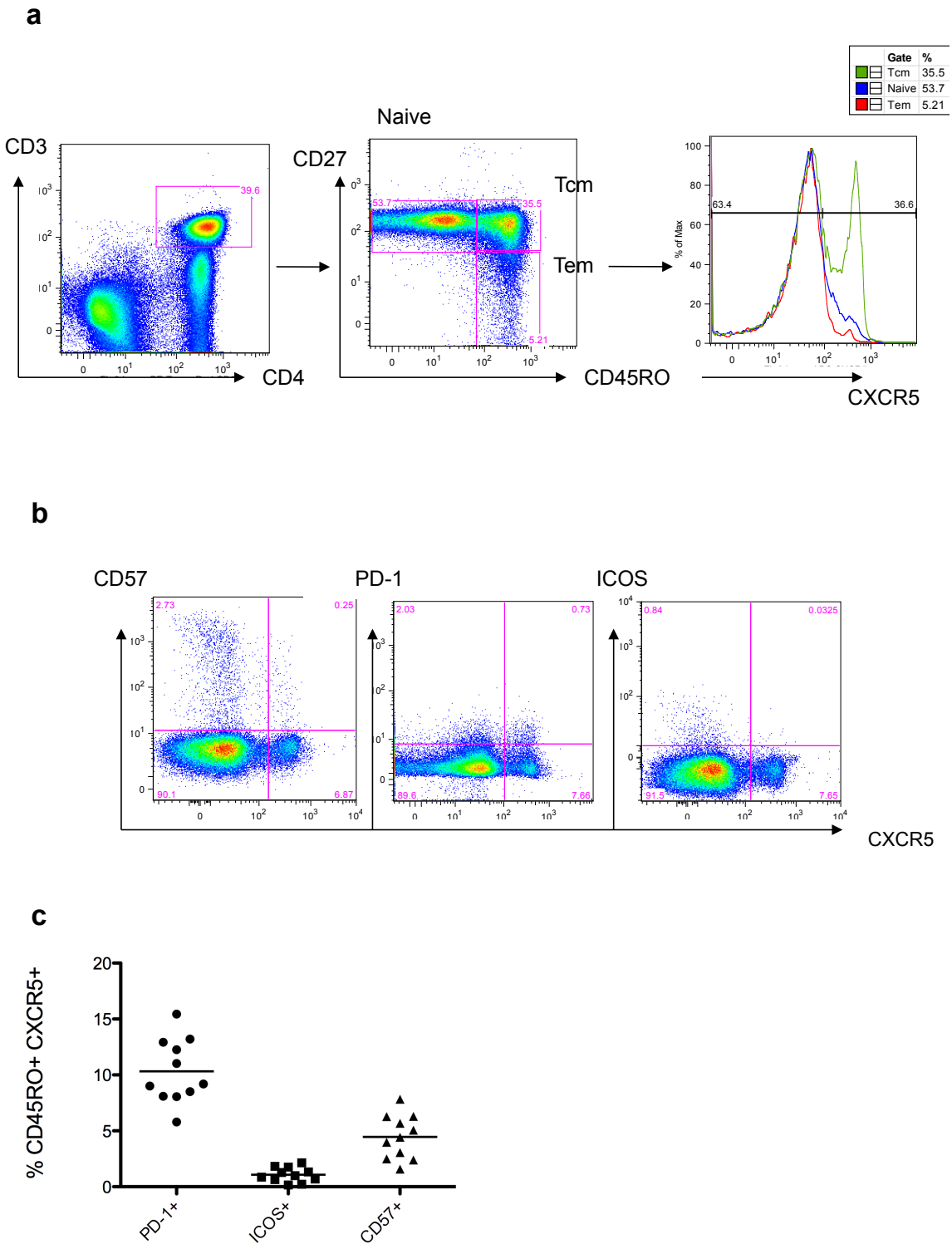

Figure 6.2 Expression of various Tfh markers by circulating CXCR5$^+$ CD4$^+$ T cells. **(a)** Representative example showing that CXCR5 expressing CD4$^+$ T cells are within the central memory (CD45RO$^+$CD27$^+$) subset in the peripheral blood. **(b)** CD57, PD-1 and ICOS expression according to the expression of CXCR5 on CD4$^+$ cells. **(c)** Frequency of blood memory CXCR5$^+$ cells expressing PD-1, ICOS and CD57 respectively. Small horizontal bars indicate mean.

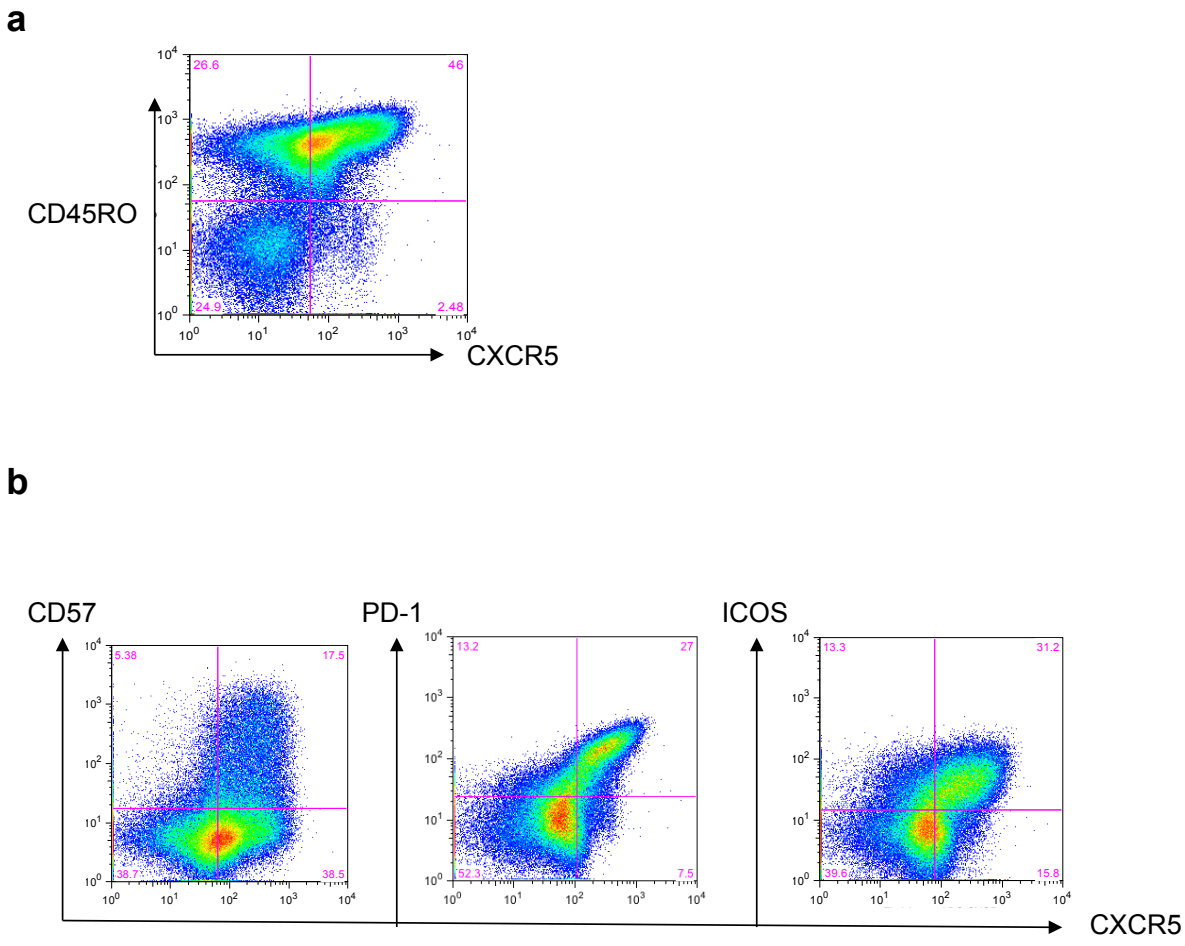

Figure 6.3 Expression of various Tfh markers by CXCR5⁺ cells from tonsil. **(a)** Representative example showing CXCR5 expression on memory CD4⁺ T cells from tonsils. **(b)** CD57, PD-1 and ICOS expression according to the expression of CXCR5 on tonsillar CD4⁺ cells.

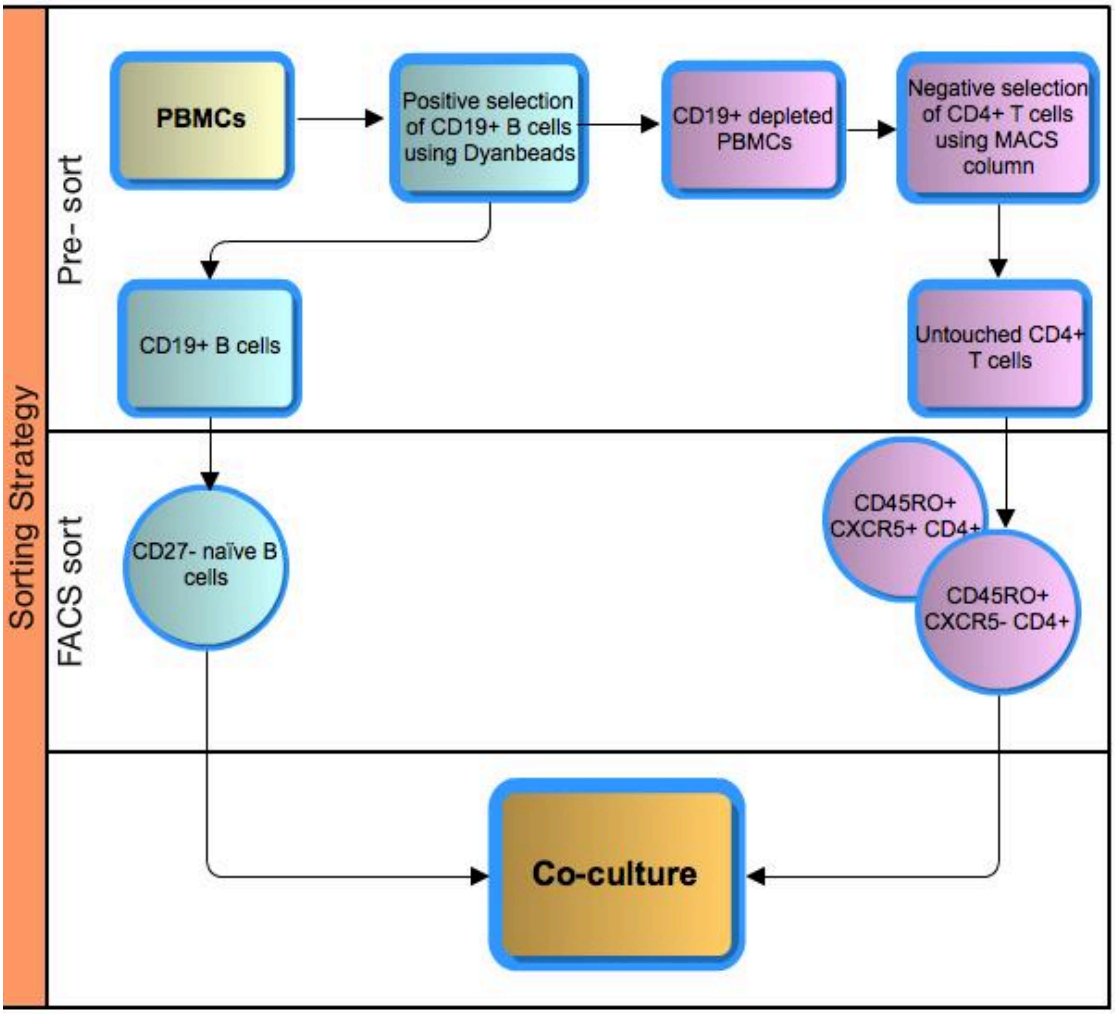

Figure 6.4 Strategy used for isolation of CXCR5^{+} and CXCR5^{-} memory CD4^{+} T cells and autologous naïve B cells for use in Tfh assays.

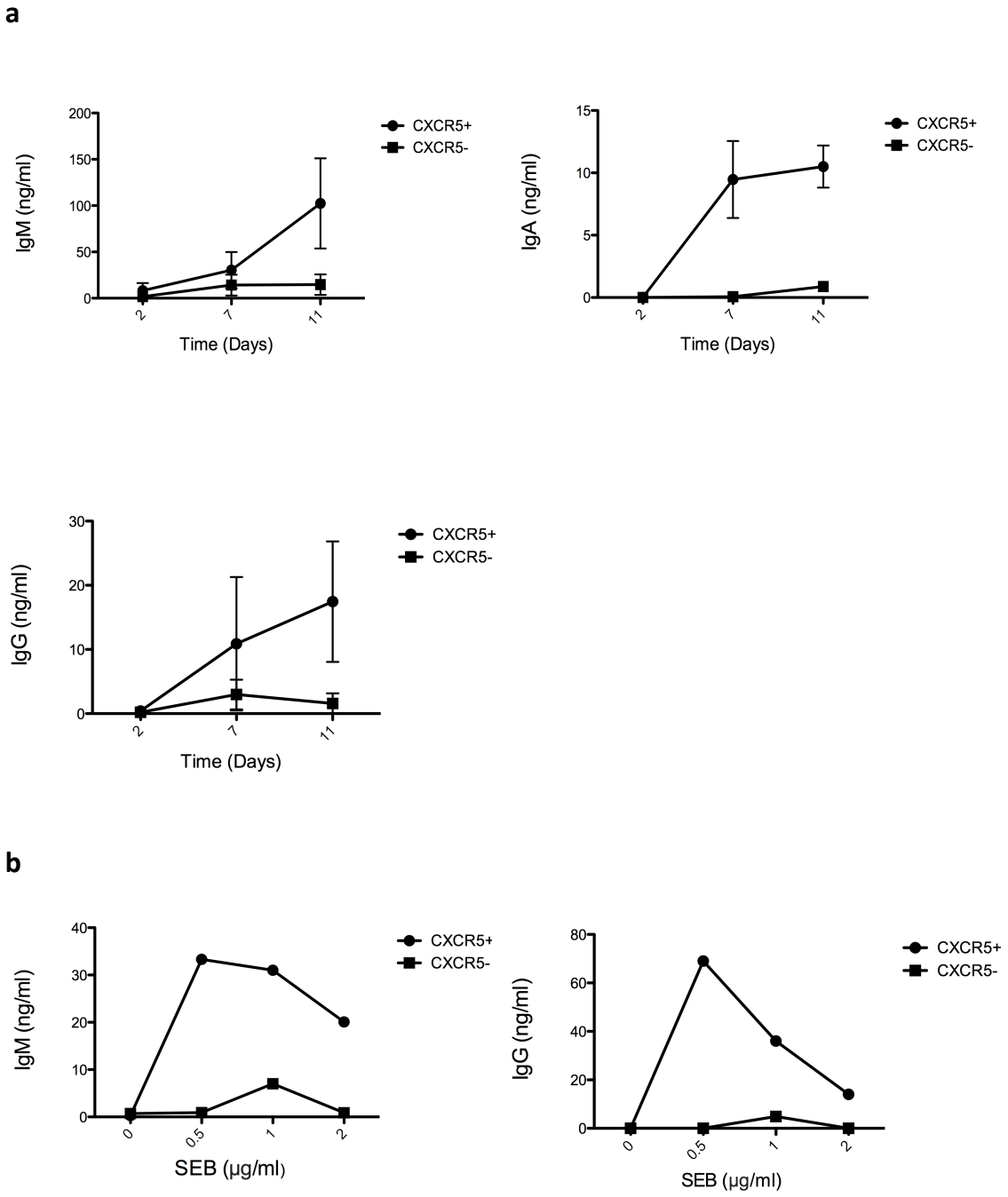

Figure 6.5 Blood CXCR5$^+$CD4$^+$ T cells induce naïve B cells to differentiate into antibody-producing plasma cells. Memory CXCR5$^+$ and CXCR5$^-$ cells were FACS-sorted from CD4$^+$ T cells enriched by negative selection. Autologous naïve B cells (CD3$^-$CD19$^+$CD27$^-$) were sorted and co-cultured with either population at 3x10^4 cells each in the presence of 1 μg/ml SEB. Ig concentration was measured in culture supernatants by ELISA. **(a)** Ig concentrations at different time points in cultures of CXCR5$^+$ or CXCR5$^-$ CD4$^+$ T cells with naïve B cells. (n=5; error bars show s.d.) **(b)** CXCR5$^+$ or CXCR5$^-$ CD4$^+$ T cells were cocultured with titrated doses of SEB of representative donor. Ig concentration measured at day 15 (n=1).

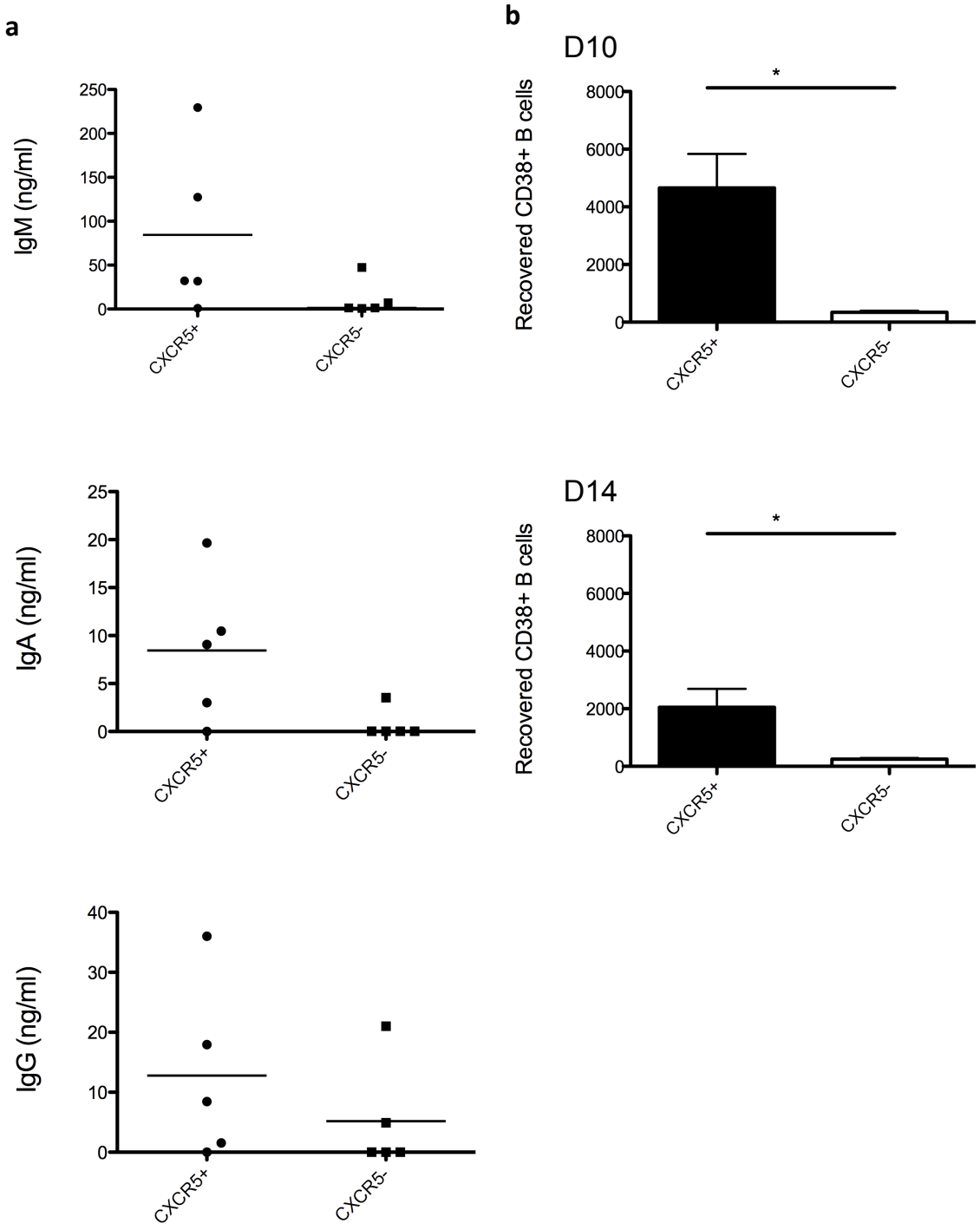

Figure 6.6 Blood CXCR5$^+$CD4$^+$ T cells induce naïve B cells to differentiate into antibody-producing plasma cells. (a) Antibody production from CXCR5$^+$ or CXCR5$^-$ CD4$^+$ T cells cocultured with naïve B cells (n=5). Ig concentration measured at day 15. Small horizontal bars indicate mean. **(b)** Viable CD38$^+$ B cells on day 10 and day 14 of culture respectively (n=5). Bars depict mean and s.d.. Differences were analysed using a paired t-test (*p< 0.05).

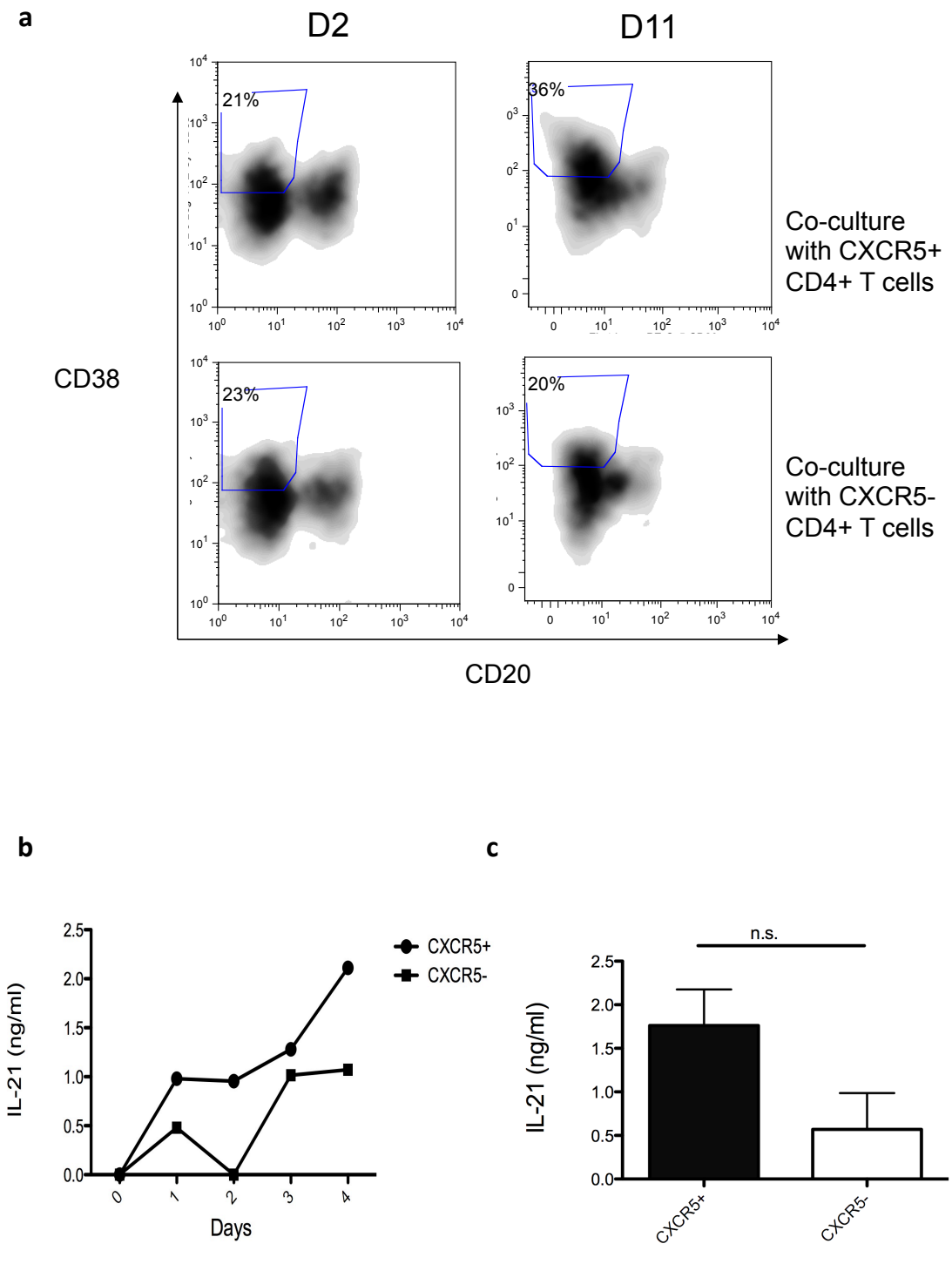

Figure 6.7 Blood CXCR5$^+$CD4$^+$ T cells induce naïve B cells to differentiate into plasmabasts. (a) CD38^{hi} CD20$^-$ plasmablasts (gated on CD3$^-$CD4$^-$ cells) in a coculture of blood CXCR5$^+$ and CXCR5$^-$ cells with naïve B cells on day 2 and 11 in the presence of SEB. **(b)** IL-21 concentrations at different time points in cocultures of CXCR5$^+$ or CXCR5$^-$ CD4$^+$ T cells with naïve B cells. **(c)** Blood CXCR5$^+$CD4$^+$ T cells produce more IL-21 when co-cultured with naïve B cells and SEB. Production of IL-21 by memory CXCR5$^+$ and CXCR5$^-$ cells co-cultured with naïve B cells in the presence of 1 μg/ml SEB. IL-21 concentration was measured in culture supernatants by ELISA on day 3 (n=3, bars show mean and s.d.). Differences were analysed using a paired t-test.

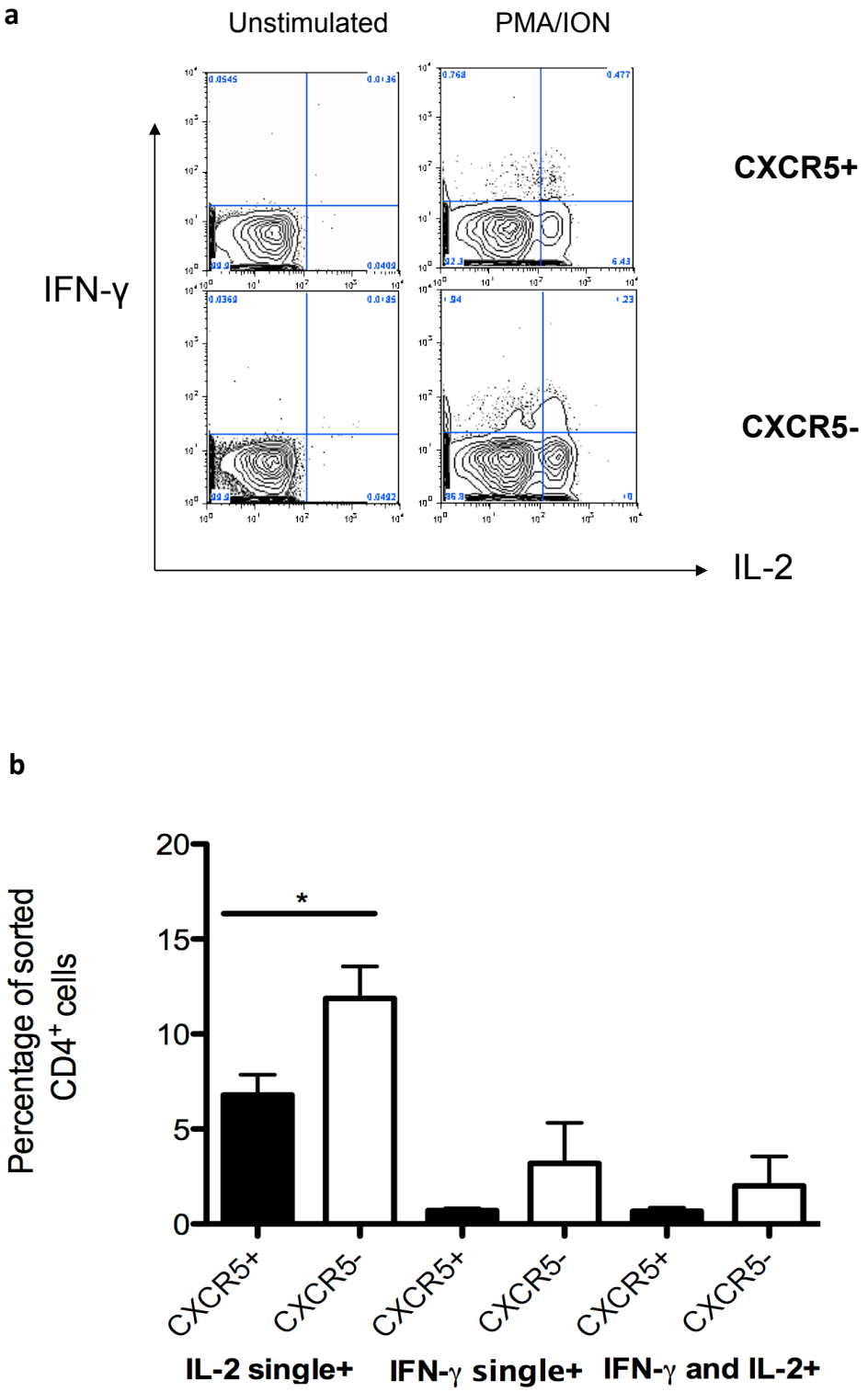

Figure 6.8 Cytokine response of CXCR5$^+$ and CXCR5$^-$ memory CD4$^+$ T cell populations to activating stimuli. (a) Expression of cytokines. PBMCs were stimulated with PMA and ION in the presence of monensin and Brefeldin A for 6 hours, and intracellular staining for IFN-γ and IL-2 was analysed. Representative data from one of three independent experiments. **(b)** Percentage of CD4$^+$CXCR5$^+$ or CXCR5$^-$ cells that produced either one or both of the cytokines (n=3, bars show mean and s.d.). Differences were analysed by an one-way ANOVA Bonferonni multiple comparison test (*p< 0.05).

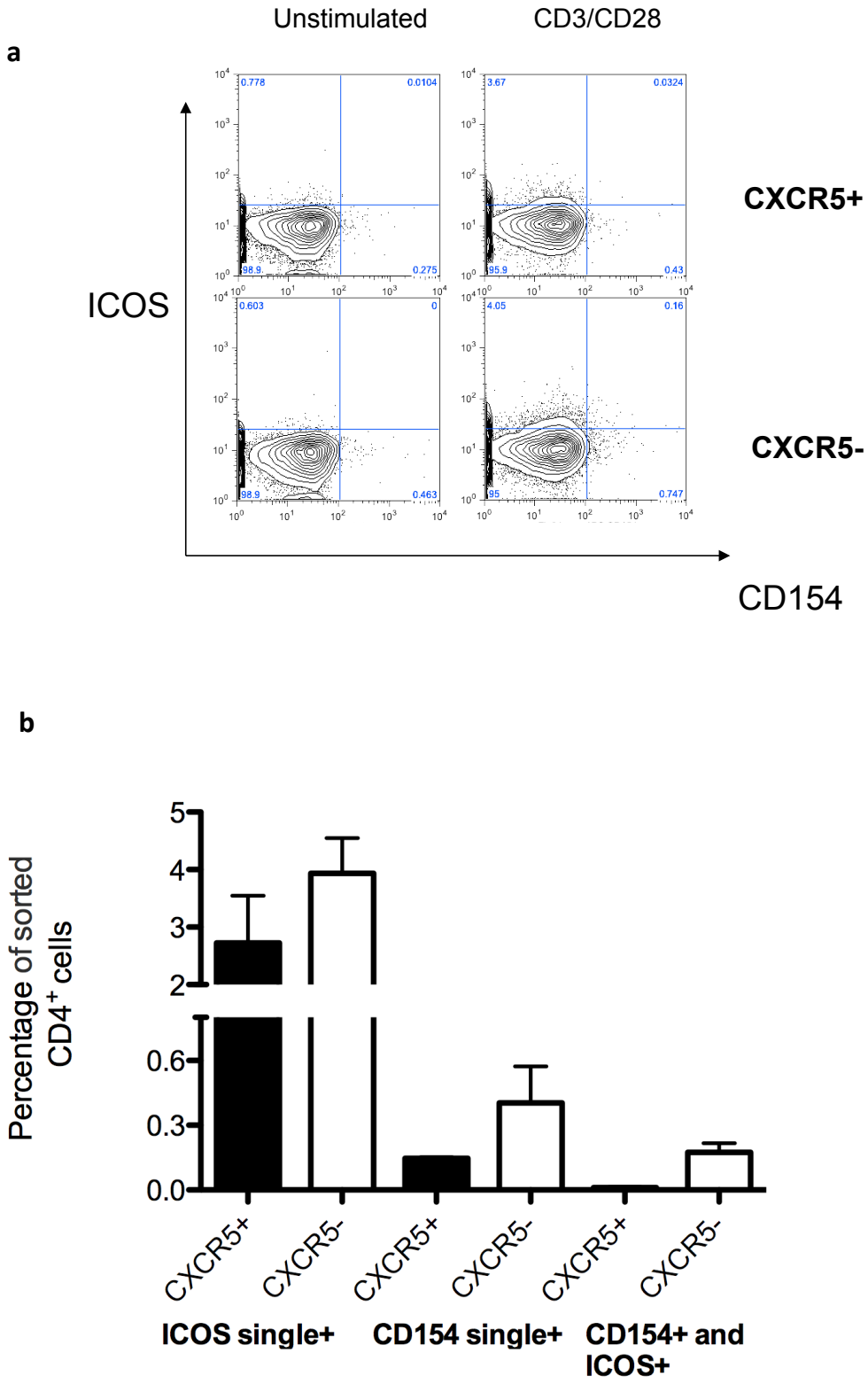

Figure 6.9 Response of CXCR5$^+$ and CXCR5$^-$ memory CD4$^+$ T cell populations to activating stimuli. **(a)** Expression of CD154 and ICOS. PBMCs were stimulated with plate-bound CD3 and soluble anti-CD28 for 48hours. Surface expression of CD154 and ICOS was analysed. Representative data from one of three independent experiments. **(b)** Expression of co-stimulatory molecules and cytokines by CXCR5$^+$ and CXCR5$^-$ cells after stimulation (n=3, bars showed mean and s.d.). Differences were analysed by an one-way ANOVA Bonferonni multiple comparison test.

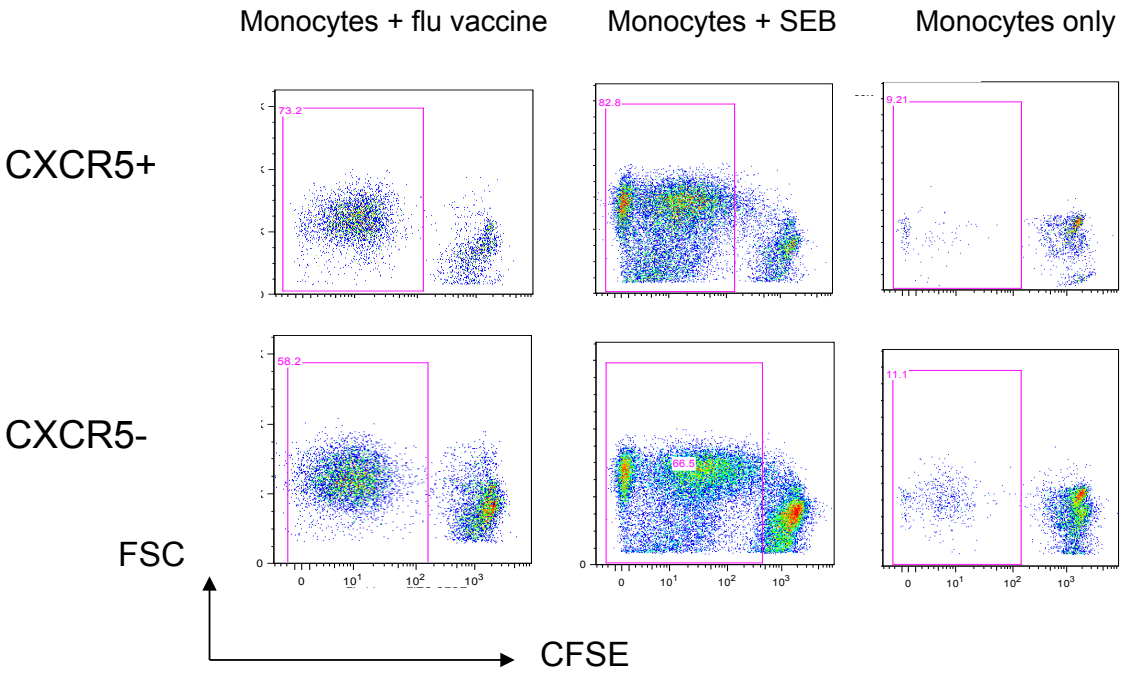

Figure 6.10 Proliferation of CXCR5$^+$ and CXCR5$^-$ memory CD4$^+$ T cell populations in response to monocytes pulsed with inactivated flu vaccine. CFSE-labeled blood CXCR5$^+$ and CXCR5$^-$ cells were cultured with autologous monocytes incubated with inactivated flu vaccine antigens. Cell proliferation was analysed on day 5. Representative data from one of the two independent experiments.

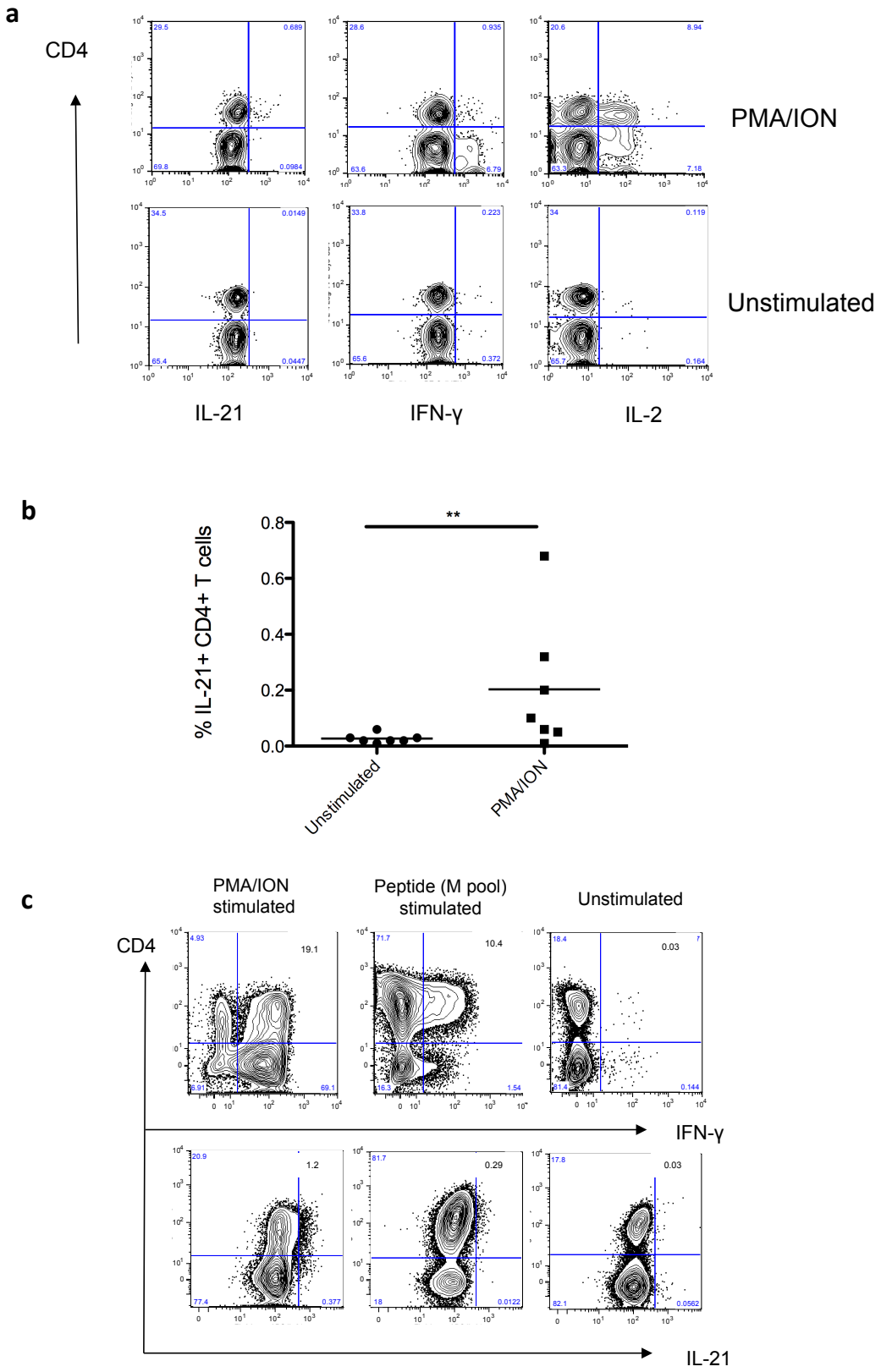

Figure 6.11 Use of intracellular staining to assess IL-21 production by CD4⁺ T cells. (a) Intracellular staining for IL-21, IFN-γ and IL-2 of PMA/ION-stimulated PBMCs. **(b)** Percentage of CD4⁺ T cells producing IL-21 in response to PMA/ION stimulation in different donors (n=7). Small horizontal bars indicate mean. Differences were analysed using a paired t-test (**p< 0.01). **(c)** Intracellular staining for IL-21 and IFN-γ of peptide-stimulated and PMA/ION-stimulated T cell lines (Representative data from four experiments).

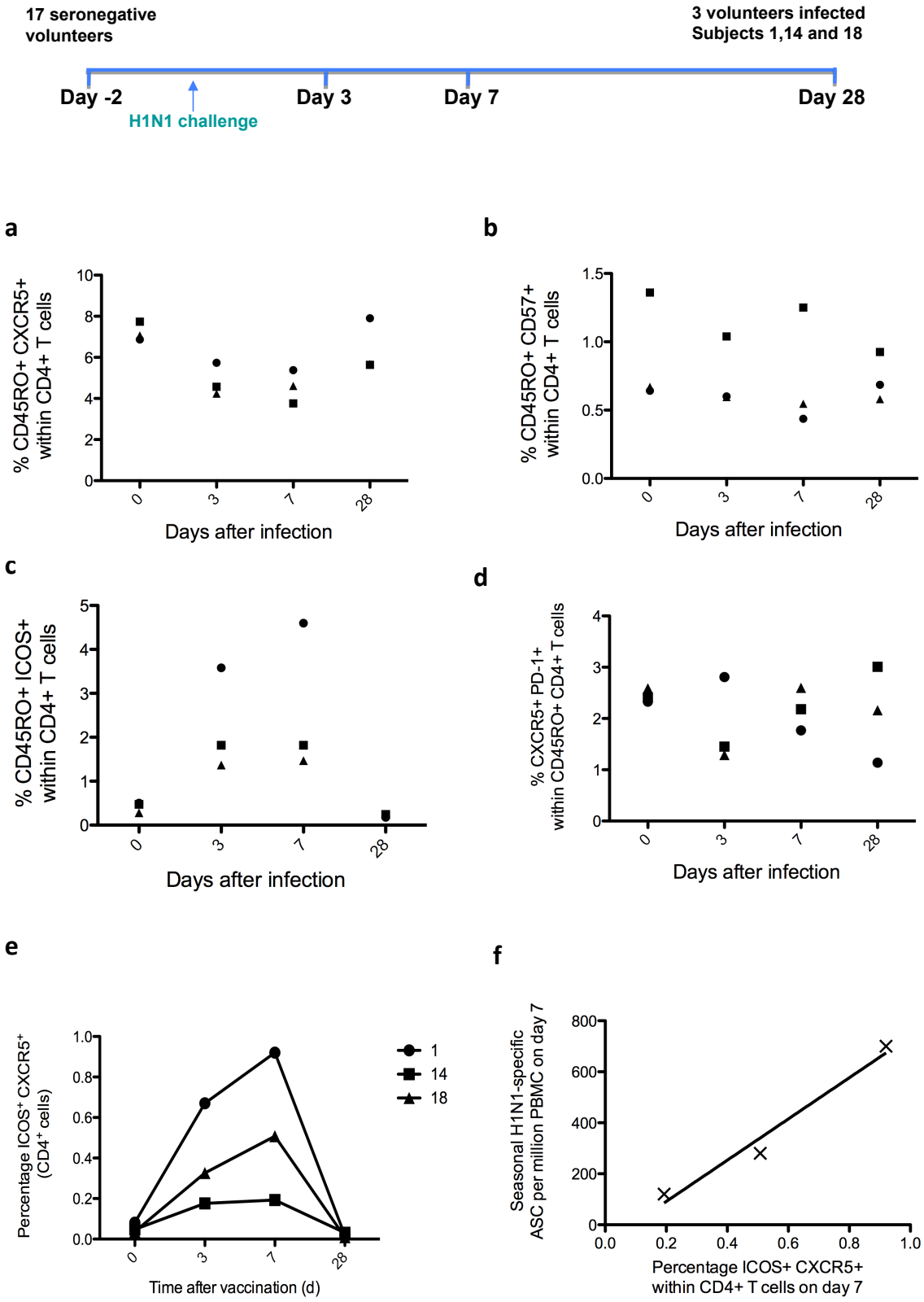

Figure 6.12 Expression of various Tfh markers on CD4⁺ T cells in the peripheral blood at different timepoints after a live influenza challenge. Percentage of **(a)** CXCR5⁺, **(b)** CD57⁺ and **(c)** ICOS⁺ cells memory (CD45RO⁺) cells within the CD4⁺ population of the three infected individuals (subjects 1, 14 and 18) as analysed by flow cytometry. **(d)** Percentage of memory CD4⁺ T cells co-expressing both CXCR5 and PD-1. **(e)** Percentage of ICOS⁺ CXCR5⁺ cells within the CD4⁺ population in the three subjects and **(f)** their relationship with antibody-secreting cells on day 7 as determined by B cell ELISpot.

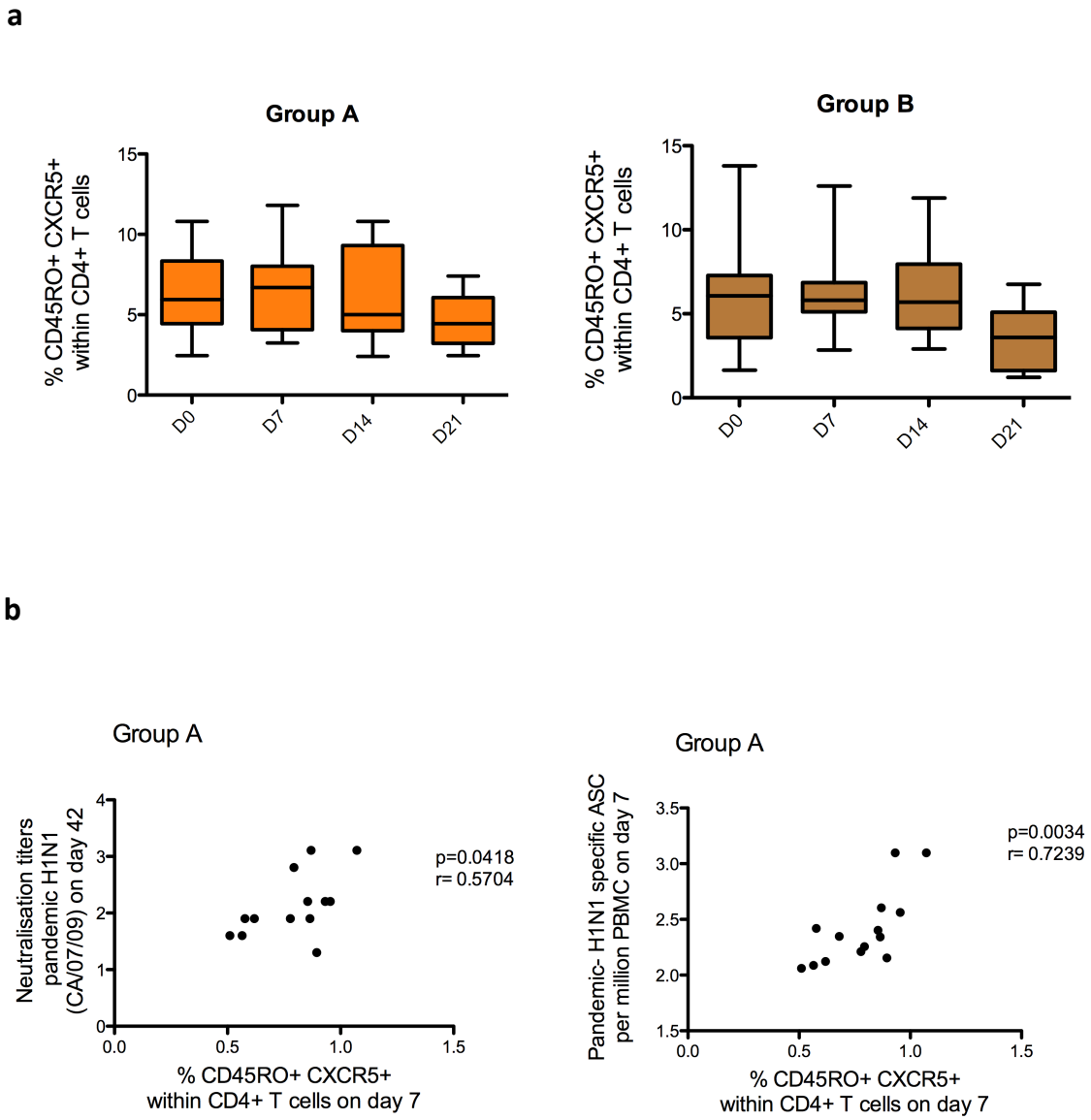

Figure 6.13 Frequency of memory CXCR5$^+$ CD4$^+$ T cells after influenza vaccination. (a) Volunteers from Group A (n=16) received pandemic vaccine only on day 0, while Group B (n=12) received seasonal vaccine on day 0, then pandemic vaccine on day 21. Percentage of CXCR5$^+$ memory (CD45RO$^+$) cells within the CD4$^+$ population was analysed by flow cytometry. In the box-and-whisker plots the horizontal line represents the median, the boundaries of the box represent the upper and lower quartiles, the whiskers represent min to max. **(b)** Relationship between CXCR5$^+$ memory cells within the CD4$^+$ population and antibody response was analysed in Group A where volunteers were vaccinated with one vaccine only. Following log transformation of pandemic H1N1-specific ASCs on day 7, microneutralization titers at the trial endpoint (day 42), and the frequency of CXCR5$^+$ memory cells within the CD4$^+$ population, a Spearman correlation analysis was performed.

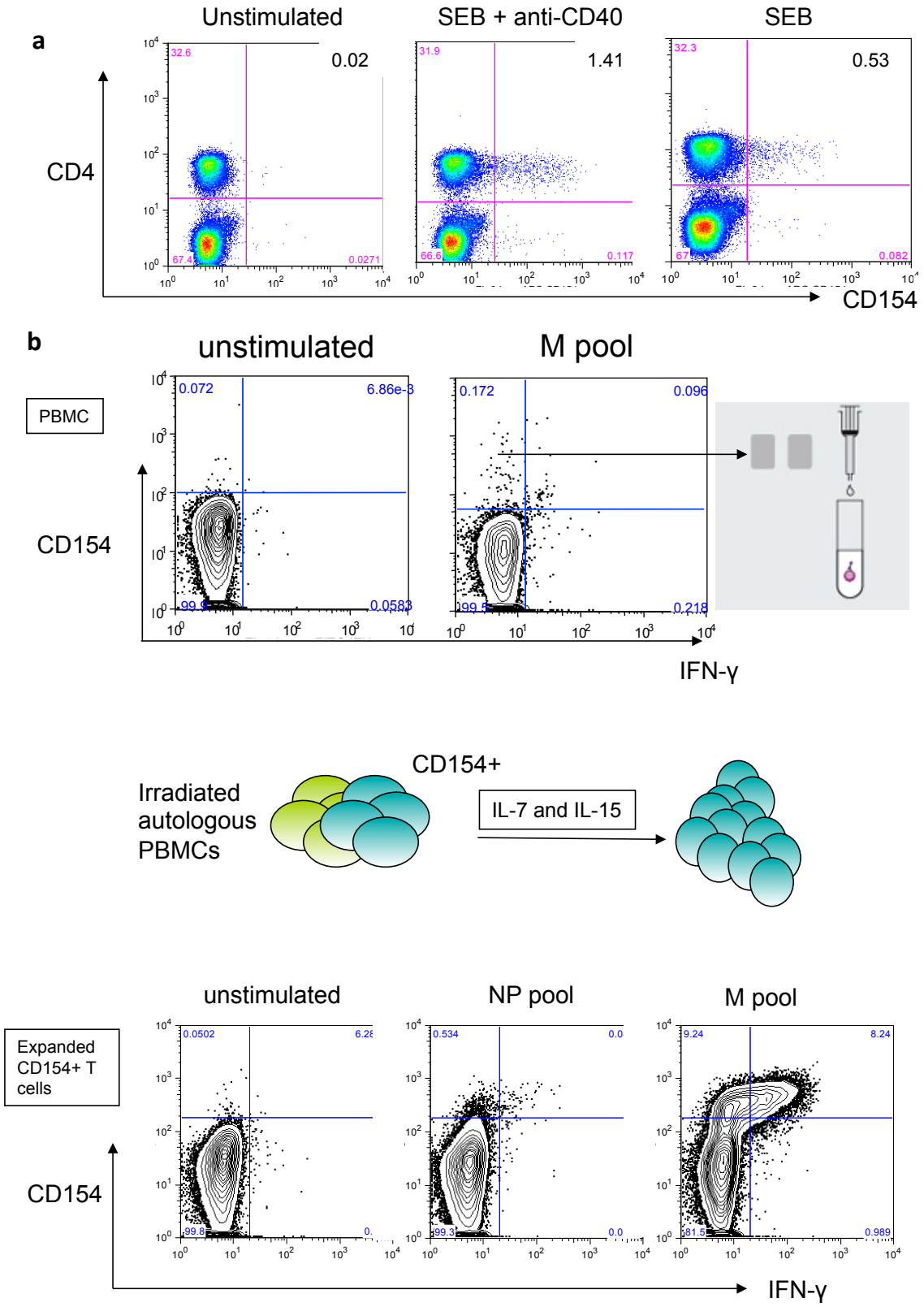

Figure 6.14 Development of a method for assessing the ability of flu-specific CD4⁺ T cells to provide help for B cells. (a) CD154 staining of stimulated PBMCs. PBMCs were stimulated with SEB, with or without anti-CD40. Use of anti-CD40 yielded a better staining. Representative data from one of three independent experiments. **(b)** Isolation and expansion of flu-specific CD4⁺ T cells. CD4⁺ T cells specific for a M peptide pool were isolated based on their CD154 expression and expanded in the presence of IL-7 and IL-15 for 21 days. The resulting cell lines responded to a M pool but not a NP peptide pool.

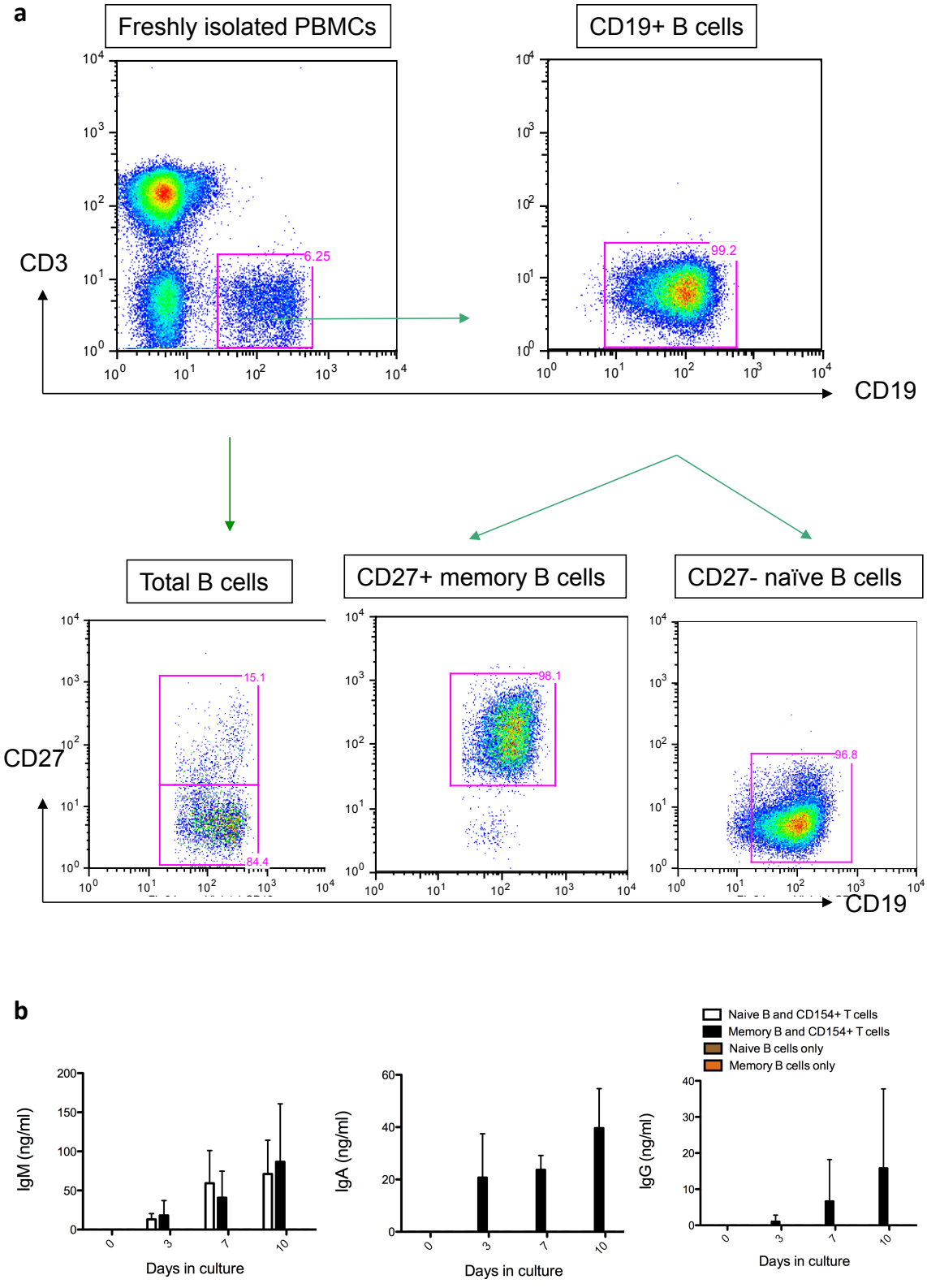

Figure 6.15 Development of a method for assessing the ability of flu-specific CD4⁺ T cells to provide help for B cells. (a) Isolation of memory and naïve B cells. Staining before and after sorting is shown. **(b)** Ig production by B cells after co-culturing with antigen-specific CD4⁺ T cells and SEB. Ig production was measured by ELISA. Data from three cell lines (two being M-specific, one being NP specific) from two different donors is shown. Bars depict mean and s.d..

Chapter 7

General discussion

7.1 T cells in acute infection

T cells are a crucial component of anti-viral immunity, and an understanding of how protective responses in viral infection are generated and maintained will aid vaccine design. T cell responses are important in controlling viral infections, for example primary infection with EBV is characterized by $CD8^+$ T cells which produce cytokines and cytolysins to kill target cells (Callan et al., 2000; Klenerman and Hill, 2005), while in herpes simplex virus (HSV) infections $CD4^+$ T cells mediate long-term control of infection (Manickan et al., 1995; Schmid and Mawle, 1991). Acute infection in particular, induces an effective immune response to completely eliminate the virus thus allowing the quality of antiviral T cell responses to be explored. How these memory $CD8^+$ and $CD4^+$ T cells directed against viral infection are maintained throughout life remains an active area of research (Sprent and Surh, 2001). Most importantly, identifying immune correlates of protection will be a prerequisite in developing any successful vaccine targeting cellular immune functions.

In this project, I focused on understanding the nature of protective cell-mediated immunity against acute influenza infection in humans. Current vaccines against influenza virus depend on generating strain-specific humoral responses to induce high-affinity neutralizing antibodies. This strategy does not offer protection against a board range of circulating viruses and any emerging pandemic strain. In contrast, a strategy targeting the induction of T cell responses which are mainly directed against the conserved internal proteins may be effective against multiple influenza strains. Despite the fact that virus-specific $CD4^+$ and $CD8^+$ T cell responses are elicited against influenza virus, their precise protective roles remained to be fully elucidated.

In Chapter 3, I described the kinetics of influenza-specific T cells during an acute influenza infection. Interesting comparisons could be drawn from my findings in the experimental influenza infection model to other studies of acute infection. Previous studies into the generation of memory T cells in acute viral infection have been carried out in murine model infection such as lymphocytic choriomeningitis virus (LCMV) or vaccinia (Harrington et al., 2002; Murali-Krishna et al., 1998); or in humans using vaccination with live attenuated viral vaccines. LCMV and vaccinia are reported to drive a massive $CD8^+$ T cell expansion in mice, resulting in up to 100,000-fold increase in frequency of antigen-specific $CD8^+$ T cells (Harrington et al., 2002; Murali-Krishna et al., 1998). In the context of humans, $CD8^+$ T cell responses to the live attenuated yellow fever virus vaccine (YFV-17D) and to the smallpox vaccine Dryvax have been analysed longitudinally. The durability of protective immunity after an acute infection lasts for years – for example YFV-17D is capable of generating neutralizing antibody responses that persist for up to 40 years (Pulendran, 2009), making it one of the most effective vaccines ever developed. Both of these live attenuated viral vaccines induce an acute 'infection' that is rapidly cleared with minimal clinical symptoms, as it is able to replicate in humans only to a sufficient extent that enables induction of potent B and T cell responses. Thus it provides a good opportunity to study how acute infections induce highly polyfunctional and long-lived CD4 and CD8 responses (Akondy et al., 2009; Gaucher et al., 2008; Miller et al., 2008). Immunization with both vaccines induced a massive expansion of $CD8^+$ T cells that were highly specific. Similar kinetics for $CD4^+$ responses of mixed Th1 and Th2 profile were observed (Gaucher et al., 2008; Santos et al., 2008; Wrammert et al., 2009). The peak of response was observed at day 15 post immunization, where 4-13% of peripheral $CD8^+$ T cells expressed both CD38 and HLA-DR. The number of activated $CD8^+$ T cells decreased after day 15 and returned to baseline levels by day 30 post-immunization (Miller et al., 2008). Both effector and memory T cells generated after YFV-17D and Dryvax immunization were polyfunctional, with most cells exhibiting three or more functions (at least IFN-γ, TNF-α and IL-2) (Miller et al., 2008; Precopio et al., 2007).

The use of a challenge model allows us to follow the kinetics and magnitude of influenza-specific T cells longitudinally before, during the acute phase, and after infection. Comparing acute influenza infection to YFV-17D and Dryvax immunization, first of all, the proliferation of antigen-specific T cells is short-lived in both challenge models and in the studies of yellow fever and smallpox vaccines, as the majority of effector $CD8^+$ T cells die by apoptosis following

viral clearance, resulting in a small pool of long-term memory T cells. My challenge models, however, reveal some differences in kinetics between primary and secondary infection. The peak of $CD8^+$ effector T cell responses to yellow fever and smallpox vaccine peaked only two weeks after vaccination, while an expansion of influenza-specific $CD4^+$ T cells was observed on day 7 post infection. In contrast, T cells elicited in response to chronic infections (e.g. HCV and HBV) take longer to develop (Thimme et al., 2002; Thimme et al., 2003). Secondly, both T cell responses induced by acute influenza infection and by yellow fever and smallpox vaccines were highly specific with minimal bystander effects. Thirdly, in my challenge models and in the studies of yellow fever and smallpox vaccines, memory T cells are highly polyfunctional. Therefore, although my challenge model displayed an expansion of T cell responses that are mainly CD4 restricted, my results shared a number of common features with the reported models, demonstrating that an acute infection leads to the generation of antigen-specific T cells that demonstrate broad specificity, high magnitude, polyfunctionality and high poliferative potential. Importantly, each individual is challenged with a broad variety of pathogens throughout their lifetime and adaptive T and B cell responses are required for long-term protection. As pre-existing memory T cells are essential in generating secondary immune responses, it is important to study the impact of acute infection on pre-existing T cell memory. The studies on live attenuated yellow fever virus vaccine (YFV-17D) and smallpox vaccine did not address the involvement of pre-existing memory T cells in an immune response. The influenza challenge model is unique in a way as it allows us to study memory influenza- specific T cells generated as a result of repeated antigenic exposure and to address some questions regarding the magnitude, breadth and functional quality of T cell memory responses.

7.2 $CD4^+$ T cells in influenza infection

In the challenge studies in Chapter 3 and 4, a relationship between the number of pre-existing influenza-specific T cells and disease severity after challenge was identified. $CD4^+$ T cell responses to synthetic peptides from core proteins of the virus correlated with a limitation of illness severity. Previously, a human challenge model similar to my approach has been used to establish a role for T cells in limiting influenza-associated illness. In subjects with an absence of specific antibodies, cytotoxic T cell responses were associated with less virus shedding after challenge (McMichael et al., 1983). However in this study, $CD8^+$ responses could not be

distinguished from $CD4^+$ responses. The target cells used were autologous PBMCs activated with PHA, so express both HLA class I and II and can be recognized by both subsets.

The present study utilized more sophisticated methods to explore the importance of $CD4^+$ T cells in protection from influenza, and to further understand some characteristics that define high quality memory $CD4^+$ T cells based on their ability to produce multiple cytokines, recognize antigens from a variant subtype and their cytotoxic potential. Memory $CD4^+$ cells are required for heterosubtypic immunity in animals infected with influenza (Guo et al., 2011; Liang et al., 1994; Powell et al., 2007; Sun et al., 2011). $CD4^+$ cells have been shown to contribute to viral clearance in many infections (Nikiforow et al., 2003; Norris et al., 2004), including influenza (Strutt et al., 2010; Teijaro et al., 2010). A potential protective role for $CD4^+$ T cells has been suggested by *in vitro* studies demonstrating cross-reactivity against previously un-encountered strains, such as against avian H5N1 by $CD4^+$ T cells primed with seasonal strains (Lee et al., 2008; McKinstry et al., 2011; Richards et al., 2010; Roti et al., 2008) or against pandemic challenge in mouse models of sequential infection (Alam and Sant, 2011). Whilst the present study highlights a potential benefit of harnessing $CD4^+$ T cell memory towards peptides that are conserved across different subtypes, one limitation of my study is that the most relevant $CD4^+$ T cells will reside in or will have to be rapidly recruited to the sites of infection i.e. respiratory tract or lymphoid tissue, which was not assessed here. It has been shown by previous studies that T cells induced by antigen activation can remain in the respiratory tract for long periods (Hogan et al., 2001; Price et al., 2009) and recall response is rapid (Lalvani et al., 1997).

Every human has a unique history of influenza infection and vaccination. The magnitude and the repertoire of influenza-specific T cells thus are determined by individual's history together with their HLA phenotype and immunological status (Boon et al., 2002). While my experimental infection model showed that a robust influenza-specific T cell response is induced upon infection (by about ten-fold), my vaccine assessment studies in Chapter 5 showed that a conventional inactivated vaccine protects by inducing strain-specific antibodies and only induces a modest T-cell response. It is known that the number of influenza-specific T cells at periphery steadily wanes after viral clearance, and T cell immunity declines substantially over the first 1-2 years (McMichael et al., 1983; Wagar et al., 2011). If the decline of peripheral T-cell memory correlates with decreased protection, it is essential to have repeated vaccination to boost a pre-existing T cell memory that is durable. There is still much we do not understand regarding the ability of the

T cells we induced in our challenge and vaccination cohort to localize to the site of infection, how they are maintained at homeostatic levels or undergo changes in phenotype and function over time.

In Chapter 6, I looked at the possible relationship between $CD4^+$ T cells and antibody production. It is well established that the generation of a high-affinity long-lived antibody responses requires the help of a subset of $CD4^+$ cells, the follicular helper T cells (Tfh). Tfh support the generation of a GC response where somatic hypermutation and affinity maturation take place, leading to the generation of memory B cells and plasma cells, which produce long-lasting antibody responses. It is particularly difficult to study human Tfh cells as it is not normally feasible to access lymphoid tissues, thus analysis is limited to cells in peripheral blood. Recent studies that used enumeration of circulating $CXCR5^+$ $CD4^+$ cells as a measure of Tfh cells demonstrated that these cells can secrete IL-21 and CXCL13, express ICOS and Bcl-6, and induce antibody production from naïve B cells (Chevalier et al., 2011; Morita et al., 2011). Although I have shown that blood $CXCR5^+$ cells represent a population of memory $CD4^+$ cells with helper functions, and demonstrated antigen-specific Tfh cells could be found in the peripheral blood of subjects which have memory T cell responses to influenza, I did not observe any change in frequency of these cells throughout influenza vaccination or infection, which highlights another problem of which markers to use to identify the "true" Tfh. There lacks a gold standard marker by which to identify the Tfh cells. Many of the markers that have been used to identify Tfh cells e.g. CXCR5, ICOS and PD-1, are also expressed by activated $CD4^+$ cells, making it hard to distinguish between the two. Even using Bcl-6 alone could not identify Tfh, as $CD4^+$ T cells rapidly express Bcl-6 after activation, long before they migrate deep into follicle and GC (Kerfoot et al., 2011; Kitano et al., 2011). How flu-specific memory $CD4^+$ T cells in the blood, that are capable of helper function, relate to $CXCR5^+$ $CD4^+$ Tfh cells remains to be determined. My study provides an insight that even blood Tfh may be phenotypically different and consist of a number of different subsets, similar to their GC counterparts.

7.3 Future studies and prospect for future vaccine development

As the present study is based on examining T cell responses in the periphery, one must not discount the role of $CD8^+$ T cells and other cell types in the site of infection, as well as an

anamnestic mucosal T cell response that may be protective. Future studies in which lung-resident or homing T cells are investigated directly by bronchial sampling techniques may offer insight into how different immune cell types orchestrate an immune response against influenza virus. It is also essential at the same time to develop standardized assays to measure efficacy and determine relevant immune correlates, such as to develop biomarkers that are indicative of a protective response.

Systems biology approaches can also be used to identify the mechanisms by which these antigen-specific T cells induce protective and effective immune responses in infected or vaccinated individuals, and allow us to further understand the multifactorial mechanisms of protection. The first examples of applying systems biology approaches to understand vaccine-induced immune responses came from studies with YFV-17D. Two independent groups identified innate gene expression signatures consisting of type I interferon, inflammasome and complement genes induced by the vaccine a few days after vaccination (Gaucher et al., 2008; Querec et al., 2009). Early gene expression signatures that predict the magnitude of adaptive immune responses ($CD8^+$ T cells and neutralizing antibody responses) to YFV-17D have been identified (Querec et al., 2009). Recently systems biology has been employed to analyse innate and adaptive responses to seasonal influenza vaccination (TIV and LAIV) in humans. This approach identified early molecular signatures that predicted seroconversion just a few days after vaccination, and shed light on the mechanisms by which effective vaccine elicited protective responses (Nakaya et al., 2011). LAIV induced a robust interferon response, similar to that of YFV-17D, while TIV induced a plasma B cell response signature.

I have yet to translate findings in this thesis to a practical use such a rational design of a vaccine that can induce protection against a broad range of circulating strains. Targeting cell-mediated immunity in an influenza vaccine is a concept aiming to reduce disease severity rather than sterilizing immunity. A recent phase IIa trial of a T cell based vaccine, a Modified Vaccinia virus Ankara vector expressing the conserved internal influenza antigens NP and M1 (MVA-NP+M1) has been shown to be safe and immunogenic (Lillie et al., 2012). This encouraging report suggests that it is possible to incorporate a T cell component in the current vaccination strategies.

7.4 Concluding remarks

This thesis provides evidence that influenza-specific $CD4^+$ T cells contribute to protection against influenza virus in humans. Due to their cross-reactive nature, influenza-specific $CD4^+$ T cells can potentially provide protection against variant virus subtypes.

References

Ahmed, R. and Akondy, R. S. (2011). Insights into human CD8(+) T-cell memory using the yellow fever and smallpox vaccines. Immunol Cell Biol *89*, 340–5.

Akondy, R. S., Monson, N. D., Miller, J. D., Edupuganti, S., Teuwen, D., Wu, H., Quyyumi, F., Garg, S., Altman, J. D., Del Rio, C., Keyserling, H. L., Ploss, A., Rice, C. M., Orenstein, W. A., Mulligan, M. J. and Ahmed, R. (2009). The Yellow Fever Virus Vaccine Induces a Broad and Polyfunctional Human Memory CD8(+) T Cell Response. Journal of Immunology *183*, 7919–7930.

Alam, S. and Sant, A. J. (2011). Infection with seasonal influenza virus elicits CD4 T cells specific for genetically conserved epitopes that can be rapidly mobilized for protective immunity to pandemic H1N1 influenza virus. J Virol *85*, 13310–21.

Alexander, J., Bilsel, P., del Guercio, M. F., Stewart, S., Marinkovic-Petrovic, A., Southwood, S., Crimi, C., Vang, L., Walker, L., Ishioka, G., Chitnis, V., Sette, A., Assarsson, E., Hannaman, D., Botten, J. and Newman, M. J. (2010). Universal influenza DNA vaccine encoding conserved CD4(+) T cell epitopes protects against lethal viral challenge in HLA-DR transgenic mice. Vaccine *28*, 664–672.

Allen, C. D., Okada, T. and Cyster, J. G. (2007). Germinal-center organization and cellular dynamics. Immunity *27*, 190–202.

Ambrose, C. S., Luke, C. and Coelingh, K. (2008). Current status of live attenuated influenza vaccine in the United States for seasonal and pandemic influenza. Influenza Other Respi Viruses *2*, 193–202.

Angelosanto, J. M. and Wherry, E. J. (2010). Transcription factor regulation of CD8+ T-cell memory and exhaustion. Immunol Rev *236*, 167–75.

Ansel, K. M., McHeyzer-Williams, L. J., Ngo, V. N., McHeyzer-Williams, M. G. and Cyster, J. G. (1999). In vivo-activated CD4 T cells upregulate CXC chemokine receptor 5 and reprogram their response to lymphoid chemokines. J Exp Med *190*, 1123–34.

Anthony, D. D. and Lehmann, P. V. (2003). T-cell epitope mapping using the ELISPOT approach. Methods *29*, 260–269.

Appay, V. (2004). The physiological role of cytotoxic CD4(+) T-cells: the holy grail? Clin Exp Immunol *138*, 10–3.

Appay, V., Dunbar, P. R., Callan, M., Klenerman, P., Gillespie, G. M., Papagno, L., Ogg, G. S., King, A., Lechner, F., Spina, C. A., Little, S., Havlir, D. V., Richman, D. D., Gruener, N., Pape, G., Waters, A., Easterbrook, P., Salio, M., Cerundolo, V., McMichael, A. J. and Rowland-Jones, S. L. (2002). Memory CD8+ T cells vary in differentiation phenotype in different persistent virus infections. Nat Med *8*, 379–85.

Appay, V., Nixon, D. F., Donahoe, S. M., Gillespie, G. M. A., Dong, T., King, A., Ogg, G. S., Spiegel, H. M. L., Conlon, C., Spina, C. A., Havlir, D. V., Richman, D. D., Waters, A., Easterbrook, P., McMichael, A. J. and Rowland-Jones, S. L. (2000). HIV-specific CD8(+) T cells produce antiviral cytokines but are impaired in cytolytic function. Journal of Experimental Medicine *192*, 63–75.

Appay, V., Zaunders, J. J., Papagno, L., Sutton, J., Jaramillo, A., Waters, A., Easterbrook, P., Grey, P., Smith, D., McMichael, A. J., Cooper, D. A., Rowland-Jones, S. L. and Kelleher, A. D. (2002). Characterization of CD4(+) CTLs ex vivo. Journal of Immunology *168*, 5954–5958.

Assarsson, E., Bui, H.-H., Sidney, J., Zhang, Q., Glenn, J., Oseroff, C., Mbawuike, I. N., Alexander, J., Newman, M. J., Grey, H. and Sette, A. (2008). Immunomic analysis of the repertoire of T-cell specificities for influenza A virus in humans. J Virol *82*, 12241–12251.

Avery, D. T., Bryant, V. L., Ma, C. S., de Waal Malefyt, R. and Tangye, S. G. (2008). IL-21-induced isotype switching to IgG and IgA by human naive B cells is differentially regulated by IL-4. J Immunol *181*, 1767–79.

Baras, B., Stittelaar, K. J., Simon, J. H., Thoolen, R. J. M. M., Mossman, S. P., Pistoor, F. H. M., van Amerongen, G., Wettendorff, M. A., Hanon, E. and Osterhaus, A. D. M. E. (2008). Cross-protection against lethal H5N1 challenge in ferrets with an adjuvanted pandemic influenza vaccine. PLoS One *3*, e1401.

Barry, J. (2004). The great influenza. The epic story of the deadliest plague in history. Viking, New York.

Basha, S., Hazenfeld, S., Brady, R. C. and Subbramanian, R. A. (2011). Comparison of antibody and T-cell responses elicited by licensed inactivated- and live-attenuated influenza vaccines against H3N2 hemagglutinin. Hum Immunol *72*, 463–9.

Bastin, J., Rothbard, J., Davey, J., Jones, I. and Townsend, A. (1987). Use of Synthetic Peptides of Influenza Nucleoprotein to Define Epitopes Recognized by Class-I-Restricted Cytotoxic Lymphocytes-T. Journal of Experimental Medicine *165*, 1508–1523.

Belser, J. A., Katz, J. M. and Tumpey, T. M. (2011). The ferret as a model organism to study influenza A virus infection. Dis Model Mech *4*, 575–9.

Belshe, R. B., Ambrose, C. S. and Yi, T. (2008). Safety and efficacy of live attenuated influenza vaccine in children 2-7 years of age. Vaccine *26 Suppl 4*, D10–6.

Belshe, R. B., Mendelman, P. M., Treanor, J., King, J., Gruber, W. C., Piedra, P., Bernstein, D. I., Hayden, F. G., Kotloff, K., Zangwill, K., Iacuzio, D. and Wolff, M. (1998). The efficacy of live attenuated, cold-adapted, trivalent, intranasal influenzavirus vaccine in children. N Engl J Med *338*, 1405–12.

Belz, G. T., Wodarz, D., Diaz, G., Nowak, M. A. and Doherty, P. C. (2002). Compromised influenza virus-specific CD8(+)-T-cell memory in CD4(+)-T-cell-deficient mice. J Virol *76*, 12388–93.

Bergen, R., Black, S., Shinefield, H., Lewis, E., Ray, P., Hansen, J., Walker, R., Hessel, C., Cordova, J. and Mendelman, P. M. (2004). Safety of cold-adapted live attenuated influenza vaccine in a large cohort of children and adolescents. Pediatr Infect Dis J *23*, 138–44.

Betts, M. R., Nason, M. C., West, S. M., De Rosa, S. C., Migueles, S. A., Abraham, J., Lederman, M. M., Benito, J. M., Goepfert, P. A., Connors, M., Roederer, M. and Koup, R. A. (2006). HIV nonprogressors preferentially maintain highly functional HIV-specific CD8(+) T cells. Blood *107*, 4781–4789.

Bevan, M. J. (1976). Cross-priming for a secondary cytotoxic response to minor H antigens with H-2 congenic cells which do not cross-react in the cytotoxic assay. J Exp Med *143*, 1283–8.

Bevan, M. J. (2004). Helping the CD8(+) T-cell response. Nat Rev Immunol *4*, 595–602.

Beyer, W. E. P., Palache, A. M., de Jong, J. C. and Osterhaus, A. D. M. E. (2002). Cold-adapted live influenza vaccine versus inactivated vaccine: systemic vaccine reactions, local and systemic antibody response, and vaccine efficacy A meta-analysis. Vaccine *20*, 1340–1353.

Bland, P. (1988). MHC class II expression by the gut epithelium. Immunol Today *9*, 174–8.

Block, S. L., Yogev, R., Hayden, F. G., Ambrose, C. S., Zeng, W. and Walker, R. E. (2008). Shedding and immunogenicity of live attenuated influenza vaccine virus in subjects 5-49 years of age. Vaccine *26*, 4940–6.

Boon, A. C., de Mutsert, G., Graus, Y. M., Fouchier, R. A., Sintnicolaas, K., Osterhaus, A. D. and Rimmelzwaan, G. F. (2002). The magnitude and specificity of influenza A virus-specific cytotoxic T-lymphocyte responses in humans is related to HLA-A and -B phenotype. J Virol *76*, 582–90.

Boon, A. C. M., de Mutsert, G., van Baarle, D., Smith, D. J., Lapedes, A. S., Fouchier, R. A. M., Sintnicolaas, K., Osterhaus, A. D. M. E. and Rimmelzwaan, G. F. (2004). Recognition of homo- and heterosubtypic variants of influenza A viruses by human CD8(+) T lymphocytes. Journal of Immunology *172*, 2453–2460.

Bossaller, L., Burger, J., Draeger, R., Grimbacher, B., Knoth, R., Plebani, A., Durandy, A., Baumann, U., Schlesier, M., Welcher, A. A., Peter, H. H. and Warnatz, K. (2006). ICOS deficiency is associated with a severe reduction of CXCR5+CD4 germinal center Th cells. J Immunol *177*, 4927–32.

Both, G. W., Sleigh, M. J., Cox, N. J. and Kendal, A. P. (1983). Antigenic drift in influenza virus H3 hemagglutinin from 1968 to 1980: multiple evolutionary pathways and sequential amino acid changes at

key antigenic sites. J Virol *48*, 52–60.

Bouvier, N. M. and Lowen, A. C. (2010). Animal Models for Influenza Virus Pathogenesis and Transmission. Viruses *2*, 1530–1563.

Breitfeld, D., Ohl, L., Kremmer, E., Ellwart, J., Sallusto, F., Lipp, M. and Forster, R. (2000). Follicular B helper T cells express CXC chemokine receptor 5, localize to B cell follicles, and support immunoglobulin production. J Exp Med *192*, 1545–52.

Bresson, J. L., Perronne, C., Launay, O., Gerdil, C., Saville, M., Wood, J., Hoschler, K. and Zambon, M. C. (2006). Safety and immunogenicity of an inactivated split-virion influenza A/Vietnam/1194/2004 (H5N1) vaccine: phase I randomised trial. Lancet *367*, 1657–64.

Brown, D. M. (2010). Cytolytic CD4 cells: Direct mediators in infectious disease and malignancy. Cellular Immunology *262*, 89–95.

Brown, D. M., Dilzer, A. M., Meents, D. L. and Swain, S. L. (2006). CD4 T cell-mediated protection from lethal influenza: Perforin and antibody-mediated mechanisms a one-two punch. Journal of Immunology *177*, 2888–2898.

Brown, D. M., Kamperschroer, C., Dilzer, A. M., Roberts, D. M. and Swain, S. L. (2009). IL-2 and antigen dose differentially regulate perforin- and FasL-mediated cytolytic activity in antigen specific CD4(+) T cells. Cellular Immunology *257*, 69–79.

Brown, D. M., Lee, S., Garcia-Hernandez Mde, L. and Swain, S. L. (2012). Multifunctional CD4 cells expressing gamma interferon and perforin mediate protection against lethal influenza virus infection. J Virol *86*, 6792–803.

Bryant, V. L., Ma, C. S., Avery, D. T., Li, Y., Good, K. L., Corcoran, L. M., de Waal Malefyt, R. and Tangye, S. G. (2007). Cytokine-mediated regulation of human B cell differentiation into Ig-secreting cells: predominant role of IL-21 produced by CXCR5+ T follicular helper cells. J Immunol *179*, 8180–90.

Burton, D. R., Poignard, P., Stanfield, R. L. and Wilson, I. A. (2012). Broadly neutralizing antibodies present new prospects to counter highly antigenically diverse viruses. Science *337*, 183–6.

Callan, M. F. C., Fazou, C., Yang, H. B., Rostron, T., Poon, K., Hatton, C. and McMichael, A. J. (2000). CD8(+) T-cell selection, function, and death in the primary immune response in vivo. Journal of Clinical Investigation *106*, 1251–1261.

Carrat, F., Vergu, E., Ferguson, N. M., Lemaitre, M., Cauchemez, S., Leach, S. and Valleron, A. J. (2008). Time lines of infection and disease in human influenza: A review of volunteer challenge studies. American Journal of Epidemiology *167*, 775–785.

Casazza, J. P., Betts, M. R., Price, D. A., Precopio, M. L., Ruff, L. E., Brenchley, J. M., Hill, B. J., Roederer, M., Douek, D. C. and Koup, R. A. (2006). Acquisition of direct antiviral effector functions by CMV-specific CD4+ T lymphocytes with cellular maturation. J Exp Med *203*, 2865–77.

Castellino, F., Galli, G., Del Giudice, G. and Rappuoli, R. (2009). Generating memory with vaccination. European Journal of Immunology *39*, 2100–2105.

Chattopadhyay, P. K., Yu, J. and Roederer, M. (2005). A live-cell assay to detect antigen-specific CD4+ T cells with diverse cytokine profiles. Nat Med *11*, 1113–7.

Chattopadhyay, P. K., Yu, J. and Roederer, M. (2006). Live-cell assay to detect antigen-specific CD4+ T-cell responses by CD154 expression. Nat Protoc *1*, 1–6.

Chen, J., Lee, K. H., Steinhauer, D. A., Stevens, D. J., Skehel, J. J. and Wiley, D. C. (1998). Structure of the hemagglutinin precursor cleavage site, a determinant of influenza pathogenicity and the origin of the labile conformation. Cell *95*, 409–17.

Chen, W., Calvo, P. A., Malide, D., Gibbs, J., Schubert, U., Bacik, I., Basta, S., O'Neill, R., Schickli, J., Palese, P., Henklein, P., Bennink, J. R. and Yewdell, J. W. (2001). A novel influenza A virus mitochondrial protein that induces cell death. Nat Med *7*, 1306–12.

Cheung, C. L., Rayner, J. M., Smith, G. J., Wang, P., Naipospos, T. S., Zhang, J., Yuen, K. Y., Webster, R. G., Peiris, J. S., Guan, Y. and Chen, H. (2006). Distribution of amantadine-resistant H5N1 avian influenza variants in Asia. J Infect Dis *193*, 1626–9.

Chevalier, N., Jarrossay, D., Ho, E., Avery, D. T., Ma, C. S., Yu, D., Sallusto, F., Tangye, S. G. and Mackay, C. R. (2011). CXCR5 expressing human central memory CD4 T cells and their relevance for

humoral immune responses. J Immunol *186*, 5556–68.

Choi, Y. S. and Baumgarth, N. (2008). Dual role for B-1a cells in immunity to influenza virus infection. J Exp Med *205*, 3053–64.

Chtanova, T., Tangye, S. G., Newton, R., Frank, N., Hodge, M. R., Rolph, M. S. and Mackay, C. R. (2004). T follicular helper cells express a distinctive transcriptional profile, reflecting their role as non-Th1/Th2 effector cells that provide help for B cells. J Immunol *173*, 68–78.

Ciuffreda, D., Comte, D., Cavassini, M., Giostra, E., Buhler, L., Perruchoud, M., Heim, M. H., Battegay, M., Genne, D., Mulhaupt, B., Malinverni, R., Oneta, C., Bernasconi, E., Monnat, M., Cerny, A., Chuard, C., Borovicka, J., Mentha, G., Pascual, M., Gonvers, J. J., Pantaleo, G. and Dutoit, V. (2008). Polyfunctional HCV-specific T-cell responses are associated with effective control of HCV replication. Eur J Immunol *38*, 2665–77.

Clark, T. W., Pareek, M., Hoschler, K., Dillon, H., Nicholson, K. G., Groth, N. and Stephenson, I. (2009). Trial of 2009 Influenza A (H1N1) Monovalent MF59-Adjuvanted Vaccine. New England Journal of Medicine *361*, 2424–2435.

Clutterbuck, E. A., Oh, S., Hamaluba, M., Westcar, S., Beverley, P. C. and Pollard, A. J. (2008). Serotype-specific and age-dependent generation of pneumococcal polysaccharide-specific memory B-cell and antibody responses to immunization with a pneumococcal conjugate vaccine. Clin Vaccine Immunol *15*, 182–93.

Co, M. D., Orphin, L., Cruz, J., Pazoles, P., Rothman, A. L., Ennis, F. A. and Terajima, M. (2008). Discordance between antibody and T cell responses in recipients of trivalent inactivated influenza vaccine. Vaccine *26*, 1990–8.

Cohen, G. B., Kaur, A. and Johnson, R. P. (2005). Isolation of viable antigen-specific CD4 T cells by CD40L surface trapping. J Immunol Methods *302*, 103–15.

Committee for Proprietary Medicinal Products-European Agency for the Evaluation of Medicinal Products (1997). Note for guidance on harmonisation of requirements for influenza vaccines. CPMP/BWP/214/96.

Corti, D., Voss, J., Gamblin, S. J., Codoni, G., Macagno, A., Jarrossay, D., Vachieri, S. G., Pinna, D., Minola, A., Vanzetta, F., Silacci, C., Fernandez-Rodriguez, B. M., Agatic, G., Bianchi, S., Giacchetto-Sasselli, I., Calder, L., Sallusto, F., Collins, P., Haire, L. F., Temperton, N., Langedijk, J. P., Skehel, J. J. and Lanzavecchia, A. (2012). A neutralizing antibody selected from plasma cells that binds to group 1 and group 2 influenza A hemagglutinins. Science *333*, 850–6.

Cox, N. J. and Subbarao, K. (1999). Influenza. Lancet *354*, 1277–1282.

Cox, N. J. and Subbarao, K. (2000). Global epidemiology of influenza: past and present. Annu Rev Med *51*, 407–21.

Cresswell, P. (2005). Antigen processing and presentation. Immunol Rev *207*, 5–7.

Cros, J. F. and Palese, P. (2003). Trafficking of viral genomic RNA into and out of the nucleus: influenza, Thogoto and Borna disease viruses. Virus Res *95*, 3–12.

Crotty, S. (2011). Follicular helper CD4 T cells (TFH). Annu Rev Immunol *29*, 621–63.

Cyster, J. G., Ansel, K. M., Reif, K., Ekland, E. H., Hyman, P. L., Tang, H. L., Luther, S. A. and Ngo, V. N. (2000). Follicular stromal cells and lymphocyte homing to follicles. Immunol Rev *176*, 181–93.

Darrah, P. A., Patel, D. T., De Luca, P. M., Lindsay, R. W., Davey, D. F., Flynn, B. J., Hoff, S. T., Andersen, P., Reed, S. G., Morris, S. L., Roederer, M. and Seder, R. A. (2007). Multifunctional TH1 cells define a correlate of vaccine-mediated protection against Leishmania major. Nat Med *13*, 843–50.

Davies, J. R. and Grilli, E. A. (1989). Natural or vaccine-induced antibody as a predictor of immunity in the face of natural challenge with influenza viruses. Epidemiol Infect *102*, 325–33.

de Bree, G. J., Daniels, H., Schilfgaarde, M., Jansen, H. M., Out, T. A., van Lier, R. A. and Jonkers, R. E. (2007). Characterization of CD4+ memory T cell responses directed against common respiratory pathogens in peripheral blood and lung. J Infect Dis *195*, 1718–25.

de Bree, G. J., van Leeuwen, E. M., Out, T. A., Jansen, H. M., Jonkers, R. E. and van Lier, R. A. (2005). Selective accumulation of differentiated CD8+ T cells specific for respiratory viruses in the human lung. J Exp Med *202*, 1433–42.

de Jong, M. D., Simmons, C. P., Thanh, T. T., Hien, V. M., Smith, G. J. D., Chau, T. N. B., Hoang, D. M., Chau, N. V. V., Khanh, T. H., Dong, V. C., Qui, P. T., Van Cam, B., Ha, D. Q., Guan, Y., Peiris, J. S. M., Chinh, N. T., Hien, T. T. and Farrar, J. (2006). Fatal outcome of human influenza A (H5N1) is associated with high viral load and hypercytokinemia. Nature Medicine *12*, 1203–1207.

de Jong, M. D., Thanh, T. T., Khanh, T. H., Hien, V. M., Smith, G. J. D., Chau, N. V., Cam, B. V., Qui, P. T., Ha, D. Q., Guan, Y., Peiris, J. S. M., Hien, T. T. and Farrar, J. (2005). Brief report - Oseltamivir resistance during treatment of influenza A (H5N1) infection. New England Journal of Medicine *353*, 2667–2672.

Debes, G. F., Bonhagen, K., Wolff, T., Kretschmer, U., Krautwald, S., Kamradt, T. and Hamann, A. (2004). CC chemokine receptor 7 expression by effector/memory CD4+ T cells depends on antigen specificity and tissue localization during influenza A virus infection. J Virol *78*, 7528–35.

Dengjel, J., Schoor, O., Fischer, R., Reich, M., Kraus, M., Muller, M., Kreymborg, K., Altenberend, F., Brandenburg, J., Kalbacher, H., Brock, R., Driessen, C., Rammensee, H. G. and Stevanovic, S. (2005). Autophagy promotes MHC class II presentation of peptides from intracellular source proteins. Proceedings of the National Academy of Sciences of the United States of America *102*, 7922–7927.

Denzin, L. K., Fallas, J. L., Prendes, M. and Yi, W. (2005). Right place, right time, right peptide: DO keeps DM focused. Immunol Rev *207*, 279–92.

Dharan, N. J., Gubareva, L. V., Meyer, J. J., Okomo-Adhiambo, M., McClinton, R. C., Marshall, S. A., George, K. S., Epperson, S., Brammer, L., Klimov, A. I., Bresee, J. S., Fry, A. M. and Grp, O.-R. W. (2009). Infections With Oseltamivir-Resistant Influenza A(H1N1) Virus in the United States. Jama-Journal of the American Medical Association *301*, 1034–1041.

Doherty, P. C., Effros, R. B. and Bennink, J. (1977). Heterogeneity of Cytotoxic Response of Thymus-Derived Lymphocytes after Immunization with Influenza-Viruses. Proceedings of the National Academy of Sciences of the United States of America *74*, 1209–1213.

Doherty, P. C., Turner, S. J., Webby, R. G. and Thomas, P. G. (2006). Influenza and the challenge for immunology. Nature Immunology *7*, 449–455.

Duvall, M. G., Precopio, M. L., Ambrozak, D. A., Jaye, A., McMichael, A. J., Whittle, H. C., Roederer, M., Rowland-Jones, S. L. and Koup, R. A. (2008). Polyfunctional T cell responses are a hallmark of HIV-2 infection. European Journal of Immunology *38*, 350–363.

Ehrhardt, C., Seyer, R., Hrincius, E. R., Eierhoff, T., Wolff, T. and Ludwig, S. (2010). Interplay between influenza A virus and the innate immune signaling. Microbes and Infection *12*, 81–87.

Eick, A. A., Wang, Z., Hughes, H., Ford, S. M. and Tobler, S. K. (2009). Comparison of the trivalent live attenuated vs. inactivated influenza vaccines among U.S. military service members. Vaccine *27*, 3568–75.

Ekiert, D. C., Friesen, R. H., Bhabha, G., Kwaks, T., Jongeneelen, M., Yu, W., Ophorst, C., Cox, F., Korse, H. J., Brandenburg, B., Vogels, R., Brakenhoff, J. P., Kompier, R., Koldijk, M. H., Cornelissen, L. A., Poon, L. L., Peiris, M., Koudstaal, W., Wilson, I. A. and Goudsmit, J. (2011). A highly conserved neutralizing epitope on group 2 influenza A viruses. Science *333*, 843–50.

Ekiert, D. C., Kashyap, A. K., Steel, J., Rubrum, A., Bhabha, G., Khayat, R., Lee, J. H., Dillon, M. A., O'Neil, R. E., Faynboym, A. M., Horowitz, M., Horowitz, L., Ward, A. B., Palese, P., Webby, R., Lerner, R. A., Bhatt, R. R. and Wilson, I. A. (2012). Cross-neutralization of influenza A viruses mediated by a single antibody loop. Nature *Sep 16; [Epub ahead of print] doi: 10.1038/nature11414.*

Ekiert, D. C. and Wilson, I. A. (2012). Broadly neutralizing antibodies against influenza virus and prospects for universal therapies. Curr Opin Virol *2*, 134–141.

Elsaesser, H., Sauer, K. and Brooks, D. G. (2009). IL-21 is required to control chronic viral infection. Science *324*, 1569–72.

Epstein, S. L. (2006). Prior H1N1 influenza infection and susceptibility of Cleveland Family Study participants during the H2N2 pandemic of 1957: an experiment of nature. J Infect Dis *193*, 49–53.

Eto, D., Lao, C., DiToro, D., Barnett, B., Escobar, T. C., Kageyama, R., Yusuf, I. and Crotty, S. (2011). IL-21 and IL-6 are critical for different aspects of B cell immunity and redundantly induce optimal follicular helper CD4 T cell (Tfh) differentiation. PLoS One *6*, e17739.

Ettinger, R., Kuchen, S. and Lipsky, P. E. (2008). The role of IL-21 in regulating B-cell function in health and disease. Immunol Rev *223*, 60–86.

Ettinger, R., Sims, G. P., Fairhurst, A. M., Robbins, R., da Silva, Y. S., Spolski, R., Leonard, W. J. and Lipsky, P. E. (2005). IL-21 induces differentiation of human naive and memory B cells into antibody-secreting plasma cells. J Immunol *175*, 7867–79.

Evavold, B. D., Sloanlancaster, J., Wilson, K. J., Rothbard, J. B. and Allen, P. M. (1995). Specific T-Cell Recognition of Minimally Homologous Peptides - Evidence for Multiple Endogenous Ligands. Immunity *2*, 655–663.

Faenzi, E., Zedda, L., Bardelli, M., Spensieri, F., Borgogni, E., Volpini, G., Buricchi, F., Pasini, F. L., Capecchi, P. L., Montanaro, F., Belli, R., Lattanzi, M., Piccirella, S., Montomoli, E., Ahmed, S. S., Rappuoli, R., Del Giudice, G., Finco, O., Castellino, F. and Galli, G. (2012). One dose of an MF59-adjuvanted pandemic A/H1N1 vaccine recruits pre-existing immune memory and induces the rapid rise of neutralizing antibodies. Vaccine *30*, 4086–94.

Fahey, L. M., Wilson, E. B., Elsaesser, H., Fistonich, C. D., McGavern, D. B. and Brooks, D. G. (2011). Viral persistence redirects CD4 T cell differentiation toward T follicular helper cells. J Exp Med *208*, 987–99.

Falasca, K., Ucciferri, C., Dalessandro, M., Zingariello, P., Mancino, P., Petrarca, C., Pizzigallo, E., Conti, P. and Vecchiet, J. (2006). Cytokine patterns correlate with liver damage in patients with chronic hepatitis B and C. Ann Clin Lab Sci *36*, 144–50.

Fan, S., Gao, Y., Shinya, K., Li, C. K., Li, Y., Shi, J., Jiang, Y., Suo, Y., Tong, T., Zhong, G., Song, J., Zhang, Y., Tian, G., Guan, Y., Xu, X.-N., Bu, Z., Kawaoka, Y. and Chen, H. (2009). Immunogenicity and protective efficacy of a live attenuated H5N1 vaccine in nonhuman primates. PLoS Pathog *5*, e1000409.

Feldmann, M., Brennan, F. M., Elliott, M. J., Williams, R. O. and Maini, R. N. (1995). TNF alpha is an effective therapeutic target for rheumatoid arthritis. Ann N Y Acad Sci *766*, 272–8.

Feng, J., Lu, L., Hua, C., Qin, L., Zhao, P., Wang, J., Wang, Y., Li, W., Shi, X. and Jiang, Y. (2011). High frequency of CD4+ CXCR5+ TFH cells in patients with immune-active chronic hepatitis B. PLoS One *6*, e21698.

Fiore, A. E., Uyeki, T. M., Broder, K., Finelli, L., Euler, G. L., Singleton, J. A., Iskander, J. K., Wortley, P. M., Shay, D. K., Bresee, J. S. and Cox, N. J. (2009). Prevention and control of seasonal influenza with vaccines: recommendations of the Advisory Committee on Immunization Practices (ACIP), 2009. MMWR Recomm Rep, 2009. *58*, 1–52.

Forrest, B. D., Pride, M. W., Dunning, A. J., Capeding, M. R., Chotpitayasunondh, T., Tam, J. S., Rappaport, R., Eldridge, J. H. and Gruber, W. C. (2008). Correlation of cellular immune responses with protection against culture-confirmed influenza virus in young children. Clin Vaccine Immunol *15*, 1042–53.

Frentsch, M., Arbach, O., Kirchhoff, D., Moewes, B., Worm, M., Rothe, M., Scheffold, A. and Thiel, A. (2005). Direct access to CD4+ T cells specific for defined antigens according to CD154 expression. Nat Med *11*, 1118–24.

Frentsch, M., Rothe, M., Radbruch, A. and Thiel, A. (2004). Antigen-reactive CD154 expression facilitates analysis and isolation of the entire repertoire of antigen-specific CD4+ T-cells. Cytometry Part A *59A*, 71–72.

Frohlich, A., Kisielow, J., Schmitz, I., Freigang, S., Shamshiev, A. T., Weber, J., Marsland, B. J., Oxenius, A. and Kopf, M. (2009). IL-21R on T cells is critical for sustained functionality and control of chronic viral infection. Science *324*, 1576–80.

Fujimoto, I., Takizawa, T., Ohba, Y. and Nakanishi, Y. (1998). Co-expression of Fas and Fas-ligand on the surface of influenza virus-infected cells. Cell Death Differ *5*, 426–431.

Galli, G., Medini, D., Borgogni, E., Zedda, L., Bardelli, M., Malzone, C., Nuti, S., Tavarini, S., Sammicheli, C., Hilbert, A. K., Brauer, V., Banzhoff, A., Rappuoli, R., Del Giudice, G. and Castellino, F. (2009). Adjuvanted H5N1 vaccine induces early CD4+ T cell response that predicts long-term persistence of protective antibody levels. Proc Natl Acad Sci U S A *106*, 3877–3882.

Gambotto, A., Barratt-Boyes, S. M., de Jong, M. D., Neumann, G. and Kawaoka, Y. (2008). Human infection with highly pathogenic H5N1 influenza virus. Lancet *371*, 1464–1475.

Garten, R. J., Davis, C. T., Russell, C. A., Shu, B., Lindstrom, S., Balish, A., Sessions, W. M., Xu, X., Skepner, E., Deyde, V., Okomo-Adhiambo, M., Gubareva, L., Barnes, J., Smith, C. B., Emery, S. L., Hillman, M. J., Rivailler, P., Smagala, J., de Graaf, M., Burke, D. F., Fouchier, R. A. M., Pappas, C., Alpuche-Aranda, C. M., López-Gatell, H., Olivera, H., López, I., Myers, C. A., Faix, D., Blair, P. J., Yu, C., Keene, K. M., Dotson, Jr, P. D., Boxrud, D., Sambol, A. R., Abid, S. H., St George, K., Bannerman, T., Moore, A. L., Stringer, D. J., Blevins, P., Demmler-Harrison, G. J., Ginsberg, M., Kriner, P., Waterman, S., Smole, S., Guevara, H. F., Belongia, E. A., Clark, P. A., Beatrice, S. T., Donis, R., Katz, J., Finelli, L., Bridges, C. B., Shaw, M., Jernigan, D. B., Uyeki, T. M., Smith, D. J., Klimov, A. I. and Cox, N. J. (2009). Antigenic and genetic characteristics of swine-origin 2009 A(H1N1) influenza viruses circulating in humans. Science *325*, 197–201.

Gaucher, D., Therrien, R., Kettaf, N., Angermann, B. R., Boucher, G., Filali-Mouhim, A., Moser, J. M., Mehta, R. S., Drake, D. R., r., Castro, E., Akondy, R., Rinfret, A., Yassine-Diab, B., Said, E. A., Chouikh, Y., Cameron, M. J., Clum, R., Kelvin, D., Somogyi, R., Greller, L. D., Balderas, R. S., Wilkinson, P., Pantaleo, G., Tartaglia, J., Haddad, E. K. and Sekaly, R. P. (2008). Yellow fever vaccine induces integrated multilineage and polyfunctional immune responses. J Exp Med *205*, 3119–31.

Ge, X. H., Tan, V., Bollyky, P. L., Standifer, N. E., James, E. A. and Kwok, W. W. (2010). Assessment of Seasonal Influenza A Virus-Specific CD4 T-Cell Responses to 2009 Pandemic H1N1 Swine-Origin Influenza A Virus. Journal of Virology *84*, 3312–3319.

Geppert, T. D. and Lipsky, P. E. (1985). Antigen presentation by interferon-gamma-treated endothelial cells and fibroblasts: differential ability to function as antigen-presenting cells despite comparable Ia expression. J Immunol *135*, 3750–62.

Gerhard, W., Mozdzanowska, K., Furchner, M., Washko, G. and Maiese, K. (1997). Role of the B-cell response in recovery of mice from primary influenza virus infection. Immunological Reviews *159*, 95–103.

Giannella, M., Alonso, M., Garcia de Viedma, D., Lopez Roa, P., Catalan, P., Padilla, B., Munoz, P. and Bouza, E. (2010). Prolonged viral shedding in pandemic influenza A(H1N1): clinical significance and viral load analysis in hospitalized patients. Clin Microbiol Infect *17*, 1160–5.

Glezen, W. P. (1996). Emerging infections: pandemic influenza. Epidemiol Rev *18*, 64–76.

Gomez-Martin, D., Diaz-Zarnudio, M., Romo-Tena, J., Ibarra-Sanchez, M. J. and Alcocer-Varela, J. (2011). Follicular helper T cells poise immune responses to the development of autoimmune pathology. Autoimmunity Reviews *10*, 325–330.

Good, K. L., Bryant, V. L. and Tangye, S. G. (2006). Kinetics of human B cell behavior and amplification of proliferative responses following stimulation with IL-21. J Immunol *177*, 5236–47.

Graf, D., Muller, S., Korthauer, U., van Kooten, C., Weise, C. and Kroczek, R. A. (1995). A soluble form of TRAP (CD40 ligand) is rapidly released after T cell activation. Eur J Immunol *25*, 1749–54.

Graham-Rowe, D. (2011). Epidemiology: Racing against the flu. Nature *480*, S2–3.

Grandea, A. G., Olsen, O. A., Cox, T. C., Renshaw, M., Hammond, P. W., Chan-Hui, P. Y., Mitcham, J. L., Cieplak, W., Stewart, S. M., Grantham, M. L., Pekosz, A., Kiso, M., Shinya, K., Hatta, M., Kawaoka, Y. and Moyle, M. (2010). Human antibodies reveal a protective epitope that is highly conserved among human and nonhuman influenza A viruses. Proceedings of the National Academy of Sciences of the United States of America *107*, 12658–12663.

Greenbaum, J. A., Kotturi, M. F., Kim, Y., Oseroff, C., Vaughan, K., Salimi, N., Vita, R., Ponomarenko, J., Scheuermann, R. H., Sette, A. and Peters, B. (2009). Pre-existing immunity against swine-origin H1N1 influenza viruses in the general human population. Proceedings of the National Academy of Sciences of the United States of America *106*, 20365–20370.

Greenberg, M. E., Lai, M. H., Hartel, G. F., Wichems, C. H., Gittleson, C., Bennet, J., Dawson, G., Hu, W., Leggio, C., Washington, D. and Basser, R. L. (2009). Response to a monovalent 2009 influenza A (H1N1) vaccine. N Engl J Med *361*, 2405–13.

Greenspan, N. and Doherty, P. C. (1982). Modification of cytotoxic T-cell response patterns by administration of hemagglutinin-specific monoclonal antibodies to mice infected with influenza A viruses. Hybridoma *1*, 149–59.

Greenwald, R. J., Freeman, G. J. and Sharpe, A. H. (2005). The B7 family revisited. Annu Rev Immunol *23*, 515–48.

Guan, Y. and Chen, H. (2005). Resistance to anti-influenza agents. Lancet *366*, 1139–40.

Guarner, J. and Falcon-Escobedo, R. (2009). Comparison of the Pathology Caused by H1N1, H5N1, and H3N2 Influenza Viruses. Archives of Medical Research *40*, 655–661.

Guo, H., Santiago, F., Lambert, K., Takimoto, T. and Topham, D. J. (2011). T cell-mediated protection against lethal 2009 pandemic H1N1 influenza virus infection in a mouse model. J Virol *85*, 448–455.

Hamad, M. (2011). Universal vaccines: shifting to one for many or shooting too high too soon! APMIS *119*, 565–73.

Hamada, H., Garcia-Hernandez Mde, L., Reome, J. B., Misra, S. K., Strutt, T. M., McKinstry, K. K., Cooper, A. M., Swain, S. L. and Dutton, R. W. (2009). Tc17, a unique subset of CD8 T cells that can protect against lethal influenza challenge. J Immunol *182*, 3469–81.

Hammad, H. and Lambrecht, B. N. (2008). Dendritic cells and epithelial cells: linking innate and adaptive immunity in asthma. Nat Rev Immunol *8*, 193–204.

Hancock, K., Veguilla, V., Lu, X., Zhong, W., Butler, E. N., Sun, H., Liu, F., Dong, L., DeVos, J. R., Gargiullo, P. M., Brammer, T. L., Cox, N. J., Tumpey, T. M. and Katz, J. M. (2009). Cross-reactive antibody responses to the 2009 pandemic H1N1 influenza virus. N Engl J Med *361*, 1945–52.

Harari, A., Cellerai, C., Enders, F. B., Kostier, J., Codarri, L., Tapia, G., Boyman, O., Castro, E., Gaudieri, S., James, I., John, M., Wagner, R., Mallal, S. and Pantaleo, G. (2007). Skewed association of polyfunctional antigen-specific CD8 T cell populations with HLA-B genotype. Proceedings of the National Academy of Sciences of the United States of America *104*, 16233–16238.

Hardtke, S., Ohl, L. and Forster, R. (2005). Balanced expression of CXCR5 and CCR7 on follicular T helper cells determines their transient positioning to lymph node follicles and is essential for efficient B-cell help. Blood *106*, 1924–31.

Harker, J. A., Lewis, G. M., Mack, L. and Zuniga, E. I. (2011). Late interleukin-6 escalates T follicular helper cell responses and controls a chronic viral infection. Science *334*, 825–9.

Harper, S. A., Fukuda, K., Uyeki, T. M., Cox, N. J. and Bridges, C. B. (2005). Prevention and control of influenza. Recommendations of the Advisory Committee on Immunization Practices (ACIP). MMWR Recomm Rep *54*, 1–40.

Harrington, L. E., Most Rv, R., Whitton, J. L. and Ahmed, R. (2002). Recombinant vaccinia virus-induced T-cell immunity: quantitation of the response to the virus vector and the foreign epitope. J Virol *76*, 3329–37.

Hassantoufighi, A., Zhang, H., Sandbulte, M., Gao, J., Manischewitz, J., King, L., Golding, H., Straight, T. M. and Eichelberger, M. C. (2010). A practical influenza neutralization assay to simultaneously quantify hemagglutinin and neuraminidase-inhibiting antibody responses. Vaccine *28*, 790–797.

Hayden, F. G., Fritz, R., Lobo, M. C., Alvord, W., Strober, W. and Straus, S. E. (1998). Local and systemic cytokine responses during experimental human influenza A virus infection. Relation to symptom formation and host defense. J Clin Invest *101*, 643–9.

Haynes, N. M., Allen, C. D., Lesley, R., Ansel, K. M., Killeen, N. and Cyster, J. G. (2007). Role of CXCR5 and CCR7 in follicular Th cell positioning and appearance of a programmed cell death gene-1high germinal center-associated subpopulation. J Immunol *179*, 5099–108.

He, X. S., Holmes, T. H., Sasaki, S., Jaimes, M. C., Kemble, G. W., Dekker, C. L., Arvin, A. M. and Greenberg, H. B. (2008). Baseline levels of influenza-specific CD4 memory T-cells affect T-cell responses to influenza vaccines. PLoS One *3*, e2574.

He, X. S., Holmes, T. H., Zhang, C. Q., Mahmood, K., Kemble, G. W., Lewis, D. B., Dekker, C. L., Greenberg, H. B. and Arvin, A. M. (2006). Cellular immune responses in children and adults receiving inactivated or live attenuated influenza vaccines. Journal of Virology *80*, 11756–11766.

He, X. S., Sasaki, S., Narvaez, C. F., Zhang, C., Liu, H., Woo, J. C., Kemble, G. W., Dekker, C. L., Davis, M. M. and Greenberg, H. B. (2010). Plasmablast-derived polyclonal antibody response after influenza vaccination. J Immunol Methods *365*, 67–75.

Hedestam, G. B. K., Fouchier, R. A. M., Phogat, S., Burton, D. R., Sodroski, J. and Wyatt, R. T. (2008). The challenges of eliciting neutralizing antibodies to HIV-1 and to influenza virus. Nature Reviews Microbiology *6*, 143–155.

Heemels, M. T. and Ploegh, H. (1995). Generation, translocation, and presentation of MHC class I-restricted peptides. Annu Rev Biochem *64*, 463–91.

Henn, V., Steinbach, S., Buchner, K., Presek, P. and Kroczek, R. A. (2001). The inflammatory action of CD40 ligand (CD154) expressed on activated human platelets is temporally limited by coexpressed CD40. Blood *98*, 1047–54.

Herfst, S., Schrauwen, E. J., Linster, M., Chutinimitkul, S., de Wit, E., Munster, V. J., Sorrell, E. M., Bestebroer, T. M., Burke, D. F., Smith, D. J., Rimmelzwaan, G. F., Osterhaus, A. D. and Fouchier, R. A. (2012). Airborne transmission of influenza A/H5N1 virus between ferrets. Science *336*, 1534–41.

Hillaire, M. L. B., van Trierum, S. E., Kreijtz, J. H. C. M., Bodewes, R., Geelhoed-Mieras, M. M., Nieuwkoop, N. J., Fouchier, R. A. M., Kuiken, T., Osterhaus, A. D. M. E. and Rimmelzwaan, G. F. (2011). Cross-protective immunity against influenza pH1N1 2009 viruses induced by seasonal influenza A (H3N2) virus is mediated by virus-specific T-cells. J Gen Virol *92*, 2339–2349.

Hintzen, R. Q., de Jong, R., Lens, S. M., Brouwer, M., Baars, P. and van Lier, R. A. (1993). Regulation of CD27 expression on subsets of mature T-lymphocytes. J Immunol *151*, 2426–35.

Ho, P. P., Young, A. L. and Truehaft, M. (1976). Plaque formation with influenza viruses in dog kidney cells. J Gen Virol *33*, 143–5.

Hoffmeister, B., Kiecker, F., Tesfa, L., Volk, H. D., Picker, L. J. and Kern, F. (2003). Mapping T cell epitopes by flow cytometry. Methods *29*, 270–281.

Hogan, R. J., Usherwood, E. J., Zhong, W., Roberts, A. A., Dutton, R. W., Harmsen, A. G. and Woodland, D. L. (2001a). Activated antigen-specific CD8+ T cells persist in the lungs following recovery from respiratory virus infections. J Immunol *166*, 1813–22.

Hogan, R. J., Zhong, W. M., Usherwood, E. J., Cookenham, T., Roberts, A. D. and Woodland, D. L. (2001b). Protection from respiratory virus infections can be mediated by antigen-specific CD4(+) T cells that persist in the lungs. Journal of Experimental Medicine *193*, 981–986.

Holmes, E. C. (2003). Error thresholds and the constraints to RNA virus evolution. Trends Microbiol *11*, 543–546.

Horimoto, T. and Kawaoka, Y. (2005). Influenza: lessons from past pandemics, warnings from current incidents. Nat Rev Microbiol *3*, 591–600.

Huber, M., Heink, S., Grothe, H., Guralnik, A., Reinhard, K., Elflein, K., Hunig, T., Mittrucker, H. W., Brustle, A., Kamradt, T. and Lohoff, M. (2009). A Th17-like developmental process leads to CD8(+) Tc17 cells with reduced cytotoxic activity. Eur J Immunol *39*, 1716–25.

Hurt, A. C., Selleck, P., Komadina, N., Shaw, R., Brown, L. and Barr, I. G. (2007). Susceptibility of highly pathogenic A(H5N1) avian influenza viruses to the neuraminidase inhibitors and adamantanes. Antiviral Res *73*, 228–31.

Ignatowicz, L., Kappler, J. and Marrack, P. (1996). The repertoire of T cells shaped by a single MHC/peptide ligand. Cell *84*, 521–529.

Ikonen, N., Strengell, M., Kinnunen, L., Osterlund, P., Pirhonen, J., Broman, M., Davidkin, I., Ziegler, T. and Julkunen, I. (2010). High frequency of cross-reacting antibodies against 2009 pandemic influenza A(H1N1) virus among the elderly in Finland. Euro Surveill *15*, 1–8.

Im, E. J., Hong, J. P., Roshorm, Y., Bridgeman, A., Letourneau, S., Liljestrom, P., Potash, M. J., Volsky, D. J., McMichael, A. J. and Hanke, T. (2011). Protective efficacy of serially up-ranked subdominant CD8+ T cell epitopes against virus challenges. PLoS Pathog *7*, e1002041.

Imai, M. and Kawaoka, Y. (2012). The role of receptor binding specificity in interspecies transmission of influenza viruses. Curr Opin Virol *2*, 160–167.

Imai, M., Watanabe, T., Hatta, M., Das, S. C., Ozawa, M., Shinya, K., Zhong, G., Hanson, A., Katsura, H., Watanabe, S., Li, C., Kawakami, E., Yamada, S., Kiso, M., Suzuki, Y., Maher, E. A., Neumann, G. and Kawaoka, Y. (2012). Experimental adaptation of an influenza H5 HA confers respiratory droplet transmission to a reassortant H5 HA/H1N1 virus in ferrets. Nature *486*, 420–8.

Ito, T., Couceiro, J. N. S. S., Kelm, S., Baum, L. G., Krauss, S., Castrucci, M. R., Donatelli, I., Kida, H., Paulson, J. C., Webster, R. G. and Kawaoka, Y. (1998). Molecular basis for the generation in pigs of influenza A viruses with pandemic potential. Journal of Virology *72*, 7367–7373.

Jaffar, Z., Ferrini, M. E., Herritt, L. A. and Roberts, K. (2009). Cutting edge: lung mucosal Th17-mediated responses induce polymeric Ig receptor expression by the airway epithelium and elevate secretory IgA levels. J Immunol *182*, 4507–11.

Jameson, J., Cruz, J. and Ennis, F. A. (1998). Human cytotoxic T-lymphocyte repertoire to influenza A viruses. Journal of Virology *72*, 8682–8689.

Jameson, J., Cruz, J., Terajima, M. and Ennis, F. R. (1999). Human CD8(+) and CD4(+) T lymphocyte memory to influenza a viruses of swine and avian species. Journal of Immunology *162*, 7578–7583.

Jayasekera, J. P., Moseman, E. A. and Carroll, M. C. (2007). Natural antibody and complement mediate neutralization of influenza virus in the absence of prior immunity. J Virol *81*, 3487–94.

Johnston, R. J., Poholek, A. C., DiToro, D., Yusuf, I., Eto, D., Barnett, B., Dent, A. L., Craft, J. and Crotty, S. (2009). Bcl6 and Blimp-1 are reciprocal and antagonistic regulators of T follicular helper cell differentiation. Science *325*, 1006–10.

Joo, H. M., He, Y. and Sangster, M. Y. (2008). Broad dispersion and lung localization of virus-specific memory B cells induced by influenza pneumonia. Proc Natl Acad Sci U S A *105*, 3485–90.

Kanegae, Y., Sugita, S., Endo, A., Ishida, M., Senya, S., Osako, K., Nerome, K. and Oya, A. (1990). Evolutionary pattern of the hemagglutinin gene of influenza B viruses isolated in Japan: cocirculating lineages in the same epidemic season. J Virol *64*, 2860–5.

Kang, S. M., Song, J. M. and Compans, R. W. (2011). Novel vaccines against influenza viruses. Virus Res *162*, 31–8.

Kannanganat, S., Ibegbu, C., Chennareddi, L., Robinson, H. L. and Amara, R. R. (2007). Multiple-cytokine-producing antiviral CD4 T cells are functionally superior to single-cytokine-producing cells. J Virol *81*, 8468–76.

Kaufhold, R. M., Field, J. A., Caulfield, M. J., Wang, S., Joseph, H., Wooters, M. A., Green, T., Clark, H. F., Krah, D. and Smith, J. G. (2005). Memory T-cell response to rotavirus detected with a gamma interferon enzyme-linked immunospot assay. J Virol *79*, 5684–94.

Keating, S. M., Bejon, P., Berthoud, T., Vuola, J. M., Todryk, S., Webster, D. P., Dunachie, S. J., Moorthy, V. S., McConkey, S. J., Gilbert, S. C. and Hill, A. V. S. (2005). Durable human memory T cells quantifiable by cultured enzyme-linked immunospot assays are induced by heterologous prime boost immunization and correlate with protection against malaria. Journal of Immunology *175*, 5675–5680.

Keitel, W. A., Couch, R. B., Cate, T. R., Six, H. R. and Baxter, B. D. (1990). Cold Recombinant Influenza-B Texas 1/84 Vaccine Virus (Crb-87) - Attenuation, Immunogenicity, and Efficacy against Homotypic Challenge. Journal of Infectious Diseases *161*, 22–26.

Kerfoot, S. M., Yaari, G., Patel, J. R., Johnson, K. L., Gonzalez, D. G., Kleinstein, S. H. and Haberman, A. M. (2011). Germinal center B cell and T follicular helper cell development initiates in the interfollicular zone. Immunity *34*, 947–60.

Killingley, B., Enstone, J., Booy, R., Hayward, A., Oxford, J., Ferguson, N. and Nguyen Van-Tam, J. (2011). Potential role of human challenge studies for investigation of influenza transmission. Lancet Infect Dis *11*, 879–86.

Kim, C. H., Rott, L. S., Clark-Lewis, I., Campbell, D. J., Wu, L. and Butcher, E. C. (2001). Subspecialization of CXCR5+ T cells: B helper activity is focused in a germinal center-localized subset of CXCR5+ T cells. J Exp Med *193*, 1373–81.

King, C. (2011). A fine romance: T follicular helper cells and B cells. Immunity *34*, 827–9.

King, C., Tangye, S. G. and Mackay, C. R. (2008). T follicular helper (TFH) cells in normal and dysregulated immune responses. Annu Rev Immunol *26*, 741–66.

Kitano, M., Moriyama, S., Ando, Y., Hikida, M., Mori, Y., Kurosaki, T. and Okada, T. (2011). Bcl6 protein expression shapes pre-germinal center B cell dynamics and follicular helper T cell heterogeneity. Immunity *34*, 961–72.

Klenerman, P. and Hill, A. (2005). T cells and viral persistence: lessons from diverse infections. Nature Immunology *6*, 873–879.

Knossow, M. and Skehel, J. J. (2006). Variation and infectivity neutralization in influenza. Immunology *119*, 1–7.

Krause, J. C., Tsibane, T., Tumpey, T. M., Huffman, C. J., Basler, C. F. and Crowe, J. E., J. (2011a). A broadly neutralizing human monoclonal antibody that recognizes a conserved, novel epitope on the globular head of the influenza H1N1 virus hemagglutinin. J Virol *85*, 10905–8.

Krause, J. C., Tsibane, T., Tumpey, T. M., Huffman, C. J., Briney, B. S., Smith, S. A., Basler, C. F. and Crowe, J. E., J. (2011b). Epitope-specific human influenza antibody repertoires diversify by B cell intraclonal sequence divergence and interclonal convergence. J Immunol *187*, 3704–11.

Kreijtz, J. H. C. M., de Mutsert, G., van Baalen, C. A., Fouchier, R. A. M., Osterhaus, A. D. M. E. and Rimmelzwaan, G. F. (2008). Cross-recognition of avian H5N1 influenza virus by human cytotoxic T-lymphocyte populations directed to human influenza a virus. Journal of Virology *82*, 5161–5166.

La Gruta, N. L., Kedzierska, K., Stambas, J. and Doherty, P. C. (2007). A question of self-preservation: immunopathology in influenza virus infection. Immunology and Cell Biology *85*, 85–92.

La Gruta, N. L., Turner, S. J. and Doherty, P. C. (2004). Hierarchies in cytokine expression profiles for acute and resolving influenza virus-specific CD8+ T cell responses: correlation of cytokine profile and TCR avidity. J Immunol *172*, 5553–60.

Lalvani, A., Brookes, R., Hambleton, S., Britton, W. J., Hill, A. V. and McMichael, A. J. (1997a). Rapid effector function in CD8+ memory T cells. J Exp Med *186*, 859–65.

Lalvani, A., Dong, T., Ogg, G., Patham, A. A., Newell, H., Hill, A. V., McMichael, A. J. and Rowland-Jones, S. (1997b). Optimization of a peptide-based protocol employing IL-7 for in vitro restimulation of human cytotoxic T lymphocyte precursors. J Immunol Methods *210*, 65–77.

Lamb, J. R., Eckels, D. D., Phelan, M., Lake, P. and Woody, J. N. (1982). Antigen-Specific Human Lymphocyte-T Clones - Viral-Antigen Specificity of Influenza Virus-Immune Clones. Journal of Immunology *128*, 1428–1432.

Lambert, L. C. and Fauci, A. S. (2010). Influenza vaccines for the future. N Engl J Med *363*, 2036–2044.

Landais, E., Saulquin, X., Scotet, E., Trautmann, L., Peyrat, M. A., Yates, J. L., Kwok, W. W., Bonneville, M. and Houssaint, E. (2004). Direct killing of Epstein-Barr virus (EBV)-infected B cells by CD4 T cells directed against the EBV lytic protein BHRF1. Blood *103*, 1408–16.

Lanzavecchia, A. (1985). Antigen-specific interaction between T and B cells. Nature *314*, 537–9.

Lau, L. L., Cowling, B. J., Fang, V. J., Chan, K. H., Lau, E. H., Lipsitch, M., Cheng, C. K., Houck, P. M., Uyeki, T. M., Peiris, J. S. and Leung, G. M. (2010). Viral shedding and clinical illness in naturally acquired influenza virus infections. J Infect Dis *201*, 1509–16.

LeBien, T. W. and Tedder, T. F. (2008). B lymphocytes: how they develop and function. Blood *112*, 1570–80.

Lee, L. Y. H., Ha, D. L. A., Simmons, C., de Jong, M. D., Chau, N. V. V., Schumacher, R., Peng, Y. C., McMichael, A. J., Farrar, J. J., Smith, G. L., Townsend, A. R. M., Askonas, B. A., Rowland-Jones, S. and Dong, T. (2008). Memory T cells established by seasonal human influenza A infection cross-react with avian influenza A (H5N1) in healthy individuals. Journal of Clinical Investigation *118*, 3478–3490.

Leekha, S., Zitterkopf, N. L., Espy, M. J., Smith, T. F., Thompson, R. L. and Sampathkumar, P. (2007). Duration of influenza a virus shedding in hospitalized patients and implications for infection control. Infection Control and Hospital Epidemiology *28*, 1071–1076.

Leonard, W. J. and Spolski, R. (2005). Interleukin-21: a modulator of lymphoid proliferation, apoptosis and differentiation. Nat Rev Immunol *5*, 688–98.

Letourneau, S., Im, E. J., Mashishi, T., Brereton, C., Bridgeman, A., Yang, H., Dorrell, L., Dong, T., Korber, B., McMichael, A. J. and Hanke, T. (2007). Design and pre-clinical evaluation of a universal HIV-1 vaccine. PLoS One *2*, e984.

Levie, K., Leroux-Roels, I., Hoppenbrouwers, K., Kervyn, A. D., Vandermeulen, C., Forgus, S., Leroux-Roels, G., Pichon, S. and Kusters, I. (2008). An adjuvanted, low-dose, pandemic influenza A (H5N1) vaccine candidate is safe, immunogenic, and induces cross-reactive immune responses in healthy adults. J

Infect Dis *198*, 642–9.

Li, I. W., Hung, I. F., To, K. K., Chan, K.-H., Wong, S. S. Y., Chan, J. F., Cheng, V. C., Tsang, O. T., Lai, S.-T., Lau, Y.-L. and Yuen, K.-Y. (2010). The natural viral load profile of patients with pandemic 2009 influenza A(H1N1) and the effect of oseltamivir treatment. Chest *137*, 759–768.

Liang, S., Mozdzanowska, K., Palladino, G. and Gerhard, W. (1994). Heterosubtypic immunity to influenza type A virus in mice. Effector mechanisms and their longevity. J Immunol *152*, 1653–1661.

Liang, X. F., Wang, H. Q., Wang, J. Z., Fang, H. H., Wu, J., Zhu, F. C., Li, R. C., Xia, S. L., Zhao, Y. L., Li, F. J., Yan, S. H., Yin, W. D., An, K., Feng, D. J., Cui, X. L., Qi, F. C., Ju, C. J., Zhang, Y. H., Guo, Z. J., Chen, P. Y., Chen, Z., Yan, K. M. and Wang, Y. (2009). Safety and immunogenicity of 2009 pandemic influenza A H1N1 vaccines in China: a multicentre, double-blind, randomised, placebo-controlled trial. Lancet *375*, 56–66.

Lillie, P. J., Berthoud, T. K., Powell, T. J., Lambe, T., Mullarkey, C., Spencer, A. J., Hamill, M., Peng, Y., Blais, M. E., Duncan, C. J., Sheehy, S. H., Havelock, T., Faust, S. N., Williams, R. L., Gilbert, A., Oxford, J., Dong, T., Hill, A. V. and Gilbert, S. C. (2012). Preliminary Assessment of the Efficacy of a T-Cell-Based Influenza Vaccine, MVA-NP+M1, in Humans. Clin Infect Dis *55*, 19–25.

Linterman, M. A., Rigby, R. J., Wong, R. K., Yu, D., Brink, R., Cannons, J. L., Schwartzberg, P. L., Cook, M. C., Walters, G. D. and Vinuesa, C. G. (2009). Follicular helper T cells are required for systemic autoimmunity. Journal of Experimental Medicine *206*, 561–576.

Lipsitch, M. and Viboud, C. (2009). Influenza seasonality: lifting the fog. Proc Natl Acad Sci U S A *106*, 3645–6.

Liu, F. and Whitton, J. L. (2005). Cutting edge: re-evaluating the in vivo cytokine responses of CD8+ T cells during primary and secondary viral infections. J Immunol *174*, 5936–40.

Lohning, M., Hutloff, A., Kallinich, T., Mages, H. W., Bonhagen, K., Radbruch, A., Hamelmann, E. and Kroczek, R. A. (2003). Expression of ICOS in vivo defines CD4+ effector T cells with high inflammatory potential and a strong bias for secretion of interleukin 10. J Exp Med *197*, 181–93.

Lucas, M., Day, C. L., Wyer, J. R., Cunliffe, S. L., Loughry, A., McMichael, A. J. and Klenerman, P. (2004). Ex vivo phenotype and frequency of influenza virus-specific CD4 memory T cells. J Virol *78*, 7284–7.

Lukacher, A. E., Morrison, L. A., Braciale, V. L., Malissen, B. and Braciale, T. J. (1985). Expression of Specific Cytolytic Activity by H-2i Region Restricted, Influenza-Virus Specific Lymphocyte-T Clones. Journal of Experimental Medicine *162*, 171–187.

MacLennan, I. C. (1994). Germinal centers. Annu Rev Immunol *12*, 117–39.

MacLennan, I. C., Toellner, K. M., Cunningham, A. F., Serre, K., Sze, D. M., Zuniga, E., Cook, M. C. and Vinuesa, C. G. (2003). Extrafollicular antibody responses. Immunol Rev *194*, 8–18.

MacLeod, M. K., David, A., McKee, A. S., Crawford, F., Kappler, J. W. and Marrack, P. (2011). Memory CD4 T cells that express CXCR5 provide accelerated help to B cells. J Immunol *186*, 2889–96.

Madan, R. P., Tan, M., Fernandez-Sesma, A., Moran, T. M., Emre, S., Campbell, A. and Herold, B. C. (2008). A prospective, comparative study of the immune response to inactivated influenza vaccine in pediatric liver transplant recipients and their healthy siblings. Clinical Infectious Diseases *46*, 712–718.

Makedonas, G. and Betts, M. R. (2006). Polyfunctional analysis of human t cell responses: importance in vaccine immunogenicity and natural infection. Springer Semin Immunopathol *28*, 209–19.

Makedonas, G. and Betts, M. R. (2011). Living in a house of cards: re-evaluating CD8+ T-cell immune correlates against HIV. Immunol Rev *239*, 109–24.

Makedonas, G., Hutnick, N., Haney, D., Amick, A. C., Gardner, J., Cosma, G., Hersperger, A. R., Dolfi, D., Wherry, E. J., Ferrari, G. and Betts, M. R. (2010). Perforin and IL-2 upregulation define qualitative differences among highly functional virus-specific human CD8 T cells. PLoS Pathog *6*, e1000798.

Mandelboim, O., Lieberman, N., Lev, M., Paul, L., Arnon, T. I., Bushkin, Y., Davis, D. M., Strominger, J. L., Yewdell, J. W. and Porgador, A. (2001). Recognition of haemagglutinins on virus-infected cells by NKp46 activates lysis by human NK cells. Nature *409*, 1055–1060.

Manickan, E., Rouse, R. J. D., Yu, Z. Y., Wire, W. S. and Rouse, B. T. (1995). Genetic Immunization against Herpes-Simplex-Virus Protection Is Mediated by Cd4(+) T-Lymphocytes. Journal of Immunology

155, 259–265.

Marazzi, I., Ho, J. S., Kim, J., Manicassamy, B., Dewell, S., Albrecht, R. A., Seibert, C. W., Schaefer, U., Jeffrey, K. L., Prinjha, R. K., Lee, K., Garcia-Sastre, A., Roeder, R. G. and Tarakhovsky, A. (2012). Suppression of the antiviral response by an influenza histone mimic. Nature *483*, 428–33.

Marshall, N. B. and Swain, S. L. (2011). Cytotoxic CD4 T cells in antiviral immunity. J Biomed Biotechnol *2011*, 954602.

Mason, D. (1998). A very high level of crossreactivity is an essential feature of the T-cell receptor. Immunology Today *19*, 395–404.

Massin, P., van der Werf, S. and Naffakh, N. (2001). Residue 627 of PB2 is a determinant of cold sensitivity in RNA replication of avian influenza viruses. J Virol *75*, 5398–404.

McCullers, J. A. (2006). Insights into the interaction between influenza virus and pneumococcus. Clin Microbiol Rev *19*, 571–582.

McElhaney, J. E., Gravenstein, S., Krause, P., Hooton, J. W., Upshaw, C. M. and Drinka, P. (1998). Assessment of markers of the cell-mediated immune response after influenza virus infection in frail older adults. Clin Diagn Lab Immunol *5*, 840–4.

McElhaney, J. E., Xie, D., Hager, W. D., Barry, M. B., Wang, Y., Kleppinger, A., Ewen, C., Kane, K. P. and Bleackley, R. C. (2006). T cell responses are better correlates of vaccine protection in the elderly. J Immunol *176*, 6333–9.

McGill, J., Heusel, J. W. and Legge, K. L. (2009). Innate immune control and regulation of influenza virus infections. Journal of Leukocyte Biology *86*, 803–812.

McHeyzer-Williams, M., Okitsu, S., Wang, N. and McHeyzer-Williams, L. (2012). Molecular programming of B cell memory. Nat Rev Immunol *12*, 24–34.

McKinstry, K. K., Strutt, T. M., Buck, A., Curtis, J. D., Dibble, J. P., Huston, G., Tighe, M., Hamada, H., Sell, S., Dutton, R. W. and Swain, S. L. (2009). IL-10 deficiency unleashes an influenza-specific Th17 response and enhances survival against high-dose challenge. J Immunol *182*, 7353–63.

McKinstry, K. K., Strutt, T. M., Kuang, Y., Brown, D. M., Sell, S., Dutton, R. W. and Swain, S. L. (2012). Memory CD4+ T cells protect against influenza through multiple synergizing mechanisms. J Clin Invest *122*, 2847–56.

McKinstry, K. K., Strutt, T. M. and Swain, S. L. (2011). Hallmarks of CD4 T cell immunity against influenza. J Intern Med *269*, 507–18.

McMichael, A. J., Gotch, F. M., Dongworth, D. W., Clark, A. and Potter, C. W. (1983a). Declining T-cell immunity to influenza, 1977-82. Lancet *2*, 762–764.

McMichael, A. J., Gotch, F. M., Noble, G. R. and Beare, P. A. (1983b). Cytotoxic T-cell immunity to influenza. N Engl J Med *309*, 13–17.

Miller, J. D., van der Most, R. G., Akondy, R. S., Glidewell, J. T., Albott, S., Masopust, D., Murali-Krishna, K., Mahar, P. L., Edupuganti, S., Lalor, S., Germon, S., Del Rio, C., Mulligan, M. J., Staprans, S. I., Altman, J. D., Feinberg, M. B. and Ahmed, R. (2008). Human effector and memory CD8+ T cell responses to smallpox and yellow fever vaccines. Immunity *28*, 710–22.

Moon, J. J., Suh, H., Li, A. V., Ockenhouse, C. F., Yadava, A. and Irvine, D. J. (2012). Enhancing humoral responses to a malaria antigen with nanoparticle vaccines that expand Tfh cells and promote germinal center induction. Proc Natl Acad Sci U S A *109*, 1080–5.

Morens, D. M., Taubenberger, J. K. and Fauci, A. S. (2008). Predominant role of bacterial pneumonia as a cause of death in pandemic influenza: implications for pandemic influenza preparedness. J Infect Dis *198*, 962–970.

Morita, R., Schmitt, N., Bentebibel, S. E., Ranganathan, R., Bourdery, L., Zurawski, G., Foucat, E., Dullaers, M., Oh, S., Sabzghabaei, N., Lavecchio, E. M., Punaro, M., Pascual, V., Banchereau, J. and Ueno, H. (2011). Human blood CXCR5(+)CD4(+) T cells are counterparts of T follicular cells and contain specific subsets that differentially support antibody secretion. Immunity *34*, 108–21.

Morris, A. G., Lin, Y. L. and Askonas, B. A. (1982). Immune interferon release when a cloned cytotoxic T-cell line meets its correct influenza-infected target cell. Nature *295*, 150–2.

Mosca, F., Tritto, E., Muzzi, A., Monaci, E., Bagnoli, F., Iavarone, C., O'Hagan, D., Rappuoli, R. and De Gregorio, E. (2008). Molecular and cellular signatures of human vaccine adjuvants. Proc Natl Acad Sci U S A *105*, 10501–6.

Mozdzanowska, K., Furchner, M., Maiese, K. and Gerhard, W. (1997). CD4+ T cells are ineffective in clearing a pulmonary infection with influenza type A virus in the absence of B cells. Virology *239*, 217–25.

Murali-Krishna, K., Altman, J. D., Suresh, M., Sourdive, D. J., Zajac, A. J., Miller, J. D., Slansky, J. and Ahmed, R. (1998). Counting antigen-specific CD8 T cells: a reevaluation of bystander activation during viral infection. Immunity *8*, 177–87.

Murphy, B. R. and Coelingh, K. (2002). Principles underlying the development and use of live attenuated cold-adapted influenza A and B virus vaccines. Viral Immunol *15*, 295–323.

Nakajima, K., Desselberger, U. and Palese, P. (1978). Recent human influenza A (H1N1) viruses are closely related genetically to strains isolated in 1950. Nature *274*, 334–9.

Nakanishi, Y., Lu, B., Gerard, C. and Iwasaki, A. (2009). CD8(+) T lymphocyte mobilization to virus-infected tissue requires CD4(+) T-cell help. Nature *462*, 510–3.

Nakaya, H. I., Wrammert, J., Lee, E. K., Racioppi, L., Marie-Kunze, S., Haining, W. N., Means, A. R., Kasturi, S. P., Khan, N., Li, G. M., McCausland, M., Kanchan, V., Kokko, K. E., Li, S., Elbein, R., Mehta, A. K., Aderem, A., Subbarao, K., Ahmed, R. and Pulendran, B. (2011). Systems biology of vaccination for seasonal influenza in humans. Nat Immunol *12*, 786–95.

National Center for Immunization and Respiratory Diseases (2009). Use of influenza A (H1N1) 2009 monovalent vaccine: recommendations of the Advisory Committee on Immunization Practices (ACIP), 2009. MMWR Recomm Rep *58*, 1–8.

Nayak, D. P., Hui, E. K. and Barman, S. (2004). Assembly and budding of influenza virus. Virus Res *106*, 147–65.

Nazaruk, R. A., Rochford, R., Hobbs, M. V. and Cannon, M. J. (1998). Functional diversity of the CD8(+) T-cell response to Epstein-Barr virus (EBV): implications for the pathogenesis of EBV-associated lymphoproliferative disorders. Blood *91*, 3875–83.

Neefjes, J., Jongsma, M. L., Paul, P. and Bakke, O. (2011). Towards a systems understanding of MHC class I and MHC class II antigen presentation. Nat Rev Immunol *11*, 823–36.

Nemes, E., Bertoncelli, L., Lugli, E., Pinti, M., Nasi, M., Manzini, L., Manzini, S., Prati, F., Borghi, V., Cossarizza, A. and Mussini, C. (2010). Cytotoxic granule release dominates gag-specific CD4(+) T-cell response in different phases of HIV infection. Aids *24*, 947–957.

Neumann, G., Noda, T. and Kawaoka, Y. (2009). Emergence and pandemic potential of swine-origin H1N1 influenza virus. Nature *459*, 931–9.

Newton, D. W., Treanor, J. J. and Menegus, M. A. (2000). Clinical and laboratory diagnosis of influenza virus infections. Am J Manag Care *6*, S265–S275.

Nicholson, K. G., Wood, J. M. and Zambon, M. (2003). Influenza. Lancet *362*, 1733–1745.

Nikiforow, S., Bottomly, K., Miller, G. and Munz, C. (2003). Cytolytic CD4(+)-T-cell clones reactive to EBNA1 inhibit Epstein-Barr virus-induced B-cell proliferation. J Virol *77*, 12088–104.

Nixon, D. E. and Landay, A. L. (2010). Biomarkers of immune dysfunction in HIV. Curr Opin HIV AIDS *5*, 498–503.

Norris, P. J., Moffett, H. F., Brander, C., Allen, T. M., O'Sullivan, K. M., Cosimi, L. A., Kaufmann, D. E., Walker, B. D. and Rosenberg, E. S. (2004a). Fine specificity and cross-clade reactivity of HIV type 1 Gag-specific CD4+ T cells. AIDS Res Hum Retroviruses *20*, 315–25.

Norris, P. J., Moffett, H. F., Yang, O. O., Kaufmann, D. E., Clark, M. J., Addo, M. M. and Rosenberg, E. S. (2004b). Beyond help: direct effector functions of human immunodeficiency virus type 1-specific CD4(+) T cells. J Virol *78*, 8844–51.

Novel Swine-Origin Influenza A (H1N1) Virus Investigation Team, Dawood, F. S., Jain, S., Finelli, L., Shaw, M. W., Lindstrom, S., Garten, R. J., Gubareva, L. V., Xu, X., Bridges, C. B. and Uyeki, T. M. (2009). Emergence of a novel swine-origin influenza A (H1N1) virus in humans. N Engl J Med *360*, 2605–2615.

Nurieva, R. I., Chung, Y., Martinez, G. J., Yang, X. O., Tanaka, S., Matskevitch, T. D., Wang, Y. H. and Dong, C. (2009). Bcl6 mediates the development of T follicular helper cells. Science *325*, 1001–5.

O'Hagan, D. T., Wack, A. and Podda, A. (2007). MF59 is a safe and potent vaccine adjuvant for flu vaccines in humans: what did we learn during its development? Clin Pharmacol Ther *82*, 740–4.

Osterholm, M. T., Kelley, N. S., Sommer, A. and Belongia, E. A. (2012). Efficacy and effectiveness of influenza vaccines: a systematic review and meta-analysis. Lancet Infectious Diseases *12*, 36–44.

Owen, R. E., Heitman, J. W., Hirschkorn, D. F., Lanteri, M. C., Biswas, H. H., Martin, J. N., Krone, M. R., Deeks, S. G., Norris, P. J. and Immunol, N. C. H. A. V. (2010). HIV+ elite controllers have low HIV-specific T-cell activation yet maintain strong, polyfunctional T-cell responses. Aids *24*, 1095–1105.

Oxford, J. S., Gelder, C. and Lambkin, R. (2005). Would you volunteer to be quarantined and infected with influenza virus? Expert Rev Anti Infect Ther *3*, 1–2.

Peiris, J. S. M., Cheung, C. Y., Leung, C. Y. H. and Nicholls, J. M. (2009a). Innate immune responses to influenza A H5N1: friend or foe? Trends in Immunology *30*, 574–584.

Peiris, J. S. M., Poon, L. L. M. and Guan, Y. (2009b). Emergence of a novel swine-origin influenza A virus (S-OIV) H1N1 virus in humans. Journal of Clinical Virology *45*, 169–173.

Peiris, J. S. M., Yu, W. C., Leung, C. W., Cheung, C. Y., Ng, W. F., Nicholls, J. M., Ng, T. K., Chan, K. H., Lai, S. T., Lim, W. L., Yuen, K. Y. and Guan, Y. (2004). Re-emergence of fatal human influenza A subtype H5N1 disease. Lancet *363*, 617–619.

Pene, J., Gauchat, J. F., Lecart, S., Drouet, E., Guglielmi, P., Boulay, V., Delwail, A., Foster, D., Lecron, J. C. and Yssel, H. (2004). Cutting edge: IL-21 is a switch factor for the production of IgG1 and IgG3 by human B cells. J Immunol *172*, 5154–7.

Pfeffer, K. (2003). Biological functions of tumor necrosis factor cytokines and their receptors. Cytokine Growth Factor Rev *14*, 185–91.

Plotkin, S. A. (2008). Correlates of vaccine-induced immunity. Clinical Infectious Diseases *47*, 401–409.

Plotkin, S. A. (2010). Correlates of Protection Induced by Vaccination. Clinical and Vaccine Immunology *17*, 1055–1065.

Powell, T. J., Strutt, T., Reome, J., Hollenbaugh, J. A., Roberts, A. D., Woodland, D. L., Swain, S. L. and Dutton, R. W. (2007). Priming with cold-adapted influenza A does not prevent infection but elicits long-lived protection against supralethal challenge with heterosubtypic virus. J Immunol *178*, 1030–1038.

Precopio, M. L., Betts, M. R., Parrino, J., Price, D. A., Gostick, E., Ambrozak, D. R., Asher, T. E., Douek, D. C., Harari, A., Pantaleo, G., Bailer, R., Graham, B. S., Roederer, M. and Koup, R. A. (2007). Immunization with vaccinia virus induces polyfunctional and phenotypically distinctive CD8(+) T cell responses. Journal of Experimental Medicine *204*, 1405–1416.

Precopio, M. L., Butterfield, T. R., Casazza, J. P., Little, S. J., Richman, D. D., Koup, R. A. and Roederer, M. (2008). Optimizing Peptide Matrices for Identifying T-Cell Antigens. Cytometry Part A *73A*, 1071–1078.

Price, G. E., Soboleski, M. R., Lo, C. Y., Misplon, J. A., Pappas, C., Houser, K. V., Tumpey, T. M. and Epstein, S. L. (2009). Vaccination focusing immunity on conserved antigens protects mice and ferrets against virulent H1N1 and H5N1 influenza A viruses. Vaccine *27*, 6512–6521.

Pulendran, B. (2009). Learning immunology from the yellow fever vaccine: innate immunity to systems vaccinology. Nat Rev Immunol *9*, 741–7.

Querec, T. D., Akondy, R. S., Lee, E. K., Cao, W. P., Nakaya, H. I., Teuwen, D., Pirani, A., Gernert, K., Deng, J. S., Marzolf, B., Kennedy, K., Wu, H. Y., Bennouna, S., Oluoch, H., Miller, J., Vencio, R. Z., Mulligan, M., Aderem, A., Ahmed, R. and Pulendran, B. (2009). Systems biology approach predicts immunogenicity of the yellow fever vaccine in humans. Nature Immunology *10*, 116–125.

Rasheed, A. U., Rahn, H. P., Sallusto, F., Lipp, M. and Muller, G. (2006). Follicular B helper T cell activity is confined to CXCR5(hi)ICOS(hi) CD4 T cells and is independent of CD57 expression. Eur J Immunol *36*, 1892–903.

Re, F., Donnini, A., Bartozzi, B., Bernardini, G. and Provinciali, M. (2005). Circulating gammadelta T cells in young/adult and old patients with cutaneous primary melanoma. Immun Ageing *2*, 2.

Rhorer, J., Ambrose, C. S., Dickinson, S., Hamilton, H., Oleka, N. A., Malinoski, F. J. and Wittes, J. (2009). Efficacy of live attenuated influenza vaccine in children: A meta-analysis of nine randomized clinical trials. Vaccine *27*, 1101–10.

Riberdy, J. M., Christensen, J. P., Branum, K. and Doherty, P. C. (2000). Diminished primary and secondary influenza virus-specific CD8(+) T-cell responses in CD4-depleted Ig(-/-) mice. J Virol *74*, 9762–5.

Richards, K. A., Chaves, F. A. and Sant, A. J. (2009). Infection of HLA-DR1 Transgenic Mice with a Human Isolate of Influenza A Virus (H1N1) Primes a Diverse CD4 T-Cell Repertoire That Includes CD4 T Cells with Heterosubtypic Cross-Reactivity to Avian (H5N1) Influenza Virus. Journal of Virology *83*, 6566–6577.

Richards, K. A., Topham, D., Chaves, F. A. and Sant, A. J. (2010). Cutting edge: CD4 T cells generated from encounter with seasonal influenza viruses and vaccines have broad protein specificity and can directly recognize naturally generated epitopes derived from the live pandemic H1N1 virus. J Immunol *185*, 4998–5002.

Riley, S., Kwok, K. O., Wu, K. M., Ning, D. Y., Cowling, B. J., Wu, J. T., Ho, L.-M., Tsang, T., Lo, S.-V., Chu, D. K. W., Ma, E. S. K. and Peiris, J. S. M. (2011). Epidemiological characteristics of 2009 (H1N1) pandemic influenza based on paired sera from a longitudinal community cohort study. PLoS Med *8*, e1000442.

Rivino, L., Messi, M., Jarrossay, D., Lanzavecchia, A., Sallusto, F. and Geginat, J. (2004). Chemokine receptor expression identifies Pre-T helper (Th)1, Pre-Th2, and nonpolarized cells among human CD4+ central memory T cells. J Exp Med *200*, 725–35.

Rogers, G. N. and Paulson, J. C. (1983). Receptor Determinants of Human and Animal Influenza-Virus Isolates - Differences in Receptor Specificity of the Hemagglutinin-H-3 Based on Species of Origin. Virology *127*, 361–373.

Roman, E., Miller, E., Harmsen, A., Wiley, J., von Andrian, U. H., Huston, G. and Swain, S. L. (2002). CD4 effector T cell subsets in the response to influenza: Heterogeneity, migration, and function. Journal of Experimental Medicine *196*, 957–968.

Roman, F., Vaman, T., Kafeja, F., Hanon, E. and Van Damme, P. (2010). AS03(A)-Adjuvanted influenza A (H1N1) 2009 vaccine for adults up to 85 years of age. Clin Infect Dis *51*, 668–77.

Rosenkrands, I., Vingsbo-Lundberg, C., Bundgaard, T. J., Lindenstrom, T., Enouf, V., van der Werf, S., Andersen, P. and Agger, E. M. (2011). Enhanced humoral and cell-mediated immune responses after immunization with trivalent influenza vaccine adjuvanted with cationic liposomes. Vaccine *29*, 6283–91.

Rota, P. A., Wallis, T. R., Harmon, M. W., Rota, J. S., Kendal, A. P. and Nerome, K. (1990). Cocirculation of two distinct evolutionary lineages of influenza type B virus since 1983. Virology *175*, 59–68.

Roti, M., Yang, J., Berger, D., Huston, L., James, E. A. and Kwok, W. W. (2008). Healthy human subjects have CD4+ T cells directed against H5N1 influenza virus. Journal of Immunology *180*, 1758–1768.

Rudolph, M. G., Stanfield, R. L. and Wilson, I. A. (2006). How TCRs bind MHCs, peptides, and coreceptors. Annu Rev Immunol *24*, 419–66.

Sad, S., Marcotte, R. and Mosmann, T. R. (1995). Cytokine-induced differentiation of precursor mouse CD8+ T cells into cytotoxic CD8+ T cells secreting Th1 or Th2 cytokines. Immunity *2*, 271–9.

Sallusto, F., Geginat, J. and Lanzavecchia, A. (2004). Central memory and effector memory T cell subsets: Function, generation, and maintenance. Annual Review of Immunology *22*, 745–763.

Sallusto, F. and Lanzavecchia, A. (2009). Heterogeneity of CD4+ memory T cells: functional modules for tailored immunity. Eur J Immunol *39*, 2076–82.

Santos, A. P., Matos, D. C., Bertho, A. L., Mendonca, S. C. and Marcovistz, R. (2008). Detection of Th1/Th2 cytokine signatures in yellow fever 17DD first-time vaccinees through ELISpot assay. Cytokine *42*, 152–5.

Sasaki, S., Jaimes, M. C., Holmes, T. H., Dekker, C. L., Mahmood, K., Kemble, G. W., Arvin, A. M. and Greenberg, H. B. (2007). Comparison of the influenza virus-specific effector and memory B-cell responses to immunization of children and adults with live attenuated or inactivated influenza virus vaccines. J Virol *81*, 215–28.

Schaerli, P., Willimann, K., Lang, A. B., Lipp, M., Loetscher, P. and Moser, B. (2000). CXC chemokine receptor 5 expression defines follicular homing T cells with B cell helper function. J Exp Med *192*, 1553–62.

Scheible, K., Zhang, G., Baer, J., Azadniv, M., Lambert, K., Pryhuber, G., Treanor, J. J. and Topham, D. J. (2011). CD8+ T cell immunity to 2009 pandemic and seasonal H1N1 influenza viruses. Vaccine *29*, 2159–2168.

Schmid, D. S. and Mawle, A. C. (1991). T-Cell Responses to Herpes-Simplex Viruses in Humans. Reviews of Infectious Diseases *13*, S946–S949.

Schmolke, M. and García-Sastre, A. (2010). Evasion of innate and adaptive immune responses by influenza A virus. Cell Microbiol *12*, 873–880.

Scholzen, T. and Gerdes, J. (2000). The Ki-67 protein: From the known and the unknown. Journal of Cellular Physiology *182*, 311–322.

Schulman, J. L. and Kilbourne, E. D. (1965). Induction of Partial Specific Heterotypic Immunity in Mice by a Single Infection with Influenza A Virus. J Bacteriol *89*, 170–174.

Schweiger, B., Bruns, L. and Meixenberger, K. (2006). Reassortment between human A(H3N2) viruses is an important evolutionary mechanism. Vaccine *24*, 6683–6690.

Seder, R. A., Darrah, P. A. and Roederer, M. (2008). T-cell quality in memory and protection: implications for vaccine design. Nat Rev Immunol *8*, 247–58.

Sester, U., Fousse, M., Dirks, J., Mack, U., Prasse, A., Singh, M., Lalvani, A. and Sester, M. (2011). Whole-blood flow-cytometric analysis of antigen-specific CD4 T-cell cytokine profiles distinguishes active tuberculosis from non-active states. PLoS One *6*, e17813.

Sette, A., Moutaftsi, M., Moyron-Quiroz, J., McCausland, M. M., Davies, D. H., Johnston, R. J., Peters, L., Benhnia, M. R. E. I., Hoffmann, J., Su, H. P., Singh, K., Garboczi, D. N., Head, S., Grey, H., Felgner, P. L. and Crotty, S. (2008). Selective CD4(+) T cell help for antibody responses to a large viral pathogen: Deterministic linkage of specificities. Immunity *28*, 847–858.

Seubert, A., Monaci, E., Pizza, M., O'Hagan, D. T. and Wack, A. (2008). The adjuvants aluminum hydroxide and MF59 induce monocyte and granulocyte chemoattractants and enhance monocyte differentiation toward dendritic cells. J Immunol *180*, 5402–12.

Shinya, K., Hatta, M., Yamada, S., Takada, A., Watanabe, S., Halfmann, P., Horimoto, T., Neumann, G., Kim, J. H., Lim, W., Guan, Y., Peiris, M., Kiso, M., Suzuki, T., Suzuki, Y. and Kawaoka, Y. (2005). Characterization of a human H5N1 influenza A virus isolated in 2003. Journal of Virology *79*, 9926–9932.

Shope, R. E. (1931). SWINE INFLUENZA : III. FILTRATION EXPERIMENTS AND ETIOLOGY. J Exp Med *54*, 373–385.

Simpson, N., Gatenby, P. A., Wilson, A., Malik, S., Fulcher, D. A., Tangye, S. G., Manku, H., Vyse, T. J., Roncador, G., Huttley, G. A., Goodnow, C. C., Vinuesa, C. G. and Cook, M. C. (2010). Expansion of Circulating T Cells Resembling Follicular Helper T Cells Is a Fixed Phenotype That Identifies a Subset of Severe Systemic Lupus Erythematosus. Arthritis and Rheumatism *62*, 234–244.

Singanayagam, A., Wood, V. and Chalmers, J. D. (2011). Factors associated with severe illness in pandemic 2009 influenza a (H1N1) infection: implications for triage in primary and secondary care. J Infect *63*, 243–51.

SJ, F., LW, E., VR, R. and AM, S. (2004). Principles of virology. Molecular biology, pathogenesis, and control of animal viruses. 2nd edition, ASM Press, Washington, DC, USA,.

Skehel, J. (2009). An overview of influenza haemagglutinin and neuraminidase. Biologicals *37*, 177–178.

Skehel, J. J. and Wiley, D. C. (2000). Receptor binding and membrane fusion in virus entry: the influenza hemagglutinin. Annu Rev Biochem *69*, 531–569.

Small, C.-L., Shaler, C. R., McCormick, S., Jeyanathan, M., Damjanovic, D., Brown, E. G., Arck, P., Jordana, M., Kaushic, C., Ashkar, A. A. and Xing, Z. (2010). Influenza infection leads to increased susceptibility to subsequent bacterial superinfection by impairing NK cell responses in the lung. J Immunol *184*, 2048–2056.

Small, P. A., J. and Morris, J. G., J. (2010). Influenza vaccination of children and infection rates in the community. JAMA *303*, 2355–6; author reply 2356.

Smith, G. J. D., Vijaykrishna, D., Bahl, J., Lycett, S. J., Worobey, M., Pybus, O. G., Ma, S. K., Cheung, C. L., Raghwani, J., Bhatt, S., Peiris, J. S. M., Guan, Y. and Rambaut, A. (2009). Origins and evolutionary genomics of the 2009 swine-origin H1N1 influenza A epidemic. Nature *459*, 1122–1125.

Smith W, A. C. . L. P. (1933). A virus obtained from influenza patients. Lancet *1*, 66–68.

Snelgrove, R. J., Goulding, J., Didierlaurent, A. M., Lyonga, D., Vekaria, S., Edwards, L., Gwyer, E., Sedgwick, J. D., Barclay, A. N. and Hussell, T. (2008). A critical function for CD200 in lung immune homeostasis and the severity of influenza infection. Nat Immunol *9*, 1074–83.

Soghoian, D. Z., Jessen, H., Flanders, M., Sierra-Davidson, K., Cutler, S., Pertel, T., Ranasinghe, S., Lindqvist, M., Davis, I., Lane, K., Rychert, J., Rosenberg, E. S., Piechocka-Trocha, A., Brass, A. L., Brenchley, J. M., Walker, B. D. and Streeck, H. (2012). HIV-Specific Cytolytic CD4 T Cell Responses During Acute HIV Infection Predict Disease Outcome. Science Translational Medicine *4*, 123–125.

Soghoian, D. Z. and Streeck, H. (2010). Cytolytic CD4(+) T cells in viral immunity. Expert Rev Vaccines *9*, 1453–63.

Sospedra, M. and Martin, R. (2006). When T cells recognize a pattern, they might cause trouble. Current Opinion in Immunology *18*, 697–703.

Spolski, R. and Leonard, W. J. (2009). IL-21 and T follicular helper cells. Int Immunol *22*, 7–12.

Sprent, J. and Surh, C. D. (2001). Generation and maintenance of memory T cells. Curr Opin Immunol *13*, 248–54.

Stephenson, I., Nicholson, K. G., Hoschler, K., Zambon, M. C., Hancock, K., DeVos, J., Katz, J. M., Praus, M. and Banzhoff, A. (2008). Antigenically distinct MF59-adjuvanted vaccine to boost immunity to H5N1. N Engl J Med *359*, 1631–1633.

Stephenson, I. and Zambon, M. (2002). The epidemiology of influenza. Occup Med (Lond) *52*, 241–7.

Strutt, T. M., McKinstry, K. K., Dibble, J. P., Winchell, C., Kuang, Y., Curtis, J. D., Huston, G., Dutton, R. W. and Swain, S. L. (2010). Memory CD4+ T cells induce innate responses independently of pathogen. Nat Med *16*, 558–64, 1p following 564.

Strutt, T. M., McKinstry, K. K. and Swain, S. L. (2009). Functionally diverse subsets in CD4 T cell responses against influenza. J Clin Immunol *29*, 145–150.

Subbramanian, R. A., Basha, S., Shata, M. T., Brady, R. C. and Bernstein, D. I. (2010). Pandemic and seasonal H1N1 influenza hemagglutinin-specific T cell responses elicited by seasonal influenza vaccination. Vaccine *28*, 8258–67.

Suguitan, Jr, A. L., McAuliffe, J., Mills, K. L., Jin, H., Duke, G., Lu, B., Luke, C. J., Murphy, B., Swayne, D. E., Kemble, G. and Subbarao, K. (2006). Live, attenuated influenza A H5N1 candidate vaccines provide broad cross-protection in mice and ferrets. PLoS Med *3*, e360.

Sun, J., Madan, R., Karp, C. L. and Braciale, T. J. (2009). Effector T cells control lung inflammation during acute influenza virus infection by producing IL-10. Nature Medicine *15*, 277–284.

Sun, J. C., Williams, M. A. and Bevan, M. J. (2004). CD4(+) T cells are required for the maintenance, not programming, of memory CD8(+) T cells after acute infection. Nature Immunology *5*, 927–933.

Sun, K., Ye, J., Perez, D. R. and Metzger, D. W. (2011). Seasonal FluMist vaccination induces cross-reactive T cell immunity against H1N1 (2009) influenza and secondary bacterial infections. J Immunol *186*, 987–993.

Swain, S. L., Agrewala, J. N., Brown, D. M., Jelley-Gibbs, D. M., Golech, S., Huston, G., Jones, S. C., Kamperschroer, C., Lee, W. H., McKinstry, K. K., Roman, E., Strutt, T. and Weng, N. P. (2006). CD4(+) T-cell memory: generation and multi-faceted roles for CD4(+) T cells in protective immunity to influenza (vol 211, pg 8, 2006). Immunological Reviews *213*, 256–256.

Swain, S. L., McKinstry, K. K. and Strutt, T. M. (2012). Expanding roles for CD4(+) T cells in immunity to viruses. Nat Rev Immunol *12*, 136–48.

Tan, P. T., Heiny, A. T., Miotto, O., Salmon, J., Marques, E. T. A., Lemonnier, F. and August, J. T. (2010). Conservation and Diversity of Influenza A H1N1 HLA-Restricted T Cell Epitope Candidates for Epitope-Based Vaccines. Plos One *5*, –.

Taubenberger, J. K. and Morens, D. M. (2008). The pathology of influenza virus infections. Annual Review of Pathology-Mechanisms of Disease *3*, 499–522.

Teijaro, J. R., Verhoeven, D., Page, C. A., Turner, D. and Farber, D. L. (2010). Memory CD4 T cells direct protective responses to influenza virus in the lungs through helper-independent mechanisms. J Virol *84*, 9217–26.

The Writing Committee of the World Health Organization (WHO) Consultation on Human Influenza A/H5 (2005). Avian Influenza A (H5N1) Infection in Humans. N Engl J Med *353*, 1374–85.

Thimme, R., Bukh, J., Spangenberg, H. C., Wieland, S., Pemberton, J., Steiger, C., Govindarajan, S., Purcell, R. H. and Chisari, F. V. (2002). Viral and immunological determinants of hepatitis C virus clearance, persistence, and disease. Proc Natl Acad Sci U S A *99*, 15661–8.

Thimme, R., Wieland, S., Steiger, C., Ghrayeb, J., Reimann, K. A., Purcell, R. H. and Chisari, F. V. (2003). CD8(+) T cells mediate viral clearance and disease pathogenesis during acute hepatitis B virus infection. J Virol *77*, 68–76.

Thomas, P. G., Keating, R., Hulse-Post, D. J. and Doherty, P. C. (2006). Cell-mediated protection in influenza infection. Emerg Infect Dis *12*, 48–54.

Thompson, W. W., Shay, D. K., Weintraub, E., Brammer, I., Bridges, C. B., Cox, N. J. and Fukuda, K. (2004). Influenza-associated hospitalizations in the United States. Jama-Journal of the American Medical Association *292*, 1333–1340.

Thompson, W. W., Shay, D. K., Weintraub, E., Brammer, L., Cox, N., Anderson, L. J. and Fukuda, K. (2003). Mortality associated with influenza and respiratory syncytial virus in the United States. Jama-Journal of the American Medical Association *289*, 179–186.

Tobery, T. W. and Caulfield, M. J. (2004). Identification of T-cell epitopes using ELISpot and peptide pool arrays. Methods Mol Med *94*, 121–32.

Topham, D. J. and Doherty, P. C. (1998). Clearance of an influenza A virus by CD4+ T cells is inefficient in the absence of B cells. J Virol *72*, 882–5.

Topham, D. J., Tripp, R. A. and Doherty, P. C. (1997). CD8+ T cells clear influenza virus by perforin or Fas-dependent processes. J Immunol *159*, 5197–200.

Topham, D. J., Tripp, R. A., Sarawar, S. R., Sangster, M. Y. and Doherty, P. C. (1996). Immune CD4+ T cells promote the clearance of influenza virus from major histocompatibility complex class II -/- respiratory epithelium. J Virol *70*, 1288–91.

Townsend, A. R. M., Gotch, F. M. and Davey, J. (1985). Cyto-Toxic T-Cells Recognize Fragments of the Influenza Nucleoprotein. Cell *42*, 457–467.

Trapani, J. A. and Smyth, M. J. (2002). Functional significance of the perforin/granzyme cell death pathway. Nat Rev Immunol *2*, 735–747.

Treanor, J. J., Kotloff, K., Betts, R. F., Belshe, R., Newman, F., Iacuzio, D., Wittes, J. and Bryant, M. (1999). Evaluation of trivalent, live, cold-adapted (CAIV-T) and inactivated (TIV) influenza vaccines in prevention of virus infection and illness following challenge of adults with wild-type influenza A (H1N1), A (H3N2), and B viruses. Vaccine *18*, 899–906.

Treanor J, W. P. (2003). Immune correlates of protection against influenza in the human challenge model. Dev Biol (Basel) *115*, 97–104.

Ulmer, J. B., Donnelly, J. J., Parker, S. E., Rhodes, G. H., Felgner, P. L., Dwarki, V. J., Gromkowski, S. H., Deck, R. R., Dewitt, C. M., Friedman, A., Hawe, L. A., Leander, K. R., Martinez, D., Perry, H. C., Shiver, J. W., Montgomery, D. L. and Liu, M. A. (1993). Heterologous Protection against Influenza by Injection of DNA Encoding a Viral Protein. Science *259*, 1745–1749.

van Assen, S., de Haan, A., Holvast, A., Horst, G., Gorter, L., Westra, J., Kallenberg, C. G., Telgt, D. S., Palache, A. M., Giezeman, K. M. and Bijl, M. (2011). Cell-mediated immune responses to inactivated trivalent influenza-vaccination are decreased in patients with common variable immunodeficiency. Clin Immunol *141*, 161–8.

Van Kerkhove, M. D., Mumford, E., Mounts, A. W., Bresee, J., Ly, S., Bridges, C. B. and Otte, J. (2011). Highly pathogenic avian influenza (H5N1): pathways of exposure at the animal-human interface, a systematic review. PLoS One *6*, e14582.

van Kooten, C. and Banchereau, J. (2000). CD40-CD40 ligand. J Leukoc Biol *67*, 2–17.

van Leeuwen, E. M., Remmerswaal, E. B., Vossen, M. T., Rowshani, A. T., Wertheim-van Dillen, P. M., van Lier, R. A. and ten Berge, I. J. (2004). Emergence of a CD4+CD28- granzyme B+, cytomegalovirus-specific T cell subset after recovery of primary cytomegalovirus infection. J Immunol *173*, 1834–41.

van Riel, D., Munster, V. J., de Wit, E., Rimmelzwaan, G. F., Fouchier, R. A. M., Osterhaus, A. D. M. E. and Kuiken, T. (2007). Human and avian influenza viruses target different cells in the lower respiratory tract of humans and other mammals. Am J Pathol *171*, 1215–1223.

Vinuesa, C. G., Tangye, S. G., Moser, B. and Mackay, C. R. (2005). Follicular B helper T cells in antibody responses and autoimmunity. Nat Rev Immunol *5*, 853–65.

Virgin, H. W., Wherry, E. J. and Ahmed, R. (2009). Redefining chronic viral infection. Cell *138*, 30–50.

Vogelzang, A., McGuire, H. M., Yu, D., Sprent, J., Mackay, C. R. and King, C. (2008). A fundamental role for interleukin-21 in the generation of T follicular helper cells. Immunity *29*, 127–37.

Vyas, J. M., Van der Veen, A. G. and Ploegh, H. L. (2008). The known unknowns of antigen processing and presentation. Nat Rev Immunol *8*, 607–18.

Waffarn, E. E. and Baumgarth, N. (2011). Protective B cell responses to flu–no fluke! J Immunol *186*, 3823–9.

Wagar, L. E., Rosella, L., Crowcroft, N., Lowcock, B., Drohomyrecky, P. C., Foisy, J., Gubbay, J., Rebbapragada, A., Winter, A. L., Achonu, C., Ward, B. J. and Watts, T. H. (2011). Humoral and cell-mediated immunity to pandemic H1N1 influenza in a Canadian cohort one year post-pandemic: implications for vaccination. PLoS One *6*, e28063.

Wagner, H. (2009). The immunogenicity of CpG-antigen conjugates. Adv Drug Deliv Rev *61*, 243–7.

Wagner, H., Heit, A., Schmitz, F. and Bauer, S. (2004). Targeting split vaccines to the endosome improves vaccination. Curr Opin Biotechnol *15*, 538–42.

Wang, Z., Tobler, S., Roayaei, J. and Eick, A. (2009). Live attenuated or inactivated influenza vaccines and medical encounters for respiratory illnesses among US military personnel. JAMA *301*, 945–53.

Warnatz, K., Bossaller, L., Salzer, U., Skrabl-Baumgartner, A., Schwinger, W., van der Burg, M., van Dongen, J. J., Orlowska-Volk, M., Knoth, R., Durandy, A., Draeger, R., Schlesier, M., Peter, H. H. and Grimbacher, B. (2006). Human ICOS deficiency abrogates the germinal center reaction and provides a monogenic model for common variable immunodeficiency. Blood *107*, 3045–52.

Webster, R. G. and Askonas, B. A. (1980). Cross-Protection and Cross-Reactive Cyto-Toxic T-Cells Induced by Influenza-Virus Vaccines in Mice. European Journal of Immunology *10*, 396–401.

Welsh, R. M. and Fujinami, R. S. (2007). Pathogenic epitopes, heterologous immunity and vaccine design. Nature Reviews Microbiology *5*, 555–563.

Welsh, R. M. and Selin, L. K. (2002). No one is naive: The significance of heterologous T-cell immunity. Nature Reviews Immunology *2*, 417–426.

Wherry, E. J. (2011). T cell exhaustion. Nat Immunol *12*, 492–9.

Whittle, J. R. R., Zhang, R. J., Khurana, S., King, L. R., Manischewitz, J., Golding, H., Dormitzer, P. R., Haynes, B. F., Walter, E. B., Moody, M. A., Kepler, T. B., Liao, H. X. and Harrison, S. C. (2011). Broadly neutralizing human antibody that recognizes the receptor-binding pocket of influenza virus hemagglutinin. Proceedings of the National Academy of Sciences of the United States of America *108*, 14216–14221.

Wiley, D. C. and Skehel, J. J. (1987). The structure and function of the hemagglutinin membrane glycoprotein of influenza virus. Annu Rev Biochem *56*, 365–94.

Wilkinson, T. M., Li, C. K., Chui, C. S., Huang, A. K., Perkins, M., Liebner, J. C., Lambkin-Williams, R., Gilbert, A., Oxford, J., Nicholas, B., Staples, K. J., Dong, T., Douek, D. C., McMichael, A. J. and Xu, X. N. (2012). Preexisting influenza-specific CD4+ T cells correlate with disease protection against influenza challenge in humans. Nat Med *18*, 274–80.

Wolff, T. and Ludwig, S. (2009). Influenza Viruses Control the Vertebrate Type I Interferon System: Factors, Mechanisms, and Consequences. Journal of Interferon and Cytokine Research *29*, 549–557.

Woodland, D. L. (2003). Cell-mediated immunity to respiratory virus infections. Current Opinion in Immunology *15*, 430–435.

Woodland, D. L. and Randall, T. D. (2004). Anatomical features of anti-viral immunity in the respiratory tract. Seminars in Immunology *16*, 163–170.

World Health Organization (2007). Clinical management of human infection with avian influenza A (H5N1) virus.

World Health Organization (2009). Antiviral use and the risk of drug resistance: pandemic (H1N1) 2009 briefing note 12.

World Health Organization Global Surveillance Network (2011). Manual for the laboratory diagnosis and virological surveillance of influenza.

Wrammert, J., Miller, J., Akondy, R. and Ahmed, R. (2009). Human Immune Memory to Yellow Fever and Smallpox Vaccination. Journal of Clinical Immunology *29*, 151–157.

Wrammert, J., Smith, K., Miller, J., Langley, W. A., Kokko, K., Larsen, C., Zheng, N. Y., Mays, I., Garman, L., Helms, C., James, J., Air, G. M., Capra, J. D., Ahmed, R. and Wilson, P. C. (2008). Rapid cloning of high-affinity human monoclonal antibodies against influenza virus. Nature *453*, 667–71.

Wright PF, N. G. and Y, K. (2007). Fields Virology: Orthomyxoviruses. 5th edition, Lippincott Williams & Wilkins., Philadelphia, PA.

Wright PF, W. R. (2001). Fields virology, vol. 1, of Orthomyxoviruses. 4th edition, Williams and Wilkins, Philadelphia.

Wu, J., Zhong, X., Li, C. K., Zhou, J. F., Lu, M., Huang, K. Y., Dong, M., Liu, Y., Luo, F. J., Du, N., Chui, C., Liu, L. Q., Smith, N. M., Li, B., Shi, N. M., Song, L. F., Gao, Y., Wang, D. Y., Wang, X., Zhu, W. F., Yan, Y., Li, Z., Chen, J. T., McMichael, A. J., Yin, W. D., Xu, X. N. and Shu, Y. (2010). Optimal vaccination strategies for 2009 pandemic H1N1 and seasonal influenza vaccines in humans. Vaccine *29*, 1009–16.

Wucherpfennig, K. W. (2004). T cell receptor crossreactivity as a general property of T cell recognition. Molecular Immunology *40*, 1009–1017.

Xu, R., Ekiert, D. C., Krause, J. C., Hai, R., Crowe, J. E., J. and Wilson, I. A. (2010). Structural basis of preexisting immunity to the 2009 H1N1 pandemic influenza virus. Science *328*, 357–60.

Yap, K. L., Ada, G. L. and Mckenzie, I. F. C. (1978). Transfer of Specific Cytotoxic T-Lymphocytes Protects Mice Inoculated with Influenza-Virus. Nature *273*, 238–239.

Yassine, H. M., Lee, C. W., Gourapura, R. and Saif, Y. M. (2010). Interspecies and intraspecies transmission of influenza A viruses: viral, host and environmental factors. Anim Health Res Rev *11*, 53–72.

Yellin, M. J., Sippel, K., Inghirami, G., Covey, L. R., Lee, J. J., Sinning, J., Clark, E. A., Chess, L. and Lederman, S. (1994). CD40 molecules induce down-modulation and endocytosis of T cell surface T cell-B cell activating molecule/CD40-L. Potential role in regulating helper effector function. J Immunol *152*, 598–608.

Yu, D., Rao, S., Tsai, L. M., Lee, S. K., He, Y., Sutcliffe, E. L., Srivastava, M., Linterman, M., Zheng, L., Simpson, N., Ellyard, J. I., Parish, I. A., Ma, C. S., Li, Q. J., Parish, C. R., Mackay, C. R. and Vinuesa, C. G. (2009). The transcriptional repressor Bcl-6 directs T follicular helper cell lineage commitment. Immunity *31*, 457–68.

Yue, F. Y., Lo, C., Sakhdari, A., Lee, E. Y., Kovacs, C. M., Benko, E., Liu, J., Song, H., Jones, R. B., Sheth, P., Chege, D., Kaul, R. and Ostrowski, M. A. (2010). HIV-specific IL-21 producing CD4+ T cells are induced in acute and chronic progressive HIV infection and are associated with relative viral control. J Immunol *185*, 498–506.

Zamarin, D., Ortigoza, M. B. and Palese, P. (2006). Influenza A virus PB1-F2 protein contributes to viral pathogenesis in mice. J Virol *80*, 7976–7983.

Zhu, F. C., Wang, H., Fang, H. H., Yang, J. G., Lin, X. J., Liang, X. F., Zhang, X. F., Pan, H. X., Meng, F. Y., Hu, Y. M., Liu, W. D., Li, C. G., Li, W., Zhang, X., Hu, J. M., Peng, W. B., Yang, B. P., Xi, P., Wang, H. Q., Zheng, J. S. and Control, T. M. C. D. (2009). A Novel Influenza A (H1N1) Vaccine in Various Age Groups. New England Journal of Medicine *361*, 2414–2423.

Zhu, J. and Paul, W. E. (2008). CD4 T cells: fates, functions, and faults. Blood *112*, 1557–69.

Zhu, J. and Paul, W. E. (2009). Heterogeneity and plasticity of T helper cells. Cell Res *20*, 4–12.

Zhu, J. and Paul, W. E. (2010). CD4+ T cell plasticity-Th2 cells join the crowd. Immunity *32*, 11–3.

Zhu, J., Yamane, H. and Paul, W. E. (2010). Differentiation of effector CD4 T cell populations (*). Annu Rev Immunol *28*, 445–89.

Zielinski, C. E., Corti, D., Mele, F., Pinto, D., Lanzavecchia, A. and Sallusto, F. (2011). Dissecting the human immunologic memory for pathogens. Immunol Rev *240*, 40–51.

Appendix I. HLA status of volunteers in the challenge studies.

	H3N2- 2008												H1N1-2009			H1N1- 2010		
HLA/Status	FLU002-7	FLU003-08	FLU004-10	FLU005-2	FLU006-9	FLU008-3	FLU012-16	FLU013-18	B004-19	B005-15	B006-14	B008-23	B009-20	B012-16	B017-02	B021-08	4032-01	4046-18
A*01								1							1			
A*0101					1		1				1						1	
A*02			1									1						
A*0201				1			1			1								1
A*03						1												
A*0301	1		1											1		1		
A*11									1				1					
A*2402									1							1		1
A*2501										1							1	
A*26								1										
A*2601				1														
A*2901											1			1				
A*3101																		
A*3303		1																
A*3601					1													
A*6801	1	1											1					
B*07						1												
B*0702	1		1									1			1			1
B*08						1		1										
B*0801			1				1								1		1	
B*13								1										
B*1501																		1
B*18				1						1		1					1	
B*3501													1	1		1		
B*3503									1									
B*3701					1													
B*3901							1											
B*3906																1		
B*4001				1						1								
B*4403(07/13/26/30/32/36)		1																
B*4403(01/13/26/30/32/36)											1			1				
B*5101									1									
B*5201													1					
B*5701	1	1									1							
B*5802					1									1				
Bw4	1	1			1			1	1		1		1	1				
Bw6	1		1	1		1	1	1	1	1		1	1		1	1	1	1
Cw*0303																		1
Cw*0304				1						1								
Cw*0401								1					1	1		1		
Cw*06					1													
Cw*06(02/03/07)	1				1						1							
Cw*07		1				1		1										
Cw*07(01/06/16)		1	1	1			1					1			1		1	
Cw*07(02/10/13)	1		1									1			1	1		1
Cw*12(02/08)													1					
Cw*12(03/06)							1		1	1							1	
Cw*1502									1									
Cw*1601											1			1				
DRB1*0101												1		1				1
DRB1*0103													1			1		
DRB1*03						1		1										
DRB1*0301			1															
DRB1*0401		1		1					1								1	
DRB1*0403																		1
DRB1*0701	1	1									1			1		1		
DRB1*09						1												
DRB1*11								1										
DRB1*1101												1						
DRB1*13							1											
DRB1*13(01/35/51/59/61)	1						1				1				1			
DRB1*13(02/34/41)										1					1			
DRB1*14(01/26)									1									
DRB1*15					1													
DRB1*15(01/06/09/12)			1	1	1					1							1	
DRB1*15(02/08/14)													1					
DRB3	1		1			1	1	1	1	1	1	1			1			
DRB4	1	1		1		1			1		1			1		1	1	1
DRB5			1	1	1					1			1				1	
DQB1*02		1	1			1		1			1			1		1		
DQB1*03						1												
DQB1*03(01/04/09/10/13)				1				1				1					1	
DQB1*03(02/07/08/11)		1							1						1			1
DQB1*03(03/12/15)	1																	
DQB1*05									1			1	1	1		1		1
DQB1*06					1													
DQB1*06(01/06)													1					
DQB1*06(02/03/07/08/10)	1						1										1	
DQB1*06(02/03/07/10/11)			1	1	1					1	1							
DQB1*06(05/09/12/17/18)							1			1					1			

Appendix II. Number of peptides from each of the subtypes that were used in this study

	A/California/07/2009(H1N1)	A/New York/ 04&05 (H3N2)	A/BR/59/2007 (H1N1)
HA	70	74	75
NA	58	64	58
NP	61	68	61
M1	31	34	31
M2	11	13	11
NS1	26	30	28
NS2	14	17	13
PB2	94	104	94
PB1	94	101	94
PA	89	96	89
PB1-F2		10	6

Appendix III.

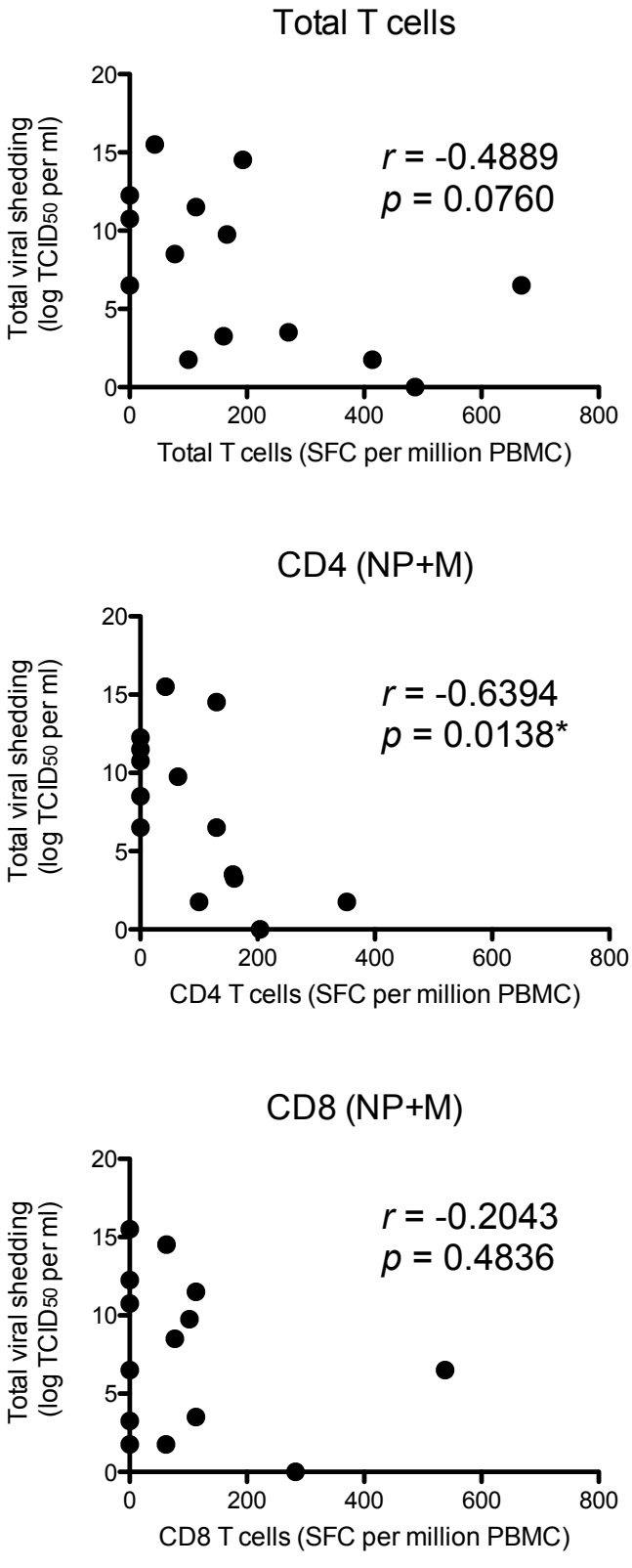

Appendix III. Relationship between influenza-specific T cell responses and viral shedding. Correlations between influenza-specific total, $CD4^+$ and $CD8^+$ T cell responses to internal proteins (NP and M) and total viral shedding in volunteers infected with H3N2 (WS/67/05). Total viral shredding was calculated based on summation of the amount of viral shredding measured daily in the seven-day period. All tests were run by Spearman rank correlation test. A *p* value of less than 0.05 was considered significant (*$p < 0.05$).